Poonam Singh

Development and characterization of cellulose based systems for the entrapment and delivery of probiotic bacteria

· U C ·

UNIVERSIDADE DE COIMBRA

Development and characterization of cellulose based systems for the entrapment and delivery of probiotic bacteria

Poonam Singh

UNIVERSIDADE DE COIMBRA

Reality is merely an illusion

Strive not to be a success, but rather to be of value
Albert Einstein

To move the world, we must first move ourselves
Socrates

Acknowledgements

Foremost, I would like to express my gratitude to Prof. Björn Lindman, who gave me this wonderful opportunity. His scientific expertise, support and care helped me to overcome setbacks and stay focused during my doctorate studies. Even though I asked silly questions, he always listened to me patiently and tried to build on the scientific background. Without his enduring help, this dissertation would not have been possible.

Prof. Maria Graça Miguel welcomed me wholeheartedly not only at the workplace but also in a new family, which helped me to have a remarkable professional experience. Her energy, warmth, and love towards science and humanity kept me motivated in hard times.

I would like to gratefully and sincerely thank Dr. Bruno Medronho, who has helped in every single step of this journey and has been a dedicated advisor to me. He has not only given theoretical knowledge but also life lessons helping me to grow mentally. He constantly and convincingly conveyed a spirit of adventure regarding research and writing.

I am very much thankful to all three of them for encouraging the use of consistent notation in my writings and for carefully reading and commenting on countless revisions of this manuscript.

I am thankful to Prof. Artur Valente, for guiding me time to time in my research and helping me with the paperwork and bureaucracy in the University.

Sincere thanks to Prof. Jordi and Prof. Gemma for hosting me for secondments and making my research fruitful even in short stays.

I would like to thank Prof Gabriela, Dr. Isabel to let me work the microbiology part in their labs and Dr. Tiago Santos to help me with toxicity studies.

I am thankful to Nuno Carvalho who has always promptly helped me with all the questions I had related to my project, University rules and financial details of the resources available.

I want to thank Dr. Filipe Antunes and Dr. Luis Alves to help me overcome my apprehensions and giving me advice on certain aspects of my project.

The heartiest thanks to Elodie, Solange, Cátia and Maria to listen to all my insane conversations

Table of contents

List of Abbreviations

BCCM: Belgian coordinated collections of microorganisms
BIBAFOODS: Biopolymer Based Food Delivery Systems
CA: Citric acid
Cfu/ml: colony forming unit per milliliter
Cht: Chitosan
CMC, NaCMC: Sodium carboxymethyl cellulose
DAPI: (4',6-diamidino-2-phenylindole)
FC: Flow Cytometry
FDA: Food and drug administration
FTIR: Fourier transform infrared spectroscopy
GC: Gas chromatography
Gen: Genipin
GI: Gastrointestinal tract
GRAS: Generally recognized as safe
HEC: Hydroxyethyl cellulose
LA: lactobacillus acidophilus
LAB: lactic acid bacteria
LGG: *Lactobacillus rhamnosus* GG
MP: Macroparticles
Mp: Microparticles
MS: Mass-spectrometry
PBS: Phosphate buffer saline
PI: Propidium iodide
SC: Sodium caseinate
SEM: Scanning electron microscopy
SGF: Simulated gastric fluid
SIG: Simulated intestinal fluid
SL: Soy lecithin
SSF: Simulated salivary fluid
TGA: Thermogravimetric analysis
W/W: Water-in-water
α CD: Alpha cyclodextrin
β CD: Beta cyclodextrin
γ CD: Gamma cyclodextrin

Abstract

Probiotics are increasing their popularity in the market, as their health benefits are being progressively recognized by the public. They are already included in some foods and representing global sales above $30 billion. There is, however, a key issue that concerns the scientists: in order to promote their beneficial effects in the host, probiotics must survive the harsh conditions of the gastrointestinal (GI) tract and should be able of reaching the large intestine to enable colonization.

A possible approach to overcome this issue is to entrap the bacteria in suitable matrices, which ideally maintain the bacteria viable and culturable along with other preservation compounds through the GI tract and capable to provide its controlled release.

This project mainly aimed at developing biopolymer-based systems to be used in food applications. Food and drug administration (FDA) approved cellulose based derivatives were selected and mixed with different polymers/compounds as additives/emulsifiers/prebiotics to enhance the viability of bacteria, create more stable delivery systems and sustain the different storage conditions as well as maintaining the viability for a minimum of 30 days.

Therefore, in this work, novel micro- and macroparticles, based on carboxymethyl cellulose (CMC) and chitosan (Cht) (cross-linked or not with genipin), were successfully prepared in aqueous media either by drop-wise addition or via nozzle-spray methods. The crosslinked particles are robust, thermally resistant and less sensitive to pH changes. On the other hand, the physical systems are pH sensitive presenting a remarkable swelling at pH 7.4, while little swelling is observed at pH 2.4. Model probiotic bacteria (*Lactobacillus rhamnosus* GG) were successfully encapsulated in the CMC-Cht based particles with acceptable viability count.

In a subsequent step, different cyclodextrins (CDs) were used in the particle formulation and their potential prebiotic effect evaluated. The morphology of the systems depends on the CD used and this may be related to different "host-guest" interactions between the CDs and the CMC-Cht matrix thus affecting the polymer organization and overall particle microstructure. Among the CDs tested, β-CD was observed to be one of the most efficient molecules to enhance the survival of the cells.

In order to improve the developed particles in terms of aggregation and colloidal stability, different food grade compounds were included in the formulations, such as caseinate and soy

lecithin.

Apart from the micro- and macro particles other methods were used to entrap probiotics such as the formation of water-in-water (W/W) emulsions based on gelatin and CMC. Depending on the conditions, the mixtures can lead to the formation of W/W emulsion droplets and model probiotic bacteria could be successfully entrapped with surprisingly high viability count.

Finally, cellulose-based edible films with CMC and HEC (hydroxyethyl cellulose) cross-linked with citric acid (CA) were also developed under mild conditions. Films with tunable mechanical properties and swelling ability could be obtained by varying the HEC/CMC ratio and the amount of CA. It is salient to notice that some of the systems tested can be considered prebiotics since the viability count of model probiotic bacteria, entrapped in CMC-Cht particles, was considerably improved after the incorporation of CDs and gelatin in the formulation.

Further studies on the aging and behavior of the particles in simulated gastrointestinal fluids were performed. Particles loaded with caseinate, soy lecithin or cyclodextrins showed an improved viability of LGG even after one month storage at 25 ℃. In most of the cases, matrices were also capable to efficiently protect the cells from the simulated harsh gastric conditions with a remarkable viability in comparison to naked probiotic. The cellulose-based particles developed were also evaluated regarding their effect on an intestinal cell line and the results indicate that the systems are reasonably mild for the cells and thus encouraging for future applications.

Overall, all the systems developed in this work could efficiently entrap and preserve viable bacteria thus being promising matrices for food applications.

Sumário

Os probióticos têm visto a sua popularidade no mercado aumentar em grande medida devido ao reconhecimento do público dos seus efeitos benéficos para a saúde. Eles já são incluídos em muitos produtos alimentares que representam um total global de vendas de cerca de 30 mil milhões de dólares. No entanto, existe uma questão central que continua a preocupar os cientistas. Para que os probioticos exerçam os seus efeitos benéficos no hospedeiro eles têm que sobreviver às condições particularmente adversas do sistema gastrointestinal e atingir o intestino grosso com viabilidade aceitável para uma colonização eficiente. Uma possível estratégia para ultrapassar os obstáculos impostos pelo trato gastrointestinal reside na proteção dos probióticos em matrizes apropriadas par ao efeito. Idealmente estes sistemas em combinação com outros compostos serão capazes de manter as bactérias viáveis e cultiváveis ao longo do trato gastrointestinal e promover a sua libertação no sítio apropriado.

Este projeto tem como objetivo principal o desenvolvimento de sistemas baseados em biopolímeros para aplicações na área alimentar. Foram selecionados derivados de celulose aprovados pela agência para os alimentos e medicamentos (FDA) e misturados com outros polímeros e compostos como agentes emulsificantes, prebióticos, ciclodextrinas para aumentar a viabilidade das bactérias probióticas e criar vetores de entrega mais estáveis e capazes de resistir a diferentes condições de armazenamento e manter uma viabilidade aceitável durante pelo menos 30 dias. Tendo isto em consideração, neste trabalho foram desenvolvidas novas micro e macro partículas à base de carboximetilcelulose (CMC) e quitosano (Cht) (reticuladas ou não com genipina) em meio aquoso através de um procedimento de adição gota-a-gota ou spray. As partículas reticuladas são robustas e termicamente resistentes e pouco sensíveis a variações de pH. Por outro lado, os sistemas físicos são mais sensíveis às variações de pH apresentando uma turgescência assinalável a pH 7.4 enquanto a turgescência a pH 2.4 é menosprezável. Neste trabalho foram encapsuladas bactérias probioticas modelo (*Lactobacillus rhamnosus* GG) em partículas de CMC-Cht com viabilidade aceitável. Numa etapa subsequente, diferentes ciclodextrinas (CDs) foram usadas na formação das partículas e avaliado o seu eventual efeito prebiótico. A morfologia dos sistemas é fortemente dependente do tipo de CD usado e tal fato pode estar relacionado com as diferentes interações "hospedeiro-hospede" entre CDs e a componentes da matriz de CMC-Cht que eventualmente afetam a organização dos polímeros e

microestrutura das partículas. De entre as CDs testadas, a β-CD foi aquela que se mostrou mais eficiente no aumento da viabilidade dos probióticos. De forma a melhorar a estabilidade das partículas em termos de minimizar a agregação, foram usados na formulação diferentes compostos de qualidade alimentar como caseinato de sódio e lecitina.

Para além da formação das micro e macro partículas foram desenvolvidos outros sistemas para "aprisionar" os agentes probióticos como emulsões de água-em-água (W/W) à base de CMC e gelatina. Dependendo das condições, estas misturas podem levar à formulação de emulsões onde é possível aprisionar de forma satisfatória e com surpreendente elevada viabilidade as bactérias probióticas modelo.

Finalmente foram ainda desenvolvidos filmes comestíveis à base dos derivados de celulose CMC e hidroxietilcelulose (HEC) reticulados com ácido cítrico. As propriedades mecânicas e de turgescência podem ser ajustadas dependendo do rácio HEC/CMC e concentração de ácido cítrico. É importante notar que alguns dos sistemas desenvolvidos comportam-se como prebióticos pois a viabilidade das bactérias probióticas modelo aumentou consideravelmente depois da incorporação de CDs ou gelatina na formulação.

Foram realizados ainda alguns estudos de envelhecimento e comportamento das partículas em fluidos gastrointestinais artificiais. As partículas com caseinato de sódio, lecitina e CDs demonstraram um melhoramento na viabilidade depois de armazenadas um mês a 25 ºC. Na maior parte dos casos, as matrizes polimericas desenvolvidas foram capazes de proteger de forma muito satisfatória as células próbioticas das condições adversas impostas pelos sucos gástricos artificiais resultando em viabilidades assinaláveis em comparação com as bactérias não protegidas.

As partículas desenvolvidas à base de celulose foram ainda avaliadas tendo em conta o seu impacto numa linha celular intestinal e os resultados indicam que os sistemas são relativamente inócuos para as células intestinais.

De forma geral, os sistemas desenvolvidos no decorrer deste trabalho conseguem de forma eficiente encapsular e preservar a viabilidade dos agente probióticos e portanto podem ser consideradas matrizes promissoras para futuras aplicações alimentares.

Graphical Abstract
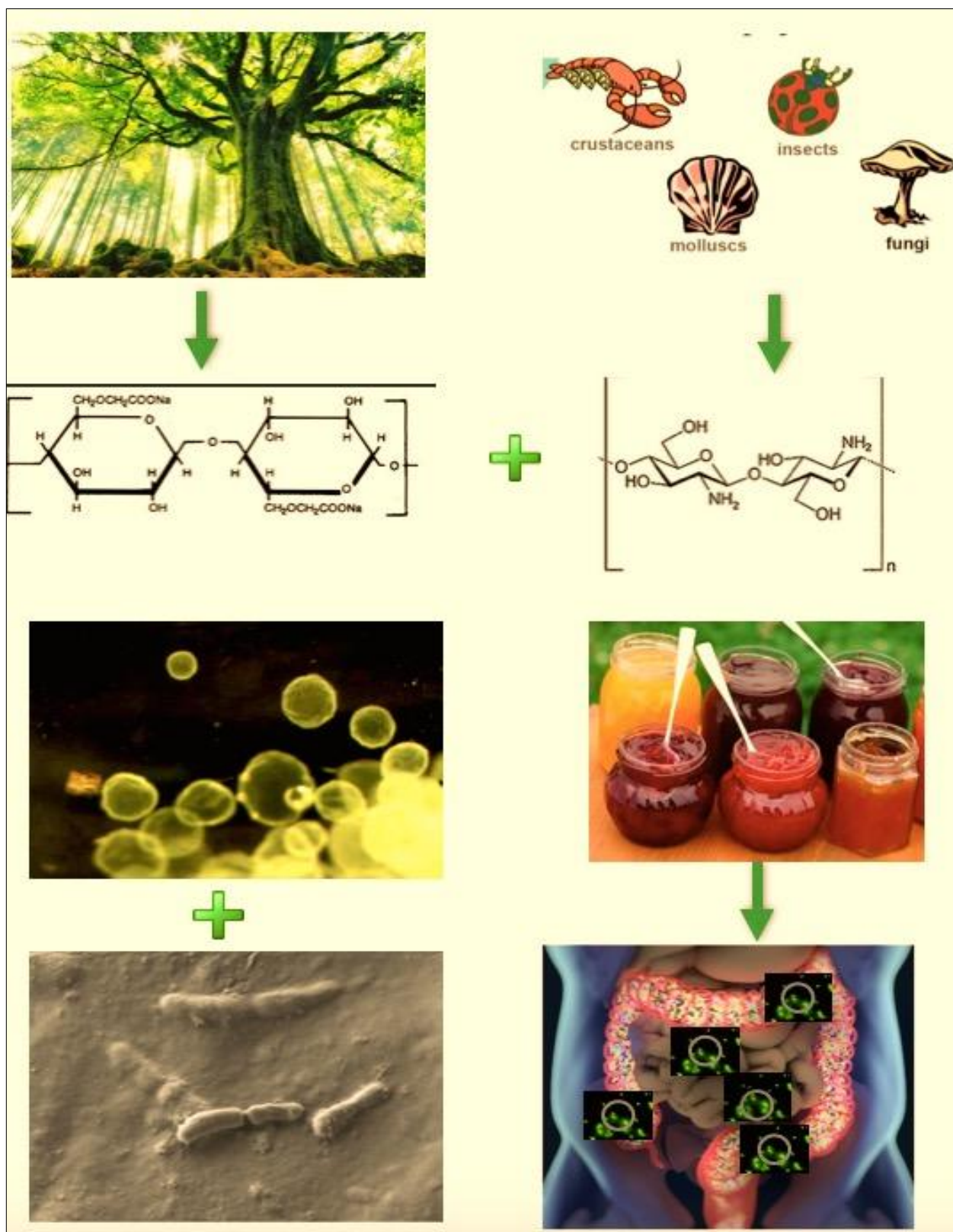
List of publications included in the thesis

I.   Singh, P., Medronho, B., Alves, L., Miguel, M. G., & Lindman, B. (2017). Development of carboxymethyl cellulose-chitosan hybrid micro- and macroparticles for encapsulation of probiotic bacteria. Carbohydrate Polymers, 175, 87-95.

II.   Singh, P., Medronho, B., Miguel., Esquena J. (2018) On the encapsulation and viability of probiotic bacteria in edible carboxymethyl cellulose-gelatin water-in-water emulsions. Food Hydrocolloids, 75, 41-50.

III. Singh, P., Medronho, B., Valente, J.M., Miguel, M. G., & Lindman, B. Exploring the prebiotic effect of cyclodextrins on probiotic bacteria entrapped in carboxymetyl cellulose-chitosan particles (Accepted in Colloids and Surfaces B).

IV.   Singh, P., Magalhaes, S., Alves, L., Antunes, F., Miguel, M. G., & Lindman, B., Medronho, B. Encapsulation of *Lactobacillus rhamnosus* in cellulose based edible films (Submitted to Carbohydrate Polymers).

V.   Singh, P., Medronho, B., Santos, T., Nunes, I., Miguel, M. G., & Lindman, B. *In vitro*, shelf life, stability and cytotoxicity studies of *Lactobacillus rhamnosus* GG entrapped CMC-Cht based particles (in preparation).

x

Publication not included in this thesis

I. Soukoulis, C., <u>Singh, P</u>., Macnaughtan, W., Parmenter, C., & Fisk, I. D. (2016). Compositional and physicochemical factors governing the viability of Lactobacillus rhamnosus GG embedded in starch-protein based edible films. Food Hydrocolloids, 52, 1, 876-887.

II. <u>Singh, P</u>., Duarte, H., Alves, L., Antunes, F., Moigne, N.L., Dormanns, J., Duchemin, B., Mark P. Staiger, M. P., & Medronho, B. (2015). From Cellulose Dissolution and Regeneration to Added Value Applications — Synergism Between Molecular Understanding and Material Development, Cellulose- Fundamental Aspects and Current Trends, Dr. Matheus Poletto (Ed.), ISBN: 978-953-51-2229-6, InTech, <u>DOI: 10.5772/61402</u>.

III. Srinath Murali, S., Kumar, S., <u>Singh, P</u>., Balu, K., Seena, S., Ferreira, M., Sobral, A. Synthesis, characterization and antimicrobial properties of chitosan-gelatin-Ag loaded ZnO nano bio-composite for wound healing applications (in preparation)

IV. <u>Singh, P</u>., Medronho, B., Miguel, M. G., & Lindman, B. Application of CMC Cht particles in food system, *in vitro*, shelf life and sensory studies. (In preparation)

Scientific contribution Report

Paper I

I performed all the experimental work and wrote the paper together with the co-authors.

Paper II

I performed all the experimental work and wrote the paper together with the co-authors.

Paper III

I performed all the experimental work and wrote the paper together with the co-authors.

Paper IV

I performed more than half of the experimental work and wrote the paper together with the co-authors

Paper V

I performed all the experimental work, except the toxicity part and wrote the paper together with the co-authors

Part I

1 Introduction and thesis overview
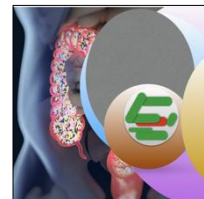
Functional foods are often defined as systems "designed to have physiological benefits and/or reduce the risk of chronic disease beyond basic nutritional functions" [1]. They may be similar in appearance to conventional food and consumed as part of a regular diet and, since the concept was introduced more than 30 years ago, functional foods have gained increased attention [2,3]. In this respect, probiotic bacteria arise as a valuable ingredient for functional foods and suggested of being capable to treat different diseases or health problems [4].

These are living microorganisms which are said to provide beneficial health effects to the host by replenishing natural GI microbiota [5,6]. However, probiotic bacteria when taken orally are very often inactivated by the harsh acidic stomach conditions and, consequently, the effectiveness of probiotics intake depends very much on the number of viable cells capable to pass the GI tract [7,8]. Thus, the development of smart delivery systems for food and biomedical applications, capable to entrap, protect, transport and appropriately deliver the active agent is not only interesting from a fundamental point of view but very important, particularly for food applications [9].

Delivery systems for food and biomedical applications combine aspects of biology, chemistry, and engineering. However, optimum understanding while designing a delivery vehicle required to rationalize and overcome the physiological limitation (i.e. temperature, pH, ionic strength, etc.) without any harmful effect to the cells and the tissues [10,11].

There are different formulations to deliver the probiotics, varying in the viability, advantages, and effectiveness of bacterial/yeast cells in the human intestine. The survival time of probiotic bacteria should be within a certain limit not only while incorporated in a formulation process, but also in both in vitro and in vivo [12]. Systems not only differ in providing protection to probiotic bacteria but also the dosage forms and survival rate after going through

harsh GI tract conditions [13]. Nevertheless, it is becoming essential to have systems that can smartly deliver the encapsulated material, be it a drug, food component or nutraceutical, in vivo [14]. As mentioned above, several physiological obstacles can delay or prevent the delivery of probiotic bacteria in a safe and effective way [15,16].

Different strategies have been explored to protect probiotics from the harsh conditions of the GI tract (i.e. low pH, bile salts and enzymes) and microencapsulation is among the most popular methods [17]. In this respect, three-dimensional biopolymer matrixes due to their often favorable biocompatibility and biodegradability profiles are being widely used as efficient vehicles to deliver therapeutic agents [18,19].

These hydrophilic systems (commonly defined as hydrogels) can be natural or synthetic and are used in a vast number of products in industrial and environmental areas [20,21]. The microcapsules are often formed by different approaches such as interfacial emulsion polymerization, ionic coacervation, and sol-gel immobilization, using biocompatible macromolecules, such as polysaccharides and proteins, as encapsulating agents [22].

Commercial formulations are generally food-based products, either in form of tablets or capsules to be taken orally like other health supplements [13]. The food products that have these bacteria added during their production, such as chocolates and ice cream, are observed to provide health benefits of interest [23,24].

Consequently, this work focuses essentially on the use of biocompatible macromolecules that are different cellulose-based derivatives, chitosan and nontoxic cross-linkers such as genipin and citric acid to develop novel smart delivery systems (e.g. micro and macro particles, films, and emulsions) capable to entrap viable and culturable cells and protect them from simulated GI conditions. There are plenty of recognized uses and studies on Cht and CMC, but surprisingly little work involves both biopolymers simultaneously.

This is a very attractive approach because of the abundance of these polymers, which may facilitate an industrial scale up. A few exceptions involve the synthesis of inorganic nanoparticles in CMC-Cht matrixes [11,25], the formation of hybrid hydrogels for yeast cell growth and the development of CMC-Cht nanoparticles after enzymatic hydrolysis of the biopolymers [26]. To our knowledge, their potential to form entrapping and delivery systems for probiotics has only been reported in one occasion using a physical layer-by-layer approach to form a nanostructured material (i.e. probiotic bacteria surrounded by alternated layers of Cht and

CMC) [27].

This work also aims at evaluating the effect of prebiotic agents in the formulations, study the temperature and aging (storing) effect on probiotic viability and, finally, evaluate the effect of the systems developed in an intestinal cell line.

Outline of the thesis

This treatise is mainly divided in two parts. Part I consists of chapters focusing on the general aspects related to probiotics (section 2), biopolymers encapsulation (section 3), delivery vehicles and storage (section 4) and viability and toxicity studies (section 5). A brief overview of the main techniques, methodology and most relevant achievements is given in section 6, while the the main characterization methods are introduced in section 7.

In the second part, the scientific papers that resulted from this work are compiled and are mainly based on four major topics: 1) designing and characterizing novel delivery vehicles; 2) entrapment of model probiotic bacteria (*Lactobacillus rhamnosus*) in the developed systems and the effect of prebiotics; 3) studying the release and viability of probiotics in simulated gastrointestinal model fluids and 4) evaluating the storage stability and interaction of the developed systems with an intestinal cell line.

2 Gut microbiota, probiotics and prebiotics
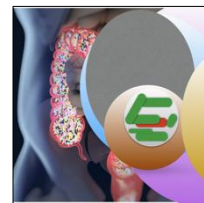
2.1 Gut microbiota

The human gut mucosa consists of more than 100 trillion microbes which are estimated to be ten times more than the human cells. The gastrointestinal (GI) tract anchors a diverse community of obligate and facultative anaerobic bacteria. These bacteria are supposed to contribute to the metabolic and protective functions of the host (human) and are referred to as microbiota [28].

An adult gut is mainly formed with two bacterial phyla, *Firmicutes* and *Bacteroidetes*. Specific host pathways are linked to microbial response impacting the wellbeing of humans. In general, the microbial mechanisms and metabolism underlying their role in modification of the gut leading to its recovery are still being poorly understood. The results of these researches support the importance of gut homeostasis and, in turn, the role of dysfunction caused by the microbial viability or the functional potentiality of the populations residing in GI tract [29,30].

The gut homeostasis can be altered during the host-microbiota interaction. This interaction is mainly affected by diets, medication, environment and gene mutation.

Food nutrients like vitamins, amino acids or dietary fibers consumed by the host are broken down and converted into some metabolites by intestinal microbes. Gut bacteria feed on these metabolites that can be short-chain organic acids (SCFAs) such as propionate, butyrate or acetate synthesized from undigested complex carbohydrates during bacterial fermentation, biogenic amines (like histamine) or derived from amino acids such as serotonin or gamma-aminobutyric acid (GABA) [31,32,33,34].

The lumen model of conversion by intestinal microbes is illustrated in Figure 1. As will be discussed later, the gut microbiota can be manipulated by probiotics to enhance the beneficial effects and efficacy during treatment of many diseases [35].
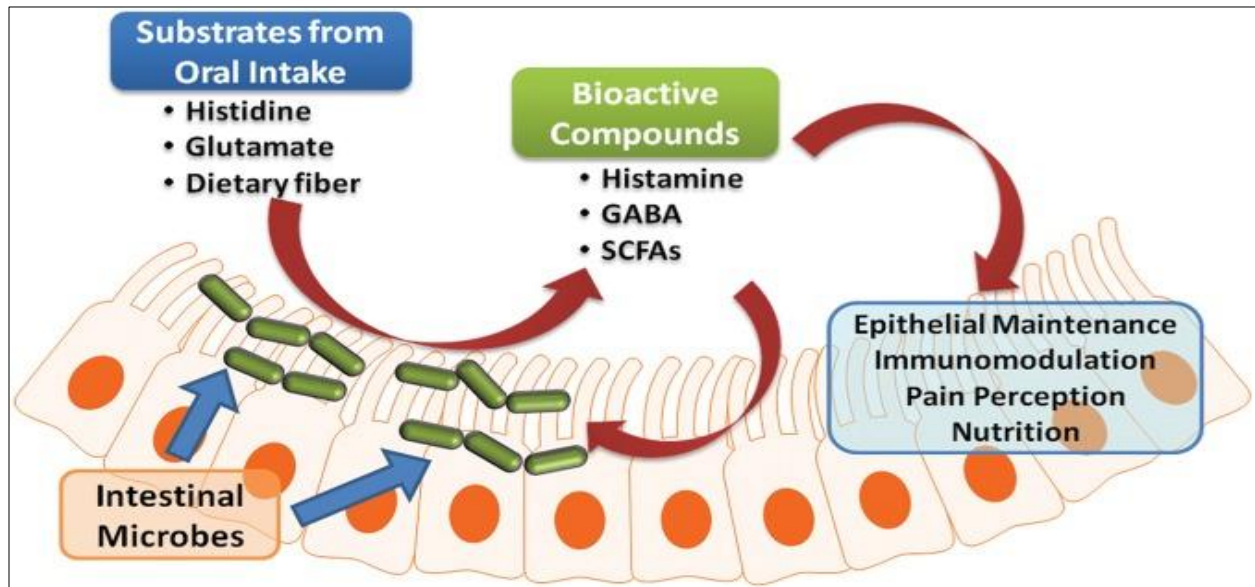
Figure 1. A depiction showing that consumed nutrients may be converted into bioactive compounds by intestinal microbes in the intestinal lumen [36].

2.2 General aspects of Probiotics

As previously discussed, probiotics are predominantly live bacteria or yeast bestowing health benefits when consumed in proper amounts [37]. According to the Food and Agriculture Organization and the World Health Organization, the minimum number of bacteria needed to provide any desired effect is suggested to be 10^6-10^7 CFU/mL (CFU is known as colony-forming units) [38]. Many scientific evidences suggest that these living microorganisms provide beneficial health effects to the host by replenishing the natural GI microbiota [39].

Probiotics are considered nutraceuticals, which balance the micro gut flora and can eliminate harmful pathogenic bacteria [40]. As a naturally occurring functional component, a vast research is being performed on their culture identification, strain selection, properties and supporting information for health benefit claims [41]. That means the characterization in a wider respect and providing clinical evidences of a health benefit.

Therefore, any culture/strain is not probiotic unless it meets this requirement [42,43]. Some convincing effects attributed to probiotics include the improvement of the aberrant microbiota conditions in different cases such as atopic dermatitis, necrotising enterocolitis, pouchitis and possibly irritable bowel syndrome [44]. The difficulty in these studies is the direct link to causing the betterment of these diseases [45].

5

The increasing consideration on how to aid the health benefits has led to the need for attentiveness in the field of probiotics. If we look to the standard definitions of probiotics and simplify, it can be inferred as "a health benefit to the host". However, according to regulatory guidelines, the use of this phrase can't be advertised on commercial products. The reason leading to this restriction is 'lack of satisfactory evidence' proving the benefit of such microbes (probiotics) selectively increasing or sustaining the flourishing gut [46].

2.3 Mechanism of action of probiotics

The human body has more than 500 different probiotic strains. If the microflora equilibrium is maintained, Gram positive and Gram negative bacteria colonized in the intestinal tract may employ correlative effects [47,48]. *Lactobacillus (L.) L. acidophilus*, *L. rhamnosus, L. helveticus, Bifidobacterium (B.) infantis, B. lactis. lactogg, L. bulgaricus, L. plantarum, L. salivarus, B. bifidum, L. reuteri, L. casei, S. thermophilus,* and *B. coagulans* are some of the most common strains which are nowadays used in food and pharmaceutical formulations. *L. acidophilus* and *L. casei we*re among the earliest probiotics known for their health benefits [49].

Nowadays, *Lactobacillus* species and Bifidobacteria are the two majorly commercialized strains. *Streptococcus (S.) thermophilus* is used in pharmaceutical applications and in yoghurts apart from lactic acid bacteria (LAB) [50]. The consequences of having microbes embanking the intestinal tract are mostly marked in the early development, when shifts in the feeding mode occur from breast-feeding to formula feeding and during the introduction of solid food as the fetus has a sterile GI tract. Imbalances of the intestinal microflora may cause gastrointestinal dysfunctions and this has been inferred while studying the mechanisms of action of probiotics in human health [51]. Some examples of the proposed mechanisms are summarized in Figure 2.

There is a general assumption that viable bacteria are required to have a beneficial effect but the recent studies have shown bacterial DNA sequences may provide the same effects as live bacteria and non-viable probiotics and microbial cell wall components are the least likely to cause safety concerns. However, further studies elaborating *in vitro* and *in vivo* trials and incorporation of non-viable strains in products are needed to prove this claim [52,53].
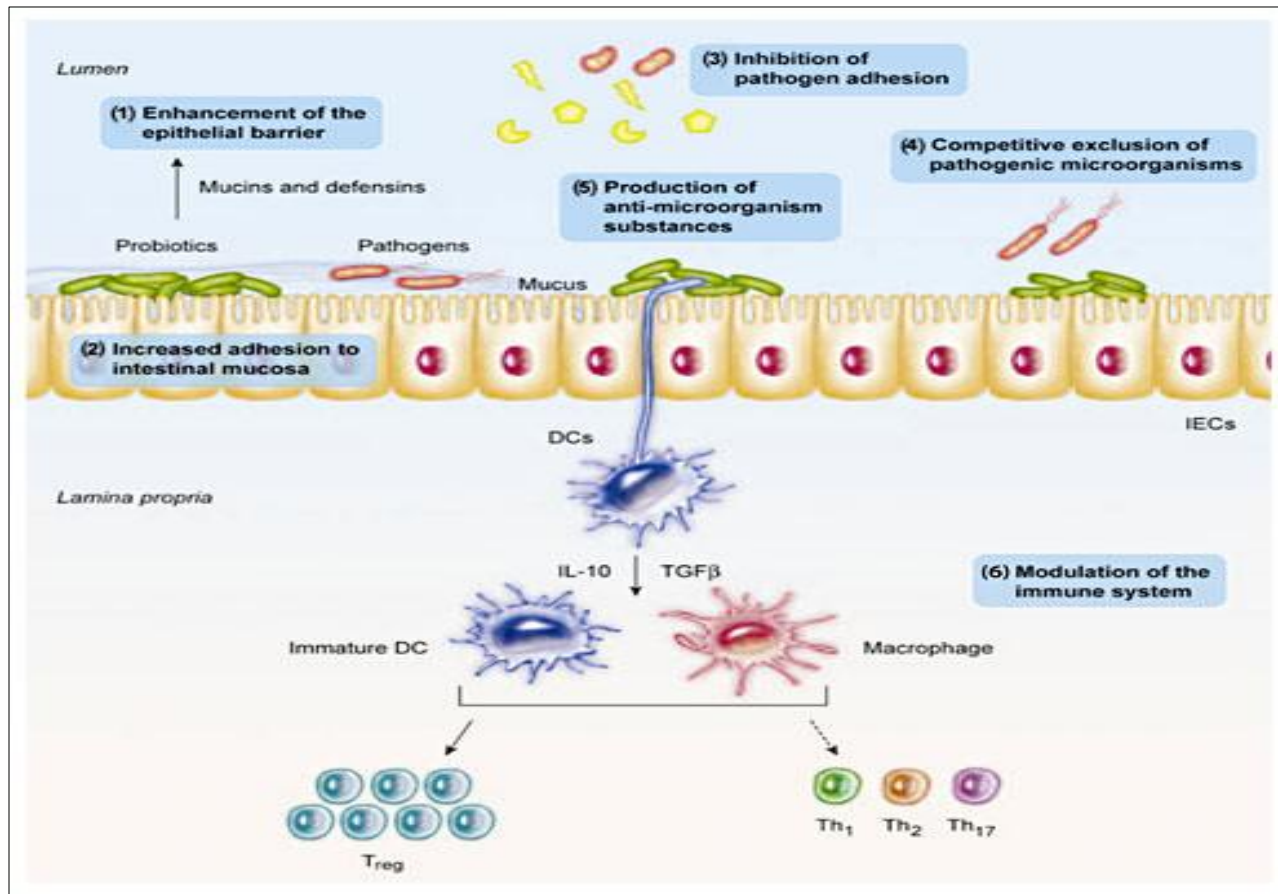
Figure 2. A depiction of major probiotic mechanisms of action in a lumen model of the human (host) [54].

2.4 Clinical benefits claimed for probiotics

The most commonly used microorganisms are bifidobacteria, lactic acid bacteria and certain types of yeast. These strains are among the most tried probiotics [55,56]. In respect to the beneficial effects, probiotics have been reported to shorten or even prevent diarrhea and respiratory tract infections, reduce the risk of necrotizing enterocolitis in premature infants, mitigation of lactose intolerance symptoms, treatment of food allergy, binding of toxins and pathogens from ingested foods or from the GI tract [57,58].

Other related studies claim the medical benefit of the probiotics even in cancer but none of those studies identify clinical improvements to probiotic-induced microbiota changes [59,60]. The application of probiotics might also show a positive impact on immunomodulation, as the

nutrients may be broken down into metabolites by microbes affecting regulatory functions in the host, although the mechanisms of action are still not clear [36].

Sherwood Gorbach and Barry Goldwin isolated for the first-time *Lactobacillus rhamnosus* GG (LGG), ATCC 53103 (the letters have been taken by the surname letters GG) from the fecal samples of a healthy human adult. The reasons why it was identified as a potential probiotic strain is its resistance to harsh acid environment and bile salts, easy handling/growth characteristics and adhesion competency to the intestinal epithelial layer [61]. It is a gram-positive, bacterium strain of the *Lactobacillus rhamnosus* species, a facultative anaerobe that resides in the GI mucosa and mouth of healthy humans [62].

It is one of the most widely studied probiotic strains, used in a variety of marketable probiotic products with satisfactory results in human intervention studies [61]. It should be noticed that lactic acid bacteria are strain specific in relation to their health benefits [63,64]. *L. rhamnosus* GG (or simply LGG) is easily grown and handled due to the lack of pathogenicity. LGG is believed to help maintaining a good balance of bacteria in the stomach and intestines by preventing the growth of other harmful bacteria.

Comprehensive research on LGG [65] probiotic response has suggested that this bacterium has the capability to reduce gastrointestinal irritation categorically for illness in kids [66]. Diarrhea caused by *Clostridium difficile*, antibiotic intake and the duration of infectious diarrhea is also observed to be alleviated by the consumption of *Lactobacillus rhamnosus* GG based products [67,68,69].

B. longum has been suggested to inhibit the origin of colon, liver and mammary tumors generated by the food mutagen (2-amino-3-methylimidazo[4,5-f]quinolone), possibly by suppressing the cancer producing microbes or their promoters [70]. *B. longum* may also induce changes in the glycolytic flux and the regulation of internal pH of the gastrointestinal tract by causing a rise in the content of ammonium in the cytoplasm due to deamination of amino acids [71].

2.5   *Probiotics and society*

Since olden times, probiotics have been consumed basically in the form of traditional fermented foods [72]. However, the scientific community has recently proposed that, in general, the

fermented foods do not necessarily contain living microorganisms [73]. In cases of beer and wine, the purification involves a microorganism removal step. In other fermented foods, microbes are often inactivated by heat treatment. For instance, when bread is baked and sauerkraut is canned or packed these foods are nutritious but might or might not contain probiotic activity. Therefore, in order to preserve the live microbe cells in the commercial products, the inactivation step should be moderated during the manufacturing process [74,75,76].

In the market there is a plethora of dairy based probiotic products, mostly yoghurt and dairy based drinks, but it is quite unusual to find dehydrated products. Other than yoghurt, the probiotic containing popular products used around the world are: kefir: a fermented dairy product; sauerkraut & kimchi: prepared with fermented cabbage and other vegetables; kombucha: a black tea from Japan; coconut kefir: a dairy-free option; miso: a traditional Japanese spice; tempeh: fermented soybean from Indonesia; balted gherkin pickles; brine-cured olives, raw cheese, apple cider vinegar and natto from Japan [77,78]. Most of these products containing probiotics are easily accessible and are sold with little or no exclusivity and restriction to the people [75]. They have already a recognized market, predominantly due to our eating habits. [79].

As previously mentioned, the majority of the consumed probiotics products in daily life are fermented milks, mostly flavored yogurt drinks and juice or juice concentrates [80]. As juices normally have a low pH, extra precaution is required to incorporate probiotics and keep their viability acceptable. Milk has a naturally excellent buffering capacity and is a favorable carrier for different probiotic strains [81]. As stated before, other probiotic niche products involve dairy based items like ice cream, cheese, kefir, candy, and chocolate [82]. Furthermore, there is a whole new market for a relatively new and a bigger product category that implicitly includes breast-milk substitutes, milks for older babies and special infant formulas [83]. As expected, the legislation for infant formulas is extremely rigorous and requires strict control and documentation of the strains used [84].

The stability and survival of probiotics is strain specific. The strain classification is not always distinct, and the coherent description of viable counts is often not described on the package labels. When it comes to the estimation of the market size for the products with health claims, the assessment becomes highly convoluted. Despite the fact there are plenty of products advertised and labeled as probiotics, only a few of them have been evaluated in scientific trials

involving humans [85].

2.6 Prebiotics

Prebiotics were initially defined as non-digestible ingredients stimulating the growth and activity of certain species of bacteria inside human colon, hence improving the health of the host [86]. Later, the definition was revised and now considers prebiotics as a class of selectively fermented ingredients that allow specific changes, both in the composition and/or activity in the gastrointestinal microflora, conferring some sort of benefit [87,88]. Prebiotics do not get absorbed in the upper part of the gastrointestinal tract; hence they enter the colon and serve as a substrate for the endogenous bacteria, thereby directly providing the host with energy and metabolic substrates [89].

Some of the advantages after the intake of dietary fibers are mentioned in Table 1. The production of lactic and short-chain carboxylic acids as end products of the fermentation has been confirmed during *in vitro* and *in vivo* studies [90].

Table 1. Benefits of intake of prebiotics on the GI tract [91].

Effects on upper GI tracts	Resistance to digestion
	Retarded gastric emptying
	Increased oro-caecal transmit time
	Reduced glucose absorption and low glycaemic index
	Hyperplasia of the small intestinal epithelium
	Stimulation of secretion of intestinal hormonal peptides
Effects on lower GI tract	Acting as food for colonic microbiota
	Acting as substrates for colonic fermentation
	Production of fermentation end products (mainly SCFAs)
	Stimulation of saccharolytic fermentation
	Acidification of the colonic content
	Hyperplasia of the colonic epithelium
	Stimulation of secretion of colonic hormonal peptides
	Bulking effect on stool production
	Regularization of stool production (frequency and consistence)

Prebiotics are generically recognized to be resistant to gastric harsh acidity conditions,

often described as non-digestible poly- or oligosaccharides that provide a valuable effect to the host by selectively stimulating the growth and/or activity of one or a limited number of beneficial bacteria in the colon [3,21]. For instance, the fermentation of oligofructose in the colon due to the presence of intestinal microflora has been suggested to confer several beneficial effects, including the increase of probiotics in the colon, enhancement of calcium absorption, shortened gastrointestinal transit time and even decrease of the blood lipid levels [92].

The main source of prebiotics are fibers and carbohydrates, such as resistant starch, wheat bran, inulin or other short oligosaccharides of glycosidic residues such as fructose in fructooligosaccharides (FOS) or galactose in galactooligosaccharides [93,94]. To date the most studied prebiotics are FOS, inulin and oligofructose [95,96]. Nevertheless, many other oligosaccharides such as xylo-oligosaccharides, pectic oligosaccharides, palatinose and pullulan derivatives have also been object of research [88,97]. Different prebiotic benefits have been reported including the relieve from constipation, suppression of diarrhea, amelioration of intestinal infection, reduction of osteoporosis and atherosclerosis, as well as reduced cardiovascular disease, etc [89].

In recent years, a new strategy has been developed using probiotics in combination with prebiotics, such as oligosaccharides, resulting in the so called "synbiotics" [98,99]. The combined effects of the two compounds improve the probiotic colonization or metabolic effect. When the patients suffering from ulcerative colitis were treated with a synbiotic approach, the outcome was more effective than when the probiotics or prebiotics were used separately [100]. The beneficial synbiotic effect was also reported in colorectal cancer prevention [59] or in very general positive regulation of the microbiota and therefore it is regarded as a very appealing approach [101,102].

3   Polymers in aqueous solution
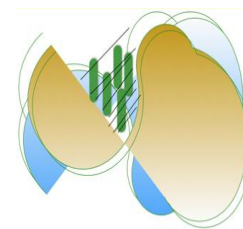
Polymers are biological (e.g. proteins, nucleic acids and polysaccharides) and non-biological (e.g. polystyrene) macromolecules having high molecular mass. Polymers can be classified based on their source (natural or synthetic), backbone of the polymer chain (linear or branched or cross-linked), composition (homopolymer or copolymer), polymerization (addition or condensation) and mechanical properties (elastomers, fibers,liquid resins or plastics) [103].

The properties of a polymer depend on the constituting monomer units and their arrangement (such as stereochemistry of the linkage). Characterization of a polymer includes its molecular weight, molar volume, density, degree of polymerization (DP), crystallinity etc. Of special significance are the interactions of the polymer molecules with cosolutes and solvents [104].

Polymers can have no charge, a net negative or a positive charge due to the different functional groups such as carboxylate, sulphate or ammonium. When polymers are charged, they are known as polyelectrolytes. Typically, polyelectrolytes have a higher solubility in water than neutral polymers due to the entropy of the counterions [105,106].

Of a particular interest in this work were the polymers with natural origin such as proteins (e.g. gelatin, casein) and polysaccharides (e.g. cellulose derivatives, chitosan), which have a large significance in the food industry. Polymers with both polar and nonpolar character are termed amphiphilic and these have a strong tendency to associate in an aqueous environment.

In solution, polymers may associate to form complex three-dimensional networks and these can also be due to entanglements. The 3D structure may be capable of entrapping large volumes of the solvent. The resulting material is often a jelly-like soft structure also called hydrogel [107]. The hydrogels can be formed by interactions such as entanglements, electrostatics, and crystallite formation, termed as physical hydrogels or via linking polymer chains with a chemical reaction, giving covalent or chemical gels. The cross-linking is expected to improve the mechanical properties of the hydrogels [108]. Figure 3 demonstrates the formation of two

different kinds of hydrogels.
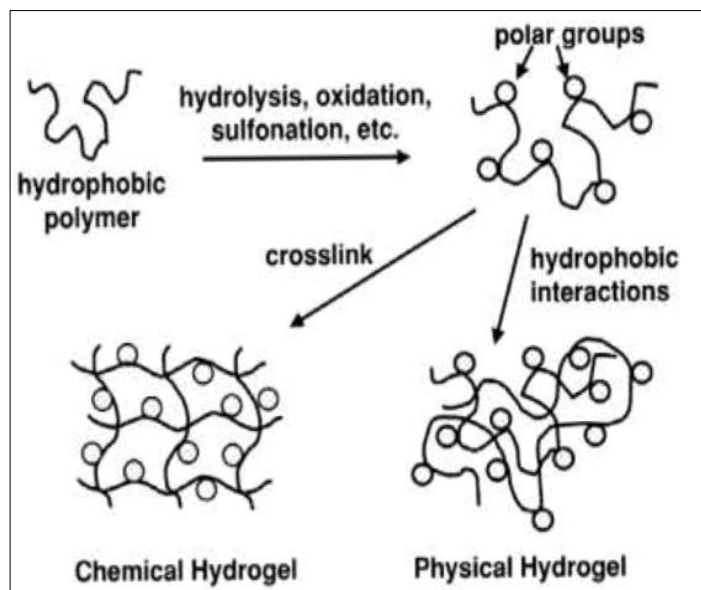
Figure 3. A simple illustration showing formation of chemically cross-linked and physical hydrogels [109].

When two polymers are mixed in the same solvent it is important to consider the phase behavior of the ternary mixtures. This consideration is crucial in order to understand the application of the end product which can be as diverse as biopolymer gels, coacervates, emulsions, etc [110]. For the development of improved formulations for the food and pharmacy industries, it is highly relevant to understand the effect of all different parameters controlling their phase behavior. Often this is not an easy task as these formulations may be rather complex with many ingredients [111].

The Flory-Huggins theory is the most common approach to rationalize the polymer phase behavior [112]. Often, mixtures may display a segregative or an associative phase separation as the illustration in Figure 4 shows.
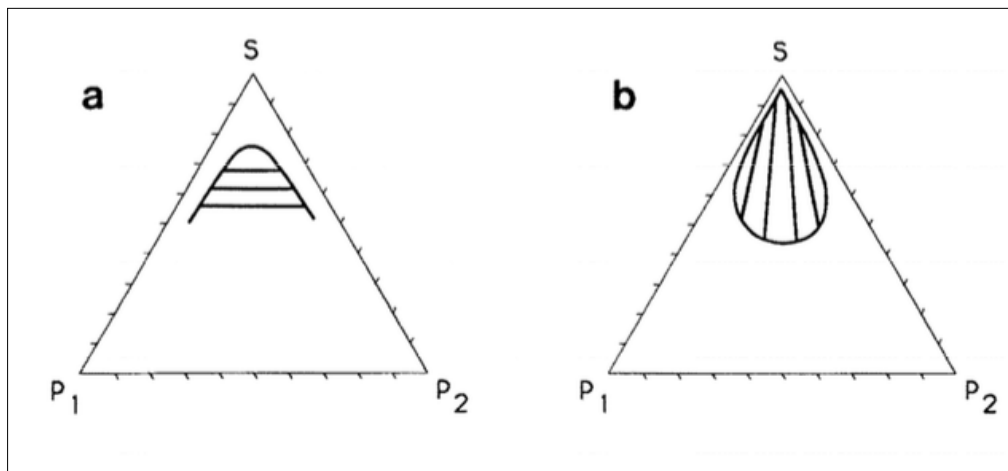
Figure 4. Ternary phase diagrams of two polymers in a solvent showing a) segregative and b) an associative phase behavior [113].

A segregative phase separation is achieved when there is an effective repulsion between two polymers, whereas an associative phase separation depends upon sufficient attraction. Obviously, the polymer-solvent (water) interactions cannot be neglected. Flory-Huggins calculations denote that even though two polymeric components mix ideally, segregative phase separation may occur due to differences in polymer-solvent interactions [114,115].

In the segregative phase separation, each phase is enriched in one of the polymers while in the associative phase separation one phase is rich in both the polymers and the other is rich in solvent (depleted in both polymers) [116]. Studies on polymer association have mostly dealt with aqueous mixtures of oppositely charged polyelectrolytes having an effective attraction. This phenomenon is termed complex coacervation; here two or more species interact on a molecular level forming complexes and aggregates [117]. Several studies have also been reported to study the transitions between associative and segregative behavior in mixtures as a result of adding salt or neutralizing with acid/base, etc. The encapsulation technology makes use of the polymer mixing behavior in solution to develop and improve formulations [118].

4   Probiotic entrapment and delivery
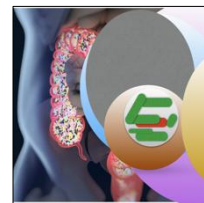
Several physiological changes can delay or prevent the delivery of viable probiotic bacteria into the gut [58]. Therefore, the development of an efficient delivery system capable to entrap, protect, transport and deliver appropriately probiotics is a key issue [119]. Delivery systems for food and biomedical applications require knowledge from interdisciplinary fields. Different strategies have been explored to protect probiotics from the harsh conditions of the gastrointestinal tract (i.e. low pH, bile salts and enzymes) for example by microencapsulation [120]. Microencapsulation is a very popular way to entrap probiotic bacteria [121].

The microcapsules are often formed by different mechanisms such as interfacial emulsion polymerization, ionic coacervation, or sol-gel immobilization. As we will see later, biocompatible macromolecules, such as polysaccharides and proteins, are preferred as encapsulating agents [122]. Moreover, many different colloidal systems can be used for encapsulation in food formulations, including oil-in-water (O/W) emulsions, liposomes, coacervates, etc. [123].

Encapsulation may shield bacteria cells from dehydration and may help to maintain the cell membrane structure and fluidity, minimizing the negative impact of osmotic stresses to their biodegradability [124]. In this respect, hydrogels are being widely used as efficient vehicles to deliver therapeutic agents including probiotics [19,125]. These hydrophilic three-dimensional polymeric matrices are capable to entrap different components [126]. Many hydrogel-based systems have been developed to deliver probiotics into the GI tract either in conventional pharmaceutical systems or in non-conventional commercial traditional products [13].

4.1   *Insight into the preparation methods for probiotic carriers*

There are various methods to prepare encapsulation vectors which may be summarized as follows.

The *extrusion method* is the simplest approach and is being used since olden times in hydrocolloid systems. This method is preferred due to the reasonably inexpensive operation conditions and safety of the deliverable. Briefly, it requires a liquid-forming core and a solution or melt assembling to form a barrier. This process involves the formation of particles either by dripping i.e. extrusion of a liquid through a nozzle and its hardening or emulsification and later solidification of the liquid droplets. In figure 5 some extrusion based methods to form particles are depicted. Of particular interest for this work is ionic gelation [127].

In *spray drying*, a dispersion of a material of interest, for instance drug molecules or cells in a concentrated liquid is formed. The liquid going to the sprayer can be a solution, an emulsion or a suspension as shown in Figure 5d [128].

Another way to form capsules is the layer-by-layer assembly by a stepwise film formation through exposing colloids cores to polyelectrolytes of alternating charge as exemplified in Figure 5e [129].
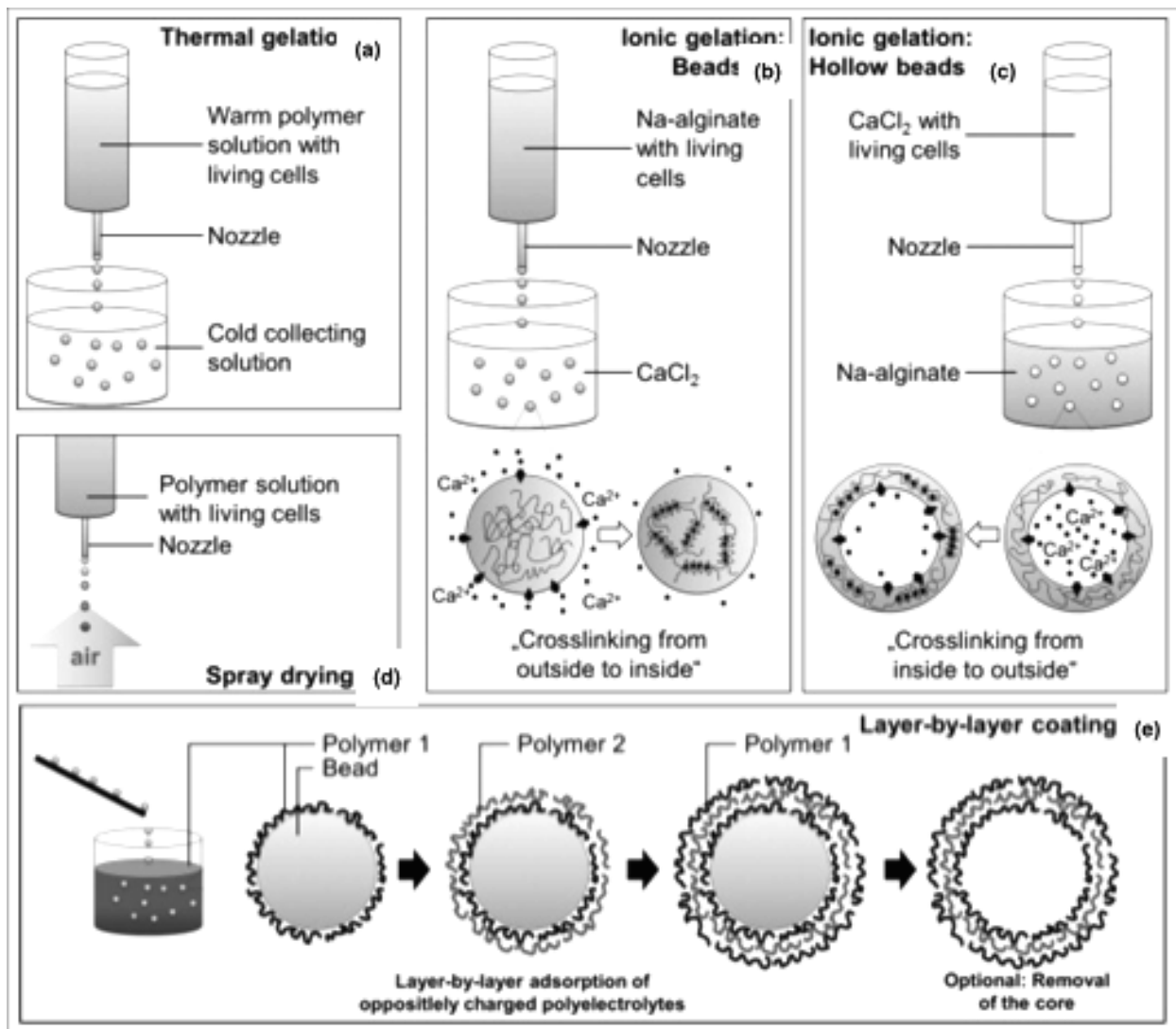
Figure 5. Encapsulation methods based on dripping: a) Thermal gelation (b), production of beads (c) and hollow beads (d) spray drying (e) layer by layer coating [127].

The chemical encapsulation, also known as *complex coacervation*, occurs when capsules are produced by water-soluble polymers containing different charges, which associate. It involves association of the two polymer solutions, one forming a core and the other wrapping around the material of interest. In this respect, gelatin is often used with several other natural or synthetic anionic water-soluble polymers to form complex coacervates for encapsulation [130]. The approximate size of the capsules produced is typically ca. 20-800 μm in diameter and 80-90 % of the weight is due to the core material. Very often the particles are cross-linked to provide

extra mechanical resistance [131].

The interfacial polymerization is associated with the encapsulation of a variety of core materials, including aqueous solutions, water-immiscible liquids and solids. Because the polymer formation is confined to the interface, reactants will more likely encounter the growing polymer chain instead of other monomers. Interfacial polymerization comprises the reaction among di-, tri- or multi-functionalized monomers.

From the reactivity and concentration of the monomers, the characteristics of the resulting polymer might be predicted. The properties of the resultant polymer are regulated by the stability of the solvent interface and how many reactive groups are present on each of the monomers [132].

An important difference between bulk polymerization and interfacial polymerization is that, in the latter, higher molecular weights can be achieved at mild reaction conditions. Precipitation of the polymer at the interface might happen in a well-defined molecular weight range, with similar polydispersity as in bulk polymerization [133].

Amines, alcohols, etc. are generally nucleophilic reactants found in one of the phases whereas the electrophilic reactants, such as acid chlorides, isocyanates, etc. stay in the other phase. For the encapsulation of microorganisms or cells, these are mixed with a hydrophilic monomer in an organic phase and a hydrophobic monomer will be added later to form a shell on the surface [134,135] as shown in Figure 6.
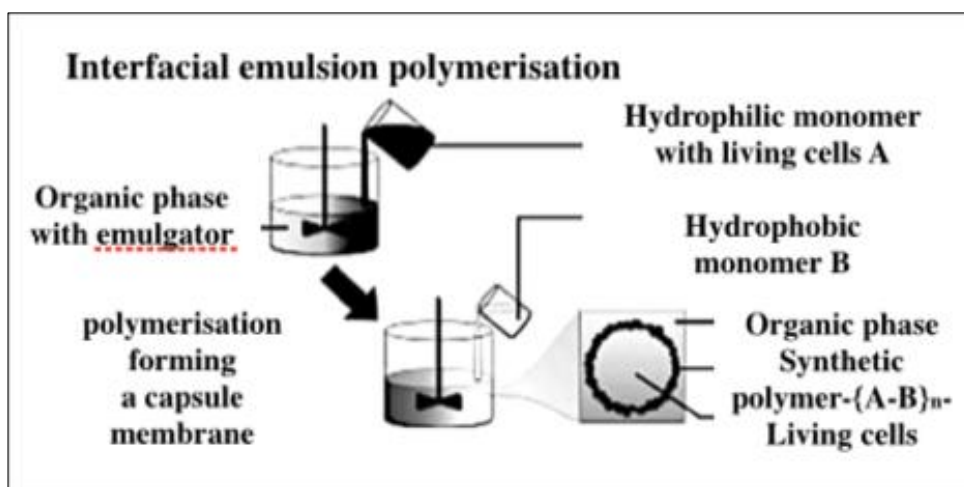
Figure 6. Schematic representation of Interfacial polymerization [127].

The *emulsification technique* consists in using a homogeneous mixture of a polymer suspension and oil as dispersion medium to form beads further collected by filtration. In this process, the bead size obtained has been reported to be within ca. 25 μm to 2 mm. Moreover, cross-linking might be performed to make the beads more robust. In the presented work, edible water-in-water emulsions have been developed to encapsulate model probiotics [136].

The *spray-cooling* method is like freeze-drying, in which a bioactive compound is atomized through a pneumatic nozzle into a vessel to produce very refined droplets with a molten matrix of low melting point [135]. Solidification of the liquid droplet leads to the encapsulation of the bioactive molecule. However, this is an expensive process and thus not easily scalable [138].

4.2 *Effect of encapsulation on the stability of probiotics during storage*

The success of probiotic preparations depends on a combination of many factors such as the type of probiotic, particle size, composition of the matrix and the storage condition [139]. The shelf life determination or storage studies are imperative along with a viability study under GI conditions (bioavailability) for an oral formulation [140].

The targeted products can be refrigerated or non-refrigerated foodstuffs. Therefore, temperature is a critical factor for the viability of probiotic bacteria in any food matrix [141]. For example, in a study at low temperatures (≤4 ℃), the survival of *lactobacillus acidophilus* (LA) and some bifidobacteria was maintained for several weeks [142]. Mosilhey in 2003 found that micro encapsulated LA can resist up to 15 weeks at 5 ℃, which is ideal for refrigerated dairy products [143]. In another study, the efficacy of freeze-dried cultures was found to be higher for low temperature storage (at 4°C) and under an oxygen-free atmosphere [144].

Refrigeration may help to provide longer shelf lives to certain products but, at the same time, it may affect the probiotic viability [145]. When antioxidants are added to the carrier, the oxygen and moisture interference was minimized and the storage stability of probiotic bacteria increases [146]. Therefore, it was suggested that the storage of probiotics at reasonably high temperatures, moisture content and oxygen-rich atmosphere, are generally unfavorable conditions that decrease the viability of probiotics over time [147].

4.3 Encapsulation systems developed in the thesis

Polymer association may lead to the formation of different systems eligible for delivery purposes. Particles and films are among the possible structures with potential use in probiotic entrapment and when formed by non-toxic and biocompatible compounds, these systems may find applications in the pharmaceutical and food areas.

Hydrogels and the microgels obtained from aqueous mixtures of polyelectrolytes have structural features somehow analogous to epidermis of human skin; the density of the network can be tuned by the polymer concentration to display different degrees of porosity. This gives the ability to design the systems according to the application. In this subsection some of the main strategies followed to entrap probiotics will be discussed.

4.3.1 Extrusion

The polymers selected to develop the first system described in paper I, which are CMC and Cht, are capable to form coacervates due to the gelation properties of these two oppositely charged macromolecules with or without a cross-linking agent (genipin) [148,149]. Therefore, the encapsulation of biomolecules, drugs or probiotics into hydrogel particles can be performed by a dripping method as schematized in Figure 7. Often, the minimum size of the particle obtained through this method is ca. 1 mm [150].

As discussed above, in this approach one polymer solution is dropped into another by a syringe and, because of the electrostatic interaction between oppositely charged polymers, these start to aggregate at the interface of the droplet. Depending on the diffusion of polymer and solvent molecules, one may get homogenous solid particles or core-shell particles [151]. The size of the particles can be controlled using different dropping systems such as syringes of different needle diameter or a nozzle spray (Figure 7b). Both methods shown in Figure 7 were applied for the production of CMC-Cht particles and encapsulation of LGG. Some of the different morphologies of the particles obtained are shown in Figure 8. The extrusion method was followed in papers I, III and V.
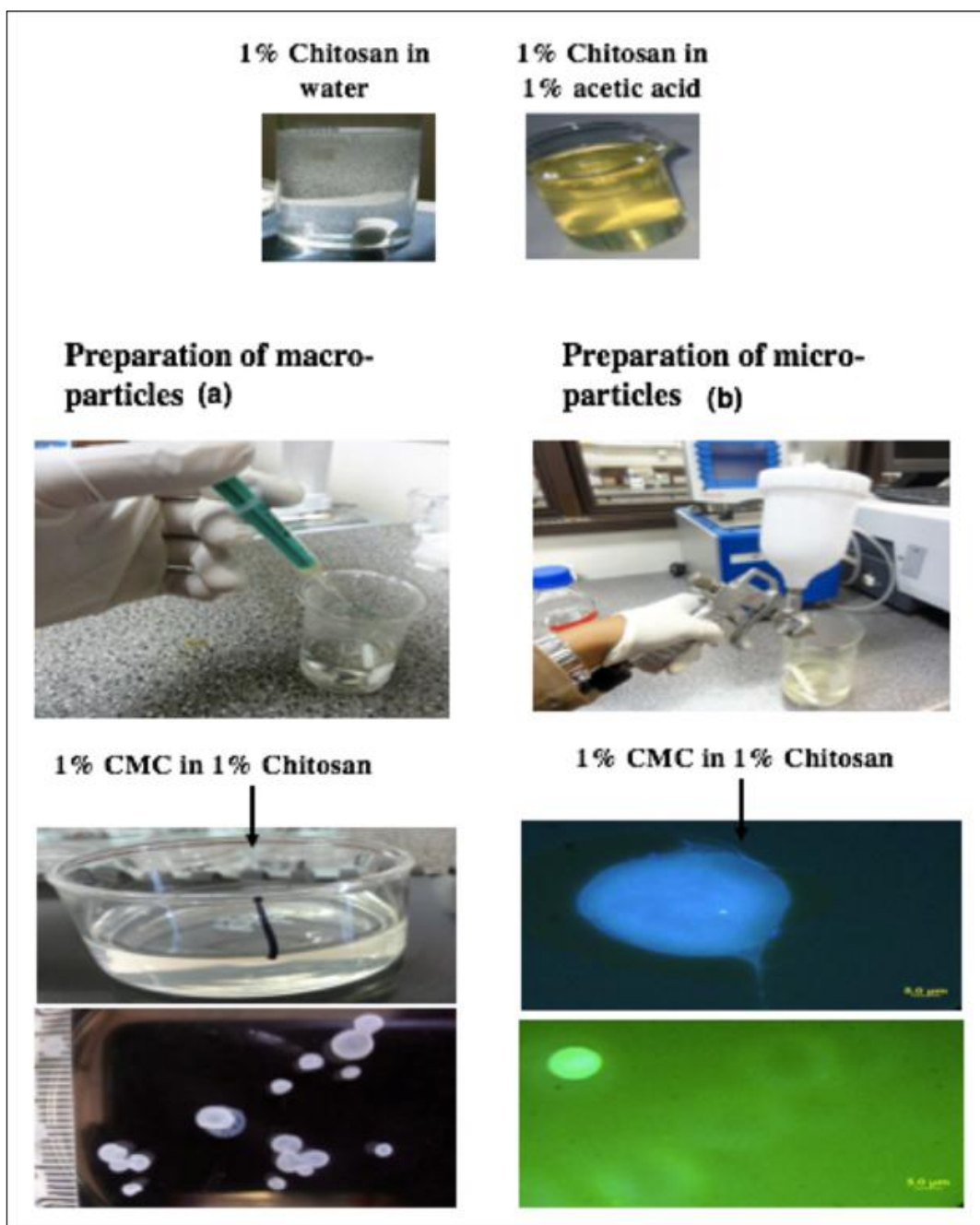
Figure 7. Schematic representation of the preparation of a) CMC-Cht macro (ca. 1-2 mm) and b) micro (ca. 5-10 μm) particles using 1wt% aqueous solutions of CMC and Cht.
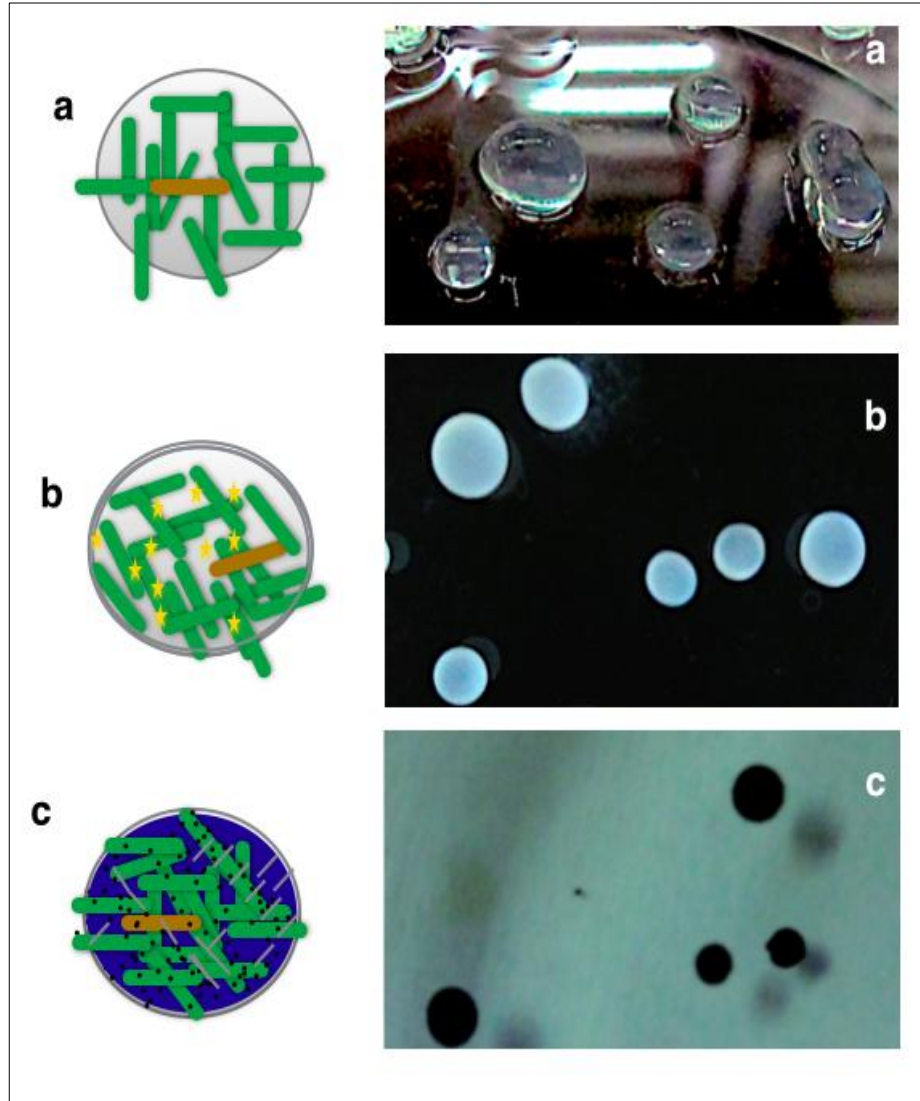
Figure 8. Pictures and illustrations of developed systems with bacteria (green/orange rods) encapsulated in a) physical CMC/Cht macroparticles b) CMC/Cht macroparticles containing β-cyclodextrin/sodium caseinate/soy lecithin c) CMC/Cht macroparticles with genipin

4.3.2 *Emulsion templating*

The W/W emulsion method, in contrast to the extrusion technique, can be easily scaled up and the diameter of the produced beads can be considerably smaller (ca. 25 μm–2 mm) [152]. Moreover, since these emulsions are only composed of water and biopolymers (no oil or surfactant is used) they are inexpensive and far friendlier for bacteria than standard emulsions [153].

The probiotic bacteria or other compounds of interest can be mixed with one of the polymer solutions and then dispersed into another solution of an incompatible polymer [154]. One of the polymers may be chosen to present a sol–gel transition at the physiological temperature [155]. Therefore, one polymer solution remains as a viscous liquid and the other jellifies. Additionally, the whole solution can be converted to a gel form by adding an appropriate cross-linker.

Emulsification is a very common approach for encapsulation in pharmaceutical industry but the use of W/W emulsions is poorly explored despite the tremendous potential. For example, stabilized W/W emulsions can be developed for fat-free food products. The W/W approach was followed in Paper II for the preparation of gelatin and CMC based W/W emulsions.

4.3.3   Encapsulation in film matrices

Entrapment of probiotics in thin edible films can be very interesting for smart packaging purposes [156]. Depending on the application of the films, the probiotics can be either mixed with the polymer before casting and curing or soaked afterwards to incorporate the bacteria mainly close to the air-film interface. The bacteria may diffuse and get adsorbed into the film during its swelling and solvent uptake.

The formation of edible films/coatings is a more efficient approach which ensures generally better probiotic delivery and viability than the direct application on the food surface [157]. In paper III, films were obtained by mixing different amounts of cellulose derivatives and citric acid at different casting conditions.

4.4   An ideal delivery system

During the probiotic encapsulation or entrapment, the carrier might exhibit different transport properties which are strongly dependent on its structure, chemical composition and the degree of cross-linking. As discussed before, an important aspect to consider is that apart from the mechanical and/or chemical boundary against incoming and outgoing molecules, the carrier should provide enough nutrients so the probiotics survive and, if possible, multiply and grow [158].

Moreover, any waste that directly influences the cell survival should easily diffuse out of

the carrier. Entrapped biomolecules and bacteria, if away from the boundary of the matrices, are expected to receive a diminished amount of nutrients [159]. As the mass transfer will only be sufficient for the cells close to the periphery of the system, higher cell densities can assist considerable mass transfer [160,161, 162,163]. This suggests that systems with greater surface area-to-volume ratio may be preferred in providing the right conditions to support viable cells. An "ideal" delivery system is illustrated in Figure 9 showcasing some of the most important properties.
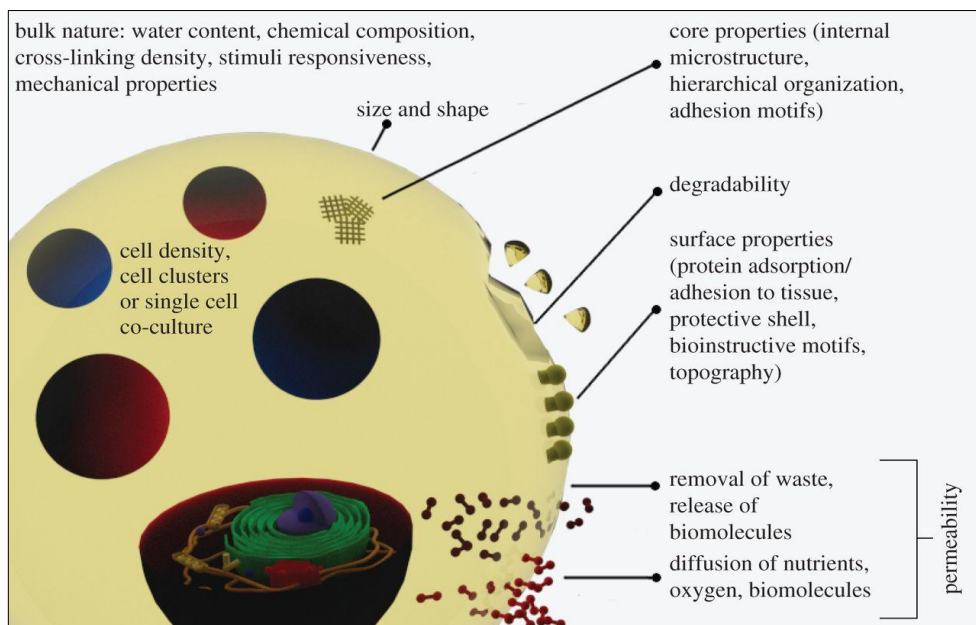
Figure 9. A scheme outlining the properties of the microcapsules for the encapsulation of cells [163].

5 Probiotics in the gastrointestinal passage
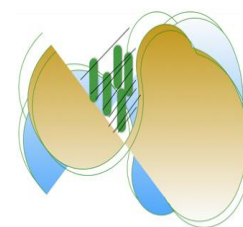
As mentioned earlier, the GI microbiota might change as per host physiology and diet. These factors exist in a continuous correlation, regulating the initial acquisition, regenerative alteration and conditional stability of the gut ecosystem. Gut microbiota has been shown to have paramount importance for human health and eventually can be enhanced with beneficial probiotic bacteria [164].

However, an important constraint is that the bacteria must reach the intestine in an acceptable viable number to produce any relevant impact. In this section some general but important details of the GI tract are introduced.

5.1 General features of the gastrointestinal tract

The essential endeavor to architect a system for encapsulation/entrapment of probiotic bacteria is to have an efficient release in the gut. Hence, it is necessary to consider the complex physiology of the GI tract.

After taking any food orally, it passes through the mouth, where we have saliva, to the esophagus in 2 s; from the esophagus, it will take only 10–14 s to reach the stomach [165].

The stomach is highly acidic, with pHs ranging from 1.2 to 2.4. Gastric glands, which together secrete 400–800 ml of gastric juice at each meal, are necessary to activate the enzymes. Pepsin cleaves peptide bonds. Secretion by the gastric glands is stimulated by the hormone gastrin [166]. Hence, it is expected that the highest viability loss of bacteria happens under gastric conditions. However, the transit time (generally considered to be 1-2 h) through the stomach and the pH vary with many factors, like age, medical condition, eating habits etc. [157]

The food entrapping bacteria should enter the small intestine after the passing through the gastric system [167,168]. The enzymes present in the villi are aminopeptidases that attack the amino terminal (N-terminal) of peptides producing amino acids, disaccharidases that convert disaccharides into their monosaccharide subunits, maltase which hydrolyzes maltose into

glucose, sucrose that hydrolyzes sucrose into glucose and fructose and lactase converting lactose into glucose and galactose [169].

The pH of the small intestine varies throughout its length; the proximal region is more acidic than the distal one. The pH range is ca. 6.15 to 7.8 and the transit time can range from 1.6 h to 9.5 h. Some recent studies suggest that the site of action of probiotics is not only restricted to the large intestine. In fact, their delivery into the small intestine has been reported to provide health benefits [170]. The schematic illustration of different segments and conditions of GI is depicted in Figure 10.

Absorption Barriers
- Double mucus layer
- Brush border membrane enzymes

Stomach
- Acidic pH
- Pepsin

Small Intestine
- Alkaline pH
- Pancreatic and intestinal digestive enzymes

Colon
- Microbiota (10^{12}-10^{14} CFU/g)
- Bacterial proteases
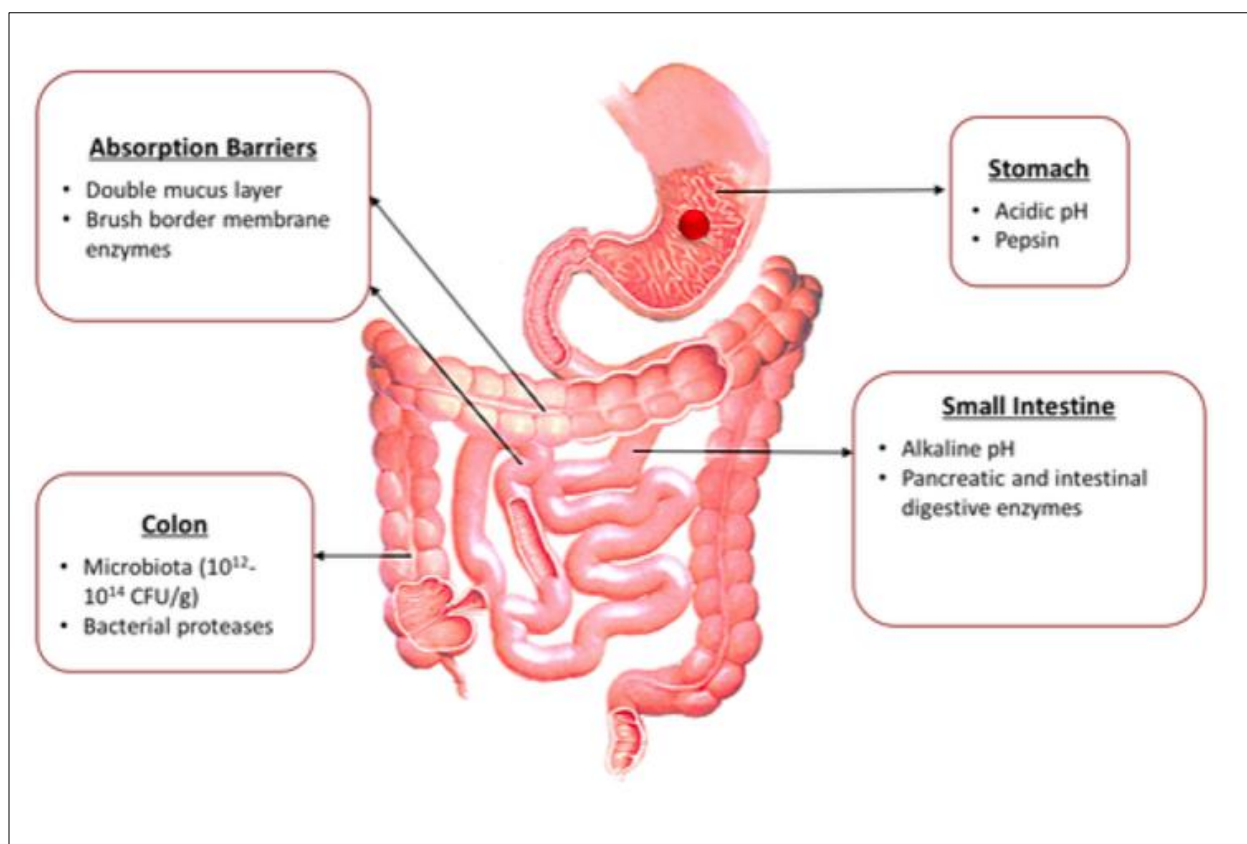
Figure 10. Representation of the gastrointestinal passage and the factors to take into consideration while designing an oral delivery vehicle.

If the particles loaded with bacteria can resist the physiological conditions found in the small intestine, they may reach the large intestine. Like the small intestine, the large intestine also has a different pH in the ascending and descending colon, ranging from 5.26 to 7.02 [171].

The slurry of digested food that passes from the small intestine into the large intestine called chyme. It is expected that the matrix where bacteria are encapsulated, while traveling through the GI tract, loses water as the contents are compacted into faeces and this may also affect the viability of the bacteria. In contrast to the other parts of the GI, in the large intestine a large number of indigenous bacterial species can be found and this microflora may assist the targeted probiotic delivery by degrading some of the polysaccharides [172]. This dissolution mechanism has been utilized as a concept in triggering the release for small drugs, but to the best of our knowledge, has not been systematically explored for the delivery of probiotics.

The GIT conditions in this study are mimicked ((simulated salivary fluid (SSF), simulated gastric fluid (SGF) and simulated gastric fluid (SIF)) using a general standardized and practical static digestion method [167,173].

5.2 Intestinal mucosa and cytotoxicity

The intestinal mucosa is an important organ of defense providing a barrier against the antigens encountered by the enteric route, and most foreign antigens are excluded by the intestine's mucosal barrier. Therefore, it is important to assess the effect of any developed particles on the intestinal epithelial [174]. The Caco-2 cells express several morphological and functional properties characteristic of small bowel enterocytes. To mimic the steric conditions in the intestine in vivo, Caco-2 cells are cultured on permeable filter inserts.

These cells serve as a model for epithelial cells, providing many advantages due to their simplicity and reproducibility [175]. Hence, this allows the comparison of laboratory results to the actual application in humans as Caco-2 cells express many enzymes and transporter proteins present in normal human intestinal epithelium. Cytotoxicity studies were performed in Paper V.

6 Materials used to develop encapsulation systems
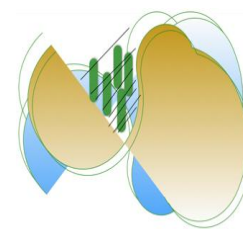
6.1 *Cellulose and cellulose derivatives*

Cellulose constitutes the primary structure of a plant cell [176]. It has certainly an impactful role among the raw materials to be used in a sustainable future [177]. Cellulose is a particularly stable polysaccharide due to its crystalline nature; cellulose cannot be hydrolysed by weak acids and bases [178]. The size of the cellulose molecules is derived from the average degree of polymerization [179]. The average molecular weight is estimated by multiplying the degree of polymerization with the molecular mass of a single anhydroglucopyranose unit (AGU) [180]. Each AGU has three hydroxyl groups (one primary and two secondary moieties that represent more than 30% by weight), except for the terminal units.

Most of the solvent systems used so far for cellulose have a limited capacity of dissolution. Moreover, most of them are toxic and expensive hence making them not suitable for food applications [181]. Hence, cellulose derivatives are an attractive alternative. Cellulose ethers are high molecular weight compounds produced by replacing the hydrogen atoms of hydroxyl groups in the anhydroglucose units of cellulose with alkyl or substituted alkyl groups as represented in Figure 11A [182]. The commercially important properties of cellulose ethers are determined by their molecular weights, chemical structure and distribution of the substituent groups, degree of substitution and molar substitution. These properties generally affect solubility, viscosity in solution, surface activity, and stability against biodegradation, heat, hydrolysis and oxidation [183,184].

Among the cellulose derivatives, CMC is highly relevant for the food domain but also finds applications in flocculation, detergents, textiles, paper, drugs, and oil well drilling operations [185]. CMC can be used in food applications as it is FDA approved and can be produced at low cost. Moreover, it is a biocompatible water-soluble derivative of cellulose commercially available in high purity forms [186]. All these features make CMC highly attractive for other advanced applications such as in the biomedical area [187]. CMC is produced

from cellulose with carboxymethyl groups (-CH$_2$-COOH) bound to some of the hydroxyl groups by the alkali-catalyzed reaction of cellulose with chloroacetic acid, [188], the structure is shown in Figure 11 B.

Another interesting cellulose derivative is HEC which is often used as a gelling and thickening agent. It is widely used in cosmetics, cleaning solutions, and other household products. Hydroxyethyl cellulose and methyl cellulose are frequently used with hydrophobic drugs in capsule formulations to improve the bioavailability of the drugs in the gastrointestinal fluids [189]. It is a nonionic, water-soluble polymer, made by reacting ethylene oxide with alkali-cellulose under rigidly controlled conditions, and the structure can be seen in Figure 11C [190].
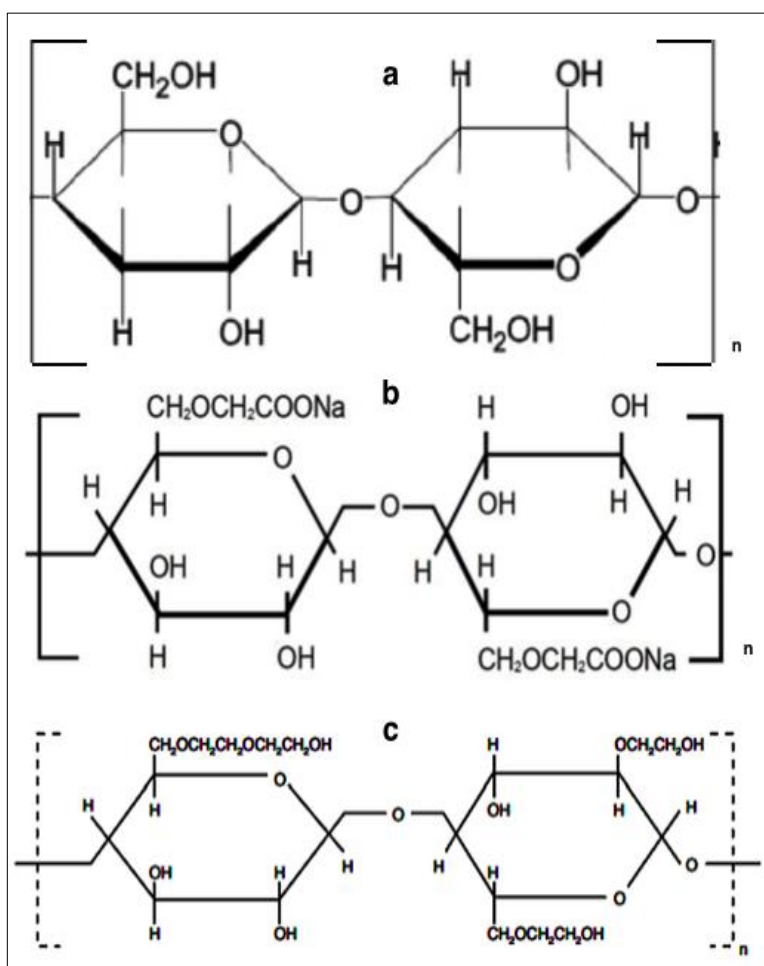
Figure 11. Schematic illustration of structure of a) cellulose b) CMC and c) HEC.

Cellulose based hydrogels can be used as matrices to incorporate nanoparticles as they are hydrophilic, biodegradable, biocompatible, transparent, low cost, and non-toxic. Hence, they can serve as multifunctional carriers in different industries as reported by [148].

Some of the cellulose derivatives have been used for encapsulation of drugs and probiotics but there is no systematic study using CMC to encapsulate bacteria.

6.2   *Chitosan*

Chitin or poly (β-(1→4)-*N*-acetyl-d-glucosamine) is a natural polysaccharide synthesized by an enormous number of living organisms [191]. It occurs as ordered crystalline microfibrils, which form structural components in the exoskeleton of arthropods [192]. It is the second most abundant natural polymer after cellulose and occurs also in the cell walls of fungi and yeast [193]. The two most utilized commercial sources of chitin are crab and shrimp shells and its extraction during industrial processing is done through acid treatment by dissolving the calcium carbonate followed by alkaline treatment to dissolve proteins [194]. A decolorization step is followed to remove pigments and obtain a colorless pure chitin [195].

Chitin is transformed to chitosan by partial deacetylation under alkaline conditions. Chitosan is a non-toxic, biocompatible, linear polysaccharide, a copolymer comprising randomly distributed b (1→4) linked d-glucosamine and N-acetyl-d-glucosamine [196]. The composition is dictated by the degree of acetylation that is the fraction of acetyl-glucosamine units present. It can be classified as a charged cationic polyelectrolyte having a pK_a value of approximately 6.5 [197] and thus chitosan is soluble under acidic conditions [198].

6.3   *Cross-linkers*

Genipin (Gen) is extracted from a fruit called Gardenia jasminoides Ellis [205]. Chemically it is termed as cyclopenta pyran-4-carboxylic acid or 1,4 a-alpha,5,7 a-alpha-tetrahydro-1-hydroxy-7-(hydroxymethyl)-, methyl ester [199]. The commonly used cross-linkers have the capacity to harm live cells but, due to its low toxicity, genipin is an attractive choice for cross-linking [200]. If we consider human cells like 3T3 fibroblasts, genipin showed 10000 times less cytotoxicity than glutaraldehyde. Genipin can act as an anti-inflammatory agent or even insulate neuronal cells from stress-induced cytotoxicity [201,202].

Genipin can cross-link chitosan forming bluish gels. According to Butler, the cross-links are formed by two reactions. Firstly, the ester group on the genipin molecule is replaced by a secondary amide linkage, as can be observed in Figure 12a. Then, in the second step, the methylamine reaction takes place via a nucleophilic attack of C_3 carbon on the primary amine activating the opening of the dihydropyran ring (Figure 12b) [203].
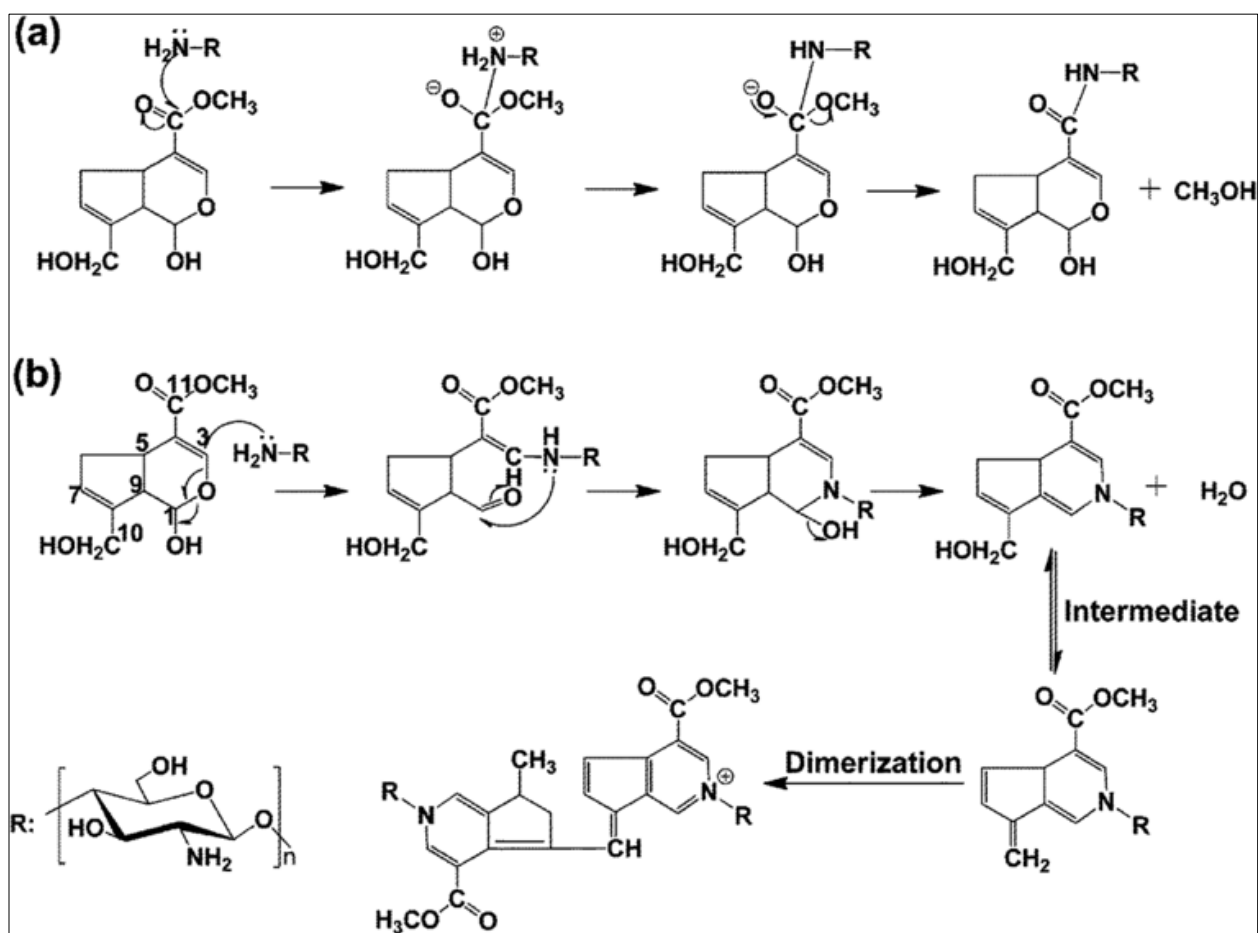
Figure 12. Diagram showing mechanism of cross-linking chitosan (a polymer containing a primary amine group) with genipin [204].

The radical reaction generates the dimerization during the cross-linking; hence genipin forms bonds with the molecules containing heterocyclic structures with a primary amine group [205]. This cross-linking mechanism has been suggested to occur in chitosan but can also be assumed for other systems involving molecules that contain primary amine groups such as some of the proteins [206].

On the other hand, CA has been suggested to cross-link cellulose derivatives under certain conditions [207]. It has a high potential in the biomaterial field, due to its excellent biocompatibility, hydrophilicity, non-toxicity and biological functions [208]. CA is widely used in food and drug industry because of its inexpensiveness [209]. Different mechanisms have been proposed in the literature to explain the cross-linking reaction of cellulose derivatives with CA [210]; essentially they involve the formation of an ester between the carboxylic acid function of CA and the hydroxyls of cellulose derivatives [211].

6.4   Cyclodextrins, phospholipids, casein and gelatin

Cyclodextrins (CDs) are cyclic oligosaccharides, which are non-branched oligomeric cycloamyloses composed of a-(1→4) d-glucopyranoside units [212,213]. They comprise three main structures; alpha (α), beta (β) and gamma (γ)-cyclodextrin [214,215] as shown in Figure 13 and the helical segments of the polysaccharide contain six to eight glucose monomer units, respectively, with a cavity depth of 0.7–0.8 nm [216].

The natural β-CD used in many pharmaceutical formulations throughout the world [217] is generally recognized as safe (GRAS) by the FDA and is listed in the European Pharmacopoeia (Ph.Eur.), US, Pharmacopoeia (USP/NF) and Japanese Pharmaceutical Codex (JPC) [218,219,220]
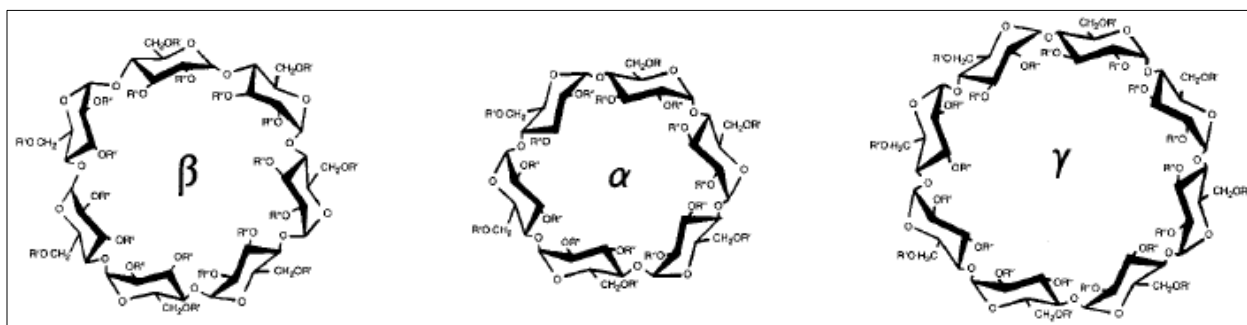
Figure 13. Structures of beta (β) alpha (α), and gamma (γ)-cyclodextrin showing the difference in the size of the cavity due to the different number of glucose units.

As a dietary supplement, the ascertained daily oral dose for β-CD is suggested to be 500 mg/day [221]. As we will see later, CDs were evaluated as possible prebiotics since they do not

get adsorbed in the upper gastrointestinal tract. The work based on the prebiotic effect of CD is compiled in paper III.

Phospholipids (PL) composed of hydrophobic tails and hydrophilic heads are amphiphilic molecules which can self-assemble into spherical and closed structures composed of lipid bilayers and called liposomes [222]. As they contain both water-loving and repelling parts they are interesting carrier materials for the delivery of compounds [223]. PLs can efficiently increase the bioavailability of drugs and have a strong affinity for cell membranes. Among the list of PLs, lechitin should be highlighted since apart from the beneficial encapsulating and emulsifier properties, lecithin is also established as an antioxidant [224]. Lecithin can also modify the surface activity of proteins and other polyelectrolytes with a net charge, by reducing the hydrophobic attraction and increasing the steric repulsion [225,226].

For instance, the interaction between lecithin and whey protein concentrate (WPC) in oil-in-water emulsions was studied by Dickinson & Yamamoto and the results suggested that there was an increase in gel strength due to the formation of a complex between added lecithin and whey protein in the bulk aqueous phase and at the surface of emulsion droplets [227].

In the presented work, the effect of lecithin on the stability of cellulose-based particles was evaluated and described in paper V.

Surface-active ingredients derived from milk can be naturally extracted; they possess colloid stabilizing properties [228]. Milk is mainly composed of two different protein classes, caseins and soluble proteins. Caseins and whey proteins make up, respectively, around 80 and 20 wt % of the proteins in milk [229]. The differences between these two proteins lie in the amino acid composition and the physicochemical character [230].

Casein is essential to human nutrition because of its emulsifying properties and amino-acid composition. Casein micelles are typically made up of α -, β- and κ-casein proteins and their gelation has been exploited for probiotic encapsulation in order to have both viable and plentiful cells in the GI tract [15]. For instance, the microencapsulation of *Lactobacillus rhamnosus* GG (LGG) in gelled whey protein isolates during *in vitro* stomach incubation [231] and during *ex-vivo* digestion [232] could maintain viable cells when exposed to harsh conditions [233].

Other examples show that milk proteins can have a beneficial effect on the viability of the entrapped probiotics. For example, *Lactobacillus paracasei* and *Bifidobacterium lactis* were encapsulated by emulsification in milk protein microparticles, [234] which led to an enhanced

33

encapsulation performance and ability to withstand simulated gastric conditions. Spray dried whey proteins were also explored to protect *Bifidobacterium* Bb-12 during a model *in vitro* digestion and the data suggests a clear positive impact [235]. Hence, milk proteins (i.e. casein) were also considered during this work to improve the stability of the LGG cells in the cellulose-based matrices as shown in Figure 14.

Figure 14. CMC-Cht particles a) without any additive, with b) SL and c) SC.

Gelatin is an amphoteric thermally reversible gelling agent hence highly appropriate for encapsulation [236]. It is extensively used in food and medicince, because it is non-toxic, biodegradable, bioactive and inexpensive. It contains both cationic and anionic groups. Gelatin nanoparticles can be prepared by coacervation or by an emulsion method [237].

Gelatin is an excellent candidate for incorporation with anionic gel forming polysaccharides, such as gellan gum and CMC. These polymers are water-soluble at pH >6, as both have a net negative charge. However, a strong interaction is observed at a pH below the isoelectric point of gelatin as its net charge becomes positive and gellan gum or CMC are negatively charged [238]. The work involving gelatin in W/W emulsions is referred to in paper II.

7   Characterization methods
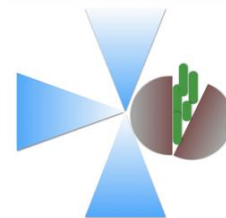
When a novel delivery vehicle is developed it is important to characterize it in order to understand the effect of the different parameters on its structural, entrapment and release properties. In this work several techniques were used to characterize the different cellulose based systems and are next briefly introduced.

Thermogravimetric analysis (TGA) is a thermal analysis technique capable to characterize different materials with complementary information provided by differential scanning calorimetry (DSC) [239]. TGA can provide details on the mass loss and on the transitions related to thermal and/or oxidative stabilities and the compositional properties of materials as a function of temperature or time in a controlled atmosphere [240]. The work flow illustration is shown in Figure15.
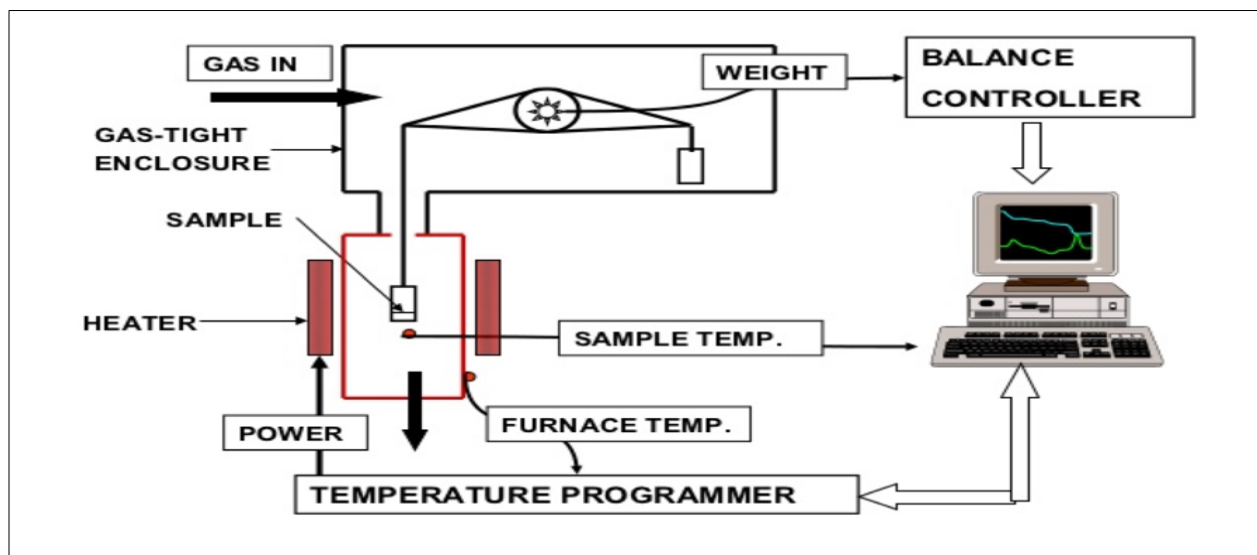
Figure 15. A schematic representation of the basic work-flow in a TGA instrument.

TGA is very useful to understand the thermal stability and moisture content of polymers

and their mixtures such as composites, particles, films/hydrogels etc. for an efficient application of these materials in a final product [241].

Fourier Transform Infrared spectroscopy (FTIR) provides quantitative and qualitative characterization for organic and inorganic samples by identifying the chemical bonds in the molecules. FTIR helps to analyze the chemical compounds in products like paints, polymers, coatings, pharmaceuticals, foods etc. [242]. The FTIR spectrum is generally a distinctive molecular fingerprint that can be used to screen and scan samples for many different libraries of components [243]. The operating principle is described in Figure 16. It is an effective instrument for the detection of functional groups and covalent bonding information corresponding, for instance, to the effect of using a cross-linker [244].
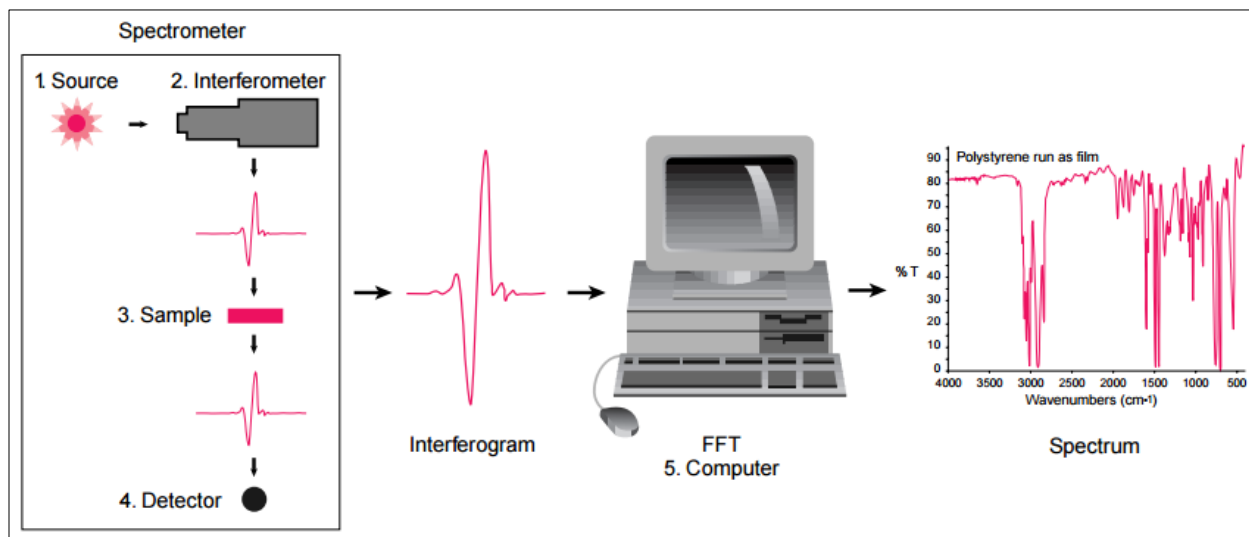
Figure 16. An illustration of the operating principle of a FTIR spectrometer.

FTIR may give complementary data or can be coupled with other molecular spectroscopic techniques such as TGA, Gas Chromatography-Mass Spectrometry (GC/MS), UV/Vis spectroscopy etc. [245].

Scanning Electron Microscope (SEM) is a technique utilizing focused beams of electrons to create an image of the surface of an object. Topographical, compositional and morphological specifications can be inferred by the high-resolution, three-dimensional images produced by SEM [246]. In the presented work, SEM was used to investigate the morphology of the developed carrier systems and to evaluate the positions of the entrapped bacteria. The working

principle of SEM is shown in Figure 17a. An image of freeze-dried CMC-Cht particle with SL can be seen in Figure 17 b; its morphological characterization is in Figure 17 c and the entrapped bacteria within the particle surface can be observed in Figure 17 d.
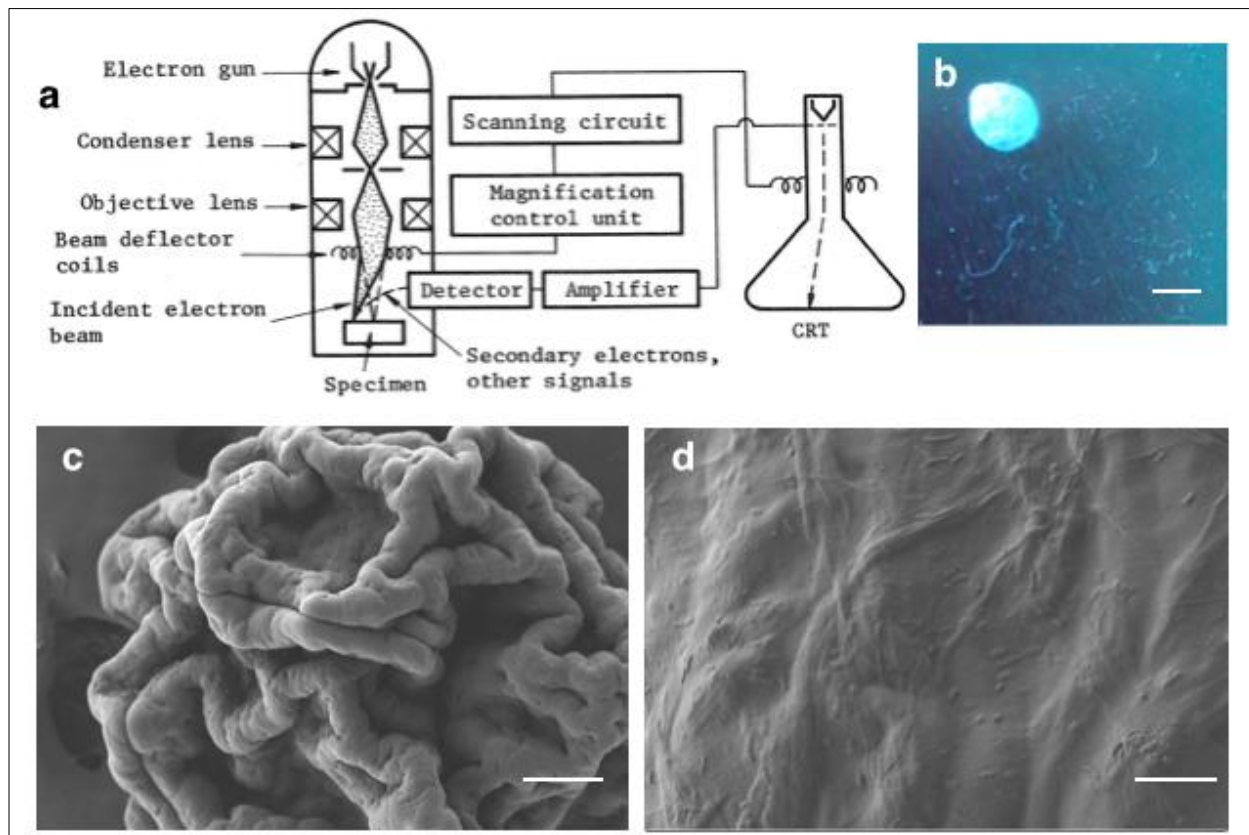
Figure 17. a) The depiction of the working principles of SEM, b) picture of a freeze-dried macro particle of CMC-Cht with SL; scale bar represents 2 mm, c) image showing the surface structure; scale bar represents 100 μm, d) encapsulated bacteria could be observed on the smooth surface; scale bar represents 20 μm.

The *swelling degree* can be measured to infer the influence of the degree of chemical or physical cross-linking on the swelling properties of a given matrix. This is particularly relevant for the hydrophilic films and particles developed in this work and the information extracted can be used to rationalize the solvent uptake of the carriers at different pHs as well as their release features [247].

The *plate counting method* (also known as spread plate) was used to monitor the growing colony of bacteria in a nutrient medium. The colony becomes visible to the naked eye and the number of colonies on a plate can be counted with a microplate reader [248]. Depending on the

source, there might be thousands, millions or even billions of microorganisms per milliliter of sample. Plate counting is one of the most fundamental microbiological techniques used to determine the number of viable (i.e. living) cells in a sample [249]. The colony-forming unit (CFU or cfu) gives a measure of the viable bacterial or fungal cells. Figure 18 shows how the colonies of LGG bacteria look like on De Man, Rogosa and Sharpe (MRS) agar plates. MRS is a selective culture medium designed to favor the fruitful growth of *Lactobacillus* spp.
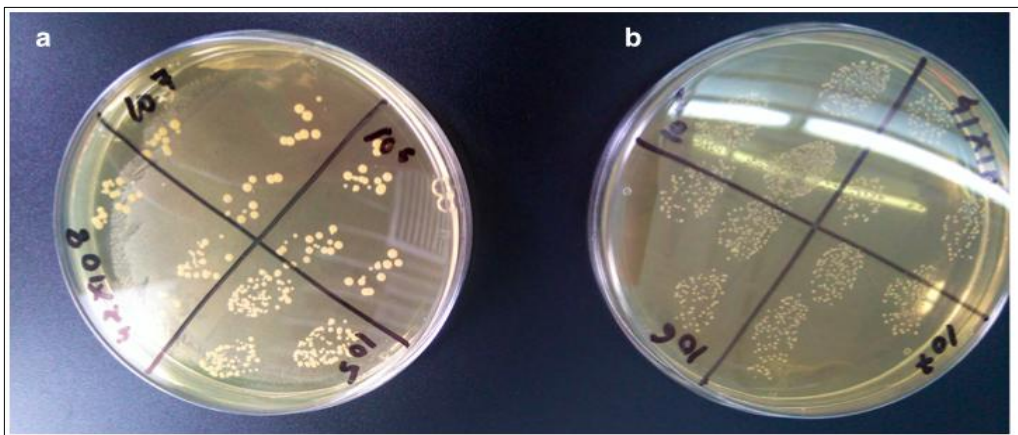
Figure 18. Images of MRS agar plates used to enumerate viability of (a) naked b) encapsulated LGG bacteria stored at room temperature.

Flow cytometry (FC) is used to study the properties of one cell at a time. FC is automated to measure the size and granularity of single cells. It is a reasonably fast method, which can count 10000 cells in less than one minute. Three to six relevant properties or components can be determined in a single sample, cell by cell. However, the sample preparation is often time consuming [250]. Figure 19a demonstrates the working principle of a flow cytometer whereas in Figures 19b and c an example of a dot plot and histogram can be observed. The dot plot shows the total population of the bacterial cells collected from the sample while a histogram represents the count of live cells in the same sample.
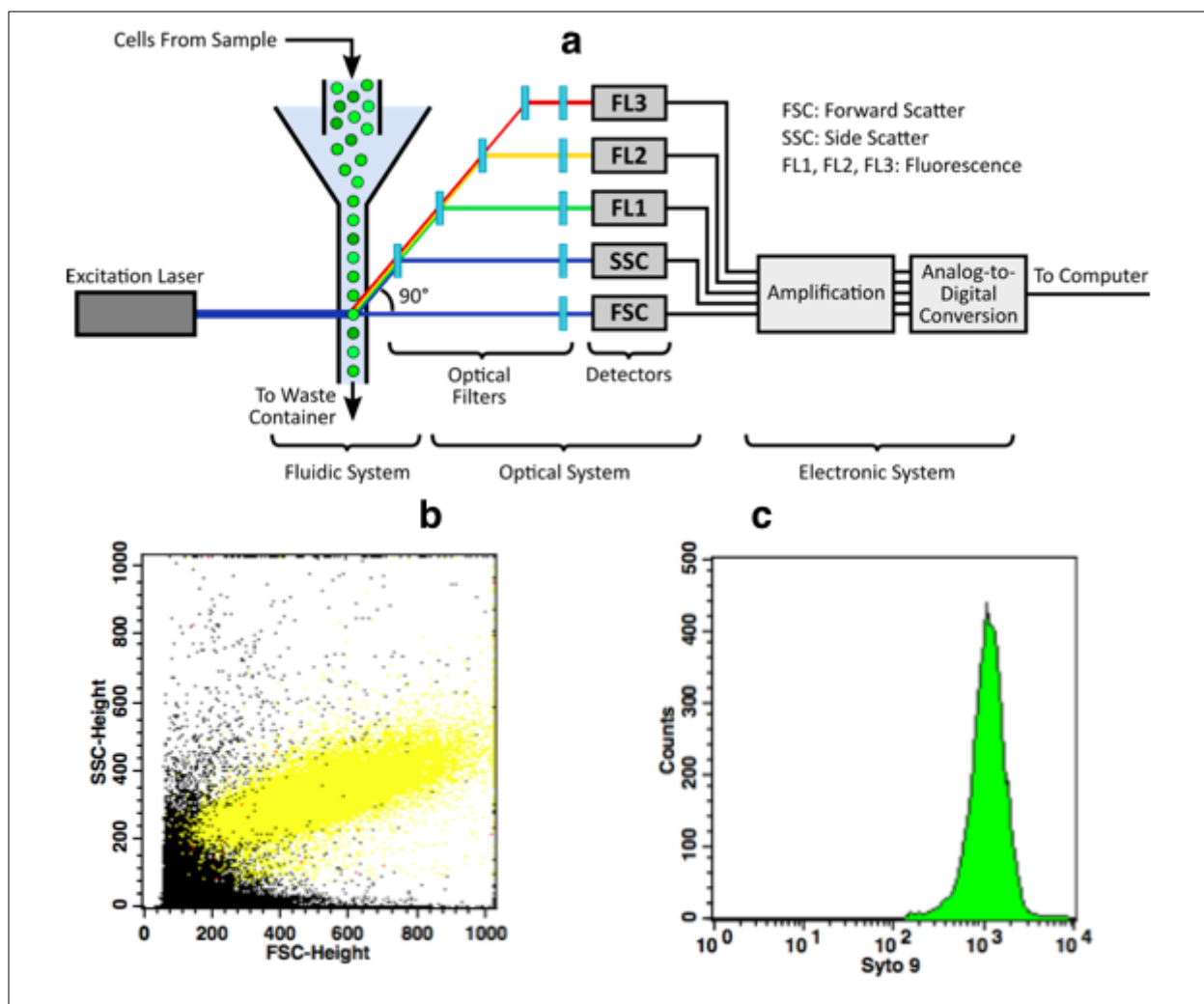
Figure 19. a) Schematic depiction of the flow cytometry fundamentals b) dot plot c) histogram of a CMC-Cht particle cross-linked with genipin exposed to SSF conditions.

Typically, the sample that is run in a flow cytometer is a suspension of monodisperse (that should be single and unclumped) cells. As mentioned, only one cell at a time passes through a laser beam giving the fluorescence and scattering pattern [251]. In the presented work, plate counting and flow cytometry were used as complementary techniques to have an appropriate understanding of the encapsulation and release of probiotics.

As some bacteria might be alive but not grow on the selected solid medium and can only be enumerated using flow cytometery, two distinct terms are used in this work to characterize the survivability of bacteria. The count with flow cytometry is termed "viability" whereas with plate count it is termed "culturability".

Fluorescence microscopy allows the detection of bacteria directly from the sample without any previous isolation step. The viability of microbial cells is not related to their capability to form colonies on an agar-based medium but is directly related to the cell's physiological activity [252]. Therefore, using appropriate dyes, fluorescence microscopy can be a very convenient technique to distinguish between viable and non-viable bacteria. This method has been extensively used in this work to evaluate the viability of bacteria in the different cellulose based matrices and also when exposed /released to the different simulated GI media.

The two main dyes used in the work were DAPI (4',6-diamidino-2-phenylindole) and the Live/Dead kit containing Syto 9 and Propidium Iodide (PI). Initially DAPI was used but as it stains both live and dead cells it is not trivial to evaluate the viability. On the other hand, the Live/Dead kit gives a clear distinction between live and dead cells. While the Syto9 stains both live and dead cells, the propidium iodite (PI) stains only dead cells. A typical image of the LGG stained with Live/Dead kit is shown in Figure 20.
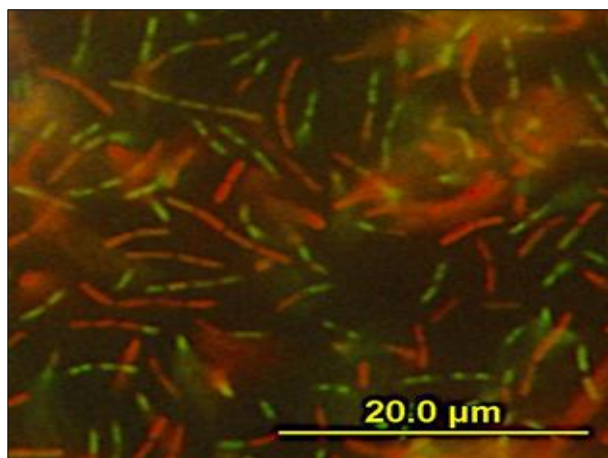
Figure 20. A fluorescence microscopy image of LGG bacteria stained with the Live/Dead Invitrogen kit (contains PI and Syto9). The dead bacteria appear as red rods while the living bacteria appear as green rods.

Optical microscopy is a very useful tool to study large objects, such as the W/W emulsions prepared in this work and also to follow the variation in size with composition, pH and temperature, this is described in paper II.

Rheometry is useful to characterize the viscoelastic and flow properties of different materials. Generally, the viscoelastic properties of a certain material that undergoes gelation can be monitored by a rheometer, with virtually no disturbance of its microstructure [253]. It is particularly useful to study gel-like systems such as the hydrogels and wet films produced in this work, by determining the viscoelastic and flow properties. A cone-plate measuring geometry is exemplified in Figure 21a. The cross-linking effect can be studied by dynamic measurements within the linear regime as illustrated in Figure 21 b.
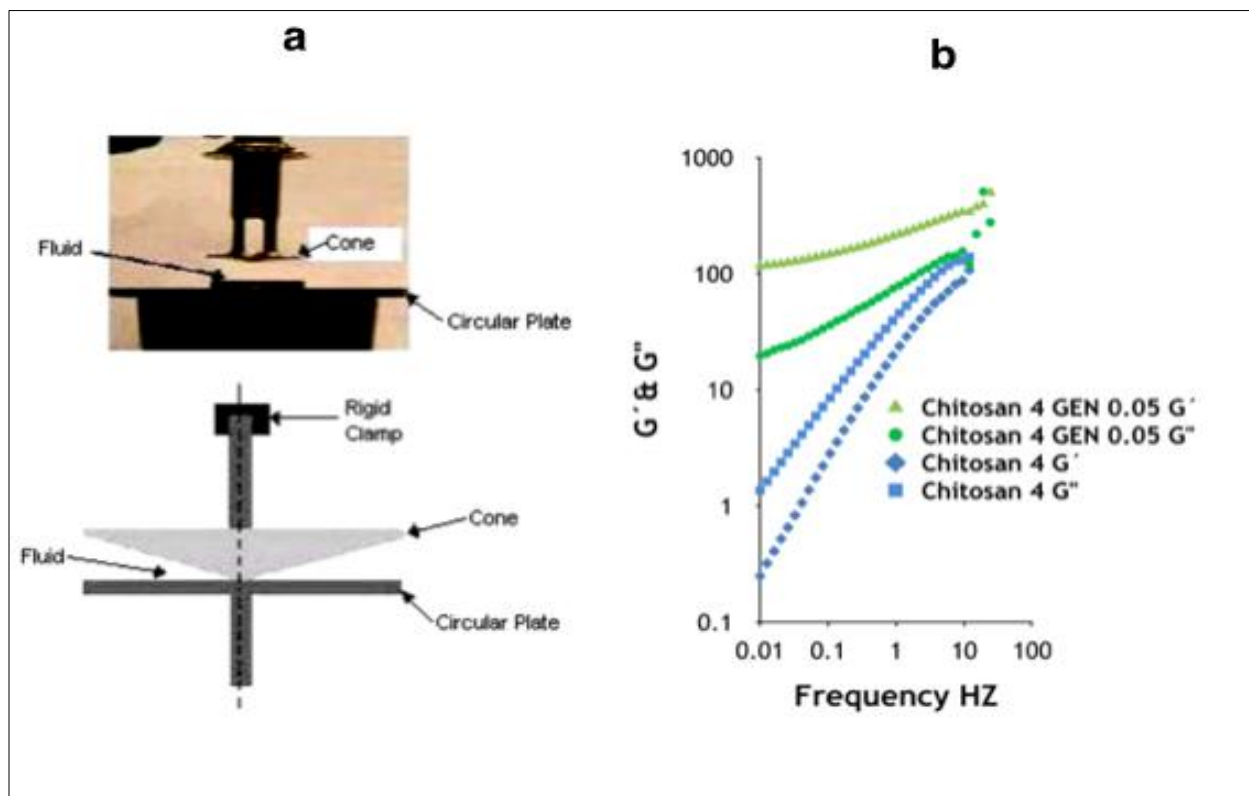
Figure 21. Diagram showing a) the basic structure of a rheometer using a cone-plate geometry b) the frequency sweep showing the changing elastic modulus (G)' and viscous modulus (G)'' in a chitosan solution with and without genipin.

In our work, rheological studies were mainly performed to evaluate the viscoelastic profile of the cross-linked HEC and CMC wet films with citric acid. The effects of temperature and polymer concentration on gelation were also investigated and are compiled in Paper IV.

8 Summary of the Papers
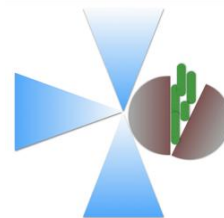
8.1 Development of CMC-chitosan macro and micro particles as delivery vehicles

The main objective of this part of the work was to design new bio-based CMC-Cht particles to efficiently encapsulate model probiotic LGG. Physically and chemically cross-linked particles were obtained from the associative phase separation of the oppositely charged polymers CMC and Cht. The micro- and macrobeads prepared were characterized by a set of different techniques to understand the physico-chemical properties, swelling behavior, morphology and bacteria viability.

The zeta potential of the microparticles was found to be ca. +60 to +70 mV and the particles were stable at room temperature and during the encapsulation process. However, centrifugation and filtration during the washing steps can induce aggregation. Particles chemically cross-linked with genipin showed an average zeta potential of around -8 mV (due to the reaction of genipin with the charged amino groups) and particles were more susceptible to aggregation. The method of preparation is shown in a schematic illustration in Figure 22.
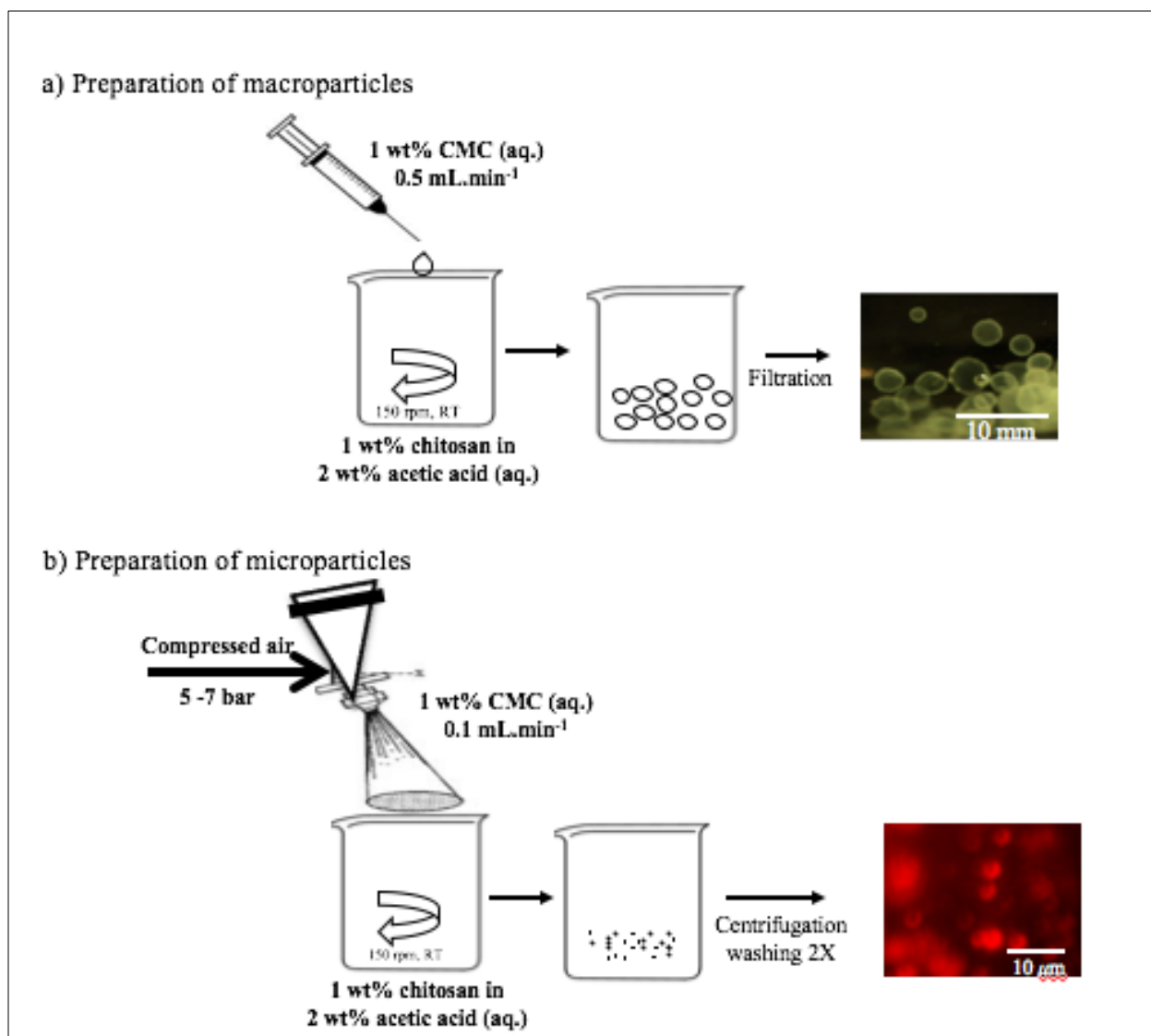
Figure 22. Schematic representation of the macroparticle (a) and microparticle (b) preparation by drop-wise addition and nozzle spray, respectively. Two typical microscopy pictures of the beads obtained are shown.

The FTIR spectrum of the physical CMC-Cht gel was very similar to that of the cross-linked system. However, in the cross-linked system it was possible to identify the amide II band at 1544 cm^{-1}; this is characteristic of the N-H deformation, which results from the formation of secondary amides due to the reaction between the genipin ester and hydroxyl groups and the Cht amino groups; the cross-linking mechanism is presented in Figure. 12.

The TGA results for native CMC and Cht showed a small (5–10%) mass loss for the first decomposition step and a more significant mass loss (50–55%) for the second step. The data

44

showed that CMC is more stable than Chitosan. In the particles, the same two main degradation steps can be identified with a ca. 25% mass loss in the first step and a more significant mass loss (35-45%) in the second step. The loss of water in these particle systems was substantially higher than for the native polymer. Interestingly, in the non-cross-linked particles, a second degradation step was dominated by the more stable polymer (i.e. CMC) while the cross-linked samples showed a second degradation step lower than for the physical gel system. Overall, the TGA data indicated that the obtained chemical and physical gel particles are thermally stable in the temperature range suitable for probiotic bacteria.

These systems were highly sensitive to pH changes, with the equilibrium size of the macroparticles being strongly pH dependent. The swelling and transition to a more expanded state is typically controlled by the osmotic pressure exerted by the mobile counterions neutralizing the network charges. The observed swelling behavior of the CMC-Cht particles is very suitable for the delivery of probiotics in the intestinal tract since particles undergo little swelling at pH values (2-4) typical for the stomach, while they undergo considerable swelling at pH conditions typically found in the intestinal tract (pH ≈ 8).

SEM images show a high density of LGG rods at the surface confirming the integrity of the bacterial cells after encapsulation, Figure 23.
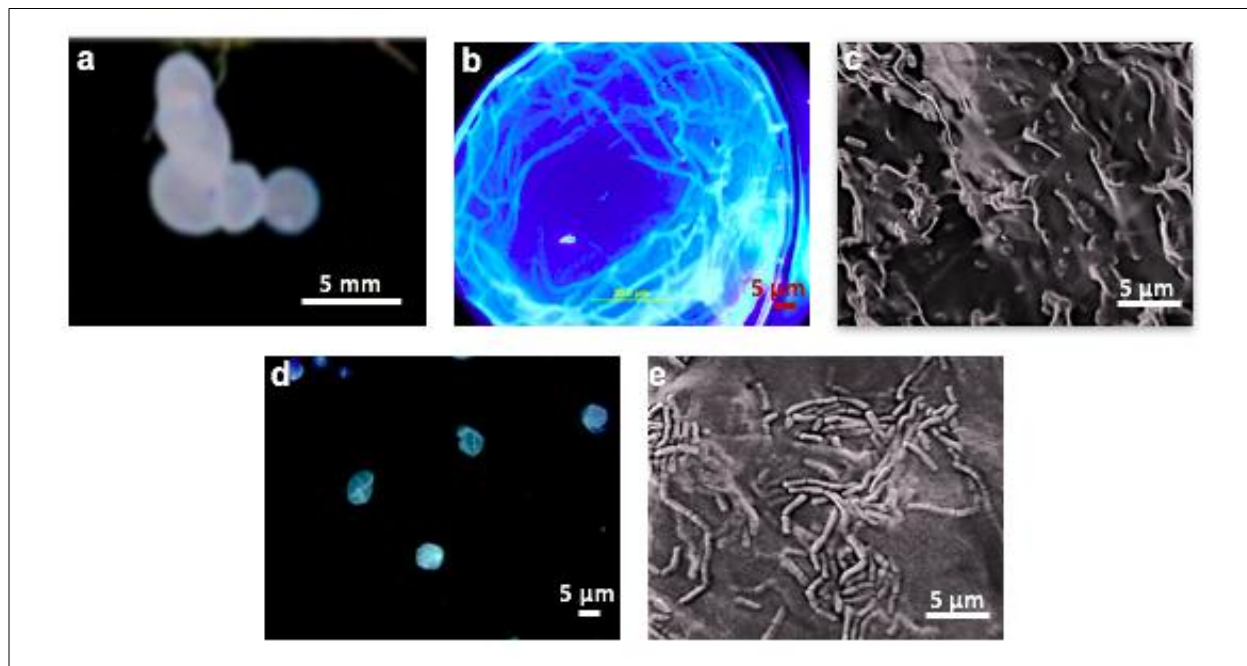
Figure 23. Images of LGG-doped particles. a, b and c) light micrograph, fluorescense image and SEM of CMC-Cht macroparticles, respectively. d and e) are fluorescense image and SEM of CMC-Cht microparticles, respectively. The scale bar in A represents 5 mm while all the other scale bars represent 5 µm. The DAPI dye was used in the fluorescense microscopy tests.

The culturability of LGG in the CMC-Cht systems was checked by plate counting (colony-forming units (CFUs)) and viability by using a fluorescense Dead/Alive kit. The counting of un-encapsulated or naked LGG cells was 11 ± 0.1 Log CFU/mL. After incorporation of LGG in the physical particles a survivability reduction to 6.8 ± 0.1 Log CFU/mL cells was observed. The decrease in culturability was slightly higher for the cross-linked system (6.1 ± 0.1 Log CFU/mL) partially due to the CMC-Cht matrix effect (low porosity) and because some bacteria may remain trapped in the dense gel particles and not be released.

8.2 Prebiotic effect of cyclodextrins

The CDs were assumed to have potential prebiotic effects and also to offer a higher versatility than their precursor starch or other typically studied prebiotics; this is attributed to their "host-guest" features. As discussed in the first paper, the formation of CMC-Cht micro and macroparticles could efficiently entrap probiotic bacteria. However, it was found that the incorporation of β-CD improves the encapsulation efficiency (EE), both in micro- and macroparticles, from ca. 63 % in the non-doped systems to ca. 93 % for the β-CD containing particles.

In paper III, the prebiotic effect of different CDs on encapsulated LGG in a CMC-Cht matrix was studied. It was found that all the CDs tested greatly improve the viability count of LGG probiotic cells entrapped in the CMC-Cht macrobeads; the initial viability values are similar to those of the naked bacteria. If the viability count of naked bacteria resembles the encapsulated ones, efficiency of encapsulation system is considered to be high. The culturability count was comparable to the effect of known prebiotic carbohydrates such as HPMC or starch. The differences in these counts among CDs were minor but still statistically relevant. The presence of CDs changes the morphology of the CMC-Cht macroparticles (Figure 24); for example, while the system without CDs is apparently less porous, with a smoother surface (i.e. "a" and "e") the system doped with α-CD (i.e. "b" and "f") shows a fiber-like pattern at the surface. These arrangements can be deduced from Figure 24.

46
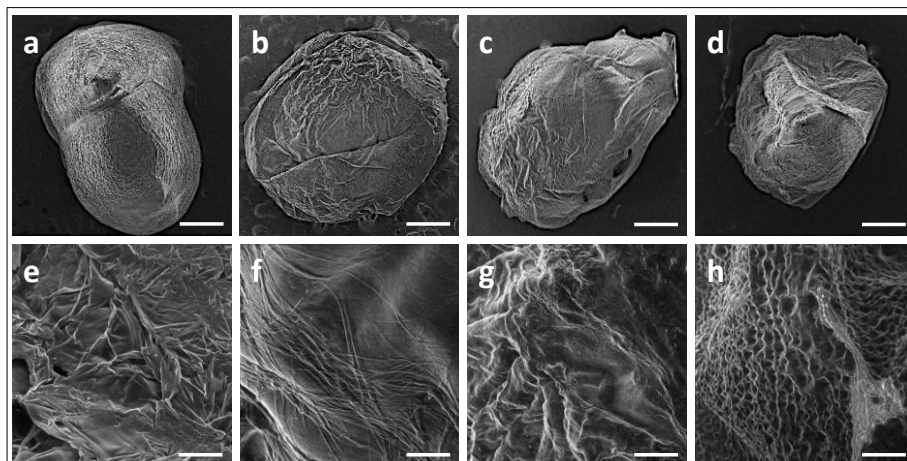
Figure 24. SEM Images of CMC-Cht macroparticles without CD (a and e), with α-CD (b and f), with β-CD (c and g) and with γ-CD (d and h). The top row shows individual macroparticles (scale bar represents 500 μm) while the bottom row displays zoomed areas (scale bars represent 20 μm). In all cases the concentration of CDs used was 1 wt.%.

As the β-CD showed the highest culturability among all different CDs evaluated it was selected to study the effect when incorporated in CMC-Cht particles regarding the storage stability and *in vitro* survivability in simulated gastrointestinal fluids.

Upon incorporation of β-CD, the T_m at the main degradation step increases to 264 ºC (Figure 25). The increase of the molecular order of the blend structure has been referred to the formation of H-bonds between the hydroxyl groups of β-CD and those in CMC and Cht. This hypothesis agrees with the features of the first decomposition step (from 40 to 160 $^\circ$C) of CMC-Cht and CMC-Cht-β-CD related to the mass loss caused by the adsorbed water.
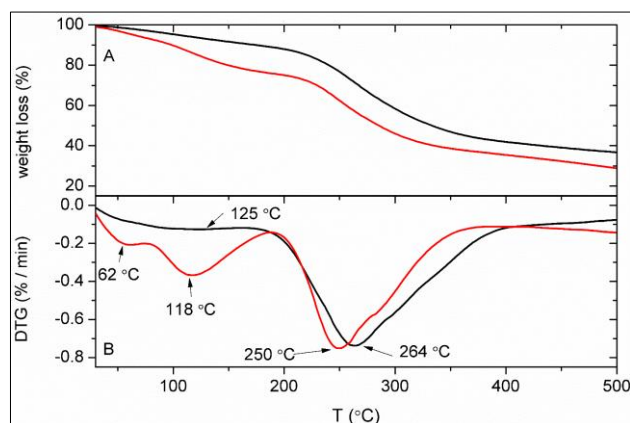
Figure 25. Thermograms (A) and corresponding derivative thermogravimetric analysis (DTG) (B) of CMC-Cht without (red lines) and with β –CD (black lines).

From the *in vitro* tests, it can be concluded that when the particles had β-CD in their composition, the bacterial cell survival after the SGF treatment for 120 minutes was much enhanced, in comparison with the naked LGG. Moreover, the higher stability even at room temperature during the evaluation of 1 month, possibly suggests an extended application range of sensitive synbiotics to non-refrigerated, long shelf-life food and pharmaceutical products.

The improved survivability upon incorporation of CDs may be related not only to the fact that they can effectively work as prebiotics and carbon sources for the enhancement of probiotic cell growth and proliferation, but it is also plausible that during the particle formation, the β-CD interacts with the CMC-Cht polymer matrix, in particular chitosan, thus decreasing its anti-bacterial effect on the viability.

8.3 Viability, toxicity and stability of probiotic bacteria entrapped in cellulose-based particles

Sodium caseinate (SC) and soy lecithin have been reported to stabilize different systems, such as emulsions, due to the combination of electrostatic and steric features. Hence, in order to improve the formation and stability properties of the existing CMC-Cht macroparticles, SC and SL were used. The addition of SC or SL to the formulation leads to a significant change in the particle transparency and, more importantly, reduction in their aggregation tendency. This might be related to extra electrostatic stability, since the particles become more charged upon the incorporation of SC.
SEM images show that the CMC-Cht particles are significantly porous whereas the presence of SC and SL gave a much denser structure with no visible porosity.

As the particles are formed with charged species with titrating groups, Cht, CMC and SC, they are highly sensitive to pH changes. The effect of SL and SC on the viability was also

48

studied. While the particles with SL show a decrease in the viability, the samples containing SC present a higher number of viable bacterial cells (Figure 26). The *in vitro* data revealed a strong correlation between the number of viable cells detected by flow cytometry and those of plate count techniques.
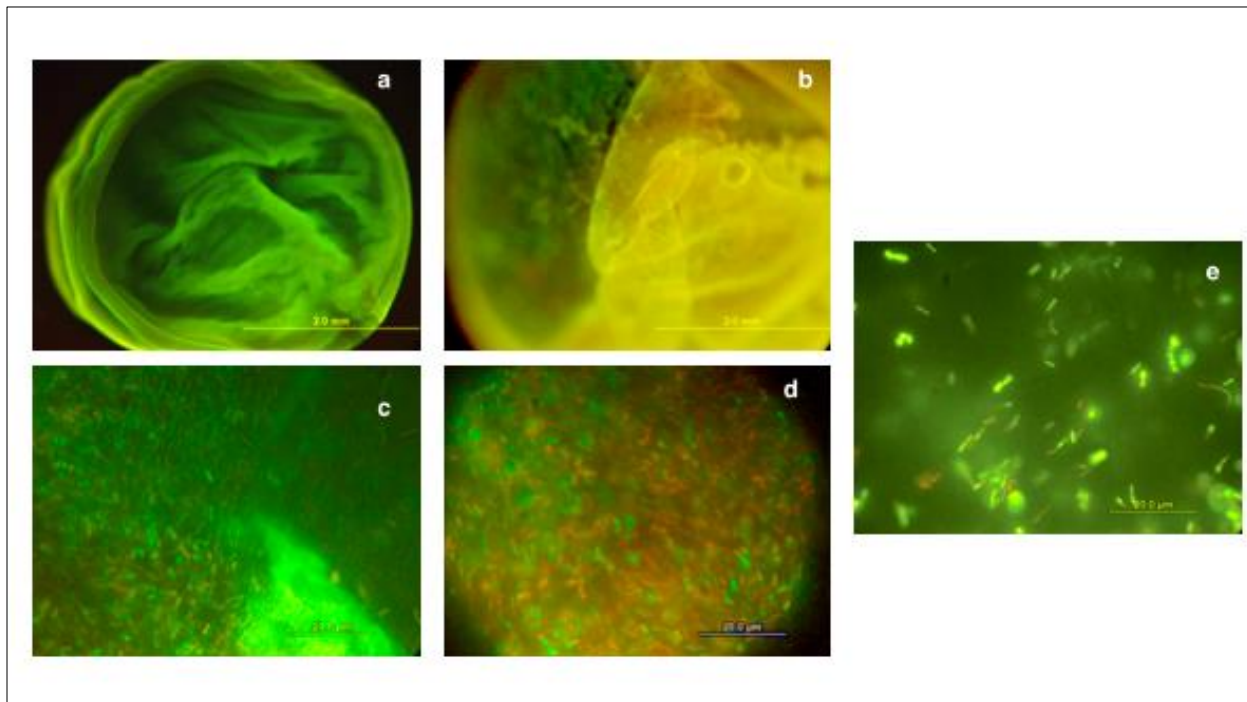
Figure 26. Images obtained through fluorescence microscope of particles with the entrapped bacteria.
a. CMC-Cht particles with casein (CS), b. CMC-Cht particles with soy lecithin (SL). The scale bar corresponds to 2 mm. c & d are magnifications of a & b, respectively. e presents the naked bacteria.
The scale bar corresponds to 20 μm

All the different particles showed a significantly higher bacterial viability after going through the simulated harsh conditions than the control.

The viability results of the systems stored at different temperatures are shown in Figure 27. It can be deduced that encapsulated bacteria have improved shelf-lifes at the three different temperatures when compared to the free bacteria. With temperature changes there is an obvious effect on the increase or decrease in the viability of the bacteria. Depending on the difference in the constituents of the systems, the culturabilty and viability were affected. The results obtained with cytotoxicity experiments demonstrate that the novel particles present a moderate to low toxicity to the cell line. Surprisingly, when the particles contain model bacteria, they show

49

enhanced viability of the cell line. The statistical analysis showed that there was a significantly higher survival rate of the encapsulated bacteria than for the free, naked cells at all the three different temperatures studied. Moreover, particles with caseinate have considerably higher viability.
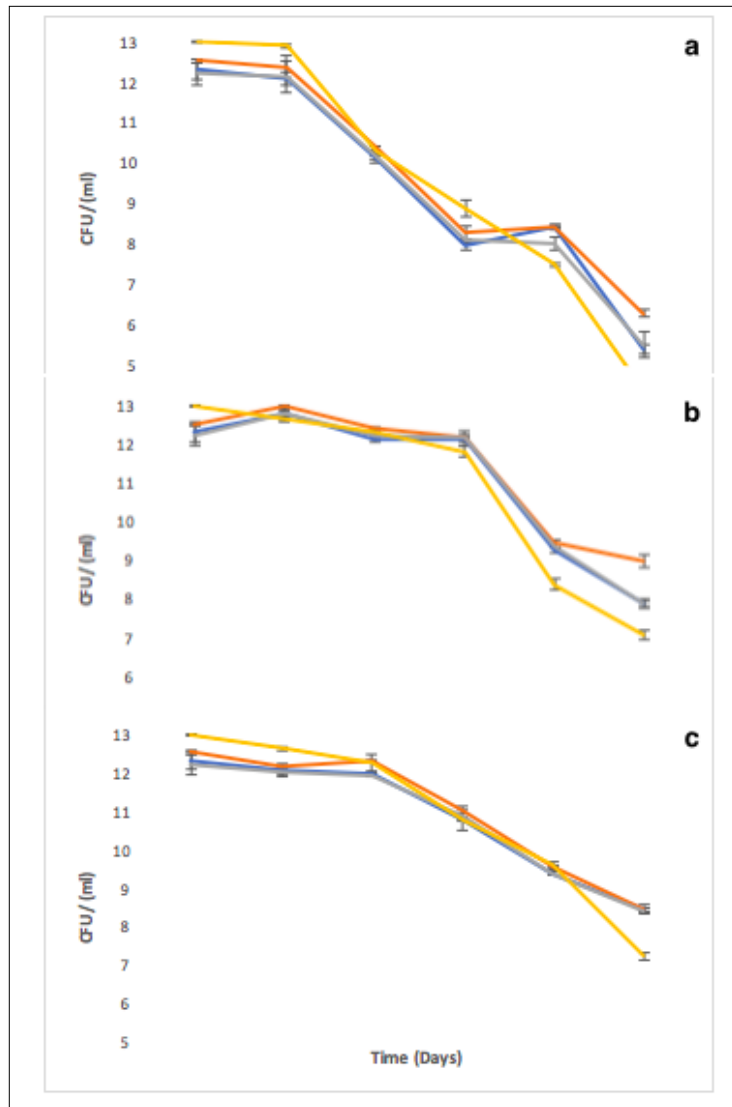
Figure 27. The graph presents the viability during storage of the samples at three different temperatures a 25 ℃, b 4 ℃ and c -20 ℃ during 30 days. Orange line refers to CMC-Cht particles with casein, Blue CMC-Cht particles, Grey CMC- Cht particles with soy lecithin and yellow is the control or the naked cells.

8.4   Encapsulation of LGG in CMC and gelatin aqueous emulsions

Systems composed of gelatin and sodium CMC were also studied in this work. For certain concentrations and temperature, aqueous mixtures of gelatin and CMC can form water-in-water (W/W) emulsion droplets. Mixtures of solutions of CMC and gelatin gave a turbid dispersion after 35 to 48 hours. Macroscopic phase separation, with two aqueous liquid phases in equilibrium, was only observed above critical polymer concentrations. As the viscosity of the continuous phase was high, phase separation was extremely slow, and took 4-7 days to be clearly visible. Since the main component in both phases is water, the refractive indices of the disperse phase and the external phase are rather similar, which results in a low contrast in the images by optical microscopy.

Depending on the ratio between the polymers, the pH of the mixtures was between 5.2 and 6.5. Under these conditions, gelatin (with an isoelectric point of ca. 4.7-5.2) and CMC (pK_a of ca. 4.3) are expected to be both negatively charged and thus coacervation is prevented. Such a system is expected to show a segregative phase separation, with the possibility of dispersion of one solution into the other. Most likely, the emulsion droplets consisted of a CMC-enriched aqueous solution, dispersed into a gelatin-rich aqueous solution (and thus the system can be denoted as a CMC-in-gelatin emulsion). The droplets had an average size of 5-10 µm.

The dispersions completely jellify when cooled down to room temperature, clearly demonstrating that gelatin is present in the external phase. Furthermore, CMC-in-gelatin emulsions can be verified by the fact that gelatin is slightly colored (yellowish) whereas CMC is colorless. During the examination, a colorless region was observed as a small separated volume located at the top of the sample vial (Figure 28) after the mixture was kept at 60ºC for several days. These simple visual observations at naked eye are supported by UV-vis measurements.
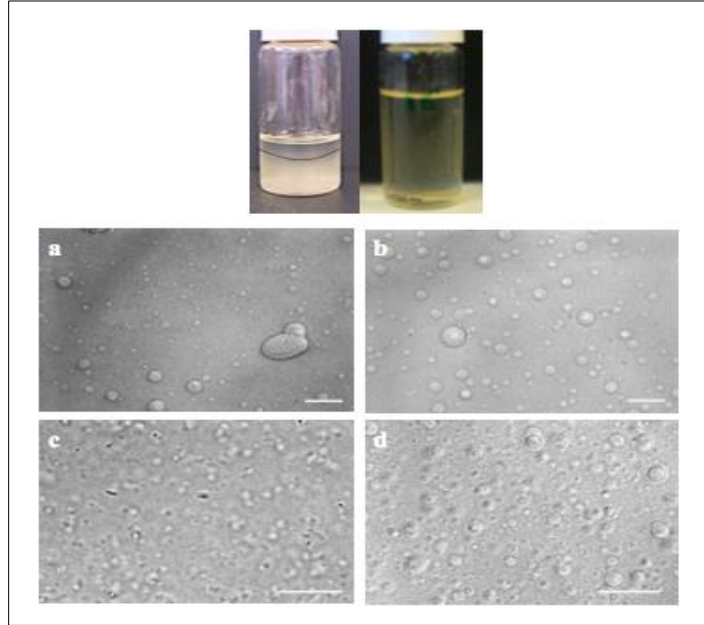
Figure 28. Top: photos of two gelatin-CMC mixtures at 60 ℃ after two days of equilibration at a constant temperature of 60 ℃. 1 wt% CMC and 15 wt% gelatin (left) and 0.2 wt% CMC and 5 wt% gelatin (right). For better visualization, the dashed line in the phase separated sample demarks the sedimentation boundary. Bottom: optical microscopy images of the CMC-gelatin systems composed of 1.2 wt % CMC and 2.8 wt% gelatin (a), 1.6 wt% CMC and 1 wt% gelatin (b), 1 wt% CMC and 7.5 wt% gelatin (c), 2 wt% CMC and 7.5 wt% gelatin (d). In all these cases, droplet-like objects can be observed indicating the formation of emulsions after mixing the phase-separated samples. The scale bars represent 20 μm.

In SEM images, a foam-like microstructure is obtained after freeze-drying, as expected for emulsion templating, showing that the bacteria are located on the surface of the macropores having a size around 50 μm.

The particles were also exposed to *in vitro* simulated digestion fluids to mimic the *in vivo* physiological conditions, considering different parameters such as concentration of digestive enzymes, pH, digestion time, salts, among others. The exposure of the naked and entrapped cells to SGF (120 minutes) followed by the SIF (120 minutes) resulted in a higher number of alive bacteria when trapped in the gelatin-CMC emulsion; the cell survival was ca. 83 and 77.5%, respectively, of the population after SGF and SIF exposure, while in the free cell case ca. 77 and 60%, respectively, were found viable. The data is shown as a bar chart in Figure 29.
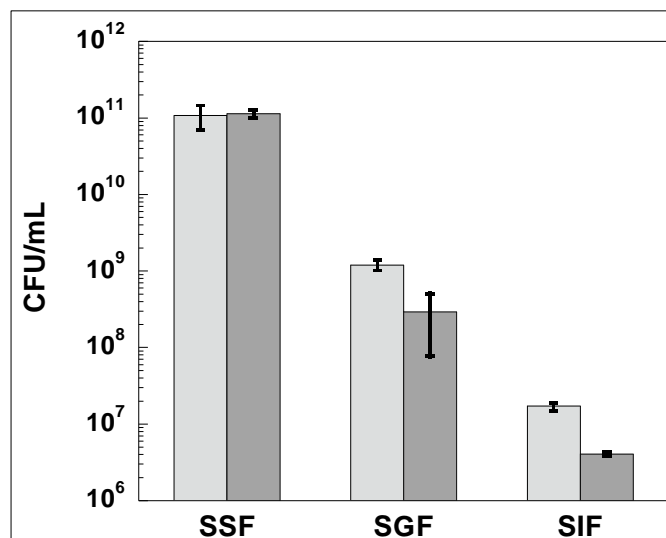
Figure 29. Culturability counts in CFU/mL of the naked (dark grey bars) and encapsulated cells in the 1% NaCMC and 7.5 % gelatin W/W emulsion (light grey bars). Data was interpreted with the plate count method after exposure of the naked and entrapped cells to Simulated Salivary, Gastric and Intestinal Fluids (SSF, SGF and SIF, respectively). The error bars represent the standard deviation.

Although the cell population declines approximately at the same rate for all the tested simulated gastro-intestinal conditions, a final 4 log CFU/ml decrease in culturability is observed for the encapsulated LGG while the loss in viability is higher, ca. 5 log CFU/ml, for the naked cells.

8.5 Edible films based on cellulose derivatives for encapsulation of bacteria

Edible films were obtained from cellulose derivatives, HEC and CMC, alone or in combination and polymers were cross-linked with citric acid (CA). The films cast were reasonably flexible and transparent, but the addition of CA followed by cross-linking resulted in less flexible, brittle films and the transparency was observed to decrease with the amount of CA. While HEC, CMC and their physical mixture dissolve in water, the cross-linked films did not. The pictures in Figure 30 show a clear distinction between native and cross-linked films of the polymers.
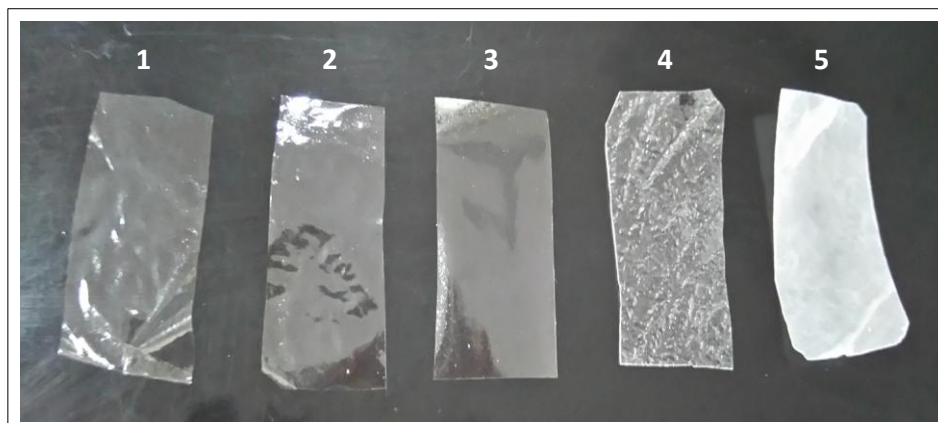
Figure 30. Photograph of cellulose-based film strips after being cast and dried in Petri dishes. 1) 1 wt% HEC; 2) 1 wt% CMC; 3) 1 wt% HEC + 1 wt% CMC; 4) 1 wt% HEC + 1 wt% CMC + 5 wt% CA; 5) 1 wt% HEC+ 1 wt% CMC + 10 wt% CA.

Characterization of the synthesized films by FTIR spectroscopy supported the completion of the esterification reaction between the cellulose derivatives and CA.

The amount of water adsorbed by the different films was measured after 24h equilibrium in distilled water. The cross-linked HEC film presented the highest swellability. Another interesting observation was related to the lower swelling of the films when the CA concentration increased; this is due to an increased rigidity of the highly cross-linked polymer network.

The rheological mechanical spectra represented in Figure 31 show a high storage modulus, G', in CMC films, almost three orders of magnitude higher than the cross-linked HEC films which behave as weak gel-like material. The combination of the two polymers resulted in films with a G' in between the values of the individual polymer films; the swelling degree was higher than for the film of CMC alone.
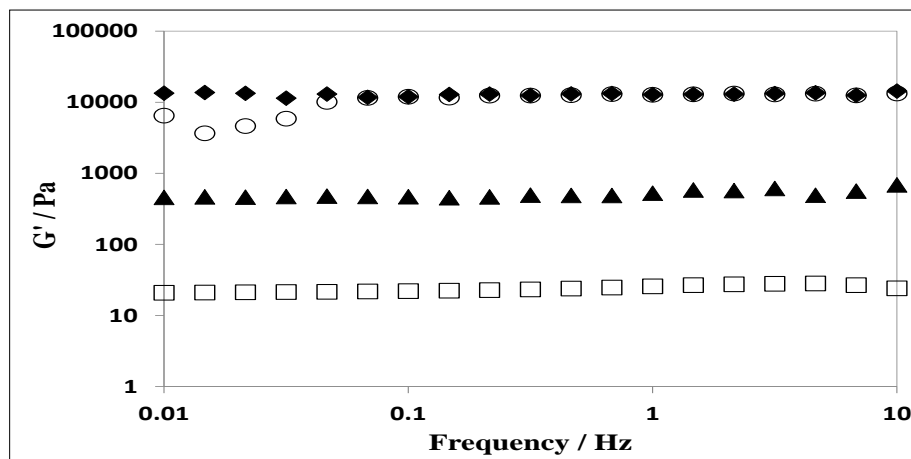
Figure 31. Mechanical spectra (frequency sweeps) of the films after 24h swelling in water at 25ºC. 1 wt% CMC + 5 wt% CA (♦); 1 wt% HEC + 5 wt% CA (□); 1 wt% HEC + 1 wt% CMC + 5 wt% CA (▲);1 wt% HEC + 1 wt% CMC + 10 wt% CA (○).

The films of cross-linked HEC or CMC alone presented a rather similar and homogenous morphology with an apparent low porosity, which contrasts to the much less denser structure and higher porosity of the non-cross-linked homologues.

The cross-linked CMC film presented the lowest cell counting at both pHs but the viability increases if HEC is added to the formulation. Moreover, the higher the content of CA the higher is the cell counting.

In general, viable LGG bacteria can be effectively entrapped in the cross-linked cellulose-based films and their release is strongly dependent on the film composition and pH of the media. The data suggested that these cellulose-based films cross-linked with CA (or related systems, such as microparticles) may be a good alternative for entrapping viable probiotics and protect them from any unfavorable food matrix properties or even from the harsh gastrointestinal conditions (e.g. low pH in the stomach).

9 Conclusions
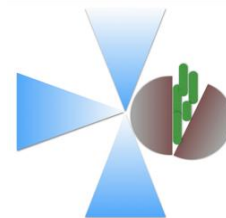
The objective of this PhD work was to develop biocompatible carriers, with FDA approved materials. The model chosen by the BIBAFOODS consortium was a probiotic bacterium, *Lactobacillus rhamnosus* GG. In the quest to achieve the objective, cellulose derivatives were chosen to develop the delivery vehicles in combination with other polymers such as chitosan and gelatin. The systems were further characterized using different techniques such as TGA, swelling ability, FTIR, zeta potential, SEM and rheology. The different systems which were designed during this study were CMC-Cht based particles, CMC-gelatin emulsions and CMC-based edible films.

The CMC-Cht particles, obtained by physical and chemical cross-linking, had tunable size depending on the method of preparation: microparticles with an average size of 5 μm prepared by nozzle-spraying and macroparticles with a mean diameter of 2 mm prepared by a drop-wise procedure. The cross-linking of the particles. achieved with genipin, was confirmed by FTIR and TGA. Viable bacteria could be entrapped in these systems. Later, a successful symbiotic combination was assessed with the influence of prebiotic oligosaccharides (CDs) on model probiotic bacteria. β-cyclodextrin was observed to considerably improve the viability count of the bacteria thus being considered a prebiotic. The particles developed were further improved in terms of their encapsulation efficiency and stability by the addition of a milk protein (SC) and a lipid (SL). Most of the systems studied were stable at pH 2.4, which is the gastric pH, and swell considerably at higher pHs, in particular at pH 7.4, close to the pH of the intestine. When pH was increased even more (pH ca. 10-11), the particles disintegrated, which may be important for the full release of the bacteria. The cross-linking of the systems as well as addition of a specific protein or lipid gave significant morphological changes.

Apart from the micro and macro particles formed by extrusion methods, novel W/W emulsions were prepared based on gelatin and CMC and used to entrap LGG. W/W emulsification can be an effective method for incorporating bacteria in fully biocompatible and

reasonably mild conditions (moderate pH and temperature), without surfactant and oil. Thus, W/W emulsions could become a platform for production of soft materials as carriers of living microorganisms. Also, the viability counts were surprisingly high in this novel inexpensive system.

As a final approach to develop one more carrier, CMC and HEC were successfully cross-linked using CA, via an esterification reaction among the COOH groups of CA and the OH groups of the cellulose derivatives, to obtain edible films. Depending on the ratio between the cellulose derivatives, and the concentration of cross-linking agent, the film properties change dramatically. Viable bacteria could be entrapped in the films after their formation via diffusion. The data suggests that the cellulose-based films cross-linked with CA may be a good alternative for entrapping viable probiotics and protect them from any unfavorable food matrix properties or even from the harsh gastrointestinal conditions (e.g. low pH in the stomach).

The bacterial cell viability was found to be high during the simulated condition of gastrointestinal passage, in all the three different storage conditions examined. Hence, the guidelines to produce a potential health benefit product are fulfilled. Together with the CMC-Cht particles containing caseinate, the gelatin-CMC W/W emulsions were among the most efficient systems to entrap LGG bacteria with high viability counts.

Fluorescence microscopy, flow cytometry, SEM and viable cell plate count confirmed the successful encapsulation and acceptable viability of LGG in essentially all cellulose-based systems, regardless of the method of preparation or presence of a cross-linking agent. The ability of the developed systems to protect *Lactobacillus rhamnosus* GG during gastrointestinal conditions assessed in a two-stage in vitro model simulating conditions in the human stomach and small intestine showed an enhancement of the viability of encapsulated bacteria in comparison to non-encapsulated bacteria.

Measurements of the toxicity of the systems on Caco-2 cell lines with and without encapsulated bacteria showed a minimum adversity to the cells. These results encouraged the establishment of the systems to be used in real food products. Overall, cellulose-based delivery vehicles, due to their inherent similarity to the extracellular matrix and mild deleterious effects, are very useful for the entrapment of viable probiotics; they may have a huge impact in the field of biotechnology and other biomedical applications. Hopefully, the results obtained during this work will contribute to the development of novel applications, particularly in the food domain.

58
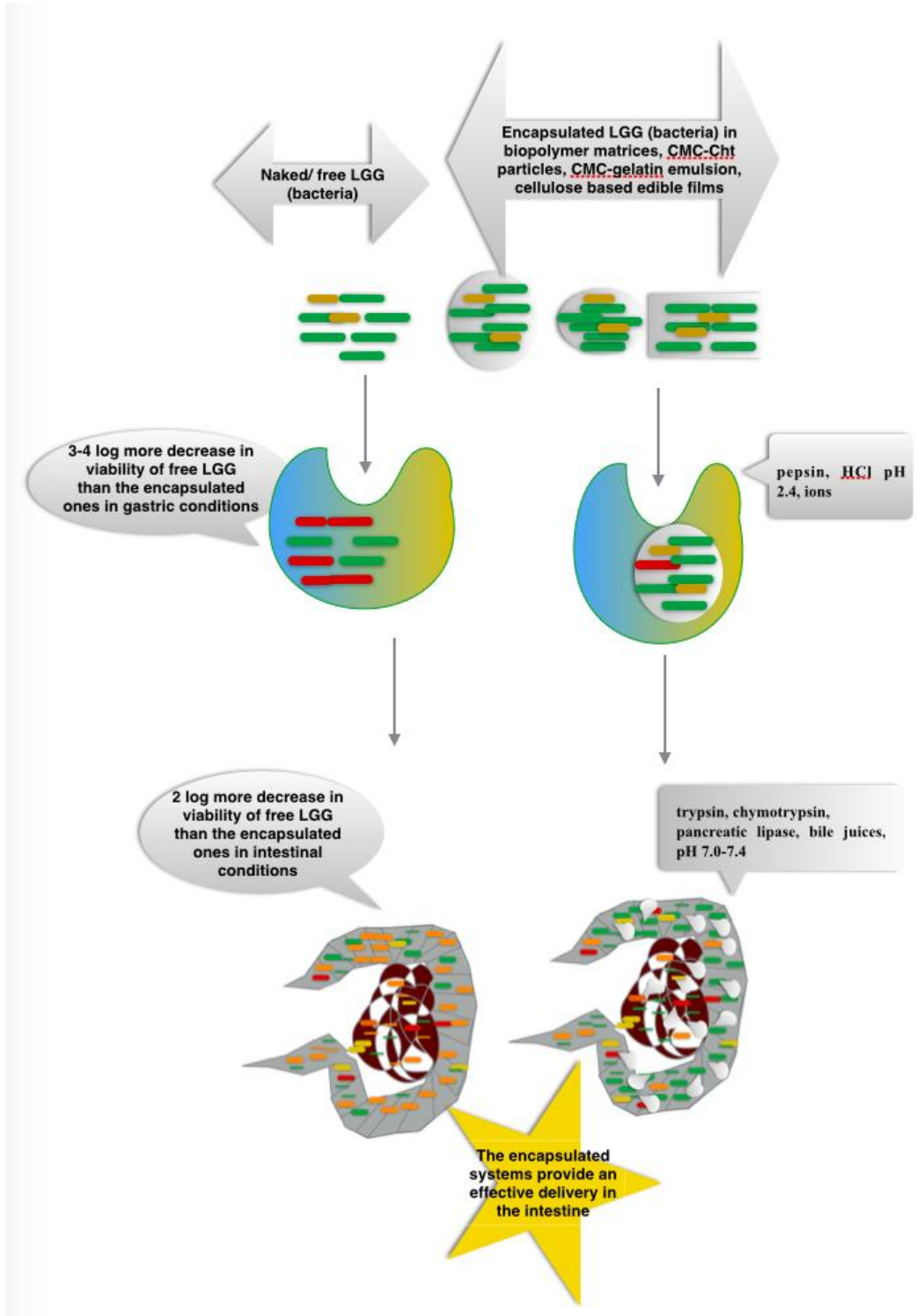
An Illustration to depict the main results of this thesis. The representation shows the importance of encapsulating probiotic bacteria to overcome the harsh conditions in the stomach and the intestine. Also, an effective release in the gut maintaining the viability suggested by FDA guidelines.

10 Future Perspective

Some of the most appealing factors of this work are related to the preparation of cost-effective and biocompatible delivery systems using cellulose derivatives as raw material. The tunable size of the CMC-Cht particles and the stability of the W/W emulsions, with the droplet size in micro scale, is a big plus as size may influence the mouthfeel (decisive parameter in oral applications). Scaling up of the synthesis of all the developed systems seems quite feasible, as only aqueous solutions of the polymers are required during the preparation. This scalability would be interesting to try in the future. In principle, the emulsions obtained using the segregative phase phenomenon in this project opens an innovative approach for the potential application in different industries, where the properties of the encapsulated material could be, for instance, affected by the hydrophobicity of the oil in standard emulsions.

Molecular techniques such as 16S ribosomal RNA sequencing and reverse transcription polymerase chain reaction are very useful to determine the viable and non-viable components of the encapsulated bacteria. The use of other molecular methods like DNA fingerprinting, RNA amplification and pulse field gel electrophoresis to study the integrity of the encapsulated bacteria could also be very useful in subsequent studies. At the same time, the influence of harsh conditions in the gut causing bacterial destruction and the release of bacterial DNA can be followed using these techniques, which are based on the separation and identification of genetic material. Again, these advanced methods could be important for a better and more complete characterization of our systems. Moreover, the adhesion properties of the delivery vehicles developed, with and without encapsulating bacteria, to the gastrointestinal cell lines should be analyzed in detail. This is an important feature when it comes to targeted delivery, which should deserve attention in the future. The Simulator of the Human Intestinal Microbial Ecosystem (SHIME) model, which has a flexible set up can be used to study the systematic release of the bacteria encapsulated in cellulose based carriers.

The functional properties of the encapsulated bacteria like antimicrobial and antioxidant activity can be interesting for future studies. For example, the metabolism of LGG such as the production of β-galactosidase and lactate can be evaluated using analytical methods and enzymatic assays. Finally, as the purpose of these developed vehicles was for food applications it would be interesting to select an appropriate food product, such as a jam, and evaluate the

potential of the developed cellulose based matrices in real food products. The long-term effects of permanent changes in the composition of the colonic microflora could also be monitored in follow-up studies.

The developed vehicles can also be used for other *in vivo* deliveries like drugs, nutraceuticals or even for cosmetic products. It would indeed be worth trying the potential of the novel formulations developed in this work with other loads apart from the probiotic bacteria.

11 References

1. Annunziata, A., & Vecchio, R. (2013). Agri-food innovation and the functional food market in Europe: Concerns and challenges. *EuroChoices*, 12, 2, 12-19.

2. Wilm, K. H. (2006). Functional food. *Chemical Technology Bedfordview-*, 24-25.

3. Roberfroid, M. B. (2000). Prebiotics and probiotics: are they functional foods? *American Journal of Clinical Nutrition*, 71(6), 1682s-1687s.

4. Tripathi, M. K., & Giri, S. K. (2014). Probiotic functional foods: Survival of probiotics during processing and storage. *Journal of Functional Foods*, 9, 225-241.

5. Cenčič, A., & Chingwaru, W. (2010). The Role of functional foods, nutraceuticals, and food supplements in intestinal health. *Nutrients*, 2, 611-625.

6. Iannitti, T., & Palmieri, B. (2010). Therapeutical use of probiotic formulations in clinical practice. *Clinical Nutrition*, 29(6), 701-725.

7. Possemiers, S., Marzorati, M., Verstraete, W., & Van, W. T. (2010). Bacteria and chocolate: a successful combination for probiotic delivery. *International Journal of Food Microbiology*, 141, 1-2.

8. Szkaradkiewicz, A. K., & Karpiński, T. M. (2013). *Probiotics and prebiotics*. J. Biol. Earth Sci, 3, M42-M47.

9. Sagalowicz, L., & Leser, M. E. (2010). Delivery systems for liquid food products. *Current Opinion in Colloid and Interface Science*, 15, 61-72.

10. Ahmed, E. M. (2015). Hydrogel: Preparation, characterization, and applications: A review. *Journal of Advanced Research*, 6, 2, 105-21.

11. Ghasemzadeh, H., Mahboubi, A., Karimi, K., & Hassani, S. (2016). Full polysaccharide chitosan- CMC membrane and silver nanocomposite: synthesis, characterization, and antibacterial behaviors. *Polymers for Advanced Technologies*, 27(9), 1204-1210. ~

12. Holzapfel, W. H., Haberer, P., Snel, J., Schillinger, U., & Huis, V. J. H. (1998). Overview of gut flora and probiotics. *International Journal of Food Microbiology*, 41, 2, 85-101.

13. Govender, M., Choonara, Y. E., Kumar, P., du Toit, L. C., van Vuuren, S., & Pillay, V. (2014). A Review of the Advancements in Probiotic Delivery: Conventional vs. Non-conventional Formulations for Intestinal Flora Supplementation. *Aaps Pharmscitech*,

15(1), 29-43.

14. James, P. H., John, R., Alex, A., & Anoop, K. R. (2014). Smart polymers for the controlled delivery of drugs - a concise overview. *Acta Pharm Sin* B, 4(2), 120-127.

15. Cook, M. T., Tzortzis, G., Charalampopoulos, D., & Khutoryanskiy, V. V. (2012). Microencapsulation of probiotics for gastrointestinal delivery. *Journal of Controlled Release*, 162, 1, 56-67.

16. Ichikawa, S., Iwamoto, S., & Watanabe, J. (2005). Formation of biocompatible nanoparticles by self-assembly of enzymatic hydrolysates of chitosan and carboxymethyl cellulose. *Bioscience Biotechnology and Biochemistry*, 69(9), 1637-1642.

17. Li, W., Zhu, Y., Ye, F., Li, B., Luo, X., & Liu, S. (2017). Probiotics in cellulose houses: Enhanced viability and targeted delivery of *Lactobacillus plantarum*. *Food Hydrocolloid*s, 62, 66-72.

18. Biquet, B., & Labuza, T. P. (1988). Evaluation of the Moisture Permeability Characteristics of Chocolate Films as an Edible Moisture Barrier. *Journal of Food Science, 53*(4), 989-998.

19. Saarela, M., Mogensen, G., Fonden, R., Matto, J., & Mattila-Sandholm, T. (2000). Probiotic bacteria: safety, functional and technological properties. *Journal of Biotechnology*, 84(3), 197-215.

20. Baldwin, E. A., Hagenmaier, R. D., & Bai, J. (2012). Edible coatings and films to improve food quality. CRC Press Llc, Boca Raton.

21. Gibson, G. R., & Roberfroid, M. B. (1995). Dietary modulation of the human colonic microbiota: introducing the concept of prebiotics. *The Journal of Nutrition*, 125, 6, 1401-12.

22. Solanki, H. K., Pawar, D. D., Shah, D. A., Prajapati, V. D., Jani, G. K., Mulla, A. M., & Thakar, P. M. (2013). Development of microencapsulation delivery system for long-term preservation of probiotics as biotherapeutics agent. *Biomed Research International*.

23. Brudnak, M. A. (2002). Probiotics as an adjuvant to detoxification protocols. *Medical Hypotheses*, 58, 5, 382-385.

24. Mohammadi, R., Mortazavian, A. M., Khosrokhavar, R., & da Cruz, A. G. (2011). Probiotic ice cream: viability of probiotic bacteria and sensory properties. *Annals of Microbiology*, 61(3), 411-424.

25. Kaihara, S., Suzuki, Y., & Fujimoto, K. (2011). In situ synthesis of polysaccharide nanoparticles via polyion complex of carboxymethyl cellulose and chitosan. *Colloids and Surfaces B- Biointerfaces*, 85(2), 343-348.

26. Long, D. D., & vanLuyen, D. (1996). Chitosan-carboxymethylcellulose hydrogels as supports for cell immobilization. *Journal of Macromolecular Science-Pure and Applied Chemistry*, A33(12), 1875-1884.

27. Priya, A. J., Vijayalakshmi, S. P., & Raichui, A. M. (2011). Enhanced Survival of Probiotic *Lactobacillus acidophilus* by Encapsulation with Nanostructured Polyelectrolyte Layers through Layer-by-Layer Approach. *Journal of Agricultural and Food Chemistry*, 59(21), 11838-11845.

28. Olsen, M. A., Myklebust, R., Kaino, T., Elbrond, V. S., & Mathiesen, S. D. (2002). The gastrointestinal tract of Adelie penguins - morphology and function. *MicrobiologyOpen*. 2, 195-204.

29. Clark J.A., Coopersmith C.M (2007). Intestinal crosstalk: A new paradigm for understanding the gut as the "motor" of critical illness. *Shock*, 28:384–393.

30. Ley R., Peterson D., Gordon J. (2006a) Ecological and evolutionary forces shaping microbial diversity in the human intestine. *Cell,* 124: 837–848

31. Ley R., Hamady M., Lozupone C., Turnbaugh P., Ramey R., Bircher J. (2008) Evolution of mammals and their gut microbes. *Science,* 320: 1647–1651

32. Guinane, C. M., & Cotter, P. D. (2013). Role of the gut microbiota in health and chronic gastrointestinal disease: Understanding a hidden metabolic organ. *Therapeutic Advances in Gastroenterology*, 6, 4, 295-308.

33. Zhang, Y. J., Li, S., Gan, R. Y., Zhou, T., Xu, D. P., & Li, H. B. (2015). Impacts of gut bacteria on human health and diseases. *International Journal of Molecular Sciences*, 16, 4, 7493-519.

34. Macfarlane S., Steed H., Macfarlane G.T. (2009). Intestinal bacteria and inflammatory bowel disease. *Crit. Rev. Clin. Lab. Sci*, 46:25–54.

35. Lee, B. J., & Bak, Y.T. (2011). Irritable Bowel Syndrome, Gut Microbiota and Probiotics. *Journal of Neurogastroenterology and Motility*, 17, 3, 252-266.

36. Hemarajata, P., & Versalovic, J. (2013). Effects of probiotics on gut microbiota: Mechanisms of intestinal immunomodulation and neuromodulation. *Therapeutic*

Advances in Gastroenterology, 6, 1, 39-51.

37. Goderska, K., Nowak, J., & Czarnecki, Z. (2008). Comparison of the growth of *Lactobacillus acidophilus* and *Bifidobacterium bifidum* species in media supplemented with selected saccharides including prebiotics. *Acta Sci. Pol*. 7, 5-20.

38. Sanders, M. E. (2003). Probiotics: Considerations for Human Health. *Nutrition Reviews*, 61, 3, 91-99.

39. Williams, N. T. (2010). Probiotics. *American Journal of Health-System Pharmacy*, 67, 6, 449-458.

40. Noomhorm, A., Anal, A. K., & Ahmad, I. (2014). Functional Foods, Nutraceuticals and Probiotics as Functional Food Components. 1-19.

41. Gupta, V, & Garg, R. (2009). Probiotics. *Indian Journal of Medical Microbiology* (ISSN: 0255-0857). 27, 3.

42. Klaenhammer, T. R. (2000). Probiotic bacteria: today and tomorrow. *The Journal of Nutrit*ion, 130.

43. Rodgers, S. (2007). Incorporation of probiotic cultures in foodservice products: an exploratory study. *J Food Serv, 18*, 108-118.

44. Singh, P., Rani, B., Chauhan, A.K., & Maheshwari, R. (2011). Healthy living with nutraceuticals. *International Research Journal of Pharmacy*, 2, 12, 12-14.

45. Hill, C., Guarner, F., Reid, G., Gibson, G. R., Merenstein, D. J., Pot, B., Morelli, L., Salminen, S. (2014). Expert consensus document: The International Scientific Association for Probiotics and Prebiotics consensus statement on the scope and appropriate use of the term probiotic. *Nature Reviews Gastroenterology and Hepatology*, 11, 8, 506-514.

46. Martin, D. R., Ramalho, M., Matos, A. P., Altun, E., & Semelka, R. C. (2015). *Gastrointestinal tract*. 593-744

47. Farstad, I. N., Norstein, J., & Brandtzaeg, P. (1997). Phenotypes of B and T cells in human intestinal and mesenteric lymph. *Gastroenterology*, 112, 1, 163-73.

48. Kandasamy, S., Vlasova, A. N., Fischer, D. D., Chattha, K. S., Shao, L., Kumar, A., Langel, S. N., Saif, L. J. (2017). Unraveling the Differences between Gram-Positive and Gram-Negative Probiotics in Modulating Protective Immunity to Enteric Infections. *Frontiers in Immunology*, 8.

49. Szajewska, H., Konarska, Z., & Kołodziej, M. (2016). Probiotic Bacterial and Fungal Strains: Claims with Evidence. *Digestive Diseases* (Basel, Switzerland), 34, 3, 251-9.

50. Zhou, H., Li, S., Chen, Y., Zhang, Q., Bai, X., Zhu, C., Liu, H., Wu, C. (2017). Evaluation of *Streptococcus thermophilus* IFFI 6038 Microcapsules Prepared Using an Ultra-fine Particle Processing System. *Aaps Pharmscitech*.

51. Snapper, S., Gevers, D., Korzenik, J., Bousvaros, A., Morgan, X., Reyes, J., Sokol, H., Ward, D. (2012). Dysfunction of the intestinal microbiome in inflammatory bowel disease and treatment. *Genome Biology*, 13, 9, 1-18.

52. Jijon H, Backer J, Diaz H, et al. DNA from probiotic bacteria modu- lates murine and human epithelial and immune function. *Gastroenterology.* 2004;126:1358 –1373.

53. Rachmilewitz D, Karmeli F, Takabayashi K, et al. Immunostimulatory DNA ameliorates experimental and spontaneous murine colitis. *Gastroenterology.* 2002;122:1428 –1441.

54. Bermudez-Brito, M., Plaza-Diaz, J., Munoz-Quezada, S., Gomez-Llorente, C., & Gil, A. (October 01, 2012). Probiotic mechanisms of action. *Annals of Nutrition and Metabolism*, 61, 2, 160-174.

55. Aureli, P., Capurso, L., Castellazzi, A. M., Clerici, M., Giovannini, M., Morelli, L., Poli, A., Zuccotti, G.V. (2011). Probiotics and health: An evidence-based review. *Pharmacological Research*, 63, 5, 366-376.

56. Gerritsen, J., Timmerman, H. M., Fuentes, S., Minnen, L. P., Panneman, H., Konstantinov, S. R., Rombouts, F. M., Rijkers, G. T. (2011). Correlation between protection against sepsis by probiotic therapy and stimulation of a novel bacterial phylotype. *Applied and Environmental Microbiology*, 77, 21, 7749-7756.

57. Salminen, S., Ouwehand, A., Benno, Y., & Lee, Y. K. (1999). Probiotics: how should they be defined? *Trends in Food Science & Technology, 10*(3), 107-110.

58. Sánchez, B., Delgado, S., Blanco-Míguez, A., Lourenço, A., Gueimonde, M., & Margolles, A. (2017). Probiotics, gut microbiota, and their influence on host health and disease. *Molecular Nutrition & Food Research*, 61, 1- 15

59. Liong, M. T. (2008). Roles of probiotics and prebiotics in colon cancer prevention: Postulated mechanisms and in-vivo evidence. *International Journal of Molecular Sciences*, 9(5), 854-863.

60. Sharafi, H., Alidost, L., Lababpour, A., Shahbani Zahiri, H., Abbasi, H., Vali, H., &

Akbari Noghabi, K. (2013). Antibacterial Activity of Probiotic *Lactobacillus plantarum* HK01: Effect of Divalent Metal Cations and Food Additives on Production Efficiency of Antibacterial Compounds. *Probiotics and Antimicrobial Proteins*, 5, 2, 121-130.

61. Doron, S., Snydman, D. R., & Gorbach, S. L. (2005). *Lactobacillus GG*: Bacteriology and Clinical Applications. *Gastroenterology Clinics of North America*, 34, 3, 483-498.

62. Nase, L., Hatakka, K., Savilahti, E., Saxelin, M., Ponka, A., Poussa, T., Korpela, R., Meurman, J. H. (2001). Effect of Long-Term Consumption of a Probiotic Bacterium, *Lactobacillus rhamnosus* GG, in Milk on Dental Caries and Caries Risk in Children. *Caries Research*, 35, 412-420.

63. Lee, Y. K., & Salminen, S. (2009). Handbook of probiotics and prebiotics. Hoboken, N.J: John Wiley & Sons.

64. Gorbach, S. L. (1990). Lactic Acid Bacteria and Human Health. *Annals of Medicine*, 22, 1, 37-41.

65. Saxelin, M. (2008). Probiotic Formulations and Applications, the Current Probiotics Market, and Changes in the Marketplace: A European Perspective. *Clinical Infectious Diseases* Chicago-, 46.

66. Horvath, A., Dziechciarz, P., & Szajewska, H. (2011). Meta-analysis: Lactobacillus rhamnosus GG for abdominal pain-related functional gastrointestinal disorders in childhood. *Alimentary Pharmacology and Therapeutics*, 33, 12, 1302-1310.

67. Marisel, S. N. (2007). Manifestations, Diagnosis, and Treatment of Strongyloides stercoralis Infection. *Annals of Pharmacotherapy*, 41, 12, 1992-2001.

68. Hawrelak, J. A., Whitten, D. L., & Myers, S. P. (2005). Is *Lactobacillus rhamnosus* GG Effective in Preventing the Onset of Antibiotic-Associated Diarrhoea: A Systematic Review. *Digestion Basel and London*, 72, 1, 51-56.

69. Szajewska, H., Gieruszczak-B. D., & Dylag, M. (2007). Meta-analysis: ondansetron for vomiting in acute gastroenteritis in children. *Alimentary Pharmacology & Therapeutics*, 25, 4, 393-400.

70. Reddy, B. S., & Rivenson, A. (1993). Inhibitory Effect of Bifidobacterium longum on Colon, Mammary, and Liver Carcinogenesis Induced by 2-Amino-3-methylimidazo-[4,5-f]quinoline, a Food Mutagen. *Cancer Research*, 53, 17, 3914.

71. Sanchez, B., Champomier-Verges, M. C., Collado, M. C., Anglade, P., Baraige, F., Sanz,

Y., de, R. G. C. G., Zagorec, M. (2007). Low-pH Adaptation and the Acid Tolerance Response of *Lara Biotype longum. Applied and Environmental Microbiology*, 73, 20, 6450-6459.

72. Gibson, G. R., Hutkins, R., Sanders, M. E., Prescott, S. L., Reimer, R. A., Salminen, S. J., Scott, K., Reid, G. (2017). Expert consensus document: The International Scientific Association for Probiotics and Prebiotics (ISAPP) consensus statement on the definition and scope of prebiotics. *Nature Reviews. Gastroenterology & Hepatology*, 14, 8, 491-502.

73. Herody, C. (2010). The legal status of microbial food cultures in the European Union: An overview. *European Food and Feed Law Review*, 5, 5, 258-269.

74. Schrezenmeir, J., & de, V. M. (2001). Probiotics, prebiotics, and synbiotics-approaching a definition. *American Journal of Clinical Nutrition*, 73.

75. Kumar, H., Salminen, S., Verhagen, H., Verhagen, H., Rowland, I., Heimbach, J., Heimbach, J., Lalonde, M. (2015). Novel probiotics and prebiotics: Road to the market. *Current Opinion in Biotechnology*, 32, 99-103.

76. de, V. M., Stegelmann, A., Richter, B., Fenselau, S., Laue, C., & Schrezenmeir, J. (January 01, 2001). Probiotics-compensation for lactase insufficiency. *American Journal of Clinical Nutrition*, 73.

77. Granato, D., Branco, G. F., Nazzaro, F., Cruz, A. G., & Faria, J. A. (January 01, 2010). Functional Foods and Nondairy Probiotic Food Development: Trends, Concepts, and Products. *Comprehensive Reviews in Food Science and Food Safety*, 9, 3, 292-302.

78. Rivera-Espinoza, Y., & Gallardo-Navarro, Y. (February 01, 2010). Non-dairy probiotic products. *Food Microbiology*, 48, 1, 1.

79. Kumar, M. N. V. R. (2000). A review of chitin and chitosan applications. *Reactive & Functional Polymers*, 46(1), 1-27.

80. Bornkessel, S., Broring, Stefanie, & Omta, S.W.F. (2015). Crossing industrial boundaries at the pharma-nutrition interface in probiotics: a life cycle perspective. *PharmaNutrition* 4 1.

81. Rijkers, G.T., Vos, W.M., de, & Brummer, R.J. (2011). Health benefits and health claims of probiotics: bridging science and marketing. *British Journal of Nutrition* 106, 9.

82. Roberts, Lesley M, McCahon, Deborah, Holder, Roger, Wilson, Sue, & Hobbs, FD

Richard. (2013). A randomised controlled trial of a probiotic 'functional food' in the management of irritable bowel syndrome. *Bmc Gastroenterology*, 13, 1, 1-10

83. Damaceno, Q. S., Souza, J. P., Nicoli, J. R., Paula, R. L., Assis, G. B., Figueiredo, H. C., Azevedo, V., Martins, F. S. (2017). Evaluation of Potential Probiotics Isolated from Human Milk and Colostrum. *Probiotics and Antimicrobial Proteins*, 9, 4, 371-379.

84. E Van Niekerk. (2011). Probiotics in premature infants: focus on necrotising enterocolitis. *South African Journal of Clinical Nutrition*; 24,3 SASPEN 2011 Conference Supplement; S35-S37.) Medpharm Publications (Pty).

85. Sanders, M. E. (2010). Substantiating Health Benefit Claims for Probiotics in the United States. 88-101.

86. Grimoud, J., Durand, H., Courtin, C., Monsan, P., Ouarne, F., Theodorou, V., & Rogues, C. (2010). In vitro screening of probiotic lactic acid bacteria and prebiotic glucooligosaccharides to select effective synbiotics. *Anaerobe*, 16(5), 493-500.

87. Serban, E. D. (2009). Probiotics, prebiotics and synbiotics in inflammatory bowel disease: Are they useful? Medicinski Razgledi. *Supplement*, 48, 2009

88. Patel, S., & Goyal, A. (2012). The current trends and future perspectives of prebiotics research: a review. 3 *Biotech*, 2(2), 115-125.

89. Gomez, B., Gullon, B., Remoroza, C., Schols, H. A., Parajo, J. C., & Alonso, J. L. (2014). Purification, Characterization, and Prebiotic Properties of Pectic Oligosaccharides from Orange Peel Wastes. *Journal of Agricultural and Food Chemistry*, 62(40), 9769-9782.

90. Bosscher, D., Van Loo, J., & Franck, A. (2006). Inulin and oligofructose as prebiotics in the prevention of intestinal infections and diseases. *Nutr Res Rev*, 19(2), 216-226.

91. Gaggìa, F., Mattarelli, P., & Biavati, B. (2010). Probiotics and prebiotics in animal feeding for safe food production. *International Journal of Food Microbiology*, 141, 1.

92. Gibson, G. R., BeatRurty, E. R., Wang, X., & Cummings, J. H. (1995). Selective stimulation of bifidobacteria in the human colon by oligofructose and inulin. *Gastroenterology*, 108, 4, 975-982.

93. Loo, J., Van Craeyveld, V., Courtin, C. M., Delcour, J. A., & Ollevier, F. (2009). Selected nondigestible carbohydrates and prebiotics support the growth of probiotic fish bacteria mono-cultures in vitro. *Journal of Applied Microbiology*, 106(3), 932-940.

94. Kolida, S., & Gibson, G. R. (2011). Synbiotics in health and disease. *Annual Review of Food Science and Technology*, 2, 373-93.

95. Alexiou, H., & Franck, A. (2008). Prebiotic inulin-type fructans: nutritional benefits beyond dietary fibre source. *Nutrition Bulletin*, 33, 3, 227-233.

96. Rurangwa, E., Laranja, J. L., Van, H. R., Delaedt, Y., Geraylou, Z., Van, W. T., Van, L. J., Ollevier, F. (2009). Selected nondigestible carbohydrates and prebiotics support the growth of probiotic fish bacteria mono-cultures *in vitro*. *Journal of Applied Microbiology*, 106, 3, 932-940.

97. Roberfroid, M. (2007). Prebiotics: The Concept Revisited. *Journal of Nutrition Baltimore and Springfield Then Bethesda*, 137, 3.

98. Roberfroid, M. B. (1998). Prebiotics and synbiotics: concepts and nutritional properties. *British Journal of Nutrition*, 80(4), S197-S202.

99. Ziemer, C. J., & Gibson, G. R. (1998). An overview of probiotics, prebiotics and synbiotics in the functional food concept: Perspectives and future strategies. *International Dairy Journal*, 8(5-6), 552 473-479.

100. Fujimori, S., Gudis, K., Mitsui, K., Seo, T., Yonezawa, M., Tanaka, S., Tatsuguchi, A., & Sakamoto, C. (2009). A randomized controlled trial on the efficacy of synbiotic versus probiotic or prebiotic treatment to improve the quality of life in patients with ulcerative colitis. *Nutrition*, 25(5), 520-525.

101. Saulnier, D. M. A., Gibson, G. R., & Kolida, S. (2008). *In vitro* effects of selected synbiotics on the human faecal microbiota composition. *Fems Microbiology Ecology*, 66(3), 516-527.

102. Fooks, L. J., Fuller, R., & Gibson, G. R. (1999). Prebiotics, probiotics and human gut microbiology. *International Dairy Journal*, 9, 1, 53-61.

103. Painter, Paul C.; Coleman, Michael M. (1997). Fundamentals of polymer science: an introductory text. *Lancaster*, 1.

104. McCrum, N. G.; Buckley, C. P.; Bucknall, C. B. (1997). *Principles of polymer engineering*. Oxford ; New York: Oxford University Press.

105. Barton, A. F. M. (1991). CRC Handbook of Solubility Parameters and Other Cohesion Parameters: Second Edition. Bosa Roca: CRC Press.

106. Billmeyer, F. W. . (1984). Textbook of polymer science. New York,N.Y: Wiley.

107. Immergut, E. H., Grulke, E. A., & Brandrup, J. (2008). Polymer handbook. New York: Wiley.

108. Berger, J.; Reist, M.; Mayer, J. M.; Felt, O.; Peppas, N. A.; Gurny, R., Structure and interactions in covalently and ionically crosslinked chitosan hydrogels for biomedical applications (2004). *Eur J Pharm Biopharm*, 57, (1), 19-34.

109. Yahia, LHocine. 2015. "History and Applications of Hydrogels". *Journal of Biomedical Sciences*. 04 (02).

110. Kammer, H. W. (1986). Thermodynamics of polymer miscibility. *Acta Polymerica*, 37, 1, 1-6.

111. Collins, E. A., Bareš, J., & Billmeyer, F. W. (1973). Experiments in polymer science. New York: Wiley.

112. Flory, P. J. (2010). Principles of Polymer Chemistry. Cornell Univ. Press.

113. Lindman, B., Khan, A., Marques, E., Miguel, M. G., Piculell, L., & Thalberg, K. (1993). Phase behavior of polymer-surfactant systems in relation to polymer-polymer and surfactant-surfactant mixtures. *Pure and Applied Chemistry*. 65, 953-958.

114. Edmond, E., & Ogston, A. G. (1968). An approach to the study of phase separation in ternary aqueous systems. *Biochemical Journal*, 109, 4, 569-576.

115. R.L. Scott (1949). J. Chem. Phys. 17279.

116. Koningsveld, R., Stockmayer, W. H., & Nies, E. (2008). Polymer phase diagrams: A textbook. Oxford: Oxford Univ. Press.

117. Piculell, L., & Lindman, B. (1992). Association and segregation in aqueous polymer/polymer, polymer/surfactant, and surfactant/surfactant mixtures: similarities and differences. *Advances in Colloid and Interface Science*, 41, 149-178.

118. Olabisi, O., Robeson, L. M., & Shaw, M. T. (1983). Polymer-polymer miscibility. New York: Academic Press.

119. Champagne, C. P., & Fustier, P. (2007). Microencapsulation for the improved delivery of bioactive compounds into foods. *Current Opinion in Biotechnology*, 18, 2, 184-90.

120. Meiners, J.-A. (2009). Micro-Encapsulation of Probiotics.

121. Đorđević, V., Paraskevopoulou, A., Mantzouridou, F., Lalou, S., Pantić, M., Bugarski, B., & Nedović, V. (2016). *Encapsulation Technologies for Food Industry*.

122. Volodkin, D. V., Petrov, A. I., Prevot, M., & Sukhorukov, G. B. (2004). Matrix

Polyelectrolyte Microcapsules: New System for Macromolecule Encapsulation. *Langmuir*, 20, 8, 3398-3406.

123. McClements, D. J. (2015). Encapsulation, protection, and release of hydrophilic active components: Potential and limitations of colloidal delivery systems. *Advances in Colloid and Interface Science*, 219, 27-53.

124. Bourtoom, T. (2008). Edible films and coatings: characteristics and properties. *Int Food Res J, 15*, 237-248.

125. Sannino, A., Demitri, C., & Madaghiele, M. (2009). Biodegradable Cellulose-based Hydrogels: Design and Applications. *Materials, 2*(2), 353-373.

126. Buwalda, S. J., Boere, K. W. M., Dijkstra, P. J., Feijen, J., Vermonden, T., & Hennink, W. E. (2014). Hydrogels in a historical perspective: From simple networks to smart materials. *Journal of Controlled Release*, 190, 254-273.

127. Vemmer, M., & Patel, A.V. (2013). Review of encapsulation methods suitable for microbial biological control agents. *Biological Control*, 67, 380–389.

128. Gharsallaoui, A., Roudaut, G., Chambin, O., Voilley, A., & Saurel, R. (2007). Applications of spray-drying in microencapsulation of food ingredients: An overview. Food Research International, 40, 9, 1107-11

129. Donath, E., Sukhorukov, G. B., Caruso, F., Davis, S. A., & Möhwald, H. (1998). Novel Hollow Polymer Shells by Colloid-Templated Assembly of Polyelectrolytes. Angewandte Chemie International Edition, 37, 16, 2201-2205.

130. de, K. C. G., Weinbreck, F., & de, V. R. (2004). Complex coacervation of proteins and anionic polysaccharides. *Current Opinion in Colloid & Interface Science*, 9, 5, 340-349.

131. Kailasapathy, K. (2002). Microencapsulation of probiotic bacteria: technology and potential applications. Wymondham, Norfolk Horizon Scientific.

132. Perignon, C., Poncelet, D., Perignon, C., Ongmayeb, G., Neufeld, R., & Frere, Y. (2015). Microencapsulation by interfacial polymerisation: Membrane formation and structure. *Journal of Microencapsulation*, 32, 1, 1-15.

133. Gill, I., & Ballesteros, A. (2000). Bioencapsulation within synthetic polymers (Part 1): sol-gel encapsulated biologicals. *Trends in Biotechnology*, 18, 7, 282-96.

134. Vorlop, K.-D., Muscat, A., & Beyersdorf, J. (1992). Entrapment of microbial cells within polyurethane hydrogel beads with the advantage of low toxicity. *Biotechnology*

Techniques, 6, 6, 483-488.

135. Rathore, S., Desai, P. M., Liew, C. V., Chan, L. W., & Heng, P. W. (2013). Microencapsulation of microbial cells. *Journal of Food Engineering*, 116, 2, 369-381.

136. Poncelet, D., Neufeld, R.J. (1996). Fundamentals of dispersion in encapsulation technology, in: Immobilized Cells - Basics and Applications: Proceedings of an International Symposium Organized Under Auspices of The Working Party on Applied Biocatalysis of the European Federation of Biotechnology Noordwijkerhout. *Elsevier*, pp. 47–54.

137. Kanmani, P., Kumar, R. S., Yuvaraj, N., Paari, K. A., Pattukumar, V., & Arul, V. (2011). Cryopreservation and microencapsulation of a probiotic in alginate-chitosan capsules improves survival in simulated gastrointestinal conditions. *Biotechnology and Bioprocess Engineering*, 16(6), 1106-1114.

138. F. Gibbs B F, Kermasha S, Alli Inteaz, Mulligan C N. (2009). "Encapsulation in the food industry: a review". *International Journal of Food Sciences and Nutrition.* 50 (3): 213-224.

139. Heenan, C. N., Adams, M. C., Hosken, R. W., & Fleet, G. H. (2004). Survival and sensory acceptability of probiotic microorganisms in a nonfermented frozen vegetarian dessert. *Lwt - Food Science and Technology*, 37, 4, 461-466.

140. Hough, G., Puglieso, M. L., Sanchez, R., & da, S. O. M. (1999). Sensory and Microbiological Shelf-Life of a Commercial Ricotta Cheese. *Journal of Dairy Science*, 82, 3, 454-459.

141. Altamirano-Fortoul, R., Moreno-Terrazas, R., Quezada-Gallo, A., & Rosell, C. M. (2012). Viability of some probiotic coatings in bread and its effect on the crust mechanical properties. *Food Hydrocolloids*, 29, 1, 166-174.

142. Sakai, K., Mishima, C, Tachiki, T., Kumagai, H. and Tochikura,T. (1987), Mortality of bifidobacteria in boiled yogurt. J. *Fermented Technol*. 65(2), 215-220.

143. Mosilhey, S. H. (2003). Influence of different capsule materials on the physiological properties of microencapsulated *Lactobacillus acidophilus*. University, Diss., 2003--Bonn.

144. Santivarangkna, C., Kulozik, U., & Foerst, P. (2007). Alternative Drying Processes for the Industrial Preservation of Lactic Acid Starter Cultures. *Biotechnology Progress*, 23,

2, 302.

145. Mathipa, M, & Thantsha, M. (2015). Cocktails of probiotics pre-adapted to multiple stress factors are more robust under simulated gastrointestinal conditions than their parental counterparts and exhibit enhanced antagonistic capabilities against *Escherichia coli* and *Staphylococcus aureus*. *Gut Pathogens*. 7, 1-14.

146. Nematollahia, A. S., Mortazavian, S., Mohammad A., & Jazaeri, S. (2016). Viability of probiotic bacteria and some chemical and sensory characteristics in cornelian cherry juice during cold storage. *Electronic Journal of Biotechnology*. 21, 49-53.

147. Soukoulis, C., Behboudi-Jobbehdar, S., Yonekura, L., Parmenter, C., & Fisk, I. (2014). Impact of Milk Protein Type on the Viability and Storage Stability of Microencapsulated *Lactobacillus acidophilus NCIMB* 701748 Using Spray Drying. *Food and Bioprocess Technology: an International Journal*, 7, 5, 1255-1268.

148. Chang, C. Y., & Zhang, L. N. (2011). Cellulose-based hydrogels: Present status and application prospects. *Carbohydrate Polymers*, 84(1), 40-53.

149. Bosnea, L.A., Moschakis, T., Biliaderis, C.G. (2014). Complex coacervation as a novel microencapsulation technique to improve viability of probiotics under different stresses. *Food and Bioprocess Technology* 7 (10), 2767–2781.

150. Oh, J.K., Drumright, R., Siegwart, D.J., Matyjaszewski, K. (2008). The development of microgels/nanogels for drug delivery applications. *Progress in Polymer Science* 33 (4), 448–477.

151. Chen, L., & Subirade, M. (2005). Chitosan/ β-lactoglobulin core-shell nanoparticles as nutraceutical carriers. *Biomaterials*, 26, 30, 6041-6053.

152. Walter, H. (1978). Cell partitioning in two-polymer aqueous phase systems. *Trends in Biochemical Sciences* 3, 97–100.

153. Doublier, J.L., Garnier, C., Renard, D., Sanchez, C. (2000). Protein-polysaccharide interactions. *Current Opinion in Colloid & Interface Science* 5 (3–4), 202–214.

154. Fang, Y.P., Li, L.B., Inoue, C., Lundin, L., Appelqvist, I. (2006). Associative and segregative phase separations of gelatin/kappa-carrageenan aqueous mixtures. *Langmuir* 22 (23), 9532–9537.

155. Hanani, Z.A.N., Roos, Y.H., Kerry, J.P. (2014). Use and application of gelatin as potential biodegradable packaging materials for food products. *International Journal of*

Biological Macromolecules 71, 94–102.

156. Soukoulis, C., Singh, P., Macnaughtan, W., Parmenter, C., & Fisk, I. D. (2016). Compositional and physicochemical factors governing the viability of *Lactobacillus rhamnosus* GG embedded in starch-protein based edible films. *Food Hydrocolloids*, 52, 876-887.

157. Muranyi, P. (2013). Functional Edible Coatings for Fresh Food Products. *J Food Process Technol, 4*, e114. 22.

158. Aiache, J. M. (1991). The Ideal Drug Delivery System: A Look into the Future. *Journal of Aerosol Medicine*, 4, 4, 323-334.

159. Corona-Hernandez, R. I., Alvarez-Parrilla, E., Lizardi-Mendoza, J., Islas-Rubio, A. R., de la Rosa, L. A., & Wall-Medrano, A. (2013). Structural Stability and Viability of Microencapsulated Probiotic Bacteria: A Review. *Comprehensive Reviews in Food Science and Food Safety, 12*(6), 614-628.

160. Keeney, M., Jiang, X. Y., Yamane, M., Lee, M., Goodman, S., & Yang, F. (2015). Nanocoating for biomolecule delivery using layer-by-layer self-assembly. *Journal of Materials Chemistry*. *B*, 3, 45, 8757-8770.

161. Ma, X., Vacek, I., & Sun, A. (2009). Generation of Alginate-Poly-L-Lysine-Alginate (APA) Biomicrocapsules: The Relationship Between the Membrane Strength and the Reaction Conditions. *Artificial Cells, Blood Substitutes, and Biotechnology*, 22, 1, 43-69.

162. Sakai, S., Mu, C., Kawabata, K., Hashimoto, I., & Kawakami, K. (2006). Biocompatibility of subsieve-size capsules versus conventional-size microcapsules. *Journal of Biomedical Materials Research Part A*, 2, 394-398.

163. Gasperini, L., Mano, J. F., & Reis, R. L. (2014). Natural polymers for the microencapsulation of cells. *Journal of the Royal Society, Interface*, 11, 100.

164. Martin, D. R., Ramalho, M., Matos, A. P., Altun, E., & Semelka, R. C. (2015). *Gastrointestinal tract*. 593-744

165. Klancke J (2003). Dissolution testing of orally disintegrating tablets. Dissolution Technologies, 6:6–8.

166. Jasion, V. S, & Burnett, B. P. (2015). Survival and digestibility of orally-administered immunoglobulin preparations containing IgG through the gastrointestinal tract in humans. *Nutrition Journal*. 14.

167. Amakiri, A.C. & Thantsha, M.S. (2016). Survival of *Bifidobacterium longum* LMG 13197 microencapsulated in Vegetal or Vegetal-inulin matrix in simulated gastrointestinal fluids and yoghurt. *Springerplus* 5, 1343.

168. Strojny, L., Bomba, A., Hijova, E., Chmelarova, A., Mojzisova, G., Bertkova, I., Koprovicova, J., Pomfy, M., Strompfova, V., & Molokacova, M. (2011). Effects of a probiotic in combination with prebiotics on intestinal lactobacilli and coliforms and activities of bacterial enzymes in 1,2-dimethylhydrazine exposed rats. *Czech Journal of Animal Science*, 56(3), 99-106.

169. Vieira, M. R., Galvao, L. C., & Fernandes, M. I. M. (2000). Relation of the disaccharidases in the small intestine of the rat to the degree of experimentally induced iron-deficiency anemia. *Brazilian journal of medical and biological research*, 33, 5, 539-44.

170. Xing, Z., Tang, W., Geng, W., Zheng, Y., & Wang, Y. (2017). In vitro and in vivo evaluation of the probiotic attributes of *Lactobacillus kefiranofaciens* XL10 isolated from Tibetan kefir grain. *Applied Microbiology and Biotechnology*, 101, 6, 2467-2477.

171. Louis, P., Scott, K. P., Duncan, S. H., & Flint, H. J. (2007). Understanding the effects of diet on bacterial metabolism in the large intestine. *Journal of Applied Microbiology*, 102, 5, 1197-1208.

172. Jaime-Fonseca, M. R., Gouseti, O., Fryer, P. J., Wickham, M. S. J., & Bakalis, S. (2016). Digestion of starch in a dynamic small intestinal model. *European Journal of Nutrition*, 55, 8, 2377-2388.

173. Minekus, M., Alminger, M., Alvito, P., Ballance, S., Bohn, T., Bourlieu, C., Carriere, F., Boutrou, R., Corredig, M., Dupont, D., Dufour, C., Egger, L., Golding, M., Karakaya, S., Kirkhus, B., Le Feunteun, S., Lesmes, U., Macierzanka, A., Mackie, A., Marze, S., McClements, D. J., Menard, O., Recio, I., Santos, C. N., Singh, R. P., Vegarud, G. E., Wickham, M. S. J., Weitschies, W., & Brodkorb, A. (2014). A standardised static in vitro digestion method suitable for food - an international consensus. *Food & Function*, 5(6), 1113-1124.

174. Lahtinen, S., Ouwehand, A., Collado, M. C., Salminen, S., Vesterlund, S., Tang, M., & Satokari, R. (2008). *Mechanisms of Probiotics*. 377-440.

175. Ingels, F., Deferme, S., Destexhe, E., Oth, M., Van, M. G., & Augustijns, P. (2002).

Simulated intestinal fluid as transport medium in the Caco-2 cell culture model. *International Journal of Pharmaceutics*, 232, 183-192.

176. Klemm, D., Philipp, B., Heinze, T., Heinze, U., Wagenknect, W., & John Wiley & Sons. (1998). Comprehensive cellulose chemistry: Vol. 1. *Weinheim: Wiley-VCH*.

177. O'sullivan, A. C. (1997). Cellulose: the structure slowly unravels. *Cellulose*. 4, 173.

178. Lindman, B., Karlström, G., & Stigsson, L. (2010). On the mechanism of dissolution of cellulose. *Journal of Molecular Liquids*, 156, 1, 76.

179. Klemm, D., Heublein, B., Fink, H. P., & Bohn, A. (2005). Cellulose: Fascinating biopolymer and sustainable raw material. *Angewandte Chemie-International Edition, 44*(22), 3358-3393.

180. Yamashiki, T., Matsui, T., Saitoh, M., Okajima, K., Kamide, K., & Sawada, T. (1990). Characterisation of cellulose treated by the steam explosion method. Part 1: Influence of cellulose resources on changes in morphology, degree of polymerisation, solubility and solid structure. *British Polymer Journal*, 22, 1, 73-83.

181. Medronho, B., Romano, A., Miguel, M. G., Stigsson, L., & Lindman, B. (2012). Rationalizing cellulose (in)solubility: reviewing basic physicochemical aspects and role of hydrophobic interactions. *Cellulose*, 19, 3, 581-587.

182. Reese, E. T., Siu, R. G., & Levinson, H. S. (1950). The biological degradation of soluble cellulose derivatives and its relationship to the mechanism of cellulose hydrolysis. *Journal of Bacteriology*, 59, 4, 485-97.

183. Wach, R. A., Mitomo, H., Yoshii, F., & Kume, T. (2001). Hydrogel of Biodegradable Cellulose Derivatives. II. Effect of Some Factors on Radiation-Induced Crosslinking of CMC. *Journal of Applied Polymer Science*, 81, 3030-3037.

184. Heinze, T., & Koschella, A. (2005). Carboxymethyl Ethers of Cellulose and Starch - A Review. *Macromolecular Symposia*, 223, 1, 13-40.

185. Fujita, H., & Homma, T. (1954). Viscosity behavior of sodium carboxy methyl cellulose in water at high dilutions. *Journal of Colloid Science*, 9, 6, 591-601.

186. Alexandar Metodiev Zhivkov (2013). Electric Properties of Carboxymethyl Cellulose, Cellulose - Fundamental Aspects, Dr. Theo G.M. Van De Ven (Ed.), *InTech*, DOI: 10.5772/56935.

187. Maftoonazad, N., Ramaswamy, H. S., & Marcotte, M. (2008). Shelf-life extension of

peaches through sodium alginate and methyl cellulose edible coatings. *International Journal of Food Science & Technology*, 43, 6, 951-957.

188. Eyler, R. W., Klug, E. D., & Diephuis, F. (1947). Determination of Degree of Substitution of Sodium Carboxymethylcellulose. *Analytical Chemistry*, 19, 1, 24-27.

189. Lohani, A., Singh, G., Bhattacharya, S. S., Hegde, R. R., & Verma, A. (2016). Tailored-interpenetrating polymer network beads of kappa-carrageenan and sodium carboxymethyl cellulose for controlled drug delivery. *Journal of Drug Delivery Science and Technology*, 31, 53- 64.

190. Myasoyedova, V. V., Zavyalov, N. A., Pokrovsky, S. A., & Krestov, G. A. (1990). Thermochemical characteristics of solutions of cellulose and its ethers and esters. *Thermochimica Acta*, 169, 111-119.

191. Ravi, K. M. N. (2000). A review of chitin and chitosan applications. *Reactive and Functional Polymers*, 46, 1, 1-27.

192. Dutta, P. K., Dutta, J., & Tripathi, V. S. (2004). Chitin and chitosan: Chemistry, properties and applications. *Journal of Scientific & Industrial Research*, 63(1), 20-31.

193. Rinaudo, M. (2006). Chitin and chitosan: Properties and applications. *Progress in Polymer Science*, 31, 7, 603-632.

194. Pillai, C. K. S., Paul, W., & Sharma, C. P. (2009). Chitin and chitosan polymers: Chemistry, solubility and fiber formation. *Progress in Polymer Science*, 34(7), 641-678.

195. Agnihotri, S. A., Mallikarjuna, N. N., & Aminabhavi, T. M. (2004). Recent advances on chitosan-based micro- and nanoparticles in drug delivery. *Journal of Controlled Release*, 100, 1, 5-28.

196. Illum, L. (1998). Chitosan and its use as a pharmaceutical excipient. *Pharmaceutical Research*, 15, 9, 1326-31.

197. Sorlier, P., Viton, C., & Domard, A. (2002). Relation between solution properties and degree of acetylation of chitosan: role of aging. *Biomacromolecules*, 3, 6.

198. Kumar, M. N. V. R. (2000). A review of chitin and chitosan applications. *Reactive & Functional Polymers*, 46(1), 1-27.

199. Liang, H.-C., Chang, W.-H., Lin, K.-J., & Sung, H.-W. (2003). Genipin-crosslinked gelatin microspheres as a drug carrier for intramuscular administration: In vitro and in vivo studies. *Journal of Biomedical Materials Research*, 65, 2, 271.

200. Jiang, F., Jiang, R., Zhu, X., Zhang, X., & Zhan, Z. (2013). Genipin inhibits TNF-α-induced vascular smooth muscle cell proliferation and migration via induction of HO-1. *Plos One*, 8, 8.

201. Yuan, Y., Chesnutt, B. M., Utturkar, G., Haggard, W. O., Yang, Y., Ong, J. L., & Bumgardner, J. D. (2007). The effect of cross-linking of chitosan microspheres with genipin on protein release. *Carbohydrate Polymers*, 68(3), 561-567.

202. Muzzarelli, R. A. A. (2009). Genipin-crosslinked chitosan hydrogels as biomedical and pharmaceutical aids. *Carbohydrate Polymers*, 77(1), 1-9.

203. Koo, H.-J., Lim, K.-H., Jung, H.-J., & Park, E.-H. (2006). Anti-inflammatory evaluation of gardenia extract, geniposide and genipin. *Journal of Ethnopharmacology*, 103, 3, 496-500.

204. Butler, M. F., Ng, Y. F., & Pudney, P. D. A. (2003). Mechanism and kinetics of the crosslinking reaction between biopolymers containing primary amine groups and genipin. *Journal of Polymer Science Part a-Polymer Chemistry*, 41(24), 3941-3953.

205. Wang, P., Zhang, A., Jin, Y., Zhang, Q., Zhang, L., Peng, Y., & Du, S. (2014). Molecularly imprinted layer-coated hollow polysaccharide microcapsules toward gate-controlled release of water-soluble drugs. *Rsc Advances*, 4, 50, 26063.

206. Klein, M. P., Hackenhaar, C. R., Lorenzoni, A. S. G., Rodrigues, R. C., Costa, T. M. H., Ninow, J. L., & Hertz, P. F. (2016). Chitosan crosslinked with genipin as support matrix for application in food process: Support characterization and beta-D-galactosidase immobilization. *Carbohydrate Polymers*, 137, 184-190.

207. Mi, F. L., Shyu, S. S., & Peng, C. K. (2005). Characterization of ring-opening polymerization of genipin and pH-dependent cross-linking reactions between chitosan and genipin. *Journal of Polymer Science Part A: Polymer Chemistry*, 43, 10, 1985-2000.

208. Coma, V., Sebti, I., Pardon, P., Pichavant, F. H., & Deschamps, A. (2003). Film properties from crosslinking of cellulosic derivatives with a polyfunctional carboxylic acid. *Carbohydrate Polymers, 51*(3), 265-271.

209. Demitri, C., Del Sole, R., Scalera, F., Sannino, A., Vasapollo, G., Maffezzoli, A., Ambrosio, L., & Nicolais, L. (2008). Novel cellulose-based superabsorbent hydrogels crosslinked with citric acid. *Journal of Applied Polymer Science, 110*(4), 2453-2460.

210. Dinelaker, B., Romheld, V. & Marschner, H. (1989), Citric acid excretion and

precipitation of calcium citrate in the rhizosphere of white lupin (*Lupinus albus* L.). *Plant, Cell & Environment*, 12: 285–292.

211. Glusker, J. P. (1980). Citrate Conformation and Chelation-Enzymatic Implications. *Accounts of Chemical Research, 13*(10), 345-352.

212. Yahia, LHocine. 2015. "History and Applications of Hydrogels". *Journal of Biomedical Sciences*. 04 (02).

213. Del Valle, E. M. M. (2004). Cyclodextrins and their uses: a review. *Process Biochemistry*, 39(9), 1033-1046.

214. Szejtli, J. (1998). Introduction and general overview of cyclodextrin chemistry. *Chemical Reviews*, 98(5), 1743-1753.

215. Loftsson, T., Vogensen, S. B., Brewster, M. E., & Konráðsdóttir, F. (2007). Effects of cyclodextrins on drug delivery through biological membranes. *Journal of Pharmaceutical Sciences*, 96, 10, 2532-2546.

216. Valente, A. J. M., Nilsson, M., & Söderman, O. (2005). Interactions between n-octyl and n-nonyl β- d-glucosides and α- and β-cyclodextrins as seen by self-diffusion NMR. *Journal of Colloid and Interface Science*, 281, 1, 218-224.

217. Malik, N. S., Ahmad, M., & Minhas, M. U. (2017). Cross-linked β-cyclodextrin and carboxymethyl cellulose hydrogels for controlled drug delivery of acyclovir. *Plos One*, 12, e0172727

218. Ayala-Zavala, J. F., Soto-Valdez, H., Gonzalaz-Leon, A., Alvarez-Parrilla, E., Martin-Belloso, O., & Gonzalez-Aguilar, G. A. (2008). Microencapsulation of cinnamon leaf (Cinnamomum zeylanicum) and garlic (Allium sativum) oils in beta-cyclodextrin. *Journal of Inclusion Phenomena and Macrocyclic Chemistry, 60*(3-4), 359-368.

219. Spears, J. K., Karr-Lilienthal, L. K., & Fahey, G. C. (2005). Influence of supplemental high molecular weight pullulan or gamma-cyclodextrin on ileal and total tract nutrient digestibility, fecal characteristics, and microbial populations in the dog. *Archives of Animal Nutrition*, 59(4), 257-270.

220. Fenyvesi, E., Vikmon, M., & Szente, L. (2016). Cyclodextrins in Food Technology and Human Nutrition: Benefits and Limitations. *Crit Rev Food Sci Nutr*, 56(12), 1981-2004.

221. Bellringer, M. E., Smith, T. G., Read, R., Gopinath, C., & Olivier, P. (1995). β-Cyclodextrin: 52-Week toxicity studies in the rat and dog. *Food and Chemical*

Toxicology, 33, 5, 367-376.

222. Wang, Y., Krull, I. S., Liu, C., & Orr, J. D. (2003). Derivatization of phospholipids. *Journal of Chromatography. B, Analytical Technologies in the Biomedical and Life Sciences*, 793, 1, 3-14.

223. Contarini, G., & Povolo, M. (2013). Phospholipids in milk fat: Composition, biological and technological significance, and analytical strategies. *International Journal of Molecular Sciences*, 14, 2, 2808-2831.

224. Deenen, L.L.M. van. (1966). Phospholipids and biomembranes. *Elsevier*.

225. Dai, L., Sun, C., Wang, D., Gao, Y., & Fraceto, L. (2016). The Interaction between Zein and Lecithin in Ethanol-Water Solution and Characterization of Zein–Lecithin Composite Colloidal Nanoparticles. *Plos One*, 11, 11.

226. Chuah, A. M., Kuroiwa, T., Ichikawa, S., Kobayashi, I., & Nakajima, M. (2009). Formation of Biocompatible Nanoparticles via the Self-Assembly of Chitosan and Modified Lecithin. *Journal of Food Science*, 74, 1.

227. Dickinson, E., & Yamamoto, Y. (1996). Viscoelastic Properties of Heat-Set Whey Protein-Stabilized Emulsion Gels with Added Lecithin. *Journal of Food Science Chicago-*, 61, 4, 811-816.

228. Singh, H., Ye, A., & Horne, D. (2009). Structuring food emulsions in the gastrointestinal tract to modify lipid digestion. *Progress in Lipid Research*, 48, 2, 92-100.

229. Havea, P. (2006). Protein interactions in milk protein concentrate powders. *International Dairy Journal*, 16, 5, 415-422.

230. Hall, W. L., Millward, D. J., Long, S. J., & Morgan, L. M. (2003). Casein and whey exert different effects on plasma amino acid profiles, gastrointestinal hormone secretion and appetite. *The British Journal of Nutrition*, 89, 2, 239-48.

231. Doherty, S. B., Auty, M. A., Stanton, C., Ross, R. P., Fitzgerald, G. F., & Brodkorb, A. (2012). Survival of entrapped *Lactobacillus rhamnosus* GG in whey protein micro-beads during simulated ex vivo gastro-intestinal transit. *International Dairy Journal*, 22, 1, 31-43.

232. Doherty, S. B., Gee, V. L., Ross, R. P., Stanton, C., Fitzgerald, G. F., & Brodkorb, A. (2011). Development and characterisation of whey protein micro-beads as potential matrices for probiotic protection. *Food Hydrocolloids*, 25, 6, 1604-1617.

233. Madureira, A. R., Amorim, M., Gomes, A. M., Pintado, M. E., & Malcata, F. X. (2011). Protective effect of whey cheese matrix on probiotic strains exposed to simulated gastrointestinal conditions. *Food Research International*, 44(1), 465-470.

234. Heidebach, T., Forst, P., & Kulozik, U. (2009). Microencapsulation of probiotic cells by means of rennet-gelation of milk proteins. *Food Hydrocolloids*, 23, 7, 1670.

235. De, Castro, C. F. P., Silva, C. D. R. E., Fritzen-Freire, C. B., Lorenz, J. G., & Sant'Anna, E. S. (2012). Bifidobacterium Bb-12 microencapsulated by spray drying with whey: Survival under simulated gastrointestinal conditions, tolerance to NaCl, and viability during storage. *Journal of Food Engineering*, 113, 2, 186-193.

236. Fernandez-Barbero, A., Suarez, I.J., Sierra-Martin, B., Fernandez-Nieves, A., de las Nieves, F.J., Marquez, M., et al. (2009). Gels and microgels for nanotechnological applications. *Advances in Colloid and Interface Science* 147–48, 88–108.

237. Kumari, A., Yadav, S. K., & Yadav, S. C. (2010). Biodegradable polymeric nanoparticles based drug delivery systems. *Colloids and Surfaces B: Biointerfaces*, 75, 1, 1-18.

238. Anal, A. K., & Singh, H. (2007). Recent advances in microencapsulation of probiotics for industrial applications and targeted delivery. *Trends in Food Science & Technology*, 18, 5, 240-251.

239. Steed, K., & Atomic Weapons Research Establishment, Aldermaston, Eng. (1970). Thermogravimetric Analysis.

240. El-Sayed, S., Mahmoud, K. H., Fatah, A. A., & Hassen, A. (2011). DSC, TGA and dielectric properties of carboxymethyl cellulose/polyvinyl alcohol blends. *Physica B: Condensed Matter*, 451 406, 4068-4076.

241. Broido, A. (1969). A simple, sensitive graphical method of treating thermogravimetric analysis data. *Journal of Polymer Science Part A-2: Polymer Physics*, 7, 10, 1761-1773.

242. Colthup, N. B., Daily, L. H., & Wiberley, S. E. (1975). "Introduction to infrared and raman spectroscopy", Academic Press, New York.

243. Lambert, J. B. (1987). "Introduction to organic spectroscopy" Macmillan, New York.

244. Koenig, J. L. (1984). Fourier transform infrared spectroscopy of polymers. *Advances in Polymer Science*. 54 (1984), 87-154.

245. Christy, A. A., Ozaki, Y., & Gregoriou, V. G. (2001). Modern Fourier transform

infrared spectroscopy. Amsterdam: *Elsevier*.

246. Hayat, M. A. (1978). Principles and techniques of scanning electron microscopy: Biological applications. Vol. 6. New York: Van Nostrand Reinhold.

247. Nicodemus, G. D., & Bryant, S. J. (2008). Cell Encapsulation in Biodegradable Hydrogels for Tissue Engineering Applications. *Tissue Engineering, Part B: Reviews*, 14, 2, 149-165.

248. Miles, A. A., Misra, S. S., & Irwin, J. O. (1938). The estimation of the bactericidal power of the blood. *Journal of Hygiene, 38*(6), 732-749.

249. Brew, J. D. (1914). A comparison of the microscopical method and the plate method of counting bacteria in milk. Geneva, N.Y: New York Agricultural Experiment Station.

250. Frankel, S. L., Binder, B. J., Chisholm, S. W., & Shapiro, H. M. (1990). A high-sensitivity flow cytometer for studying picoplankton.

251. Wyllie, A. H. (1987). The flow cytometer. *British Medical Journal* (clinical Research Ed.), 294, 6565.

252. Baschong, W., Landmann, L., & Aebi, U. (2006). Fluorescence Microscopy. Cell Biology: A Laboratory Hand Book, 5-17.

253. Janmey, P. A., & Schliwa, M. (2008). Rheology. *Current Biology*, 18, 15.

Part II - Papers

Paper I

Development of carboxymethyl cellulose-chitosan hybrid micro- and macroparticles for encapsulation of probiotic bacteria

P. Singh [a], B. Medronho [b,*], L. Alves [a], G.J. da Silva [c], M.G. Miguel [a], B. Lindman [a,d]

[a] CQC, University of Coimbra, Department of Chemistry, 3004-535 Coimbra, Portugal
[b] Faculty of Sciences and Technology (MeditBio), Ed. 8, University of Algarve, Campus de Gambelas, 8005-139 Faro, Portugal
[c] Faculty of Pharmacy and Center for Neurosciences and Cell Biology, University of Coimbra, Health Sciences Campus, 3000-5548 Coimbra, Portugal
[d] FSCN, Mid Sweden University, SE-851 70 Sundsvall, Sweden

ARTICLE INFO

ABSTRACT

Novel carboxymethyl cellulose-chitosan (CMC-Cht) hybrid micro- and macroparticles were successfully prepared in aqueous media either by drop-wise addition or via nozzle-spray methods. The systems were either physically or chemically crosslinked using genipin as the reticulation agent. The macroparticles (ca. 2 mm) formed are found to be essentially of the core-shell type, while the microparticles (ca. 5 μm) are apparently homogeneous. The crosslinked particles are robust, thermally resistant and less sensitive to pH changes. On the other hand, the physical systems are pH sensitive presenting a remarkable swelling at pH 7.4, while little swelling is observed at pH 2.4. Furthermore, model probiotic bacteria (*Lactobacillus rhamnosus* GG) was for the first time successfully encapsulated in the CMC-Cht based particles with acceptable viability count. Overall, the systems developed are highly promising for probiotic encapsulation and potential delivery in the intestinal tract with the purpose of modulating gut microbiota and improving human health.

1. Introduction

Delivery systems for food and biomedical applications are balanced approaches comprising biology, chemistry and engineering (Saarela, Mogensen, Fonden, Matto, & Mattila-Sandholm, 2000). Designing a delivery vehicle capable to overcome the physiological variations (i.e. temperature, pH, ionic strength, etc) with an efficient approach and without any harmful effect to the cells and the tissues is a challenging task. Important candidates for encapsulation and delivery in the gut are probiotic bacteria which are living microorganisms shown to provide beneficial health effects to the host by replenishing the natural gastrointestinal microbiota (Holzapfel, Haberer, Snel, Schillinger, & Huis in't Veld, 1998; Pamer, 2016; Sánchez et al., 2017).

However, the survival rate of probiotic bacteria should be within a certain limit not only while incorporated in a formulation process but also in both *in vitro* and *in vivo* situations (Tripathi & Giri, 2014). According to the Food and Agriculture Organization and the World Health Organization, the minimum number of bacteria needed to provide any desired effect is suggested to be 10^6–10^7 CFU/mL (CFU is known as colony-forming units). There are different formulations to deliver the probiotics, varying in the viability, advantages and effectiveness of bacterial cells to the human intestine (Govender et al., 2014; Martin, Lara-Villoslada, Ruiz, & Morales, 2015). The encapsulation methods may involve immobilization in a matrix using spray drying, emulsion, extrusion, gelation techniques or coating of the microorganism in multilayer systems (Haffner, Diab, & Pasc, 2016; Krasaekoopt, Bhandari, & Deeth, 2003; Soukoulis, Singh, Macnaughtan, Parmenter, & Fisk, 2016). In this respect, bio-based hydrogels (coacervation process) are being widely used as efficient vehicles to deliver therapeutic agents due to their biocompatibility and biodegradability (Haffner et al., 2016; Kanmani et al., 2011; Silva et al., 2013). These systems are typically hydrophilic three-dimensional matrices capable to entrap different molecules. Natural and synthetic hydrogels are used in products in a number of biological and environmental areas (Buwalda et al., 2014). What makes the delivery through hydrogel-based systems more exciting is that they can exhibit a wide variety of "smart" responses according to the changes in the surrounding physiological conditions (Priya James, John, Alex, & Anoop, 2014). Therefore it is possible to have, for instance, pH- or thermal-sensitive systems with delivery triggered by precise changes in those parameters (El-Sherbiny, 2010). So far, among the many hydrogel-based systems

* Corresponding author.
E-mail addresses: bfmedronho@ualg.pt, bfmedronho@portugalmail.pt
(B. Medronho).

developed, high focus has been given to sugar-based biopolymers for biocompatibility and availability reasons (Chang & Zhang, 2011). It is thus not surprising that a lot of work has been devoted to chitin and cellulose based systems, the two most abundant natural polymers on earth (Dutta, Dutta, & Tripathi, 2004; Klemm, Heublein, Fink, & Bohn, 2005; Kumar, 2000). Chitosan (Cht) is composed of α(1 → 4) 2-amino 2-deoxy β-D-glucan units randomly organized and it is obtained from the deacetylation of chitin. The tuning of the degree of deacetylation and substitution allows for obtaining polymers of different characteristics with respect to charge density and hydrophobicity, thus affecting not only the molecular interactions but also other features such as the swelling degree (Kumar, 2000). Cellulose derivatives are widely used in many different applications; one of the most suitable candidates for food or medical formulations is sodium carboxymethyl cellulose (CMC) which is typically obtained from the fibrous tissue found in plants (Kamide, 2005). Several promising physical hydrogels are prepared by mixing oppositely charged polymers. Given the proper conditions, these mixtures may form strong hydrogels due to the formation of dynamic physical interactions between entangled polymer chains (Devi & Maji, 2009; Kaihara, Suzuki, & Fujimoto, 2011; Lohani, Singh, Bhattacharya, Hegde, & Verma, 2016; Long & vanLuyen, 1996; Luo et al., 2015, 2016; Myung et al., 2008). These interlaced polymer networks (also known as interpenetrating polymer networks, IPN) are highly attractive due to the high swelling features and good stability of the three dimensional system. In this work we have focused on a semi-IPN where Cht is crosslinked while CMC is left in the linear form. The cross-linking is expected to strengthen the polyion complex and improve the mechanical properties of the hydrogels (Berger et al., 2004). Most of the cross-linking agents found in literature, such as formaldehyde or glutaraldehyde, are often toxic or disinfectant, and therefore their use is limited (Hennink & van Nostrum, 2012). Genipin, a gardenia fruit extract, was alternatively used in this work since it is safe, biocompatible with low acute toxicity profile and is regarded as promising natural cross-linking agent (Feng, Zhang, & Zhu, 2013; Klein et al., 2016; Muhamad, Fen, Hui, & Mustapha, 2011; Muzzarelli, 2009; Yuan et al., 2007). As seen above, CMC and Cht are oppositely charged biopolymers, biodegradable and frequently used in biomedical applications mainly as injectables or transplants or in the food industry but despite the recognized number of uses and studies on Cht and CMC, surprisingly little work has been done involving simultaneously both biopolymers in hybrid systems. This is a very attractive approach not only due to their safety and biocompatibility profiles but also due to their high availability which may facilitate an hypothetical process scale up. A few exceptions involve the synthesis of inorganic nanoparticles in CMC-Cht matrixes (Ghasemzadeh, Mahboubi, Karimi, & Hassani, 2016; Kaihara et al., 2011), the formation of hybrid hydrogels for yeast cell growth (Long & vanLuyen, 1996) and the development of CMC-Cht nanoparticles after enzymatic hydrolysis of the biopolymers (Ichikawa, Iwamoto, & Watanabe, 2005). However, to our knowledge, their potential to form particles for probiotic encapsulation has only been reported in one occasion where a physical layer-by-layer approach was used to form a nanostructured material (i.e. probiotic bacteria surrounded by alternated layers of Cht and CMC) (Priya, Vijayalakshmi, & Raichui, 2011). Therefore, the main objective of this work is to design new bio-based CMC-Cht particles capable to efficiently encapsulate the a model probiotic, Lactobacillus rhamnosus GG (LGG). In order to proof the concept and target different possible applications, micro- and macrobeads were prepared by different methods and characterized by a set of different techniques to understand the physico-chemical properties, swelling behavior, morphology and bacteria viability.

2. Materials and methods

2.1. Materials and chemicals

Chitosan, Cht, (extracted and purified from crab shell, deacetylation ≥ 85% and Mw of ca. 370 kDa), sodium carboxymethyl cellulose, CMC, (Mw of ca. 250 kDa with degree of substitution ca. 0.80–0.85), Rhodamine B (>95%) and 4,6-diamidino-2 phenylindole (DAPI) were purchased from Sigma-Aldrich. Genipin (98% purity) was obtained from Challenge Bioproducts Co., Ltd. Acetic acid glacial (>99.7% purity) was obtained from Panreac AppliChem. MRS broth pH 6.4 and MRS agar pH 5.7 were obtained from VWR International. The PBS buffer was prepared in the lab with disodium hydrogen phosphate, sodium chloride, potassium chloride and potassium dihydrogen phosphate, all purchased from Sigma-Aldrich. Lactobacillus rhamnosus GG LMG 18243 was bought from the Belgian Coordinated Collection of Microorganisms (BCCM). The LIVE/DEAD® BacLight™ Bacterial Viability Kit L7012 was purchased from Thermofisher Scientific, USA. Milli-Q water (18.2 MΩ cm^{-1} at 25 °C, MQ) was used for the preparation of all samples.

2.2. Preparation of the biopolymer solutions and hydrogels

An appropriate amount of Cht was first dissolved in a 1 wt% acetic acid aqueous solution with moderate heating under stirring. Likewise, CMC solutions were prepared by simply adding the desired amount of CMC powder in MQ water under constant stirring for not less than 30 min. For the hydrogels preparation two methods were used as exemplified in Fig. 1. The macrogels were formed by careful drop-wise addition of a solution of 1 wt% of CMC (50 mL) into a solution of 1 wt% of Cht (300 mL) using a manually operated syringe with a 0.7-mm cannula (Fig. 1A). The Cht solution was kept under continuous agitation to facilitate the solvent-polymer diffusion and interaction during the hardening of the gel particles. Other concentrations were initially screened but the 1 wt% (for both biopolymers) revealed the most suitable in terms of robustness of the particles formed. The hydrogel macroparticles were removed from the Cht solution (filtration) after 30 min aging. On the other hand, the microparticles were prepared in an air compressed equipment (working pressure of ca. 5–7 bar) coupled with a nozzle sprayer as illustrated in Fig. 1B. The obtained microgels were further washed with MQ water and recovered after gentle centrifugation. Both particles prepared either with the syringe or nozzle spray are found to display a reasonable narrow size distribution; ca. 5–10 μm and ca. 1.5–3 mm for micro- and macroparticles, respectively. For the preparation of chemically crosslinked beads, a 0.5 wt% (w/w) genipin solution (pH 7) was added to the 1 wt% CMC aqueous solution and later dropped into the 1 wt% Cht solution (via syringe or air pressure spray) and kept for 15 h at room temperature in order to complete the crosslinking reaction.

2.3. Growth and encapsulation of Lactobacillus rhamnosus GG

All the media and buffers were autoclaved at 121 °C for 15 min for sterilization. The freeze-dried cells of Lactobacillus rhamnosus GG were rehydrated in 5 mL MRS broth and incubated at 37 °C for 40 h in a CO$_2$ incubator and the growth was checked for two days. Visual turbidity and measurement of optical density at 600 nm confirmed the bacterial growth. The optical density was measured with UV/vis spectrophotometer (Thermo Fisher Scientific Genesys 6). To evaluate the purity of the culture, one full loop of bacteria was streaked on a MRS agar plate while a plate with pure culture was taken as control. The morphology of the colonies were compared. In a later step, 10 mL of the cultured broth were divided in ten Eppendorfs and centrifuged for 30 min at 3000 RCF. The supernatant was discarded and 1 mL of PBS was added to each of the pellets followed

A) Preparation of macroparticles
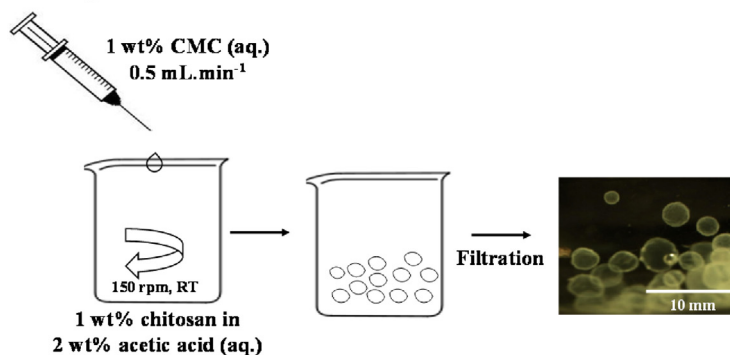
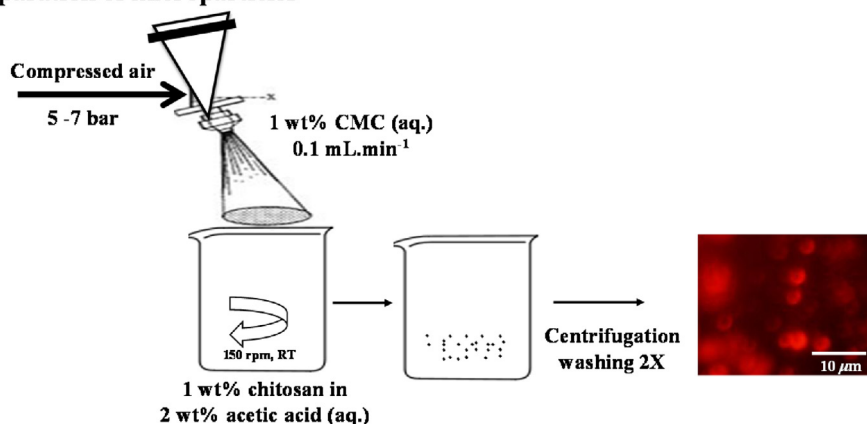## B) Preparation of microparticles

Fig. 1. Schematic representation of the macroparticles (A) and microparticles (B) preparation by drop wise addition and nozzle spray, respectively. Two typical microscopy pictures of the beads obtained are shown.

by centrifugation at 3000 RCF for 20 min. This washing procedure was repeated twice. Finally, the PBS supernatant was discarded and ten bacterial pellets were mixed with 20 mL of 1 wt% of CMC aqueous solution, forming the micro and macrobeads by adding them to 1% (w/w) Cht solution.

2.4. Evaluation of Lactobacillus rhamnosus GG Viability

To estimate the viable counts, the encapsulated bacteria was released from the particles by re-suspending in a PBS buffer solution at 37 °C for 30 min, under stirring (pH 7.4) followed by homogenization. The viability count corresponds to bacteria released from one macrobead (ca. 0.05 g) which was suspended in 1 mL of PBS buffer for the serial dilutions. In the case of microbeads, 100 μl of the suspended beads in the Cht solution were added to 1 mL of PBS buffer. Sequential dilutions were performed by dissolving the particles from each composition in the PBS buffer following the Miles and Misra approach to count the number of viable bacteria (Miles, Misra, & Irwin, 1938). All different dilutions were plated in triplicates and kept in CO_2 incubator for 48 h before the bacterial colony was counted using a colony reader. The experiments were performed in Faster BH-EN and BHG Class II Microbiological Safety Cabinets. The bacteria viability was also inferred using a Dead/Alive kit (commercial LIVE/DEAD® BacLight™). The bacteria in the particles were stained with 2 μl of SYTO 9 dye and 2 μl of propidium iodide from the kit and observed in a fluorescence Olympus microscope (100× immersion objective).

2.5. Thermogravimetric analysis (TGA)

The TGA analysis was performed on a TG 209 F3Tarsus thermogravimetric analyzer (Netzsch Instruments). Samples (ca. 8–10 mg) were weighed in alumina pans and were heated from 30 to 500 °C at a heating rate of 10 °C min^{-1} under N_2 atmosphere (flow rate of 20 mL min^{-1}).

2.6. Fourier transform infrared spectroscopy (FTIR)

The crosslinking between Cht and genipin was investigated by FTIR at 25 °C with a ATR-FTIR spectrophotometer Thermo Nicolet, IR300 (USA), using a universal ATR sampling accessory. FTIR spectral analysis was performed within the wave number range of 400–4000 cm^{-1}. A total of 256 scans were run to collect each spectrum at a resolution of 1 cm^{-1} in the transmission mode.

2.7. Scanning electron microscopy (SEM)

A VEGA3 SBH from TESCAN scanning electron microscope equipped with a selected energy dispersive X-ray microanalyser (EDX) was used to observe the morphology of the CMC-Cht particles with and without bacteria. Generally, freeze dried particles were deposited directly over the carbon tape on the support and sputtered with an approximately 6 nm thin Au/Pd film by cathodic pulverization using a SPI Module Sputter Coater before SEM analysis, during 90 s and with a current of de 15 mA. The accelerating voltage ranged from 5 to 15 kV.

2.8. Zeta potential

The zeta potential measurements were performed at a constant temperature of 25 °C on a Zetasizer Nano ZS (Malvern Instruments Ltd, Malvern, UK), using a folded capillary electrophoresis cell (Malvern Instruments). The average values of zeta potential were calculated with the data obtained from three runs of triplicates.
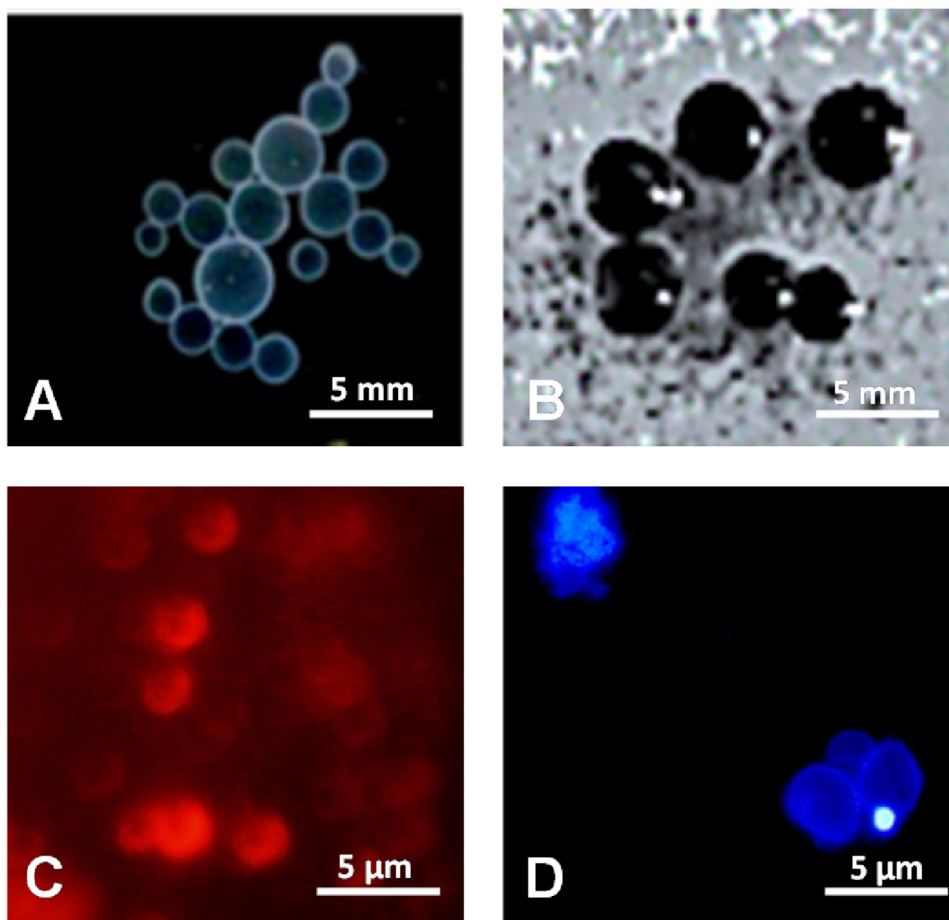
Fig. 2. Images of 1:1 (w/w) CMC-Cht non-crosslinked and crosslinked macro- and microparticles: A) A suspension of non-cross linked macroparticles imaged by optical microscopy, B) photograph of crosslinked macroparticles with genipin, C) Non-cross linked microparticles (doped with rhodamine) imaged by fluorescence microscopy, and D) chemically genipin crosslinked microparticles doped with DAPI and imaged by fluorescence microscopy. The scale bars represent 5 mm for the macroparticles (A and B) and 5 μm for the microparticles (C and D).

2.9. Optical and fluorescence microscopy

The micro and macroparticles were also observed in a fluorescence microscope (Olympus BX51 M), equipped with a 100× objective lens, a filter set type U-MNU2 (360–370 nm excitation and 400 nm dichromatic mirror) and an UV-mercury lamp (100 W Ushio Olympus). The DNA of the bacteria was stained the DAPI dye or with a Live/Dead assay to rapidly distinguish live bacteria with intact plasma membranes from dead bacteria with altered membranes. Samples without bacteria were also observed using the same conditions. The images were digitized on a computer through a video camera (Olympus digital camera DP70) and were analyzed with an image processor (Olympus DP Controller 2.1.1.176, Olympus DP Manager 2.1.1.158). The observations were carried out at room temperature. For the observation of bacteria-free macroparticles (doped with beta-rhodamine), an optical microscope equipped with a Moticam 2300 camera was also used.

2.10. pH influence on the swelling degree

The effect of pH on the swelling degree of the resulting macrobeads was studied by suspending the non-crosslinked and crosslinked macrobeads in different aqueous media at different pH (i.e. 2.5, 5.0, 7.5, 12.5). The samples were left to equilibrate for 12 h at room temperature before measuring the change in size of the particles with a vernier calliper.

2.11. Statistical analysis

The experiments were performed in triplicate and data was subjected to one-way analysis of variance (ANOVA). Multiple comparisons were performed by LSD test. Statistical significance was set at $P < 0.05$ using SPSS (SPSS Inc, USA).

3. Results and discussion

3.1. Characterization of the macro- and microparticles

The particles developed are intended to be suitable matrices for probiotic encapsulation and delivery. In particular, the main goal is to develop robust systems capable to maintain viable an acceptable number of cells while passing through the harsh conditions of the stomach before reaching the intestine. Therefore, the best conditions for the particle formation were screened and optimized during preliminary studies of different formulations. It was found that the optimum biopolymer ratio for bead formation was around 1:1 (w/w) which, taking into account the DS of CMC (0.80-0.85) and the deacetylation degree of chitosan (≥85%), gives an estimated ratio of ionizable groups of ca. to 1:1. Generally, higher amounts of Cht or CMC lead to non-uniform particles or inefficient particle formation, as increasing the concentration resulted in high viscosity and high charge accumulation. A similar optimum ratio was found for the chemically crosslinked particles. In this case, a maximum of 0.5 wt% of genipin was sufficient to obtain robust beads.
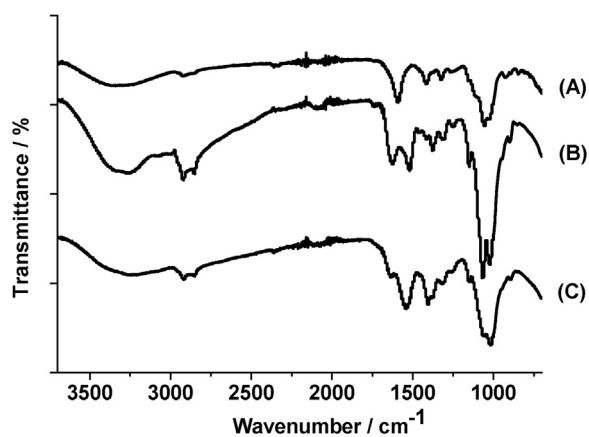
Fig. 3. FTIR spectra of a) CMC, b) Cht and c) CMC-Cht marcoparticles crosslinked with 0.5 wt% genipin.
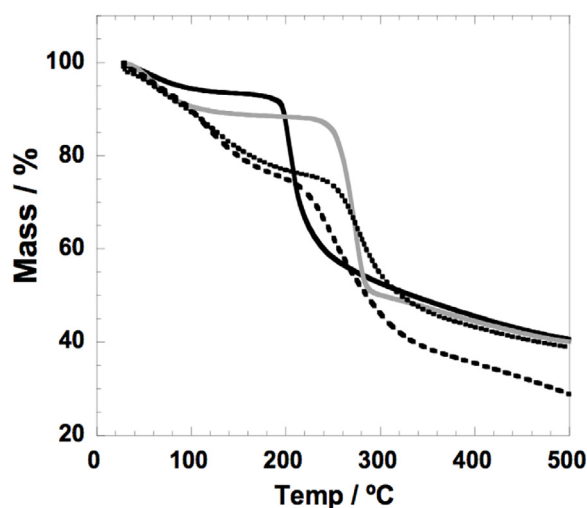

Fig. 4. TGA for native Cht (full black curve), CMC (grey curve), non crosslinked CMC-Cht (dotted black line) and crosslinked CMC-Cht (dashed black line).

In Fig. 2, the macro- and microparticles obtained with the different methods are shown. As can be seen, the macroparticles (Fig. 2A) are essentially spherical with an average size of ca. 2 mm while the microparticles (Fig. 2C) present an average size of ca. 5 μm. Moreover, the images also suggest core-shell type macroparticles, while the microparticles are apparently homogeneous. When the systems are chemically crosslinked with genipin (Fig. 2B and D) the beads go from transparent to dark blue, which strongly suggests the successful reaction between Cht and genipin (Muzzarelli, 2009).

In general, the particles resulting from the associative phase separation of mixed oppositely charged polymers are stable colloidal systems if their surfaces are overcharged with one of the polymers. Typically, particle systems with zeta potential values above ca. +40 or below −40 mV are considered to be adequately stable (i.e. no agglomeration) (Riddick, 1968). However, if neutralization is achieved (fully or partially), and consequently the net surface charge is low, aggregation can occur. In the systems developed here the zeta potential of the physical micro particles was found to be ca. +60 to +70 mV and the particles were reasonably stable. Centrifugation and filtration during the washing steps can, however, induce aggregation as can be seen in Fig. 2A where the macro particles after re-suspension in an aqueous medium are found to stick to each other. On the other hand, systems crosslinked with genipin show an average zeta potential around −8 mV (due to the reaction of genipin with the charged amino groups) and particles are more susceptible to aggregation as shown in Fig. 2D. The incorporation of LGG (negatively charged cells) further makes the particles more negatively charged thus giving a higher colloidal stability and a reduced tendency to aggregation.

In terms of mechanism, the crosslinking involves a nucleophilic attack (fast reaction) of the amino group of Cht on the C-3 olefinic carbon of genipin which results in the opening of the dihydropyran ring and the formation of a tertiary amine. The subsequent slower reaction is the formation of amide through the reaction of the amino group on Cht with the ester group of genipin (Mi, Sung, & Shyu, 2001). At the same time, polymerization can take place between genipin molecules already linked to amino groups of Cht, which could lead to the crosslinking of amino groups by short genipin copolymers (Butler, Ng, & Pudney, 2003).

In Fig. 3 a set of different FTIR spectra from the native biopolymers and the chemically crosslinked systems is shown.

The most characteristic bands of CMC can be identified in Fig. 3A; the broad absorption in the range 3100–3600 cm^{-1} can be ascribed to the stretching of the −OH groups (Jahan, Saeed, He, & Ni, 2011; Peng et al., 2009; Sun, Sun, Liu, Fowler, & Tomkinson, 2002) while the band at 2900 cm^{-1} appears due to C−H stretching (Jahan et al., 2011; Sun et al., 2002). An intense band at 1590 cm^{-1} is due to

the absorbed moisture (i.e. bending mode of water absorbed to the cellulose derivative) (Ren, Sun, Liu, Chao, & Luo, 2006). The deformation, wagging and twisting modes of the anhydroglucopyranose structure are comprised between 700 and 1500 cm^{-1}. More specifically, the absorbance bands between 1000 cm^{-1} and 1200 cm^{-1} are attributed mainly to the C−O stretching in major ether bands (Liu, Ni, Fatehi, & Saeed, 2011) while C−H deformations and wagging modes can be ascribed to the bands at ca. 1300 and 1400 cm^{-1}. The native Cht shows absorptions at ca. 1630 cm^{-1} and 1526 cm^{-1}, which are typical for the N−H bending vibrations of primary amines (Lambert, 1987). The band at ca. 1376 cm^{-1} can be ascribed to stretching of the Cht primary alcoholic group. On the other hand, the absorption bands between 1000 cm^{-1} and 1100 cm^{-1} were attributed to C−O and C−N stretching and C−C−N bending vibrations. As in the CMC case, the broad band between 3000 cm^{-1} and 3600 cm^{-1} is attributed to the O−H stretching mainly coming from absorbed water, which most likely overlaps to the amine stretching vibrations (N−H) also found in the same region (Lambert, 1987) while the bands between 2800 cm^{-1} and 3000 cm^{-1} can be assigned to the C−H stretching vibration (Colthup, Daily, & Wiberley, 1975). The FTIR spectrum of the physical CMC−Cht gel is very similar to the crosslinked system (data not shown). However, in the crosslinked system it is possible to identify the amide II band at 1544 cm^{-1}, characteristic of N−H deformation (Lambert, 1987), which results from the formation of secondary amides due to the reaction between the genipin ester and hydroxyl groups and the Cht amino groups. The peak at 1635 cm^{-1} can be ascribed to the C=O stretch in secondary amides. Additionally, it is also possible to observe augmented band intensities at ca. 1400 cm^{-1} and 1000 cm^{-1}, which can be attributed to the C−N and C−OH stretching modes, respectively, due to a higher number density after crosslinking with genipin (Lambert, 1987).

The thermogravimetric analysis (TGA) plays an important role in determining the thermal stability of materials. Fig. 4 shows the TGA of the chemical and physical gel systems. The native CMC and Cht show a small (5–10%) mass loss for the first decomposition step and a more significant mass loss (50–55%) for the second step. The data shows that CMC is more stable than the Cht (Corazzari et al., 2015). The first step consists in the evaporation of bound water while the second transition may be attributed to the complex dehydration of the saccharide rings followed by depolymerization, and pyrolytic decomposition of the polysaccharide structure with vaporization and elimination of CO_2 and other volatile products (Penichecovas, Arguellesmonal, & Sanroman, 1993; Zohuriaan & Shokrolahi, 2004).
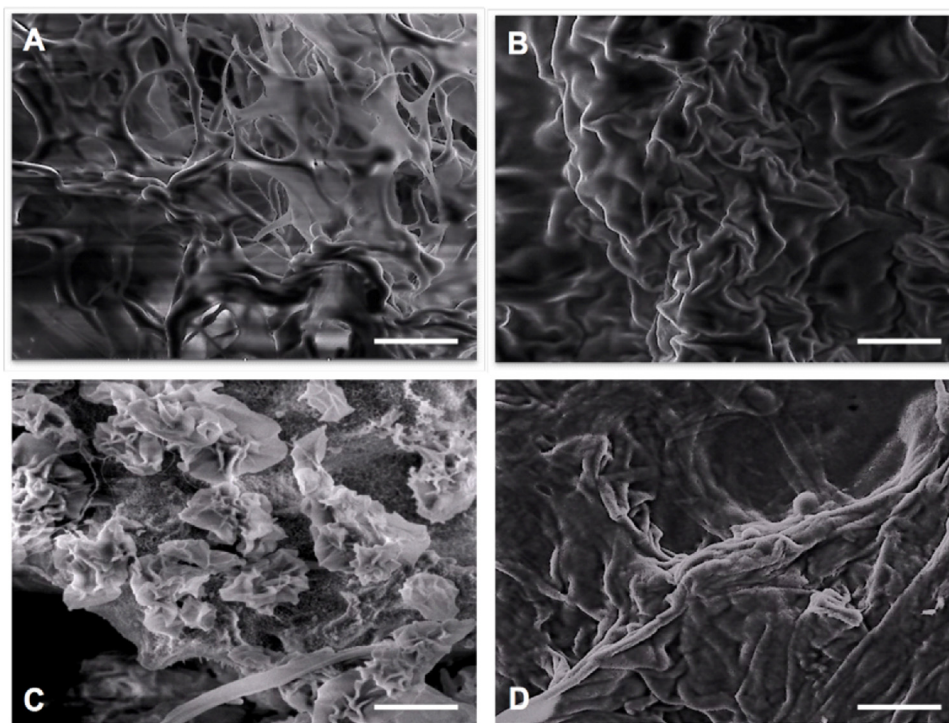
Fig. 5. SEM images of: A) non crosslinked CMC-Cht macroparticle; B) crosslinked CMC-Cht macroparticle; C) non-crosslinked CMC-Cht microparticle and D) crosslinked CMC-Cht microparticle. The scale bar represents 5 μm.

In the particle systems the same two main degradation steps can be identified with a ca. 25% mass loss in the first step and a more significant mass lost (35–45%) in the second step. The loss of water in these particle systems is substantially higher than in the native polymer. Interesting to note is that the non-crosslinked system presents a second degradation step dominated by the more stable polymer (i.e. CMC) while the crosslinked system shows the second degradation step at a higher temperature than the native Cht, but still lower than the physical gel system. Moreover, the crosslinked systems show higher values of the weight loss in this range of temperatures, probably due to a partial weakening of the Cht structure caused by the crosslinking with genipin (Klein et al., 2016). This effect has been observed in related systems such as in Cht crosslinked with tannic acid (Rivero, García, & Pinotti, 2013) and in gluteraldehyde crosslinked films (Beppu, Vieira, Aimoli, & Santana, 2007). Nevertheless, overall the TGA curves indicate that the obtained chemical and physical gel particles are thermally stable in the temperature range suitable for probiotic bacteria.

In Fig. 5 representative SEM images of the macro- and micro particles are shown. The morphologies are particularly different upon cross-linking with genipin (compare, for instance, Fig. 5A and B); while the physical gel particles, resulting from the CMC-Cht electrostatic association alone, are significantly porous, the chemical gel particles present a much denser structure with no visible porosity. This feature seems to be independent of the size of the beads. Such difference in porosity may affect the release of probiotic bacteria from the particles.

The particles are formed by the association between the oppositely charged Cht and CMC and, as mixtures of titrating polyelectrolytes, these systems are highly sensitive to pH changes. The knowledge of their swelling behavior is very relevant in particular for applications involving media of different pHs, such as in drug or probiotic delivery in the gastrointestinal system. As seen in Fig. 6, the equilibrium size of the non-crosslinked macroparticles is strongly pH dependent. The swelling (and consequently the size of the macrobeads) and transition to a more expanded state is
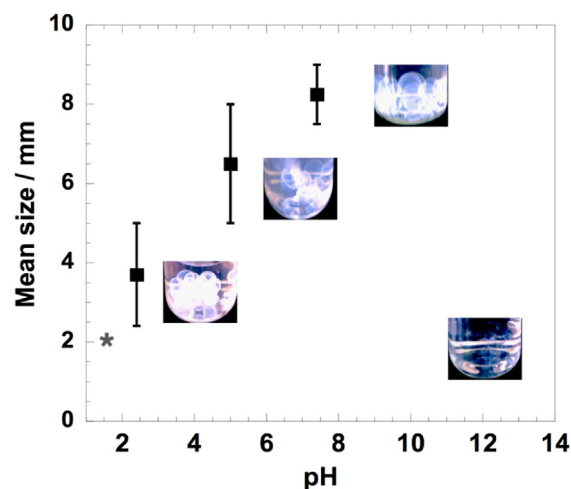
Fig. 6. Representation of the pH size dependence of the CMC-Cht macroparticles. The mean size was calculated after averaging ten samples per pH value. The grey star represents the initial average particle size (ca. 2 mm). At pH 12.5 the majority of the particles disintegrate. Photos of the macroparticles are inserted in the plot.

typically controlled by the osmotic pressure exerted by the mobile counterions neutralizing the network charges. At pH 2.4, Cht is protonated ($pKa \approx 6.5$) (Pillai, Paul, & Sharma, 2009) while at pH 5, CMC is also ionized ($pKa \approx 3.65$) (Zhivkov, 2013) and thus a lower swelling should be expected at this pH when both the oppositely charged polymers are ionized. However, as seen in Fig. 6, a large swelling is observed at pH 5. This can be related to the fact that the pKa of Cht is also dependent on the deacetylation degree and on the acid used in dissolution. For instance, pKa values of 4.5 for Cht have been reported when HCl is used in dissolution (Pillai et al., 2009). Our zeta potential data from both polymers independently in solution show that at pH 5 Cht presents less than 50% of the total charge predicted while CMC is almost fully deprotonated. These

Fig. 7. Images of LGG-doped particles. A, B and C) light micrograph, fluorescent image and SEM of CMC-Cht macroparticles, respectively. D and E) are fluorescent image and SEM of CMC-Cht microparticles, respectively. The scale bar in A represents 5 mm while all the other scale bars represent 5 μm. The DAPI dye was used in the fluorescent microscopy tests.

conditions lead to a non neutral charge conditions at pH 5 and thus to the observed extended swelling. In fact, the estimated pH range for charge neutrality is ca. 3.8. Thus, in an extra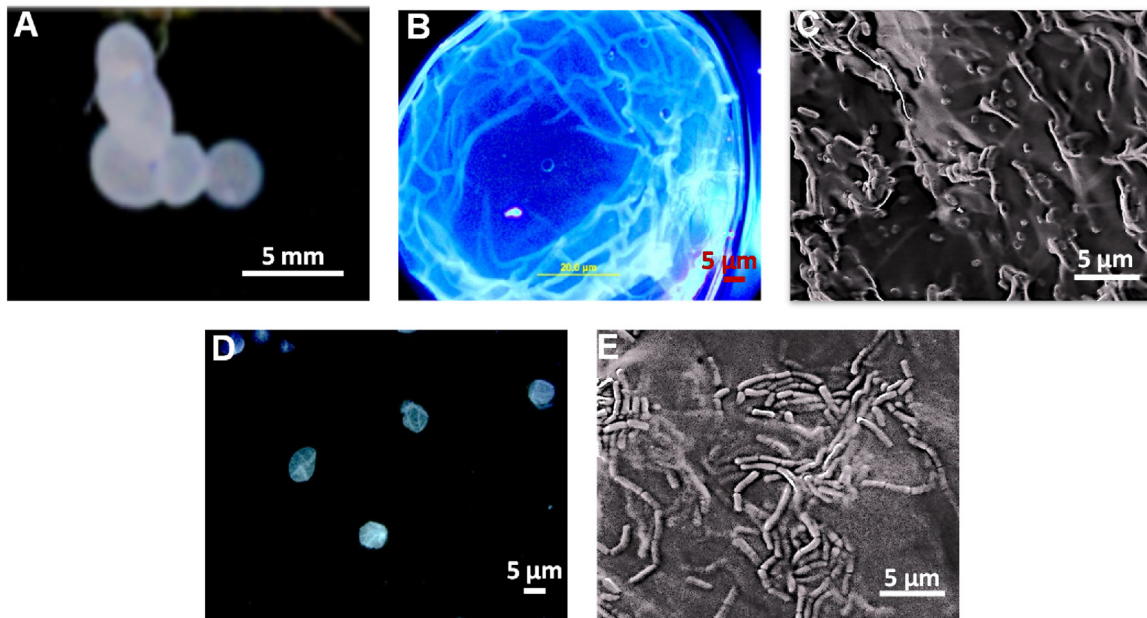 experiment, particles have been exposed to this pH and showed an average size of 2.3 mm (similar size to the native particles) with negligible swelling. The larger particles are observed at pH 7.4 where only CMC is extensively charged. At the highest pH tested (12.5), most of the macroparticles disintegrate and this can be referred to the high net charge since CMC is then fully ionized while Cht is uncharged. The observed swelling behavior of the CMC-Cht particles is very suitable for the delivery of probiotics in the intestinal tract since particles undergo little swelling at pH 2–4 (particles stable at pH values typical for the stomach) while they undergo considerable swelling at pH conditions typically found in the intestinal tract (pH ≈ 8). The delivery of probiotics under conditions mimicking those of the gastrointestinal tract will be a matter of further studies.

3.2. Probiotic encapsulation and viability

The probiotic LGG was encapsulated in the different particle formulations, as described in the Material and Methods section. Upon encapsulation, the non-crosslinked macrobeads became turbid, as observed in Fig. 7A (compare to Fig. 2A). The turbid appearance is most likely originated from the high density of bacterial cells encapsulated. This is further confirmed with the fluorescence microscopy and SEM data (Fig. 7B and C, respectively). The same is verified for the microbeads. In this case, the SEM image (Fig. 7E) shows a high density of LGG rods at the surface. Note that unlike the macrobeads no individual microbeads are observed in the SEM image probably due to the freeze-drying procedure (i.e. during solvent sublimation the particles aggregate in larger structures). The same type of morphologies is found for the related crosslinked particle systems (data not shown).

The encapsulation efficiency was estimated after mechanically disintegrating the particles in a phosphate buffer (pH = 7.4), by stirring them at 37 °C. After that, the number of entrapped cells by serial dilution was measured by drop the plate method and counts were expressed as number CFU, and calculated as EE = (Log 10N/Log 10N0) × 100, where EE stands for entrapment/encapsulation effi-

ciency, N is the number of viable entrapped bacteria released from the particles and N0 is the number of free/naked bacteria taken as control (Jantzen, Gopel, & Beermann, 2013; Lotfipour, Mirzaeei, & Maghsoodi, 2012). The physical macro- and micro particles presented an EE of ca. 62 and 66%, respectively. On the other hand, the chemically cross-linked macro- and micro particles display an EE of ca. 55 and 57%, respectively. The SEM images in Fig. 7 confirm the integrity of the bacterial cells after encapsulation. Distinct bacterial cells with intact membrane are found throughout the particles, which indicates that the chosen methods for encapsulation are suitable for cell viability. The bacterial cells are easily stained with DAPI which associates with the minor groove of double stranded DNA with a preference for the adenine-thymine basepair. However, DAPI stains the DNA of the bacteria independently if the bacteria are dead or alive. Therefore the viability of LGG in the CMC-Cht systems was checked by plate counting (colony-forming units (CFUs)) and by using a fluorescent Dead/Alive kit. The size of the particles seems not to influence the viability since the same trend and values were obtained within the calculated standard deviations (i.e. macroparticles: 2.08 ± 0.23 mm; microparticles: 7.26 ± 1.88 μm). Therefore, in Fig. 8A, the results from the plate counting method (tests in triplicate) are summarized for both macro- and microparticles. The counting of un-encapsulated or naked LGG cells was 11 ± 0.1 Log CFU/mL. After incorporation of LGG in the physical particles a viability reduction to 6.8 ± 0.1 Log CFU/mL cells was observed. The decrease in viability is slightly higher for the crosslinked system (6.1 ± 0.1 Log CFU/mL) partially due to the CMC-Cht matrix effect (low porosity as observed by SEM data) and some bacteria may remain trapped in the dense gel particles and not be released. Note that significant difference (P < 0.05) was observed for the chemical and physical systems tried thus indicating that the cross linking agent affects the viability of the bacteria. Nevertheless, since health benefits can be obtained with products containing probiotics at the standard of a minimum level of viable cells ranging from 6 to 7 Log CFU/ml (Madureira, Amorim, Gomes, Pintado, & Malcata, 2011; Mohammadi, Mortazavian, Khosrokhavar, & da Cruz, 2011), overall the encapsulation procedures preserved LGG integrity and viability with quite acceptable values for practical uses. The qualitative cell viability in the CMC-Cht particles was also evaluated by fluo-
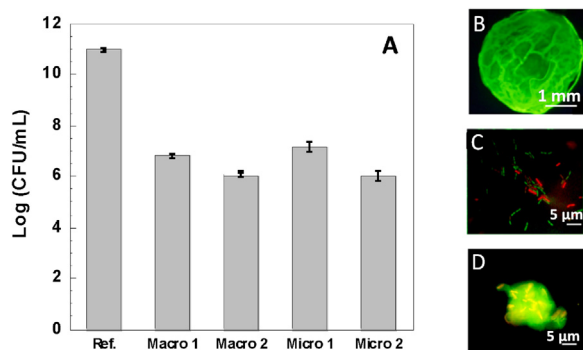
Fig. 8. Left: A) Viability counts in Log CFU/mL of the different systems developed. The unprotected LGG cells are represented as "Ref". The "Macro 1" and "Macro 2" stand for the Cht + CMC physical macroparticles and Cht + CMC chemical macroparticles, respectively, while the "Micro 1" and "Micro 2" stand for the Cht + CMC physical microparticles and Cht + CMC chemical microparticles, respectively. Right: Fluorescent microscopy images using a Dead/Alive kit. B) Macroparticle loaded with LGG and C) a zoom of the same macroparticle. D) Microparticle loaded with LGG. The scale bar for B represents 1 mm while the scale bars for C and D represent 5 μm.

rescence microscopy using a Dead/Alive kit. Both non-crosslinked macro- and micro particles are shown. In this test the viable bacteria appear as green rods while the dead bacteria are red. As can be seen in Fig. 8B, the fresh non crosslinked macroparticles are essentially green. A higher magnification (Fig. 8C) shows the individual LGG cells, high number of green rods. The images are partially blurry due to the gel density and thickness. The same high viability is found for the microparticles (Fig. 8D), in good agreement with the quantitative plate counting method. No significant differences were observed for the crosslinked systems. From the microscopy analysis of different particles and different depths of fields, the bacteria are found to be homogeneously distributed, in the core and shell of the particles.

4. Conclusions

Gut microbiota has been shown to have paramount importance in the human health and eventually can be modulated with the benefic probiotic bacteria that must reach the intestine in an acceptable viable number. Therefore, in this work novel biobased particles were developed for the encapsulation and potential delivery of probiotic bacteria in the gut. The systems were formed with food grade polymers (CMC and Cht) and, in some cases, a low toxicity cross-linking agent, genipin, was also used. Tunable size could be achieved depending on the method of preparation: microparticles with an average size of 5 μm were obtained by nozzle-spraying while macroparticles with a mean diameter of 2 mm were obtained by a drop-wise procedure. The cross-linking of the particles, confirmed by FTIR and TGA, produced significant morphological changes in the beads (i.e. the porosity decreases remarkably with cross-linking). The particles were stable at pH 2.4, which is the gastric pH, and swell considerably at higher pHs, in particular at pH 7.4 (a close pH of the intestine). Fluorescence microscopy, SEM and viable cell plate count confirmed the successful encapsulation and acceptable viability of LGG in all CMC-Cht systems, regardless of the method of preparation or presence of cross-linking agent. The cell viability was found to be reasonable and above the minimum required to produce a potential health benefit. Overall, the novel biocompatible particle systems developed are robust and display several features of interest (i.e. pH dependent swelling behaviour, high viable cell number encapsulation, thermal stability) regarding their future use for probiotic encapsulation and potential delivery in the intestinal tract. Further studies will assess the release of probiotic in

intestinal tract environmental conditions using these biocompatible systems.

References

Beppu, M. M., Vieira, R. S., Aimoli, C. G., & Santana, C. C. (2007). Crosslinking of chitosan membranes using glutaraldehyde: Effect on ion permeability and water absorption. *Journal of Membrane Science, 301*(1–2), 126–130.

Berger, J., Reist, M., Mayer, J. M., Felt, O., Peppas, N. A., & Gurny, R. (2004). Structure and interactions in covalently and ionically crosslinked chitosan hydrogels for biomedical applications. *European Journal of Pharmaceutics and Biopharmaceutics, 57*(1), 19–34.

Butler, M. F., Ng, Y. F., & Pudney, P. D. A. (2003). Mechanism and kinetics of the crosslinking reaction between biopolymers containing primary amine groups and genipin. *Journal of Polymer Science Part A—Polymer Chemistry, 41*(24), 3941–3953.

Buwalda, S. J., Boere, K. W. M., Dijkstra, P. J., Feijen, J., Vermonden, T., & Hennink, W. E. (2014). Hydrogels in a historical perspective: From simple networks to smart materials. *Journal of Controlled Release, 190*, 254–273.

Chang, C. Y., & Zhang, L. N. (2011). Cellulose-based hydrogels: Present status and application prospects. *Carbohydrate Polymers, 84*(1), 40–53.

Colthup, N. B., Daily, L. H., & Wiberley, S. E. (1975). *Introduction to infrared and Raman spectroscopy*. New York: Academic Press.

Corazzari, I., Nistico, R., Turci, F., Faga, M. G., Franzoso, F., Tabasso, S., et al. (2015). Advanced physico-chemical characterization of chitosan by means of TGA coupled on-line with FTIR and GCMS: Thermal degradation and water adsorption capacity. *Polymer Degradation and Stability, 112*, 1–9.

Devi, N., & Maji, T. K. (2009). Preparation and evaluation of gelatin/sodium carboxymethyl cellulose polyelectrolyte complex microparticles for controlled delivery of isoniazid. *Aaps PharmSciTech, 10*(4), 1412–1419.

Dutta, P. K., Dutta, J., & Tripathi, V. S. (2004). Chitin and chitosan: Chemistry, properties and applications. *Journal of Scientific & Industrial Research, 63*(1), 20–31.

El-Sherbiny, I. M. (2010). Enhanced pH-responsive carrier system based on alginate and chemically modified carboxymethyl chitosan for oral delivery of protein drugs: Preparation and in-vitro assessment. *Carbohydrate Polymers, 80*(4), 1125–1136.

Feng, H. Z., Zhang, L. M., & Zhu, C. Y. (2013). Genipin crosslinked ethyl cellulose-chitosan complex microspheres for anti-tuberculosis delivery. *Colloids and Surfaces B-Biointerfaces, 103*, 530–537.

Ghasemzadeh, H., Mahboubi, A., Karimi, K., & Hassani, S. (2016). Full polysaccharide chitosan-CMC membrane and silver nanocomposite: Synthesis, characterization, and antibacterial behaviors. *Polymers for Advanced Technologies, 27*(9), 1204–1210.

Govender, M., Choonara, Y. E., Kumar, P., du Toit, L. C., van Vuuren, S., & Pillay, V. (2014). A review of the advancements in probiotic delivery: Conventional vs. non-conventional formulations for intestinal flora supplementation. *Aaps PharmSciTech, 15*(1), 29–43.

Haffner, F. B., Diab, R., & Pasc, A. (2016). Encapsulation of probiotics: insights into academic and industrial approaches. *Aims Materials Science, 3*(1), 114–136.

Hennink, W. E., & van Nostrum, C. F. (2012). Novel crosslinking methods to design hydrogels. *Advanced Drug Delivery Reviews, 64*, 223–236.

Holzapfel, W. H., Haberer, P., Snel, J., Schillinger, U., & Huis in't Veld, J. H. J. (1998). Overview of gut flora and probiotics. *International Journal of Food Microbiology, 41*(2), 85–101.

Ichikawa, S., Iwamoto, S., & Watanabe, J. (2005). Formation of biocompatible nanoparticles by self-assembly of enzymatic hydrolysates of chitosan and carboxymethyl cellulose. *Bioscience Biotechnology and Biochemistry, 69*(9), 1637–1642.

Jahan, M. S., Saeed, A., He, Z. B., & Ni, Y. H. (2011). Jute as raw material for the preparation of microcrystalline cellulose. *Cellulose, 18*(2), 451–459.

Jantzen, M., Gopel, A., & Beermann, C. (2013). Direct spray drying and microencapsulation of probiotic Lactobacillus reuteri from slurry fermentation with whey. *Journal of Applied Microbiology, 115*(4), 1029–1036.

Kaihara, S., Suzuki, Y., & Fujimoto, K. (2011). In situ synthesis of polysaccharide nanoparticles via polyion complex of carboxymethyl cellulose and chitosan. *Colloids and Surfaces B—Biointerfaces, 85*(2), 343–348.

Kamide, K. (2005). 1 – Introduction. In *Cellulose and cellulose derivatives*. pp. 1–23. Amsterdam: Elsevier.

Kanmani, P., Kumar, R. S., Yuvaraj, N., Paari, K. A., Pattukumar, V., & Arul, V. (2011). Cryopreservation and microencapsulation of a probiotic in alginate-chitosan capsules improves survival in simulated gastrointestinal conditions. *Biotechnology and Bioprocess Engineering, 16*(6), 1106–1114.

Klein, M. P., Hackenhaar, C. R., Lorenzoni, A. S. G., Rodrigues, R. C., Costa, T. M. H., Ninow, J. L., et al. (2016). Chitosan crosslinked with genipin as support matrix for application in food process: Support characterization and beta-D-galactosidase immobilization. *Carbohydrate Polymers, 137*, 184–190.

Klemm, D., Heublein, B., Fink, H. P., & Bohn, A. (2005). Cellulose: Fascinating biopolymer and sustainable raw material. *Angewandte Chemie—International Edition, 44*(22), 3358–3393.

Krasaekoopt, W., Bhandari, B., & Deeth, H. (2003). Evaluation of encapsulation techniques of probiotics for yoghurt. *International Dairy Journal, 13*(1), 3–13.

Kumar, M. N. V. R. (2000). A review of chitin and chitosan applications. *Reactive & Functional Polymers, 46*(1), 1–27.

Lambert, J. B. (1987). *Introduction to organic spectroscopy*. New York: Macmillan.

Liu, Z. H., Ni, Y. H., Fatehi, P., & Saeed, A. (2011). Isolation and cationization of hemicelluloses from pre-hydrolysis liquor of kraft-based dissolving pulp production process. *Biomass & Bioenergy, 35*(5), 1789–1796.

Lohani, A., Singh, G., Bhattacharya, S. S., Hegde, R. R., & Verma, A. (2016). Tailored-interpenetrating polymer network beads of kappa-carrageenan and sodium carboxymethyl cellulose for controlled drug delivery. *Journal of Drug Delivery Science and Technology, 31*, 53–64.

Long, D. D., & vanLuyen, D. (1996). Chitosan-carboxymethylcellulose hydrogels as supports for cell immobilization. *Journal of Macromolecular Science-Pure and Applied Chemistry, A, 33*(12), 1875–1884.

Lotfipour, F., Mirzaeei, S., & Maghsoodi, M. (2012). Evaluation of the effect of CaCl2 and alginate concentrations and hardening time on the characteristics of Lactobacillus acidophilus loaded alginate beads using response surface analysis. *Advanced Pharmaceutical Bulletin, 2*(1), 71–78.

Luo, F., Sun, T. L., Nakajima, T., Kurokawa, T., Zhao, Y., Sato, K., et al. (2015). Oppositely charged polyelectrolytes form tough, self-healing, and rebuildable hydrogels. *Advanced Materials, 27*(17), 2722.

Luo, F., Sun, T. L., Nakajima, T., King, D. R., Kurokawa, T., Zhao, Y., et al. (2016). Strong and tough polyion-complex hydrogels from oppositely charged polyelectrolytes: A comparative study with polyampholyte hydrogels. *Macromolecules, 49*(7), 2750–2760.

Madureira, A. R., Amorim, M., Gomes, A. M., Pintado, M. E., & Malcata, F. X. (2011). Protective effect of whey cheese matrix on probiotic strains exposed to simulated gastrointestinal conditions. *Food Research International, 44*(1), 465–470.

Martin, M. J., Lara-Villoslada, F., Ruiz, M. A., & Morales, M. E. (2015). Microencapsulation of bacteria: A review of different technologies and their impact on the probiotic effects. *Innovative Food Science & Emerging Technologies, 27*, 15–25.

Mi, F. L., Sung, H. W., & Shyu, S. S. (2001). Release of indomethacin from a novel chitosan microsphere prepared by a naturally occurring crosslinker: Examination of crosslinking and polycation-anionic drug interaction. *Journal of Applied Polymer Science, 81*(7), 1700–1711.

Miles, A. A., Misra, S. S., & Irwin, J. O. (1938). The estimation of the bactericidal power of the blood. *Journal of Hygiene, 38*(6), 732–749.

Mohammadi, R., Mortazavian, A. M., Khosrokhavar, R., & da Cruz, A. G. (2011). Probiotic ice cream: Viability of probiotic bacteria and sensory properties. *Annals of Microbiology, 61*(3), 411–424.

Muhamad, I. I., Fen, L. S., Hui, N. H., & Mustapha, N. A. (2011). Genipin-cross-linked kappa-carrageenan/carboxymethyl cellulose beads and effects on beta-carotene release. *Carbohydrate Polymers, 83*(3), 1207–1212.

Muzzarelli, R. A. A. (2009). Genipin-crosslinked chitosan hydrogels as biomedical and pharmaceutical aids. *Carbohydrate Polymers, 77*(1), 1–9.

Myung, D., Waters, D., Wiseman, M., Duhamel, P. E., Noolandi, J., Ta, C. N., et al. (2008). Progress in the development of interpenetrating polymer network hydrogels. *Polymers for Advanced Technologies, 19*(6), 647–657.

Pamer, E. G. (2016). Resurrecting the intestinal microbiota to combat antibiotic-resistant pathogens. *Science, 352*(6285), 535–538.

Peng, F., Ren, J. L., Xu, F., Bian, J., Peng, P., & Sun, R. C. (2009). Comparative study of hemicelluloses obtained by graded ethanol precipitation from sugarcane bagasse. *Journal of Agricultural and Food Chemistry, 57*(14), 6305–6317.

Penichecovas, C., Arguellesmonal, W., & Sanroman, J. (1993). A kinetic-study of the thermal-degradation of chitosan and a mercaptan derivative of chitosan. *Polymer Degradation and Stability, 39*(1), 21–28.

Pillai, C. K. S., Paul, W., & Sharma, C. P. (2009). Chitin and chitosan polymers: Chemistry, solubility and fiber formation. *Progress in Polymer Science, 34*(7), 641–678.

Priya James, H., John, R., Alex, A., & Anoop, K. R. (2014). Smart polymers for the controlled delivery of drugs—A concise overview. *Acta Pharm Sin B, 4*(2), 120–127.

Priya, A. J., Vijayalakshmi, S. P., & Raichui, A. M. (2011). Enhanced survival of probiotic lactobacillus acidophilus by encapsulation with nanostructured polyelectrolyte layers through layer-by-layer approach. *Journal of Agricultural and Food Chemistry, 59*(21), 11838–11845.

Ren, J. L., Sun, R. C., Liu, C. F., Chao, Z. Y., & Luo, W. (2006). Two-step preparation and thermal characterization of cationic 2-hydroxypropyltrimethylammonium chloride hemicellulose polymers from sugarcane bagasse. *Polymer Degradation and Stability, 91*(11), 2579–2587.

Riddick, T. M. (1968). *Control of colloid stability through zeta potential and its relationship to cardiovascular disease*. Wynnewood, PA: Livingston Publishing.

Rivero, S., García, M. A., & Pinotti, A. (2013). Physical and chemical treatments on chitosan matrix to modify film properties and kinetics of biodegradation. *Journal of Materials Physics and Chemistry, 1*, 51–57.

Sánchez, B., Delgado, S., Blanco-Míguez, A., Lourenço, A., Gueimonde, M., & Margolles, A. (2017). Probiotics, gut microbiota, and their influence on host health and disease. *Molecular Nutrition and Food Research, 61*, 1–15.

Saarela, M., Mogensen, G., Fonden, R., Matto, J., & Mattila-Sandholm, T. (2000). Probiotic bacteria: Safety, functional and technological properties. *Journal of Biotechnology, 84*(3), 197–215.

Silva, J. P. S. E., Sousa, S. C., Costa, P., Cerdeira, E., Amaral, M. H., Lobo, J. S., et al. (2013). Development of probiotic tablets using microparticles: Viability studies and stability studies. *Aaps PharmSciTech, 14*(1), 121–127.

Soukoulis, C., Singh, P., Macnaughtan, W., Parmenter, C., & Fisk, I. D. (2016). Compositional and physicochemical factors governing the viability of Lactobacillus rhamnosus GG embedded in starch-protein based edible films. *Food Hydrocolloids, 52*, 876–887.

Sun, R., Sun, X. F., Liu, G. Q., Fowler, P., & Tomkinson, J. (2002). Structural and physicochemical characterization of hemicelluloses isolated by alkaline peroxide from barley straw. *Polymer International, 51*(2), 117–124.

Tripathi, M. K., & Giri, S. K. (2014). Probiotic functional foods: Survival of probiotics during processing and storage. *Journal of Functional Foods, 9*, 225–241.

Yuan, Y., Chesnutt, B. M., Utturkar, G., Haggard, W. O., Yang, Y., Ong, J. L., et al. (2007). The effect of cross-linking of chitosan microspheres with genipin on protein release. *Carbohydrate Polymers, 68*(3), 561–567.

Zhivkov, A. M. (2013). Electric properties of carboxymethyl cellulose, cellulose—Fundamental aspects. In T. G. M. Van De Ven (Ed.),. InTech. http://dx.doi.org/10.5772/56935. Available from:. http://www.intechopen.com/books/cellulose-fundamental-aspects/electric-properties-of-carboxymethyl-cellulose

Zohuriaan, M. J., & Shokrolahi, F. (2004). Thermal studies on natural and modified gums. *Polymer Testing, 23*(5), 575–579.

Paper II
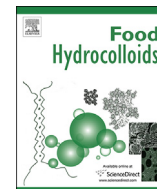
On the encapsulation and viability of probiotic bacteria in edible carboxymethyl cellulose-gelatin water-in-water emulsions

Poonam Singh [a], Bruno Medronho [b, *], Maria G. Miguel [a], Jordi Esquena [c, **]

[a] CQC, University of Coimbra, Department of Chemistry, 3004-535 Coimbra, Portugal
[b] Faculty of Sciences and Technology (MeditBio), Ed. 8, University of Algarve, Campus de Gambelas, 8005-139 Faro, Portugal
[c] Institute of Advanced Chemistry of Catalonia, Spanish National Research Council (IQAC-CSIC) and Networking Research Center on Bioengineering, Biomaterials and Nanomedicine (CIBER-BBN), Jordi Girona, 18-26, 08034 Barcelona, Spain

ARTICLE INFO

ABSTRACT

In this study, novel biobased dispersions to entrap probiotic bacteria were developed and characterized regarding their formation, microstructure and *in vitro* viability and culturability performance in model salivary, gastric and intestinal fluids. The systems are composed of type B pigskin gelatin and sodium carboxymethyl cellulose (NaCMC) which, depending on concentrations and temperature, can form water-in-water (W/W) emulsion droplets as observed by optical and fluorescence microscopy. Model probiotic bacteria, *Lactobacillus rhamnosus* GG (LGG), were successfully entrapped into the W/W emulsion droplets with surprisingly high viability. Moreover, the survival of the LGG cells, when exposed to the different model fluids, was improved after their entrapment in the W/W emulsions. Therefore, the developed dispersions display high potential for probiotic encapsulation and eventual delivery into the intestinal tract with acceptable viability.

1. Introduction

The development of efficient delivery systems for food and biomedical applications, able to encapsulate, protect, transport and deliver the active agent appropriately, remains unsolved in many aspects. One major challenge is that the carrier should deliver its content to the target area without any harmful side effect to cells and/or tissues. Probiotic bacteria arise as valuable cargo capable of treatment of different diseases or health problems (Holzapfel, Haberer, Snel, Schillinger, & Huis in't Veld, 1998; Iannitti & Palmieri, 2010; Passariello, Agricole, & Malfertheiner, 2014). These are living microorganisms, which are considered to provide beneficial health effects to the host by replenishing natural gastrointestinal microbiota. However, probiotic bacteria taken orally are very often deactivated by acidic stomach conditions, and consequently, the effectiveness of probiotics intake depends very much on the number of viable cells capable to reach the gastrointestinal tract (Shen & Cabasso, 1982).

Several physiological obstacles can delay or prevent the delivery of probiotic bacteria in a safe and effective fashion. Different strategies have been explored to protect probiotics from the harsh conditions of the gastrointestinal tract (i.e. low pH, bile salts and enzymes) such as microencapsulation (Cook, Tzortzis, Charalampopoulos, & Khutoryanskiy, 2012). Various microencapsulation methods are being studied to address the problem of protecting and effectively delivering viable probiotic bacteria that preserve its metabolic functions. The microcapsules are often formed by mechanisms such as interfacial emulsion polymerization, ionic coacervation and sol-gel inmmobilization, using biocompatible macromolecules, such as polysaccharides and proteins, as encapsulating agents (Corona-Hernandez et al., 2013; Haffner, Diab, & Pasc, 2016). In this context, many different colloidal systems can be used for encapsulation in food formulation, including oil-in-water (O/W) emulsions, liposomes, coacervates, etc (Vemmer & Patel, 2013). Much less explored is the use of water-in-water (W/W) emulsions as templates for microencapsulation of probiotics in spite of these systems finding potential applications in food and drug delivery areas (Nicolai & Murray, 2017). These systems consist of droplets of an aqueous phase dispersed into another aqueous phase and are often obtained in different aqueous mixtures of hydrophilic polymers due to their

---

* Corresponding author.
** Corresponding author.
  E-mail addresses: Bfmedronho@ualg.pt (B. Medronho), jordi.esquena@iqac.csic.es (J. Esquena).

thermodynamic incompatibility (Esquena, 2016; Frith, 2010; Grinberg & Tolstoguzov, 1997).

One of the main drawbacks of W/W emulsions is their poor stability; often fast droplet coalescence or flocculation occurs, resulting in irreversible phase separation (Frith, 2010). One strategy to increase colloidal stability is using gelifying species/reagents in the formulation which may form arrested gelled states upon temperature change, thus stabilizing the emulsion droplets (Esquena, 2016; Frith, 2010). The W/W emulsions are typically formed after segregative phase separation (repulsive interactions between the polymers), avoiding the conditions where associative phase separation (attractive interactions) may occur, and preventing the formation of coacervate particles instead of emulsion droplets (Doublier, Garnier, Renard, & Sanchez, 2000). Such segregative phase separation may eventually result in the formation of microgels, which are particularly relevant as efficient vehicles to entrap and deliver therapeutic agents due to their biocompatibility and biodegradability (Fernandez-Barbero et al., 2009; Oh, Drumright, Siegwart, & Matyjaszewski, 2008; Silva et al., 2013).

W/W can be an effective method for incorporating bacteria in fully biocompatible and reasonably mild conditions (moderate pH and temperature), without both surfactant and oil. Thus, W/W emulsions could become a platform for production of soft materials as carriers of living microorganisms. For example, probiotic bacteria could be directly introduced inside microgels. However, this process would require chemical crosslinking to prevent fast dissolution of microgels in aqueous solutions. Crosslinking might seriously affect or damage the bacteria and, in this context, alternative methods such as freeze-drying of emulsions might allow the production of novel soft biocompatible porous polymer materials with incorporated viable probiotic bacteria.

Mixtures of edible proteins and polysaccharides are particularly interesting candidates for food applications due to their biocompatibility profiles. A vast list of combinations of proteins and polysaccharides that result in segregative phase separation can be found elsewhere (Grinberg & Tolstoguzov, 1997), and it is known that stable W/W emulsions can be formulated in mixtures of such macromolecules (Esquena, 2016; Frith, 2010). Gelatin and carboxymethyl cellulose (NaCMC) were chosen for this work because of their biocompatibility, low-cost and different ionic character. NaCMC is an anionic derivative of cellulose with muco-adhesive properties, while gelatin has excellent membrane-forming ability, biocompatibility and non-toxicity features (Hanani, Roos, & Kerry, 2014; "Kamide, K., 1 - Introduction. In Cellulose and Cellulose Derivatives, Elsevier: Amsterdam, 2005; pp 1–23.,"). Moreover, due to its amphoteric nature, it is also a thermally reversible gelling agent for encapsulation, sharply increasing viscosity below ca.40 °C, which hypothetically may guarantee an enhanced colloidal stability (Esquena, 2016; Grinberg & Tolstoguzov, 1997). Depending on the concentration, temperature and pH, NaCMC and gelatin may change their protonation states and weakly attractive or segregative forces may induce the formation of complexes or separated phases.

The formation of colloidal dispersions in gelatin/NaCMC mixtures remains mostly unexplored, and in the present work, the formation of W/W emulsions is investigated and characterized. Although plate counting is a widely used method of choice for detection of live probiotics in the food industry, modern techniques such as flow cytometry provide much more information in terms of culture-independent viability assays, for example rapidity and the ability to detect dormant cells. Therefore, to improve the understanding the viability and culturability of probiotic cells the two different approaches (plate counting and flow cytometry) were used for the systems exposed to the different in vitro conditions. The main goal of this work is to determine if NaCMC/gelatin complexes and/or emulsions can be formed and used to entrap viable probiotic bacteria and eventually deliver them to the gut.

2. Experimental

2.1. Materials and methods

Sodium carboxymethyl cellulose, NaCMC, (Mw ca. 250 kDa with a degree of substitution of 0.7) and gelatin (bovine skin, Mw of ca. 50 kDa-100 kDa) were purchased from Sigma-Aldrich. *Lactobacillus rhamnosus* GG LMG 18243 (LGG) was bought from the Belgian Coordinated Collection of Microorganisms (BCCM). The MRS broth pH 6.4 and MRS agar pH 5.7 were obtained from VWR International. The PBS buffer was prepared in the lab with disodium hydrogen phosphate, sodium chloride, potassium chloride and potassium dihydrogen phosphate, all purchased from Sigma-Aldrich. Sodium bicarbonate, magnesium chloride hexahydrate, ammonium carbonate and calcium chloride (all analytical grade) were obtained from Sigma-Aldrich. The Live/Dead® BacLight™ Bacterial Viability Kit L7012, containing the fluorescent probes Syto 9 and propidium iodine, PI, was purchased from Thermofisher Scientific, USA. Milli-Q water (18.2 MΩ.cm^{-1} at 25 °C, MQ) was used for the preparation of all samples. Porcine pepsin (EC 3.4.23.1), porcine trypsin (EC 3.4.21.4), bovine chymotrypsin (EC 3.4.21.1), porcine pancreatic α-amylase (EC 3.2.1.1), porcine pancreatic lipase (EC 3.1.1.3), porcine pancreatic colipase and bile extract B8631 (porcine) were all purchased from Sigma Aldrich.

2.2.1. Gelatin-NaCMC mixtures

Aqueous stock solutions of gelatin at different concentrations (from 5 to 64 wt%) were prepared by dissolving the appropriate amount of protein in MilliQ (MQ) water at 60 °C under continuous stirring. After achieving full dissolution, the solutions were kept at 4 °C before further use. On the other hand, aqueous stock solutions of NaCMC (from 0.5 to 7 wt%) were prepared by dissolving the polymer directly in MQ water at room temperature. Different ratios of the NaCMC and gelatin stock solutions were mixed by vortex and left to equilibrate at a constant temperature (60 °C) water bath. Samples were periodically inspected (i.e. naked eye and under polarized light microscopy).

2.2.2. Preparation of salivary, gastric and intestinal fluids

The Simulated Salivary Fluid (SSF), Simulated Gastric Fluid (SGF) and Simulated Intestinal Fluid (SIF) were made up of the corresponding electrolyte stock solutions, enzymes and water as described in Minekus et al. (see Tables 1 and 2 therein for details) (Minekus et al., 2014). Briefly, the SSF was prepared using stock solutions of the following electrolytes: K$^+$ (18.8 mmol/L), Na$^+$ (13.6 mmol/L), Cl$^-$ (19.5 mmol/L), H$_2$PO$_4^-$(3.7 mmol/L), HCO$_3^-$ (13.7 mmol/L), Mg^{2+}(0.15 mmol/L), NH$_4^+$ (0.12 mmol/L), Ca^{2+}(1.5 mmol/L). In a typical example, five gelatin-CMC particles were mixed with 5 ml of SSF electrolyte stock solution. Human salivary α-amylase (EC 3.2.1.1) was further added to achieve 75 U/mL in the final mixture, followed by CaCl$_2$ (0.75 mM) and the required amount of water to dilute the stock solution of SSF. Note that the recommended contact time with the enzyme is 2 min at 37 °C (pH 7) and therefore all reagents were pre-heated before mixing.

For the SGF fluid, the electrolyte stock solution was prepared to achieve the following ion concentrations; K$^+$ (7.8 mmol/L), Na$^+$ (72.2 mmol/L), Cl$^-$ (70.2 mmol/L), H$_2$PO$_4^-$ (0.9 mmol/L), HCO$_3^-$ (25.5 mmol/L), Mg^{2+}(0.1 mmol/L), NH$_4^+$ (1 mmol/L), Ca^{2+}(0.15 mmol/L). Later, porcine pepsin (EC 3.4.23.1) was added to achieve 2000 U/mL in the SGF electrolyte mixture. 1 M HCl was added to adjust the pH to 3. Typically, the obtained gastric chyme

was kept in contact with the particles for 2 h at 37 °C (recommended conditions for digestion (Minekus et al., 2014)).

Finally, for the SIF fluid preparation, five parts of simulated gastric chyme were mixed with four parts of a SIF electrolyte stock solution composed of K^+ (7.6 mmol/L), Na^+ (123.4 mmol/L), Cl^- (55.5 mmol/L), $H_2PO_4^-$ (0.8 mmol/L), HCO_3^- (85 mmol/L), Mg^{2+} (0.33 mmol/L) and Ca^{2+} (0.6 mmol/L) to obtain a final ratio of gastric chyme to SFI of 50:50 (v/v) after addition of other recipients and water. The mixture was neutralized to pH 7.0 with 1 M NaOH. Individual enzymes were added to the digestion mixture to achieve the following activities in the final fluid: porcine trypsin (EC 3.4.21.4) 100 U/mL, bovine chymotrypsin (EC 3.4.21.1) 25 U/mL, porcine pancreatic α-amylase (EC 3.2.1.1) 200 U/mL, porcine pancreatic lipase (EC 3.1.1.3) 2000 U/mL, porcine pancreatic colipase 100 U/mL and bile extract B8631 (porcine) 10 mM. Note that the pH may need re-adjustment before finally adding water to the mixture to dilute the stock solution of SIF. Typically, the SFI fluid was kept in contact with the particles for 2 h at 37 °C (recommended conditions for intestinal digestion) and pH 7.0.

2.2.3. Optical microscopy

An Olympus model BX51TRF-6 microscope, coupled to a digital camera Olympus DP73 was used to study the phase behavior and microscopic structures of the aqueous polymer mixtures, at different pHs and concentrations in the transmission mode.

2.2.4. Morphology studies

Scanning Electron Microscopy was performed on a Hitachi TM-1000 Tabletop Microscope, operating at 5 kV, and on a VEGA3 SBH from TESCAN, 15 kV, equipped with a selected energy dispersive X-ray microanalyser (EDX). These SEM were used to observe the morphology of the NaCMC-gelatin particles with and without LGG bacteria. Generally, freeze dried particles were deposited directly onto the carbon tape on the support and sputtered with approximately 6 nm thin Au/Pd film by cathodic pulverization using a SPI Module Sputter Coater, during 90 s and with a current of 15 mA.

2.2.5. Growth and entrapment of Lactobacillus rhamnosus GG

All culture media and buffers were autoclaved for sterilization at 121 °C for 15 min. Freeze-dried cells of *Lactobacillus rhamnosus* GG were rehydrated in 5 mL MRS broth and incubated at 37 °C for 40 h in a CO_2 incubator and the growth was checked during two days. When the broth became turbid, the bacterial growth was visually confirmed by the optical density and was compared with the non-inoculated broth. To evaluate the purity of the bacteria, one inoculation loop with bacteria was streaked on a MRS agar plate while a plate with pure sterilized culture was treated as control. The optical density was measured with UV/vis spectrophotometer. In a later step, 10 mL of the cultured broth were divided in 10 eppendorfs and centrifuged for 30 min at 3000 rpm. The supernatant was discarded and 1 ml PBS was added to each of the pellets followed by centrifugation at 3000 rpm for 20 min. This washing procedure was repeated twice. Finally, the PBS rich supernatant was discarded. 5 bacterial pellets were mixed with 20 ml of 1 wt% of NaCMC aqueous solution and 5 bacterial pellets were mixed with 20 ml of 7.5 wt% gelatin aqueous solution, both equilibrated at 40 °C.

2.2.6. Evaluation of LGG proliferation: plate counting and fluorescence

The fresh gelatin-NaCMC particles were transferred to a PBS buffer solution at 37 °C for 30 min. The counts of bacteria cells were performed by adding 100 μl of the suspended particles to 1 ml of PBS buffer. Sequential dilutions were performed by dissolving the particles from each composition in the PBS buffer following the Miles and Misra approach to count the number of culturable bacteria (Miles, Misra, & Irwin, 1938). All different dilutions were plated in triplicates and kept in CO_2 incubator for 48 h before the bacterial colony was counted using a colony reader. For the particles treated with different gastrointestinal fluids (*in vitro* tests), the procedure was rather similar. After exposing the particles to the different fluids, samples were centrifuged at 3000 relative centrifugal force (rcf) for 10 min at 4 °C. The particles (or what remains from them) were re-suspended in 900 μL of phosphate buffer (0.1 M, pH 7.0) followed by gentle shaking at room temperature for 15 min. Sequential dilutions and plating in MRS agar was performed as previously described to estimate the number of culturable cells. The experiments were performed in Faster BH-EN and BHG Class II Microbiological Safety Cabinets. The bacteria viability was also inferred using a Dead/Alive kit (commercial LIVE/DEAD® *Bac*Light™). The bacteria in the NaCMC-gelatin particles were stained with 2 μl of SYTO 9 dye from the kit and observed in a fluorescence Olympus microscope (100× immersion objective).

2.2.7. Flow cytometry

Analysis was performed using a FACSCalibur flow cytometer (BD Biosciences) equipped with a 488 nm argon ion laser. Green fluorescence was measured at 530/30 nm (FL1) and red fluorescence was measured above 670 nm (FL3). Data analysis was performed using BD Cell Quest Pro software. The fluorescent probes Syto 9 (3.34 mM in DMSO) and propidium iodine (PI) (20 mM in DMSO) were used to stain all bacteria and the ones with the membrane compromised, respectively. These probes were used to make the working solutions. Typically, 5 μL of live/dead working solution was added to 5 μL of diluted particle sample and 490 μL of filtered PBS. The mixture was further incubated at 37 °C for 15 min in an incubator. The collected data was analyzed by drawing a region around the Syto 9 positive cells (R1) and discriminating the PI positive cells (R2—dead cells) from the ones only labeled with Syto 9 (R1 and not R2—live cells). Heat killed bacteria (90 °C for 15 min) were used as positive control whereas free bacteria were used as a negative control. At least 40000 events gated on R1 were collected for analysis.

2.3. Statistical analysis

All experiments and analysis were run in triplicate. All quantitative data are presented as mean ± standard deviation. Excel software was used to perform statistical analysis and $p < 0.05$ indicates the statistical significance.

3. Results and discussion

3.1. Phase behavior of Gelatin-NaCMC mixtures

Depending on the gelatin/NaCMC ratio, the pH of the mixtures was generally between 6.3 and 7.3. In these conditions, gelatin (isoelectric point of ca. 4.7—5.2) and NaCMC (pKa of ca. 4.3 (Tian et al., 2006)) are expected to be both negatively charged, and thus, coacervation is prevented. After mixing the polymer solutions, a turbid dispersion appeared but after ca. 35—48 h, macroscopic phase separation (two aqueous liquid phases in equilibrium), could be observed above critical polymer concentrations. Such behavior suggests a segregative phase separation, with formation of two immiscible aqueous liquid phases caused by repulsive interactions between the two water soluble polymers.

The vials presented on top of Fig. 1 illustrate phase separation. Slow sedimentation (left image) and rather complete phase separation (right image) can be both visually observed at naked eye, despite the fact that W/W systems are highly transparent. The slower velocity of sedimentation (left image) can be related to a
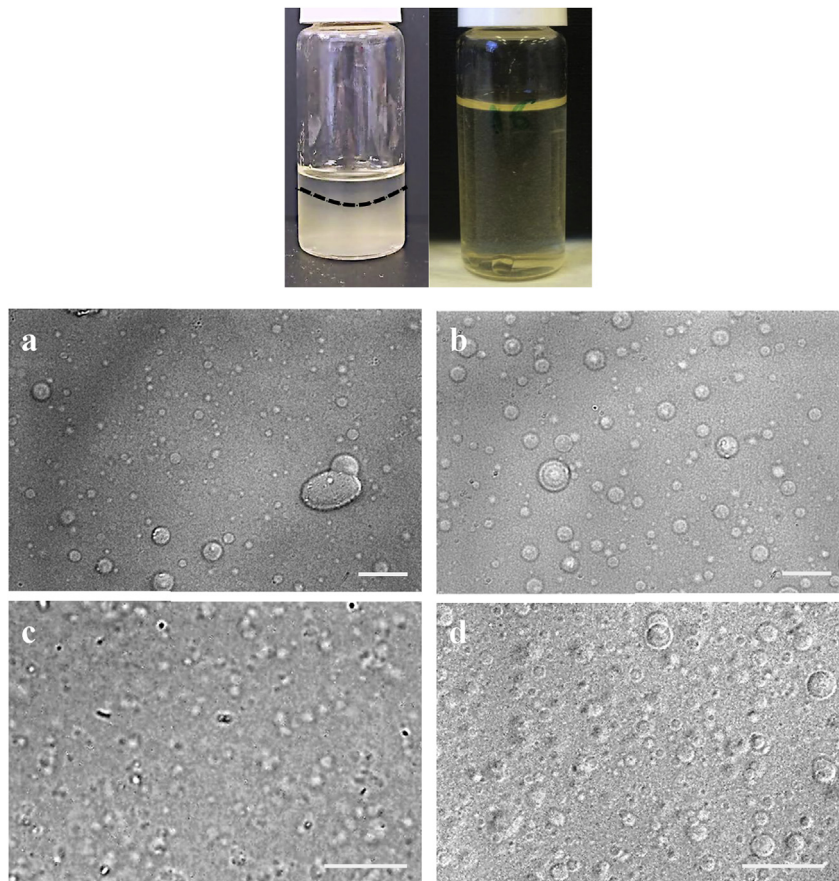
Fig. 1. Top: photos of two Gelatin-NaCMC mixtures at 60 °C after two days of equilibration at constant temperature of 60 °C. 1 wt% NaCMC and 15 wt% gelatin (left) and 0.2 wt% NaCMC and 5 wt% gelatin (right). For better visualization, the dashed line in the phase separated sample demarks the sedimentation boundary. Bottom: optical microscopy images of the NaCMC-gelatin systems composed of 1.2 wt NaCMC and 2.8 wt% gelatin (a), 1.6 wt% NaCMC and 1 wt% gelatin (b), 1 wt% NaCMC and 7.5 wt% gelatin (c), 2 wt% NaCMC and 7.5 wt% gelatin (d). In all these cases, droplet-like objects can be observed indicating the formation of emulsions after mixing the phase-separated samples. The scale bars represent 20 μm.

higher viscosity, since this sample contained 15 wt% gelatin, whereas the gelatin concentration was 5 wt% in the sample that shows more advanced phase separation. The W/W emulsions originated from segregative phase separation can be prepared by applying mechanical agitation. A collection of optical microcopy images displaying typical emulsion droplets, from different NaCMC and gelatin compositions, is also shown in Fig. 1.

Macroscopic phase separation was not observed for most of the compositions tested (e.g. Fig. 1a and b), during at least 3 days of equilibrium at 60 °C. Most likely, this slow sedimentation can be attributed to a small difference in density between the two phases. Moreover, one should consider that the viscosity of the continuous phase might be rather high. Consequently, phase separation can be extremely slow requiring longer periods to be clearly observed. Since the main component in both phases is water, the refractive indexes of the disperse phase and the continuous phase are rather similar which results in a low contrast in the images by optical microscopy. This small difference in refractive index also causes the emulsions to be rather transparent, instead of white or milky, as typically observed in other systems. It was striking to observe the good colloidal stability of the dispersions, with absence of short-term sedimentation even though the droplets have an average size ca. 5–10 μm. These observations seem to confirm that colloidal dispersions most probably consist of water-in-water emulsions, given the liquid nature of the two phases and the probable small differences in macroscopic properties (refractive index and density) between these two phases. Note that, the observations of these

emulsions require temperatures higher than 35 °C, which is the gelling point of gelatin. Most likely, the emulsion droplets consist of a NaCMC-enriched aqueous solution, dispersed into a gelatin-rich aqueous solution (and thus the system can be denoted as NaCMC-in-gelatin emulsion) because the dispersions completely jellify when cooled down to room temperature, clearly demonstrating that gelatin is present in the continuous phase. Further, the NaCMC-in-gelatin emulsions can be verified by the fact that gelatin is slightly colored (yellowish) whereas NaCMC is colorless and, after several days at 60 °C, a colorless region is observed as a small separated volume located at the top of the sample vial (see, for instance, Fig. 1, top-left image). This can be attributed to the migration of less dense NaCMC droplets to the top of the sample. This creaming seems to be rather slow which, as mentioned before, can be related to the small difference in density between the NaCMC and the gelatin aqueous solutions. The formation of NaCMC-in-gelatin emulsions is also consistent to the fact that NaCMC was added in rather small concentrations with respect to gelatin. As described in literature, water-in-water droplets are constituted by the phase with smaller volume, whereas the large-volume phase tends to become the continuous phase (Esquena, 2016; Frith, 2010). Moreover, when increasing the Gelatin/NaCMC composition ratio, it was observed that the volume of the yellowish region (rich in gelatin), located at the sample bottom, increases. These simple visual observations at naked eye are supported by UV-vis measurements as described in the SI section. Therefore, it can be concluded that the system has a segregative phase separation and

the colloidal dispersions observed at 60 °C are indeed NaCMC-in-gelatin W/W emulsions. Due to the observed non-equilibrium features and presence of kinetically arrested structures, the equilibrium phase diagram of the NaCMC-gelatin system is currently under investigation. Nevertheless, qualitatively the behavior is rather similar to the phase diagrams reported for several binary mixtures of milk proteins, including whey, amylopectin and gelatin, with other neutral polysaccharides, such as xyloglucan or maltodextrin (Grinberg & Tolstoguzov, 1997).

3.2. Influence of pH on the W/W emulsions

The interactions between the two polymers can be tuned by pH or ionic strength, which can lead to a rich phase behavior. In fact, depending on pH and ionic strength, associative and segregative phase separation have been reported to occur, even simultaneously (Fang, Li, Inoue, Lundin, & Appelqvist, 2006). However, it should be noted that such situation is not expected to occur at equilibrium and thus it represents kinetically trapped states. In our system, Fig. 2 shows how pH affects the W/W emulsion structure for the 1 wt% NaCMC and 7.5 wt% gelatin (a, b, c) and 1 wt% NaCMC and 15 wt% gelatin samples (d, e, f).

No major changes are observed in the W/W emulsions for the lower gelatin concentration (i.e. 7.5 wt%) while the average size seems to change slightly for the highest gelatin concentration (i.e. 15 wt%). At pH 3 (Fig. 2a), the NaCMC should be neutral (pKa of ca. 4.3 (Tian et al., 2006)) while the gelatin should be weakly positively charged (isoelectric point ca. 4.7–5.2). On the other hand, at pH 5.7 and 10 (Fig. 2b and c, respectively) both polymers should be negatively charged. Typically, the segregation can arise from thermodynamic incompatibility, which may be highly dependent on molecular conformation. The repulsion between polymer chains can be electrostatic in nature (i.e. like charges) or due to restrictions in the free conformational movement of the polymers. This behavior depends strongly on molecular weight: short molecules tend to restrict free conformation states of long linear chain molecules. Therefore, repulsive interactions are expected to be present in mixtures of the polymers without electrostatic attraction and clearly distinct molecular weights, such as in the case of gelatin and NaCMC, at pH values far from their respective isoelectric points.

Henceforth, the conditions are beneficial for segregative phase separation either by mixing a nonionic (or weakly charged) polymer, carboxymethyl cellulose, with a protonated polymer (gelatin at pH 3) or by mixing two negatively charged polymers (cases at pH 5.7 and 10), and this might be the reason why W/W emulsions are observed in the studied pH range. A thorough study of the influence of pH and ionic strength on the phase behavior of NaCMC-gelatin aqueous mixed system will be addressed in the future.

3.3. Entrapment of LGG in the W/W emulsions

The first part of the paper describes the formation of emulsion droplets in the NaCMC-gelatin system, at 60 °C. Rather than the extensive characterization of these systems, the main objective of the work is to evaluate if these W/W emulsion systems can be used to entrap viable probiotic bacteria. Accordingly, the cell viability in the NaCMC-gelatin system was qualitatively evaluated, at 37 °C, by fluorescence microscopy using the Syto 9 dye from the Dead/Alive kit (Fig. 3). For the 1 wt% NaCMC and 7.5 wt% gelatin, W/W emulsions trapping LGG are observed (Fig. 3a and b). The average size of the emulsion droplets is apparently not greatly affected. The green emission is a signature of stained cells and such emission is clearly observed in the NaCMC aqueous droplets thus demonstrating a higher affinity of bacteria for the NaCMC aqueous phase. This preferential location of bacteria in the NaCMC phase is probably caused by electrostatic attraction between the negatively charged NaCMC and the positive charges of bacterial membrane lipids. Moreover, it can be observed that the green emission is more intense at the interface of the emulsion drops, which seems to be covered with adsorbed bacteria. This observation indicates that bacteria are adsorbed at the W/W interface. This is not surprising and has been reported before (Fisher, 1981; Walter, 1978). It is known that adsorption of spherical particles in liquid/liquid interfaces depends both on particle size and interfacial tension, and thus bacteria adsorbs on interfaces more strongly when interfacial tension is higher (Fisher, 1981; Walter, 1978). The mechanism of adsorption is probably the same as that described for Pickering emulsions (Balakrishnan, Nicolai, Benyahia, & Durand, 2012; Nicolai & Murray, 2017), considering that the energy of adsorption of homogeneous spherical particles, ΔE, follows the equation

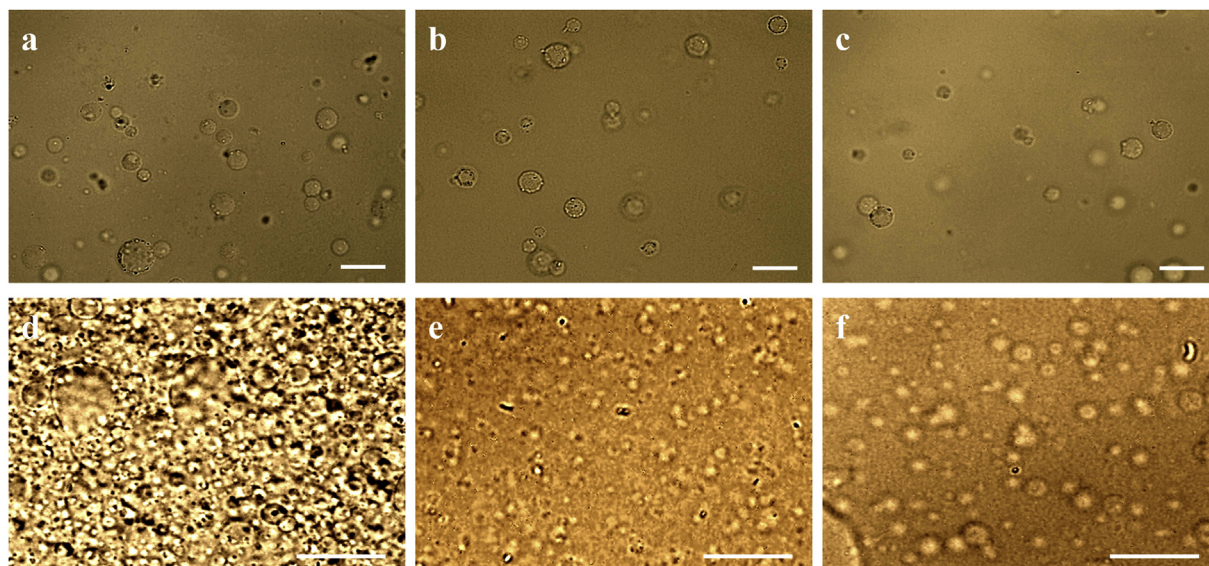

Fig. 2. Optical microscopy images of W/W emulsions from the 1 wt% NaCMC and 7.5 wt% gelatin (a, b and c) and 1 wt% NaCMC and 15 wt% gelatin (d, e and f) samples. The pH is 3.0 (a, d); 5.7 (b, e) and 10 (c, f). The scale bars represent 20 μm.
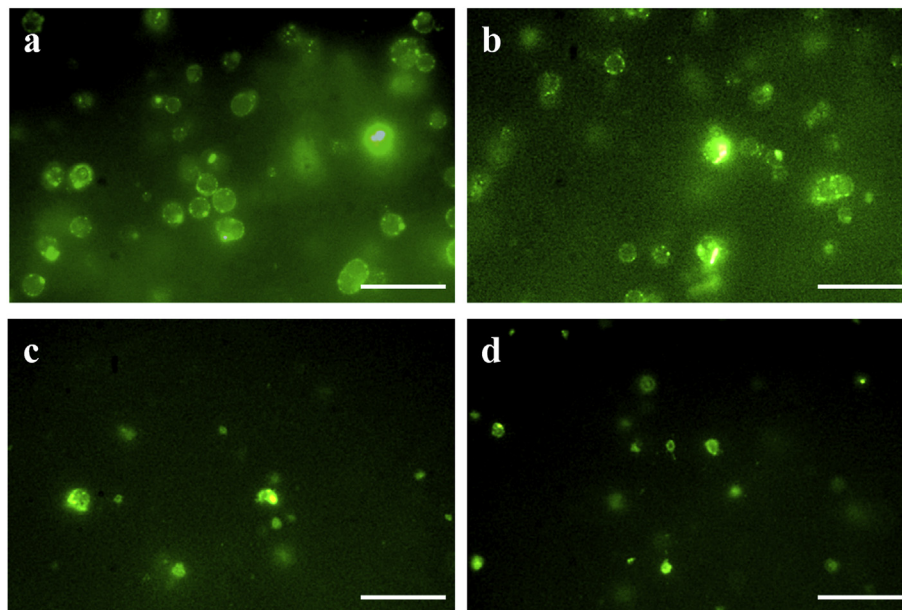
Fig. 3. Fluorescence microscopy images of W/W emulsions from the 1 wt% NaCMC and 7.5 wt% gelatin sample (a and b) and 1 wt% NaCMC and 15 wt% gelatin (c and d) at pH 5.5 and 37 °C. The samples were stained with Syto9 and green emission identifies the location of bacteria. The scale bars represent 20 μm.

$\Delta E = \pi R^2 \gamma (1-|\cos\theta|^2)$ (Aveyard, Binks, & Clint, 2003), where R^2 is the square of particle size, γ is the interfacial tension and θ is the contact angle on the interface. Bacteria typically are few micrometers in length, and this size is enough to overcome a low interfacial tension, and thus, producing a significant energy of adsorption that pushes bacteria to the interface. One can compare the images of Fig. 3 with those of W/W emulsions stabilized by particles adsorbed on the interface, shown in the literature (Balakrishnan et al., 2012; de Freitas, Nicolai, Chassenieux, & Benyahia, 2016). It has been reported that different types of particles (i.e. latex, globular proteins, silica, cellulose nanocrystals, etc) can absorb at W/W interfaces, despite the very low interfacial tension, in a similar way as traditional Pickering emulsions (Esquena, 2016; Frith, 2010), increasing the stability and thus decreasing the rate of coalescence and sedimentation. A similar mechanism is believed to occur with LGG bacteria in the NaCMC-gelatin system.

On the other hand, in Fig. 3c and d the density of brighter flocculates seems to increase. It looks like when the concentration of gelatin raises from 7.5 to 15 wt% the emulsions may become less stable in the presence of LGG, increasing the rate of phase separation. The flocculates are green and this might suggest the formation of LGG aggregates with gelatin, which, at pH 5.5, is weakly positively charged while LGG is negatively charged. In addition, the increase of density of flocculates may be related to higher adsorption of LGG to W/W interface since the affinity of the LGG to adsorb at liquid–liquid interface is expected to increase as the system composition moves away from the critical point, presumably by increasing interfacial tension (Fisher, 1981). The microstructure of the LGG cells entrapped in the W/W emulsions was further studied by SEM (Fig. 4).

Regardless of the order of mixing (i.e. LGG mixed first with NaCMC or with gelatin), a foam-like microstructure is obtained after freeze-drying (Fig. 4a and b) as expected for emulsion templating. Therefore, a macroporous solid foam have been obtained, without oil and without surfactant. This porous material has an alveolar morphology and the images show that the bacteria are located on the surface of the macropores as shown in Fig. 4c (higher magnification of Fig. 4b). The size of the macropores of the solid

material (around ≈ 50 μm) is significantly larger than the size of droplets in the emulsions (around ≈ 5 μm, as shown in Fig. 1). However, it should be noted that NaCMC-in-gelatin emulsions are rather unstable at 40 °C, with presence of phase separation (visual observations, images not shown) and consequently, the increase in size, from 5 to 50 μm, could be simply attributed to coalescence. However, one cannot discard the possibility that the increase in pore size was also influenced by the formation of ice crystals during the freeze-drying process. It has been reported that crystallization is a key factor in the appearance of large pores in the freeze-drying of microgels. For instance, Schachschal et al. have shown that freeze-drying of microgels leads to the formation of porous particles having large voids (Schachschal et al., 2011). Nevertheless, the polydispersity of the W/W emulsion, its reduced stability and the location of bacteria mainly on the W/W interface are factors that are consistent to SEM observations (Fig. 4) and support the argument that the macropores present in the final material were templated by W/W emulsion droplets. In any case, the results clearly demonstrate that bacteria can be incorporated in W/W emulsions, which are oil and surfactant-free dispersions and thus highly compatible to microorganisms. In Fig. 5, the results from the plate counting method are summarized for the particles formed with the 1 wt% NaCMC and 7.5 wt% gelatin.

The counting of the naked not entrapped LGG cells was 10.01 ± 0.14 Log CFU/mL. After incorporation of LGG in the NaCMC-gelatin W/W systems (either mixing LGG first with gelatin, "A", or mixing LGG first with NaCMC, "B") the count of the cells was not reduced. Regardless of the order of mixture, the bacterial count was found to be very close to that of naked free bacteria (i.e. "A": 9.95 ± 0.33 Log CFU/mL and "B": 9.55 ± 0.23 Log CFU/mL). If the matrix characteristics are beneficial for probiotic growth and proliferation, it is not unusual to observe similar viabilities between the reference naked bacteria and the entrapped systems (Amakiri & Thantsha, 2016; Arora, Kaur, Chopra, & Rishi, 2014; Bosnea, Moschakis, & Biliaderis, 2014; Zanjani, Tarzi, Sharifan, & Mohammadi, 2014). The high culturability estimated from the plate counting is in good agreement with the qualitative cell viability from the fluorescence microscopy using a Dead/Alive kit (Fig. 3).
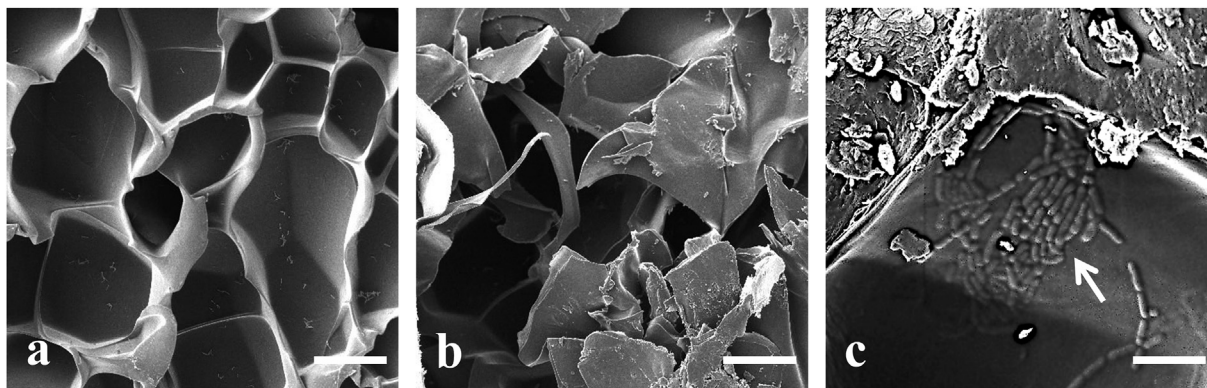
Fig. 4. Scanning electron microscopy images from 1 wt% NaCMC and 7.5 wt% gelatin doped with LGG. a) LGG was mixed with the NaCMC solution and the gelatin solution added later; b) LGG was mixed with the gelatin solution and the NaCMC solution added later; C) higher magnification of Fig. 4b showing the rod-shaped LGG cells. The arrow highlights a region crowded with LGG. The scale bars represent 50 μm (a and b) and 5 μm (c).
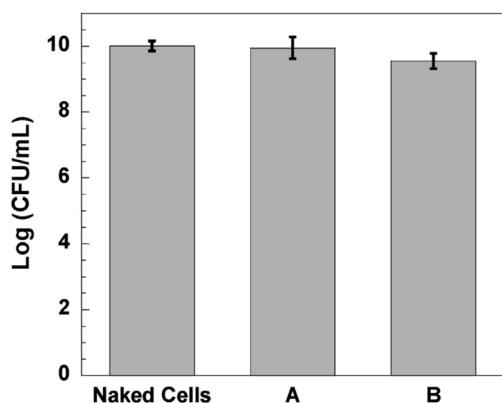

Fig. 5. Bacterial counts in Log CFU/mL of the naked free cells. LGG mixed firstly with gelatin and NaCMC added afterwards is denoted "A" and LGG mixed firstly with NaCMC and gelatin added afterwards is indicated as "B". The error bars represent the standard deviation.

Samples of NaCMC-in-gelatin emulsions were also exposed to *in vitro* simulated digestion fluids as described in section 2.2.2. The fluids used try to mimic the in vivo physiological conditions, considering different parameters such as concentration of digestive enzymes, pH, digestion time, salts, among others.

Bacteria were gated by drawing a region around Syto 9 positive events (R1), which are presented in yellow in the FSS/SCC dot plots, and only those cells were further analyzed. Note that, forward light scattering (FSC) correlates with the cell size whereas the side scattering channel (SSC) is proportional to the granularity of the cells. The cells labeled with both Syto 9 and PI (R2) have the membrane compromised (dead) and are presented in red. Live cells, only labeled with Syto 9 (R1 and not R2) are presented in green. Fluorescent signals were quantified by measuring the height of the signals. The specificity of the LIVE/DEAD BacLight stain was assessed using known ratios of live to heat-killed bacteria in flow cytometry shown in Fig. S3 (Supplementary Information). A good correlation was obtained between the percentages of PI positive and negative bacteria as a percentage of red and green colors, shown further in Fig. S4 (Supplementary Information). Red or green color can be observed on the histograms and dot plots depending on whether the cultures were dead (PI positive) or live (PI negative). Note that a standard control procedure was followed to guarantee that in the selected region only bacteria stained with probes is collected. This procedure was used to determine the shifts and

mark the controls by measuring the fluorescent of the dyes SYTO9, PI and the PBS buffer alone or in combination with the bacteria.

The effect of the model SGF is depicted in Figs. 6 and 7. It can be concluded that the cell counting was virtually the same before and after the SGF treatment for 120 min. More than 99% of the total cell population gated was found viable after the SGF treatment. Therefore, clearly the NaCMC-in-gelatin matrix has an excellent protective effect on bacteria. In any case, the soft NaCMC-in-gelatin matrix may be affected by the treatment. This aspect was not evaluated, and the number of encapsulated or released bacteria was not quantified. Most likely, the NaCMC-gelatin structure allows protection of bacteria by slowing down its release in the presence of digestive fluids. The kinetics of release of bacteria is an important aspect to be studied and it can be the scope of future works.

On the other hand, the sequential exposure of the naked and entrapped cells to SGF (120 min) followed by the SIF (120 min) resulted in a higher number of alive bacteria when trapped in the NaCMC-in-gelatin matrix; the cell survival was ca. 77.5% of the population after SGF and SIF exposure while in the free cell case ca. 60% were found metabolically viable (Figs. 8 and 9).

Although the cell population declines approximately at the same rate for all the tested simulated gastro-intestinal conditions, a final 4 log CFU/ml decrease in bacterial count is observed for the encapsulated LGG while the loss in bacterial count is higher, ca. 5 log CFU/ml, for the naked cells. Despite the obvious differences, a similar conclusion is drawn from the plate counting method, which shows a good correlation with the flow cytometry data (Fig. 10).

In conclusion, bacterial counts after treatment with simulated digestive fluids showed that NaCMC-in-gelatin dispersions protect bacteria, improving the ability to proliferate in comparison to naked bacteria. In addition, flow cytometry showed that metabolically active bacteria also increased by incorporation of bacteria into NaCMC-in-gelatin dispersions. These two concepts, proliferation by culture counting and viability determination by a Dead/Alive essay, both have shown that NaCMC-in-gelatin certainly have a protective effect on bacteria with remarkable values for practical uses (Shen & Cabasso, 1982).

4. Conclusions

The NaCMC-gelatin system was studied regarding its possibility to be used as a matrix for encapsulation of probiotic bacteria. The data suggest the formation of a segregative phase separation above critical polymer concentrations where W/W emulsions can be formed. Interestingly, colloidally stable emulsion droplets were also observed, without apparent sedimentation. Due to some
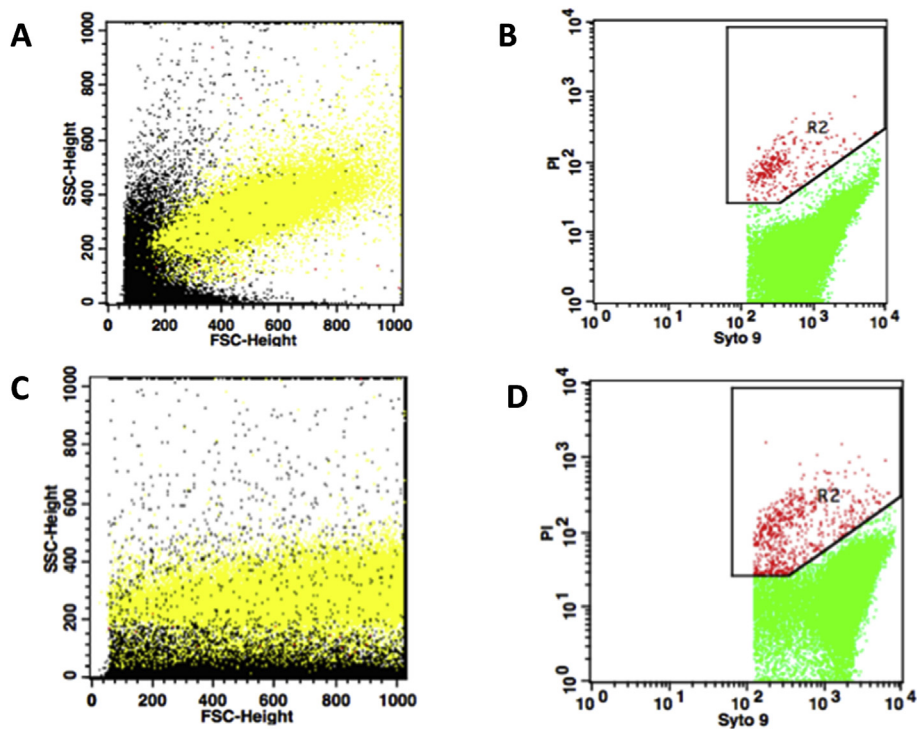
Fig. 6. Dot plots obtained after treating the particles with the simulated gastric fluid. The control (free naked cells) data is displayed on the graphics A and B while the data respective to the cells entrapped in the W/W emulsions (1% NaCMC and 7.5% gelatin) is represented on the graphics C and D. The yellow region in the FSS/SCC dot plot represents all the cells labeled with Syto 9. Red dots represent cells labeled with both Syto 9 and PI (dead cells) while the green dots represent the cells only labeled with Syto 9 (live cells).
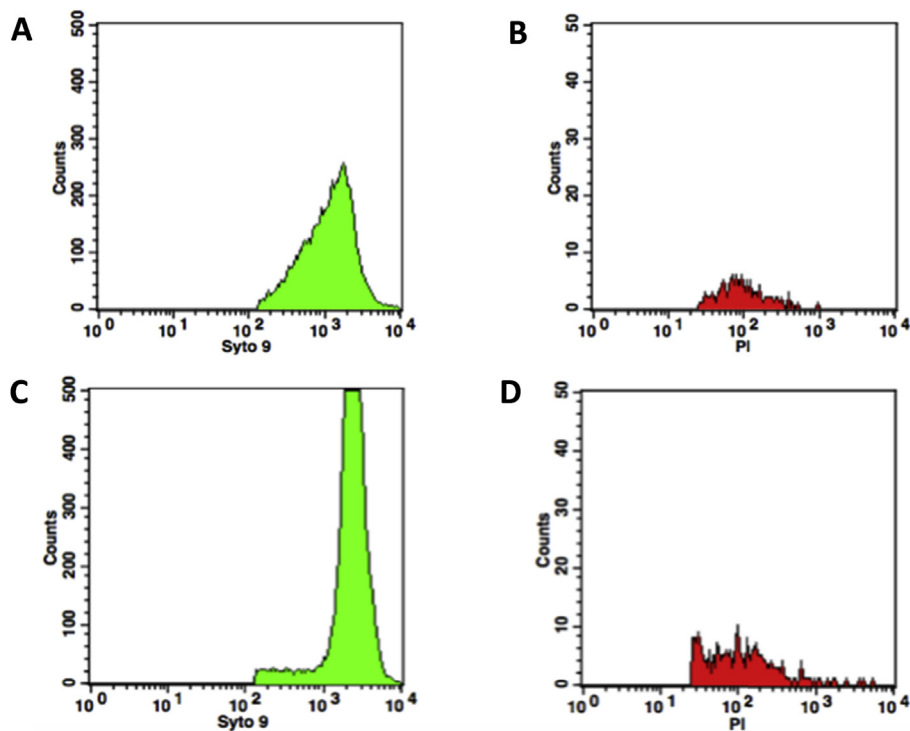

Fig. 7. Histograms obtained after simulated gastric fluid treatment of the control cells (A and B) and cells encapsulated in the 1% NaCMC and 7.5% gelatin W/W emulsions (C and D). The systems have been stained with Syto 9 and PI. The green histograms show bacteria only labeled with Syto 9 (i.e. viable) while the red histograms display the bacteria labeled with both Syto 9 and PI (i.e. dead).

peculiarities of the systems (i.e. high viscosity and low density difference), sedimentation may proceed at slow velocity.

Nevertheless, these W/W emulsions can be used to efficiently entrap LGG bacteria as demonstrated by fluorescence microscopy
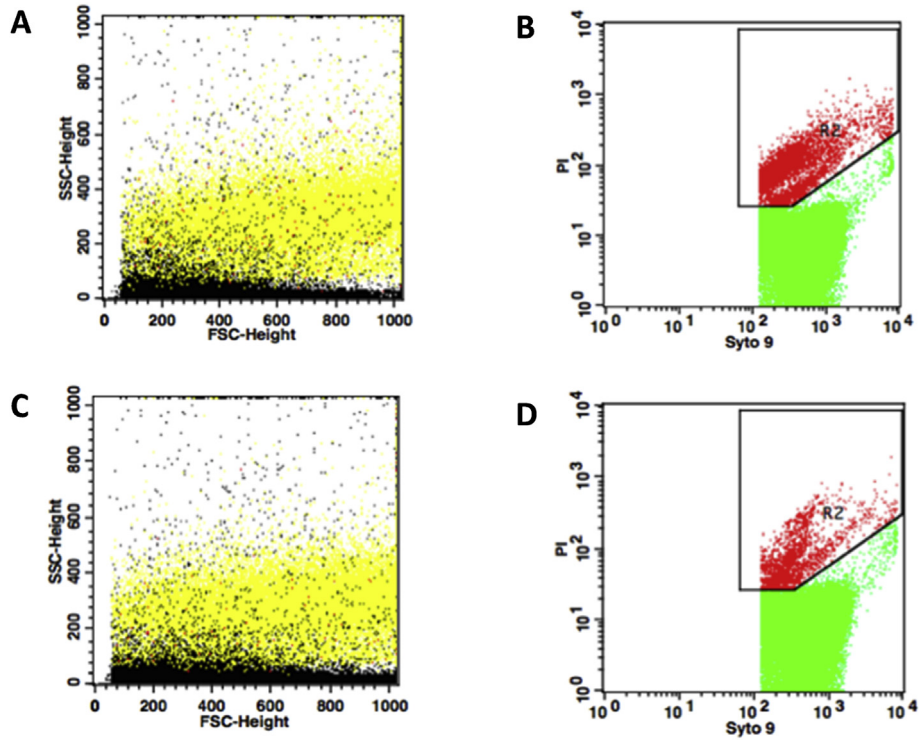
Fig. 8. Dot plots obtained after treating the particles with the simulated intestinal fluid. The control (free naked cells) data is displayed on the graphics A and B, while the data respective to the cells entrapped in the W/W emulsions (1% NaCMC and 7.5% gelatin) is represented on the graphics C and D. The yellow region in the FSS/SCC dot plot represents all the cells labeled with Syto 9. Red dots represent cells labeled with both Syto 9 and PI (dead cells) while the green dots represent the cells only labeled with Syto 9 (live cells).

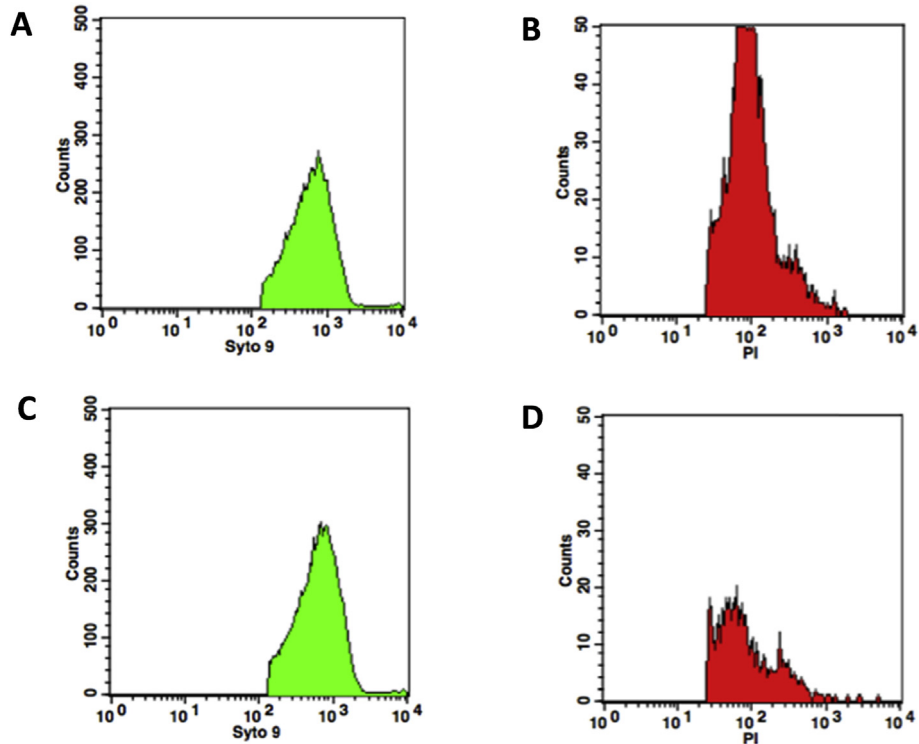**Fig. 9.** Histograms obtained after simulated intestinal fluid treatment of the control cells (A and B) and cells encapsulated in the 1% NaCMC and 7.5% gelatin W/W emulsions (C and D). The systems have been stained with Syto 9 and PI. The green histograms show bacteria only labeled with Syto 9 (i.e. metabolically viable) while the red histograms display the bacteria labeled with both Syto 9 and PI (i.e. dead).
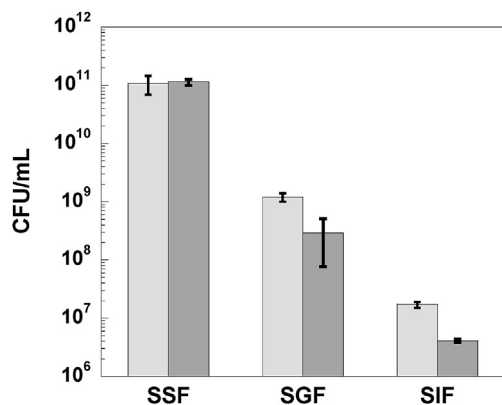
Fig. 10. Bacterial counts in CFU/mL of the naked (dark grey bars) and encapsulated cells in the 1% NaCMC and 7.5% gelatin W/W emulsion (light grey bars). Data was interpreted with the plate count method after exposure of the naked and entrapped cells to Simulated Salivary, Gastric and Intestinal Fluids (SSF, SGF and SIF, respectively). The error bars represent the standard deviation.

and SEM. The developed systems are observed not to reduce significantly the viability and culturability when exposed to different gastro-intestinal fluids. The results also showed that the encapsulation in the W/W emulsion improved the survival of the cells with values acceptable for practical uses. Therefore, this study opens a new route for the entrapment of preserved probiotic bacteria using biocompatible W/W emulsions formed by edible proteins and polysaccharides.

Acknowledgements

Appendix A. Supplementary data

Supplementary data related to this article can be found at https://doi.org/10.1016/j.foodhyd.2017.09.014.

References

Amakiri, A. C., & Thantsha, M. S. (2016). Survival of Bifidobacterium longum LMG 13197 microencapsulated in Vegetal or Vegetal-inulin matrix in simulated gastrointestinal fluids and yoghurt. *Springerplus, 5*, 1343.

Arora, S., Kaur, I. P., Chopra, K., & Rishi, P. (2014). Efficiency of double layered microencapsulated probiotic to modulate ProInflammatory molecular markers for the management of alcoholic liver disease. *Mediators of Inflammation, 2014*, 715130.

Aveyard, R., Binks, B. P., & Clint, J. H. (2003). Emulsions stabilised solely by colloidal particles. *Advances in Colloid and Interface Science, 100*, 503–546.

Balakrishnan, G., Nicolai, T., Benyahia, L., & Durand, D. (2012). Particles trapped at the droplet interface in water-in-water emulsions. *Langmuir, 28*(14), 5921–5926.

Bosnea, L. A., Moschakis, T., & Biliaderis, C. G. (2014). Complex coacervation as a novel microencapsulation technique to improve viability of probiotics under different stresses. *Food and Bioprocess Technology, 7*(10), 2767–2781.

Cook, M. T., Tzortzis, G., Charalampopoulos, D., & Khutoryanskiy, V. V. (2012). Microencapsulation of probiotics for gastrointestinal delivery. *Journal of Controlled Release, 162*(1), 56–67.

Corona-Hernandez, R. I., Alvarez-Parrilla, E., Lizardi-Mendoza, J., Islas-Rubio, A. R., de la Rosa, L. A., & Wall-Medrano, A. (2013). Structural stability and viability of microencapsulated probiotic bacteria: A review. *Comprehensive Reviews in Food Science and Food Safety, 12*(6), 614–628.

Doublier, J. L., Garnier, C., Renard, D., & Sanchez, C. (2000). Protein-polysaccharide interactions. *Current Opinion in Colloid & Interface Science, 5*(3–4), 202–214.

Esquena, J. (2016). Water-in-water (W/W) emulsions. *Current Opinion in Colloid & Interface Science, 25*, 109–119.

Fang, Y. P., Li, L. B., Inoue, C., Lundin, L., & Appelqvist, I. (2006). Associative and segregative phase separations of gelatin/kappa-carrageenan aqueous mixtures. *Langmuir, 22*(23), 9532–9537.

Fernandez-Barbero, A., Suarez, I. J., Sierra-Martin, B., Fernandez-Nieves, A., de las Nieves, F. J., Marquez, M., et al. (2009). Gels and microgels for nanotechnological applications. *Advances in Colloid and Interface Science, 147–48*, 88–108.

Fisher, D. (1981). The separation of cells and organelles by partitioning in two-polymer aqueous phases. *Biochemical Journal, 196*(1), 1–10.

de Freitas, R. A., Nicolai, T., Chassenieux, C., & Benyahia, L. (2016). Stabilization of water-in-water emulsions by polysaccharide-coated protein particles. *Langmuir, 36*, 1227–1232.

Frith, W. J. (2010). Mixed biopolymer aqueous solutions - phase behaviour and rheology. *Advances in Colloid and Interface Science, 161*(1–2), 48–60.

Grinberg, V. Y., & Tolstoguzov, V. B. (1997). Thermodynamic incompatibility of proteins and polysaccharides in solutions. *Food Hydrocolloids, 11*(2), 145–158.

Haffner, F. B., Diab, R., & Pasc, A. (2016). Encapsulation of probiotics: Insights into academic and industrial approaches. *Aims Materials Science, 3*(1), 114–136.

Hanani, Z. A. N., Roos, Y. H., & Kerry, J. P. (2014). Use and application of gelatin as potential biodegradable packaging materials for food products. *International Journal of Biological Macromolecules, 71*, 94–102.

Holzapfel, W. H., Haberer, P., Snel, J., Schillinger, U., & Huis in't Veld, J. H. J. (1998). Overview of gut flora and probiotics. *International Journal of Food Microbiology, 41*(2), 85–101.

Iannitti, T., & Palmieri, B. (2010). Therapeutical use of probiotic formulations in clinical practice. *Clinical Nutrition, 29*(6), 701–725.

Kamide, K. (2005). 1-Introduction. In *Cellulose and cellulose derivatives* (pp. 1–23). Amsterdam: Elsevier.

Miles, A. A., Misra, S. S., & Irwin, J. O. (1938). The estimation of the bactericidal power of the blood. *Journal of Hygiene, 38*(6), 732–749.

Minekus, M., Alminger, M., Alvito, P., Ballance, S., Bohn, T., Bourlieu, C., et al. (2014). A standardised static in vitro digestion method suitable for food - an international consensus. *Food & Function, 5*(6), 1113–1124.

Nicolai, T., & Murray, B. (2017). Particle stabilized water in water emulsions. *Food Hydrocolloids, 68*, 157–163.

Oh, J. K., Drumright, R., Siegwart, D. J., & Matyjaszewski, K. (2008). The development of microgels/nanogels for drug delivery applications. *Progress in Polymer Science, 33*(4), 448–477.

Passariello, A., Agricole, P., & Malfertheiner, P. (2014). A critical appraisal of probiotics (as drugs or food supplements) in gastrointestinal diseases. *Current Medical Research and Opinion, 30*(6), 1055–1064.

Schachschal, S., Adler, H. J., Pich, A., Wetzel, S., Matura, A., van Pee, et al. (2011). Encapsulation of enzymes in microgels by polymerization/cross-linking in aqueous droplets. *Colloid and Polymer Science, 289*(5–6), 693–698.

Shen, T. C., & Cabasso, I. (1982). In R. B. Seymour, & G. A. Stahl (Eds.), *Macromolecular solutions, solvent-property relationship in polymers*. New York: Pergamon Press.

Silva, J. P. S. E., Sousa, S. C., Costa, P., Cerdeira, E., Amaral, M. H., Lobo, J. S., et al. (2013). Development of probiotic tablets using Microparticles: Viability studies and stability studies. *Aaps Pharmscitech, 14*(1), 121–127.

Tian, F., Sandler, N., Gordon, K. C., McGoverin, C. M., Reay, A., Strachan, C. J., et al. (2006). Visualizing the conversion of carbamazepine in aqueous suspension with and without the presence of excipients: A single crystal study using SEM and raman microscopy. *European Journal of Pharmaceutics and Biopharmaceutics, 64*(3), 326–335.

Vemmer, M., & Patel, A. V. (2013). Review of encapsulation methods suitable for microbial biological control agents. *Biological Control, 67*, 380–389.

Walter, H. (1978). Cell partitioning in two-polymer aqueous phase systems. *Trends in Biochemical Sciences, 3*, 97–100.

Zanjani, M. A. K., Tarzi, B. G., Sharifan, A., & Mohammadi, N. (2014). Microencapsulation of probiotics by calcium alginate-gelatinized starch with Chitosan coating and evaluation of survival in simulated human gastro-intestinal condition. *Iranian Journal of Pharmaceutical Research, 13*(3), 843–852.

Paper III

Exploring the prebiotic effect of cyclodextrins on probiotic bacteria entrapped in carboxymetyl cellulose-chitosan particles

Poonam Singh[§], Bruno Medronho[‡,*], Artur J.M. Valente[†], Maria G. Miguel[§] and Björn Lindman[‖]

[§]CQC, University of Coimbra, Department of Chemistry, 3004-535 Coimbra, Portugal

[‡]Faculty of Sciences and Technology (MeditBio), Ed. 8, University of Algarve, Campus de Gambelas, 8005-139 Faro, Portugal

[†]*CQC*, University of Coimbra, Department of Chemistry, 3004-535 Coimbra, Portugal

[‖]FSCN, Mid Sweden University, SE-851 70 Sundsvall, Sweden

*Corresponding author: bfmedronho@ualg.pt

Abstract:

In this work the prebiotic effect of different cyclodextrins, CDs, on the viability of model probiotic bacteria (*Lactobacillus rhamnosus* GG) encapsulated in carboxymethyl cellulose-chitosan (CMC-Cht) hybrid particles was studied. All the CDs tested were observed to considerably improve the viability (quantitatively like common prebiotics, such as corn starch) and encapsulation efficiency when compared to the CD-free particles, as inferred by plate counting methods and fluorescence microscopy. The SEM data suggests that the morphology of the particles, the roughness of the surface and porosity, is dependent on the type of CD and may reflect different interactions between the CDs and the matrix components. The aging and stability of the samples with and without β-CD was further evaluated. Remarkably, the viability count of the CD-doped samples was still reasonably high after one month storage at room temperature with acceptable values for practical uses. Moreover, when the CMC-Cht particles were exposed to *in vitro* simulated digestion fluids and the cell survival was much enhanced when the particles contained β-CD.

Keywords: prebiotic; probiotic; carboxyl methylcellulose; chitosan; cyclodextrin

Introduction:

Delivery systems for food and biomedical applications which are able to efficiently encapsulate, protect, transport and deliver the active cargo to the target area, without any harmful side effects

35   to cells and/or tissues, constitutes an exciting academic and industrial challenge (Corona-
36   Hernandez, Alvarez-Parrilla, Lizardi-Mendoza, Islas-Rubio, de la Rosa & Wall-Medrano, 2013;
37   Haffner, Diab & Pasc, 2016). In this respect, probiotic bacteria arise as important and are
38   generally recognized to induce beneficial effects on the host's health (Holzapfel, Haberer, Snel,
39   Schillinger & Huis in't Veld, 1998; Iannitti & Palmieri, 2010; Passariello, Agricole &
40   Malfertheiner, 2014; Saarela, Mogensen, Fonden, Matto & Mattila-Sandholm, 2000). Typically,
41   probiotics (mainly bifidobacteria and lactobacilli) reside in the human colon modulating its
42   microflora, immunogenic responses or even producing certain useful compounds for the
43   host(Holzapfel, Haberer, Snel, Schillinger & Huis in't Veld, 1998). These "friendly" bacteria have
44   been suggested as aiding in the prevention of infections, reduce cholesterol levels, promoting
45   vitamin and cytokine synthesis or even having an anti-cancer effect (Pedraza, Toribio, Romo,
46   Arreola & Guevana, 2014; Strojny et al., 2011; Szkaradkiewicz & Karpiński, 2013; Truter, 2012).
47   In recent years, a new strategy has been developed using probiotics in combination with
48   prebiotics, such as oligosaccharides, resulting in the so-called "synbiotics"(Grimoud et al., 2010;
49   Roberfroid, 1998; Ziemer & Gibson, 1998). The aim is to obtain synergistic effects of the two
50   compounds by an improving of the probiotic colonisation or metabolic effect. Such a symbiotic
51   approach has been shown to be more effective than probiotics or prebiotics alone in the
52   improvement of the quality of life in patients suffering from ulcerative colitis (Fujimori et al.,
53   2009), in colorectal cancer prevention (Liong, 2008) or in very general positive regulation of the
54   microbiota (Saulnier, Gibson & Kolida, 2008), and is therefore regarded as a very appealing
55   approach. Prebiotics are generically recognized as being resistant to harsh gastric acidity
56   conditions, often described as non-digestible poly- or oligosaccharides that provide a valuable
57   effect to the host by selectively stimulating the growth and/or activity of one or a limited number
58   of beneficial bacterial species in the colon (Gibson & Roberfroid, 1995; Roberfroid, 2000). For
59   instance, the fermentation of oligofructose in the colon due to the presence of intestinal microflora
60   has been suggested to confer several beneficial effects, including the increase of probiotics in the
61   colon, enhancement of calcium absorption, shortened gastrointestinal transit time and even
62   decrease of the blood lipid levels. The main source of prebiotics are fibers and carbohydrates, such
63   as resistant starch, wheat bran, inulin or other short oligosaccharides of glycosidic residues such as
64   fructose in fructooligosaccharides (FOS) or galactose in galactooligosaccharides (Gibson &
65   Roberfroid, 1995). To date the most studied prebiotics are FOS, inulin and oligofructose
66   (Bosscher, Van Loo & Franck, 2006b; Rurangwa et al., 2009). Nevertheless, many other
67   oligosaccharides such as xylo-oligosaccharides, pectic-oligosaccharides, palatinose and pullulan
68   derivates have also been object of research (Gomez, Gullon, Remoroza, Schols, Parajo & Alonso,

2014; Patel & Goyal, 2012; Pedraza, Toribio, Romo, Arreola & Guevana, 2014; Rurangwa et al., 2009). Much less attention has been paid to cyclodextrins, CDs, which are commercially available and are generally recognized as safe (GRAS) food additives. These molecules are circular oligosaccharides composed of glucose residues linked by alpha-1,4-glicosidic bonds and have a truncated cone shape (Szejtli, 1998). Similar to common prebiotics, CDs are not digested in the upper gastrointestinal tract making them available, and longer lasting potential carbon sources, for beneficial colon bacteria (Bosscher, Van Loo & Franck, 2006a; Goderska, Nowak & Czarnecki, 2008; Kunova, Rada, Lisova, Rockova & Vlkova, 2011; Mandadzhieva, Ignatova-Ivanova, Kambarev, Iliev & Ivanova, 2011). Nevertheless, very scarce information is available on the influence of CDs on probiotic bacteria and their antibacterial activity, but it has been shown that α-CDs can maintain the growth of *Lactobacillus casei* and increase the amounts of *bifidobacteria* (Jo, Nakata, Terao, Otani & Sano, 2007). The mechanism highlighted suggests that the microbial degradation produces linear malto-oligosaccharides, which are then further hydrolyzed and fermented to absorbable and metabolisable short-chain fatty acids (Pranckute, Kaunietis, Kuisiene & Citavicius, 2014; Szejtli, 1998). Overall, the metabolic fate of ingested α-CD is similar to that of other nondigestible but fermentable carbohydrates such as resistant starch or inulin. On the other hand, γ-cyclodextrin has been suggested to improve the gut health by positively altering the microbial populations (Spears, Karr-Lilienthal & Fahey, 2005). As said, literature is surprisingly scarce in studies regarding the potential prebiotic effect of CDs and this is possibly explained by the fact that these molecules are synthesized from starch, a rather inexpensive and largely available raw material, also considered a prebiotic (Del Valle, 2004). However, apart from the academic interest, CDs and, in particular, β-CD are of interest since they can form quite stable inclusion complexes with poorly water-soluble lipophilic species, thus having a considerable potential in drug development and food industry (Del Valle, 2004). Since the 70s, CDs have been used in the food industry as food additives for carrying food-related lipophiles (e.g., vitamins, aromas, and colorants) and for inhibiting light/heat mediated food degradation and thus extending product shelf life (Fenyvesi, Vikmon & Szente, 2016). Overall, CDs can offer a higher versatility than its precursor starch (or other typical prebiotics) since they may combine "host-guest" features with potential prebiotic effects. In this work the prebiotic effect of different CDs on a model probiotic bacteria (LGG) encapsulated in a CMC-Cht matrix was studied. Moreover, the morphology, storage stability and *in vitro* viability in simulated gastrointestinal fluids were assessed.

1. Experimental

103

2.1. Materials and Methods

α-cyclodextrin (purity >98%), β-cyclodextrin (purity of >97%), γ-cyclodextrin (purity of >98%), hydroxypropyl-β-CD, hydroxypropyl methylcellulose (HPMC), corn starch, and chitosan (deacetylation ≥ 85 % and Mw of ca. 370 kDa), were purchased from Sigma-Aldrich. Sodium carboxymethyl cellulose, CMC, (Mw of ca. 250 kDa) was obtained from VWR chemicals. *Lactobacillus rhamnosus* GG LMG 18243 (LGG) was bought from the Belgian Coordinated Collection of Microorganisms (BCCM). The MRS broth pH 6.4 and MRS agar pH 5.7 were obtained from VWR International. The PBS buffer was prepared in the lab with sodium hydrogen phosphate, sodium chloride, potassium chloride and potassium dihydrogen phosphate, all purchased from Sigma-Aldrich. Sodium hydrogen carbonate, magnesium chloride hexahydrate, ammonium carbonate and calcium chloride (all analytical grade) were also obtained from Sigma-Aldrich. The Live/Dead® *Bac*Light™ Bacterial Viability Kit L7012 was purchased from Thermofisher Scientific, USA. Porcine pepsin (EC 3.4.23.1), porcine trypsin (EC 3.4.21.4), bovine chymotrypsin (EC 3.4.21.1), porcine pancreatic α-amylase (EC 3.2.1.1), porcine pancreatic lipase (EC 3.1.1.3), porcine pancreatic colipase and bile extract B8631 (porcine) were all purchased from Sigma Aldrich. Milli-Q water (18.2 MΩ.cm^{-1} at 25 °C, MQ) was used for the preparation of all samples.

2.2.1. Preparation of doped NaCMC-chitosan macroparticles

In order to evaluate the effect of different cyclodextrins on the viability of probiotic cells in CMC-Cht particles, different physical macrobeads were prepared, adapting the procedure reported before (Singh, Medronho, Alves, da Silva, Miguel & Lindman, 2017). Briefly, 1 wt% CMC aqueous solutions were mixed with 0.5 and 1 wt % α, β, γ and modified β-CDs and the macroparticles were subsequently formed by careful drop-wise addition of the different CMC doped solutions (50 mL) into 1 wt% chitosan solution (300 mL) using a manually operated syringe with a 0.7 mm cannula under continuous stirring. The hydrogel macroparticles (MP) were removed from the chitosan solution by gentle filtration after 30 minutes aging. Apart from the cyclodextrins, corn starch and HPMC were also used as model prebiotics following the same procedure as described above. Microspheres (mP) were prepared in a similar way but in an air compressed equipment (working pressure of ca. 5-8 bar) coupled with a nozzle sprayer (Singh, Medronho, Alves, da Silva, Miguel & Lindman, 2017).

135

136

2.2.2. Growth and entrapment of *Lactobacillus rhamnosus* GG

All culture media and buffers were autoclaved for sterilization at 121 ºC for 15 minutes. Freeze-dried cells of *Lactobacillus rhamnosus* GG were rehydrated in 5 mL MRS broth and incubated at 37 °C for 40 hours in a CO_2 incubator and the growth was checked during two days. When the broth became turbid, the bacterial growth was visually confirmed by the optical density using a UV/vis spectrophotometer and was compared with the non-inoculated broth. To evaluate the purity of the bacteria, one inoculation loop with bacteria was streaked on a MRS agar plate while a plate with pure sterilized culture was treated as control. In a later step, 10 mL of the cultured broth were divided in 10 eppendorfs and centrifuged for 30 minutes at 3000 rcf. The supernatant was discarded and 1 ml PBS was added to each of the pellets followed by centrifugation at 3000 rcf for 20 minutes. This washing procedure was repeated twice. Finally, the PBS rich supernatant was discarded and 5 bacterial pellets were mixed with 20 ml of 1 wt% of NaCMC aqueous solution also containing α, β, γ, modified β-CDs, corn starch or HPMC.

The encapsulation efficiency, EE, was estimated after mechanically disintegrate the particles in a phosphate buffer (pH=7.4), by stirring them at 37 °C. After that, the number of entrapped cells by serial dilution was measured by the plate method and counts were expressed as number of colony forming units (CFU), and calculated as $EE = (\log_{10}N/\log_{10}N_0) \times 100$, where N is the number of viable entrapped bacteria released from the particles and N_0 is the number of free/naked bacteria taken as control (Jantzen, Gopel & Beermann, 2013; Lotfipour, Mirzaeei & Maghsoodi, 2012).

2.2.3. Preparation of Salivary, Gastric and Intestinal Fluids

The Simulated Salivary Fluid (SSF), Simulated Gastric Fluid (SGF) and Simulated Intestinal Fluid (SIF) were made up of the corresponding electrolyte stock solutions, enzymes and water as described in tables 1 and 2. (Minekus et al., 2014).

2.2.4. Evaluation of LGG Viability: plate counting and fluorescence microscopy

The fresh CMC-Cht doped particles were transferred to a PBS buffer solution at 37 ºC for 30 minutes. The viability count corresponds to 100 μl of the suspended particles added to 1 ml of PBS buffer. Sequential dilutions were performed by dissolving the particles from each composition in the PBS buffer following the Miles and Misra approach to count the number of viable bacteria (Miles, Misra & Irwin, 1938). All different dilutions were plated in triplicates and kept in CO_2 incubator for 48 hours before the bacterial colony was counted using a colony reader. For the particles treated with the different gastrointestinal fluids (*in vitro* tests), the procedure was

171 rather similar. After exposing the particles to the different fluids, samples were centrifuged at
172 3000 rcf for 10 min at 4 °C. The particles (or what remains from them) were re-suspended in 900
173 µL of phosphate buffer (0.1 M, pH 7.0) followed by gentle shaking at room temperature for 15
174 min. Sequential dilutions and plating in MRS agar was performed as previously described to
175 estimate the number of viable cells. The experiments were performed in Faster BH-EN and BHG
176 Class II Microbiological Safety Cabinets.

177 The bacteria viability was also inferred using a Dead/Alive kit (commercial LIVE/DEAD®
178 *Bac*Light™). The bacteria in the CMC-Cht particles were stained with 2 μl of SYTO 9 dye and 2
179 μl of propidium iodide from the kit and observed in a fluorescence Olympus microscope (100x
180 immersion objective).

181 For the time evolution of the viability, the samples were storage in different conditions (25, 4 and
182 −20 ºC) and the viability assessed periodically through plate counting for one month.

183

184 **2.2.5. Thermal and Morphological studies**
185 The effect of β-CD on gel particles has been evaluated by thermal analysis gravimetry by using a
186 *TG 209 F3 Tarsus* thermogravimetric analyzer (*Netzsch Instruments*). Samples (*ca.* 10 mg) were
187 weighed in alumina pans and were heated from 30 to 500 ºC at a heating rate of 10 ºC min^{-1} under
188 N$_2$ atmosphere (flow rate of 20 mL min^{-1}).

189 Scanning Electron Microscopy (SEM) was performed on a VEGA3 SBH from TESCAN, 15 kV,
190 equipped with a selected energy dispersive X-ray microanalyser (EDX). Generally, freeze-dried
191 particles were deposited directly onto the carbon tape on the support and sputtered with
192 approximately 6 nm thin Au/Pd film by cathodic pulverization using a SPI Module Sputter Coater,
193 during 90 s and with a current of de 15mA.

194

195 **2.3. Statistical analysis**
196 The experiments were performed in triplicate and data was subjected to one-way analysis of
197 variance (ANOVA). Multiple comparisons were performed by LSD test. Statistical significance
198 was set at P<0.05 using SPSS (SPSS Inc, USA).

199

200 **Results and Discussion**
201 Recently we have reported the formation of CMC-Cht micro- and macroparticles capable to
202 efficiently entrap probiotic bacteria with acceptable viability (Singh, Medronho, Alves, da Silva,
203 Miguel & Lindman, 2017). Initial viability experiments with different molecules suggested that
204 when β-CD is used in the particle formation, a threefold increase in the probiotic viability is

observed regardless of the size of the particles (Figure 1). Moreover, it was found that the incorporation of β-CD improves the EE, both in micro and macroparticles, from ca. 63 % in the non-doped systems to ca. 93 % for the β-CD containing particles. This effect is qualitatively demonstrated in Figure 2, where the sample with β-CD has a much higher number of probiotic cells entrapped than the sample without it.
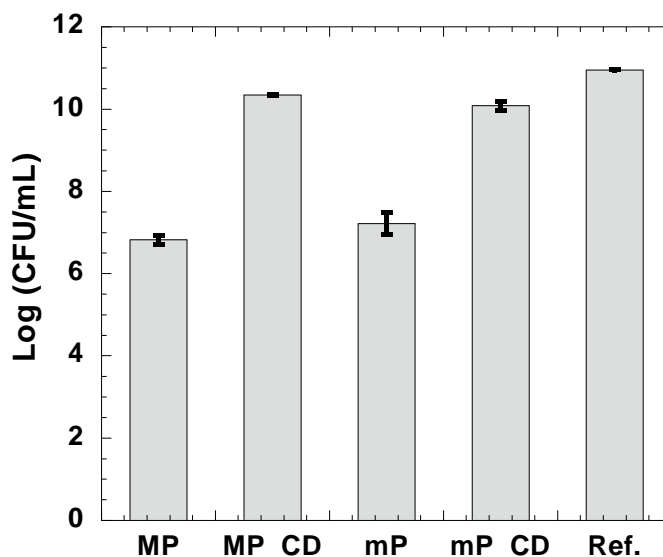
Figure 1. Bacterial counts in Log CFU/mL of CMC-Cht micro- and macro-particles with ("mP_CD"; "MP_CD") and without ("mP"; "MP") 1 wt % β-CD. The reference state is the native unprotected LGG cells denoted as "Ref."


Figure 2. The SEM images of encapsulated bacteria in (a) CMC-Cht macroparticles and (b) CMC-Cht macroparticles with β-CD. The scale bar corresponds to 2 μm.

7

234   Motivated by these findings and by the fact that the prebiotic effect of CDs has been essentially
235   neglected in literature, different CDs (1 wt%) have been used as shown in Figure 3. It is striking
236   that all the CDs tested greatly improve the viability count of LGG probiotic cells entrapped in the
237   physical CMC-Cht macrobeads. The minimum counting observed was 9.85 ± 0.13 log CFU/mL
238   for α-CD (sample #3), which, nevertheless, is still considerably higher than the viability counting
239   for CD-free CMC-Cht macrobeads (ca. 6.82 ± 0.11 log CFU/mL, see Figure 1). Overall, the
240   values are similar to the model naked bacteria (sample #7) and resemble the effect of known
241   prebiotic carbohydrates such as HPMC or starch (samples #5 and #6, respectively). The
242   differences between CDs are minor but still statistically relevant. Different concentrations have
243   been tried but the general trend is similar: β-CD and γ-CD are found to have the best performance
244   while α-CD, as mentioned above, showed the lowest enhancement in the viability counting. At
245   this stage the reason is not clear of these differences, but it might be related to the different
246   relative stability and degradation rate of the CDs (Szejtli, 1998). Before going further, it is
247   important to have an insight into the eventual effect of CD (in particular, β-CD) on the structure of
248   the particles. Figure 4 shows thermograms, and the corresponding DTG, for CMC-Cht particles in
249   the absence and presence of □-CD. The temperatures of maximum degradation rate (T_m) were
250   determined as the minimum in the derivative curve (see Figure 4B). It can be seen that the T_m
251   value for the blend, at the main degradation step (i.e., 264 ℃) is smaller than the temperatures of
252   degradation of neat chitosan and CMC: 289 and 271 ℃, respectively (El-Sayed, Mahmoud, Fatah
253   & Hassen, 2011). This plasticizing-like effect can be related to the mixture of non-compatible
254   polymers, resulting in a less structured polymer network and phase separation (Martelo et al.,
255   2012). However, upon incorporation of β-CD, the T_m at the main degradation step increases to 264
256   ℃. The increase of the molecular order of the blend structure can be understood from the
257   formation of H-bonds between the hydroxyl groups of β-CD and those in CMC and chitosan
258   (Malik, Ahmad & Minhas, 2017; Shangguan, Luo, Liu & Zheng, 2016). This hypothesis is in
259   agreement with the features of the first decomposition step (from 40 to 160 °C) of CMC-Cht and
260   CMC-Cht-β-CD related to the mass loss caused by the adsorbed freezing and non-freezing water.
261   In fact, the water loss in the β-CD-containing gel is much lower (ca. 11%) than for the
262   corresponding blend without CD (ca. 24 %); this is accompanied by a slight increase in the
263   temperature of the water loss from 118 to 125 ℃. These results clearly suggest that the
264   incorporation leads to a less swollen structure and, consequently, to a higher stability.

265

266
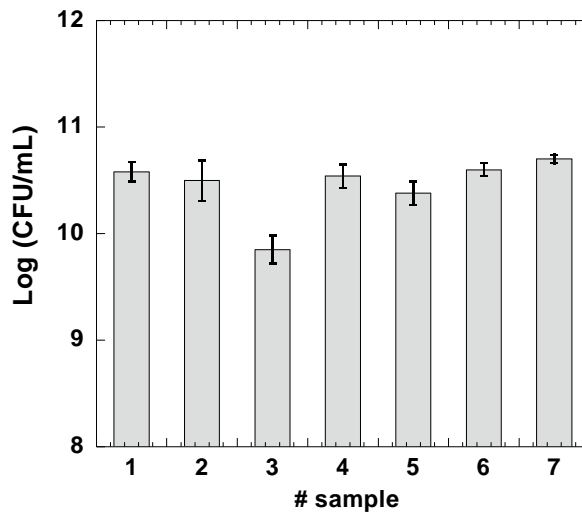
Figure 3: The bar diagram depicts the bacteria count obtained by drop plate culture method. The sample numbers are: #1: β-CD, #2: hydroxypropyl-β-CD, #3: α-CD, #4: γ-CD, #5: HPMC, #6: corn starch and #7: naked LGG (control). In all cases 1 wt% of prebiotic was used in the formation of the CMC-Cht physical macroparticles as described in the experimental section.
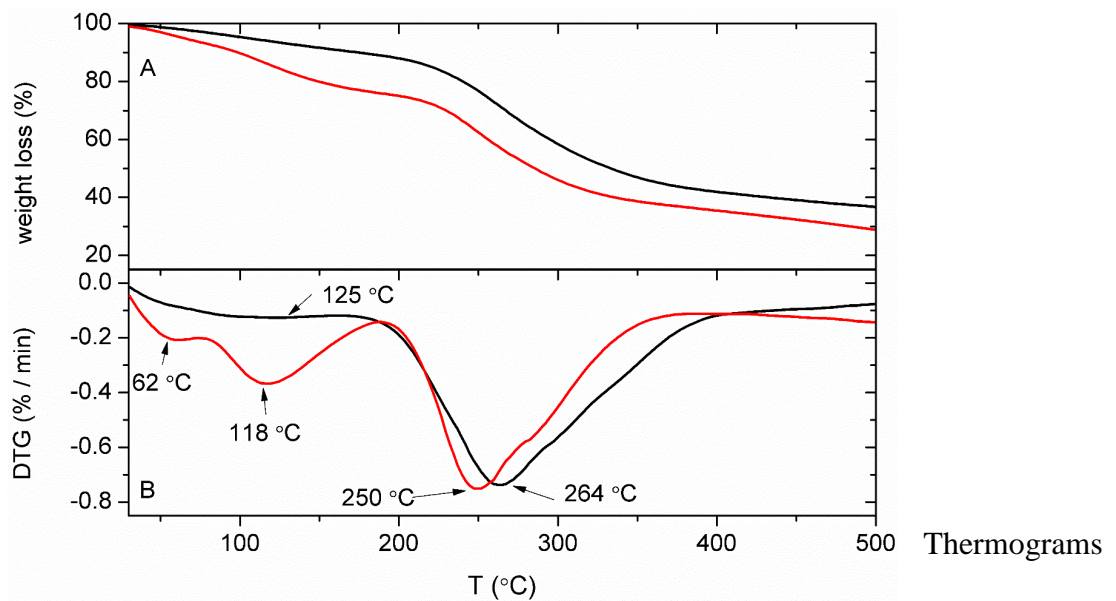
Figure 4. Thermograms (A) and corresponding DTGs (B) of CMC-Cht without (red lines) and with □-CD (black lines).

The improved viability may be related not only to the fact that CDs can effectively work as prebiotics and carbon sources for the enhancing of probiotic cell growth and proliferation but it is also plausible that during the particle formation, the β-CD interacts with the CMC-Cht polymer matrix, in particular chitosan, thus decreasing its anti-bacterial effect on the viability (Karim & Adnan, 2012; Karim, Adnan & Husain, 2012). This would also possibly explain the differences in

9

microstructure observed by SEM (Figure 5) and the consequent encapsulation efficiency. As can be observed in Figure 5, the presence of CDs changes the morphology of the CMC-Cht macroparticles. While the system without CDs is apparently less porous with a smoother surface (i.e. "a" and "e") the system doped with α-CD (i.e. "b" and "f") shows a fiber-like pattern at the surface. On the other hand, the systems doped with β-CD (i.e. "c" and "g") and γ-CD (i.e. "d" and "h") display a more rough and porous morphology.
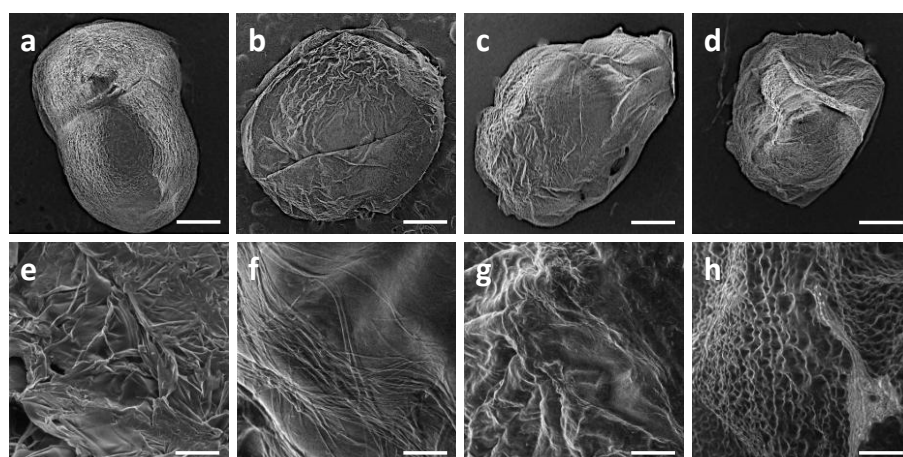
Figure 5. SEM Images of CMC-Cht macroparticles without CD (a and e), with α-CD (b and f), with β-CD (c and g) or with γ-CD (d and h). The top row shows individual macroparticles (scale bar represents 500 μm) while the bottom row displays zoomed areas (scale bars represent 20 μm). In all cases the concentration of CDs used was 1 wt%.

The qualitative cell viability in the CMC-Cht macroparticles doped with the different CDs was also evaluated by fluorescence microscopy using a Dead/Alive kit. In this test the viable bacteria appear as green rods while the dead bacteria are red. As can be seen in Figure 6, the fluorescence microscopy images provide support to the microbiological studies. While the sample with α-CD is more "orange-like" (Figure 6a) the β-CD and γ-CD samples (Figures 6b and 6c, respectively) are "greener" thus suggesting a higher number of viable cells.

10
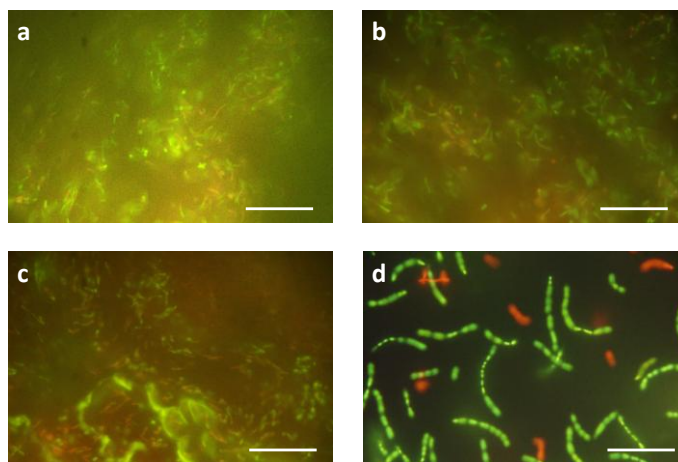
Figure 6. Fluorescent microscopy images of CMC-Cht macroparticles using the Dead/Alive kit. The macroparticles were prepared with 1 wt% a) α-CD, b) β-CD and c) γ-CD. The reference naked bacteria in the aqueous broth are shown in d). Note the images (a, b and c) are partially blurry due to the gel density and thickness after gently squeezing one macroparticle between glass plates.

Taking into account the prebiotic effect of different CDs and the price, bearing in mind possible further applications, β-CD has been selected to a further study of its influence on the stability and aging of the CMC-Cht particles as well as the particle stability in simulated *in vitro* gastrointestinal (GI) conditions. In Figure 7, the effect of the model gastric and intestinal fluids (SGF and SIF, respectively) is depicted. The fluids used try to mimic the *in vivo* physiological conditions, considering different parameters such as concentration of digestive enzymes, pH, digestion time, salts, among others.
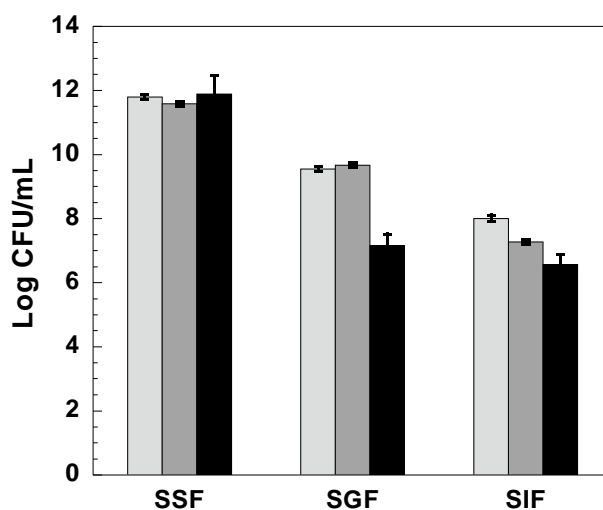
Figure 7. Bacterial counts in Log CFU/mL of the naked (black bars) and encapsulated cells in the
CMC-Cht micro- (dark grey bars) and macroparticles (light grey bars) doped with 1 wt% β-CD.
Data was interpreted with the plate count method after exposure of the naked and entrapped cells
to Simulated Salivary, Gastric and Intestinal Fluids (SSF, SGF and SIF, respectively). The error
bars represent the standard deviation.

It can be concluded that the cell survival after the SGF treatment for 120 minutes was much
enhanced, in comparison with the naked LGG, when the particles had β-CD in their composition.
Regardless of the size of the particles the bacterial counts of the β-CD based formulations was ca.
9.5 Log CFU/mL while the unprotected control cells show a viability of ca. 7.15 Log CFU/mL. To
a lower extent, the sequential exposure of the naked and entrapped cells in the β-CD doped CMC-
Cht particles to SGF (120 minutes) followed by the SIF (120 minutes) again resulted in a higher
number of viable bacteria when the cyclodextrin was present.

Additionally, the viability of LGG in the CMC-Cht macroparticles with β-CD was evaluated
for samples stored of a period of 30 days (4 and 25 ºC) and compared with naked cells (Figure 8).
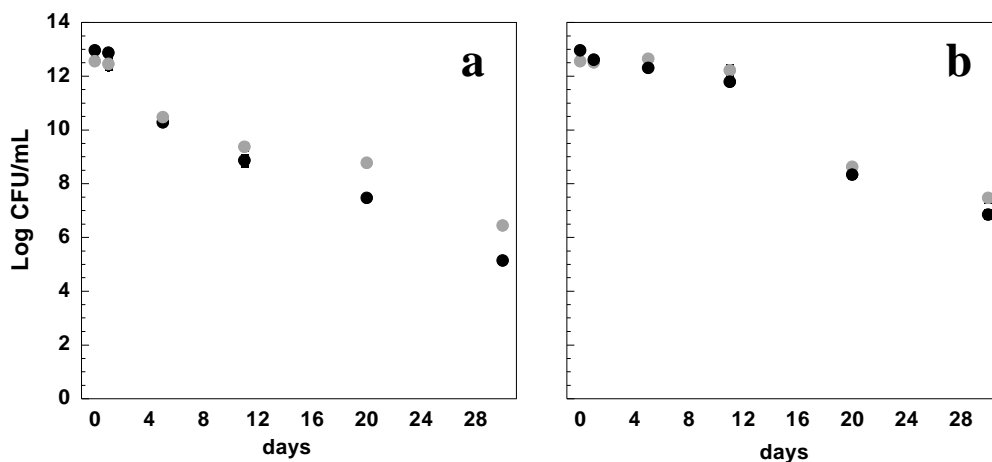
Figure 8. Viability counts of LGG in CMC-Cht macroparticles doped with 1 wt% β-CD (full grey
circles) for 30 days at a) 25ºC and b) 4ºC. The control is naked bacteria in broth (full black
circles). Data are reported as mean (±SD, $n = 3$). Note that the error bars might be within the size
of the markers.

Clearly, the viability count decreases with a slower rate when particles are doped with β-CD and,
after 30 days, the number of viable cells at room temperature (Figure 8a) is still within the 6-7 Log
CFU/ml often considered the minimum to produce health benefits in products containing

12

403 probiotics. The same effect is observed when the samples were stored at lower temperatures (i.e. 4
404 ºC). In this case, the bacterial counts are shifted to higher values and the β-CD effect was less
405 pronounced (Figure 8b) which might be explained by an expected lower degradation rate of β-CD
406 at lower temperatures.

407 Globally, the encapsulation in the CMC-Cht systems doped with β-CD improved the survival of *L.*
408 *rhamnosus* in the simulated gastro intestinal fluids with remarkable values for practical uses (i.e.
409 above 6 Log CFU/mL). Furthermore, the presence of β-CD protects LGG and improves the
410 viability keeping it at acceptable levels, even at room temperature, thus possibly extending the
411 application range of sensitive synbiotics to non-refrigerated, long shelf life food and
412 pharmaceutical products.

413

414 **Conclusion**

415 In order to create a successful synbiotic combination it is very important to evaluate the influence
416 of prebiotic oligosaccharides on probiotic bacteria. In this work, different CDs (practically not
417 investigated as a component of synbiotics) were used and it is striking that all the systems tested
418 can be considered prebiotics since the viability count of model probiotic bacteria, entrapped in
419 CMC-Cht particles, was considerably improved. The morphology of the systems depends on the
420 CD used and this may be related to different "host-guest" interactions between the CDs and the
421 CMC-Cht matrix thus affecting the polymer organization and overall particle microstructure. As a
422 consequence, the encapsulation efficiency was also observed to be much enhanced in the presence
423 of CDs. β-CD was observed to be one of the most efficient molecules to enhance the survival of
424 the cells and thus further studies on the aging of the particles and behavior in simulated
425 gastrointestinal fluids were conducted. In both cases, β-CD improved the viability of LGG even
426 after one month of storage at 25 ºC and efficiently protected the cells from the simulated harsh
427 gastric conditions with a remarkable viability count in comparison to naked probiotic. Overall,
428 CDs should be regarded as viable prebiotics in the development of synbiotics for health
429 improvement. Moreover, CDs may not only play an efficient prebiotic role but can simultaneously
430 be used to entrap less water-soluble molecules required for different biomedical and food
431 formulations which constitutes an important advantage over the traditional prebiotics.

432

433

434

435

436

References

Bosscher, D., Van Loo, J., & Franck, A. (2006a). Inulin and oligofructose as prebiotics in the prevention of intestinal infections and diseases. *Nutr Res Rev, 19*(2), 216-226.

Bosscher, D., Van Loo, J., & Franck, A. (2006b). Inulin and ologofructose as prebiotics in the prevention of intestinal infections and diseases. *Nutr. Res. Rev., 19*, 216-226.

Corona-Hernandez, R. I., Alvarez-Parrilla, E., Lizardi-Mendoza, J., Islas-Rubio, A. R., de la Rosa, L. A., & Wall-Medrano, A. (2013). Structural Stability and Viability of Microencapsulated Probiotic Bacteria: A Review. *Comprehensive Reviews in Food Science and Food Safety, 12*(6), 614-628.

Del Valle, E. M. M. (2004). Cyclodextrins and their uses: a review. *Process Biochemistry, 39*(9), 1033-1046.

El-Sayed, S., Mahmoud, K. H., Fatah, A. A., & Hassen, A. (2011). DSC, TGA and dielectric properties of carboxymethyl cellulose/polyvinyl alcohol blends. *Physica B: Condensed Matter, 406*, 4068-4076.

Fenyvesi, E., Vikmon, M., & Szente, L. (2016). Cyclodextrins in Food Technology and Human Nutrition: Benefits and Limitations. *Crit Rev Food Sci Nutr, 56*(12), 1981-2004.

Fujimori, S., Gudis, K., Mitsui, K., Seo, T., Yonezawa, M., Tanaka, S., Tatsuguchi, A., & Sakamoto, C. (2009). A randomized controlled trial on the efficacy of synbiotic versus probiotic or prebiotic treatment to improve the quality of life in patients with ulcerative colitis. *Nutrition, 25*(5), 520-525.

Gibson, G. R., & Roberfroid, M. B. (1995). Dietary Modulation of the Human Colonic Microbiota - Introducing the Concept of Prebiotics. *Journal of Nutrition, 125*(6), 1401-1412.

Goderska, K., Nowak, J., & Czarnecki, Z. (2008). Comparison of the growth of Lactobacillus acidophilus and Bifidobacterium bifidum species in media supplemented with selected saccharides including prebiotics. *Acta Sci. Pol.*(7), 5-20.

470 Gomez, B., Gullon, B., Remoroza, C., Schols, H. A., Parajo, J. C., & Alonso, J. L. (2014).
471 Purification, Characterization, and Prebiotic Properties of Pectic Oligosaccharides from Orange
472 Peel Wastes. *Journal of Agricultural and Food Chemistry, 62*(40), 9769-9782.

473 Grimoud, J., Durand, H., Courtin, C., Monsan, P., Ouarne, F., Theodorou, V., & Rogues, C.
474 (2010). In vitro screening of probiotic lactic acid bacteria and prebiotic glucooligosaccharides to
475 select effective synbiotics. *Anaerobe, 16*(5), 493-500.

476 Haffner, F. B., Diab, R., & Pasc, A. (2016). Encapsulation of probiotics: insights into academic
477 and industrial approaches. *Aims Materials Science, 3*(1), 114-136.

478 Holzapfel, W. H., Haberer, P., Snel, J., Schillinger, U., & Huis in't Veld, J. H. J. (1998). Overview
479 of gut flora and probiotics. *International Journal of Food Microbiology, 41*(2), 85-101.

480 Iannitti, T., & Palmieri, B. (2010). Therapeutical use of probiotic formulations in clinical practice.
481 *Clinical Nutrition, 29*(6), 701-725.

482 Jantzen, M., Gopel, A., & Beermann, C. (2013). Direct spray drying and microencapsulation of
483 probiotic Lactobacillus reuteri from slurry fermentation with whey. *Journal of Applied*
484 *Microbiology, 115*(4), 1029-1036.

485 Jo, A., Nakata, D., Terao, K., Otani, M., & Sano, K. (2007). New synbiotics by the combination of
486 α-cyclodextrin and lactic acid bacteria. *Proceedings of 25th Cyclodextrin Symposium in Japan*
487 *Tottori, Japan*, 144-145.

488 Karim, Z., & Adnan, R. (2012). The β-cyclodextrin-chitosan inclusion complex: Characterization
489 and application in the removal of pesticides in wastewater. *ARCH. ENVIRON. SCI., 6*, 1-12.

490 Karim, Z., Adnan, R., & Husain, Q. (2012). A beta-cyclodextrin-chitosan complex as the
491 immobilization matrix for horseradish peroxidase and its application for the removal of azo dyes
492 from textile effluent. *International Biodeterioration & Biodegradation, 72*, 10-17.

493 Kunova, G., Rada, V., Lisova, I., Rockova, S., & Vlkova, E. (2011). In vitro Fermentability of
494 Prebiotic Oligosaccharides by Lactobacilli. *Czech Journal of Food Sciences, 29*, S49-S54.

495 Liong, M. T. (2008). Roles of probiotics and prebiotics in colon cancer prevention: Postulated
496 mechanisms and in-vivo evidence. *International Journal of Molecular Sciences, 9*(5), 854-863.

497 Lotfipour, F., Mirzaeei, S., & Maghsoodi, M. (2012). Evaluation of the effect of CaCl2 and
498 alginate concentrations and hardening time on the characteristics of Lactobacillus acidophilus
499 loaded alginate beads using response surface analysis. *Adv Pharm Bull, 2*(1), 71-78.

500 Malik, N. S., Ahmad, M., & Minhas, M. U. (2017). Cross-linked β-cyclodextrin and
501 carboxymethyl cellulose hydrogels for controlled drug delivery of acyclovir. *Plos One, 12*,
502 e0172727.

503 Mandadzhieva, T., Ignatova-Ivanova, T., Kambarev, S., Iliev, I., & Ivanova, I. (2011). Utilization
504 of Different Prebiotics by Lactobacillus Spp. And Lactococcus Spp. *Biotechnology &*
505 *Biotechnological Equipment, 25*, 117-120.

506 Martelo, L., Jiménez, A., Valente, A. J. M., Burrows, H. D., Marques, A. T., Forster, M., Scherf,
507 U., Peltzer, M., & Fonseca, S. M. (2012). Incorporation of polyfluorenes into poly(lactic acid)
508 films for sensor and optoelectronics applications. *Polymer International, 61*, 1023-1030.

509 Miles, A. A., Misra, S. S., & Irwin, J. O. (1938). The estimation of the bactericidal power of the
510 blood. *Journal of Hygiene, 38*(6), 732-749.

511 Minekus, M., Alminger, M., Alvito, P., Ballance, S., Bohn, T., Bourlieu, C., Carriere, F., Boutrou,
512 R., Corredig, M., Dupont, D., Dufour, C., Egger, L., Golding, M., Karakaya, S., Kirkhus, B., Le
513 Feunteun, S., Lesmes, U., Macierzanka, A., Mackie, A., Marze, S., McClements, D. J., Menard,
514 O., Recio, I., Santos, C. N., Singh, R. P., Vegarud, G. E., Wickham, M. S. J., Weitschies, W., &
515 Brodkorb, A. (2014). A standardised static in vitro digestion method suitable for food - an
516 international consensus. *Food & Function, 5*(6), 1113-1124.

517 Passariello, A., Agricole, P., & Malfertheiner, P. (2014). A critical appraisal of probiotics (as
518 drugs or food supplements) in gastrointestinal diseases. *Current Medical Research and Opinion,*
519 *30*(6), 1055-1064.

520 Patel, S., & Goyal, A. (2012). The current trends and future perspectives of prebiotics research: a
521 review. *3 Biotech, 2*(2), 115-125.

522 Pedraza, L., Toribio, H., Romo, R., Arreola, S., & Guevana, M. (2014). Prebiotic activity of
523 xylooligosaccharides from corncob. *JCBPS Sect. A: Food Biotechnol., 4*, 01-05.

524 Pranckute, R., Kaunietis, A., Kuisiene, N., & Citavicius, D. (2014). Development of synbiotics
525 with inulin, palatinose, alpha-cyclodextrin and probiotic bacteria. *Pol J Microbiol, 63*(1), 33-41.

526 Roberfroid, M. B. (1998). Prebiotics and synbiotics: concepts and nutritional properties. *British*
527 *Journal of Nutrition, 80*(4), S197-S202.

528 Roberfroid, M. B. (2000). Prebiotics and probiotics: are they functional foods? *American Journal*
529 *of Clinical Nutrition, 71*(6), 1682s-1687s.

530 Rurangwa, E., Laranja, J. L., Van Houdt, R., Delaedt, Y., Geraylou, Z., Van de Wiele, T., Van
531 Loo, J., Van Craeyveld, V., Courtin, C. M., Delcour, J. A., & Ollevier, F. (2009). Selected
532 nondigestible carbohydrates and prebiotics support the growth of probiotic fish bacteria mono-
533 cultures in vitro. *Journal of Applied Microbiology, 106*(3), 932-940.

534 Saarela, M., Mogensen, G., Fonden, R., Matto, J., & Mattila-Sandholm, T. (2000). Probiotic
535 bacteria: safety, functional and technological properties. *Journal of Biotechnology, 84*(3), 197-
536 215.

537   Saulnier, D. M. A., Gibson, G. R., & Kolida, S. (2008). In vitro effects of selected synbiotics on
538   the human faecal microbiota composition. *Fems Microbiology Ecology, 66*(3), 516-527.

539   Shangguan, Y., Luo, G., Liu, M., & Zheng, Q. (2016). Shear induced self-thickening of
540   chitosan/β-cyclodextrin compound solution. *Rsc Advances, 6*, 110367-110374.

541   Singh, P., Medronho, B., Alves, L., da Silva, G. J., Miguel, M. G., & Lindman, B. (2017).
542   Development of carboxymethyl cellulose-chitosan hybrid micro- and macroparticles for
543   encapsulation of probiotic bacteria. *Carbohydrate Polymers, 175*, 87-95.

544   Spears, J. K., Karr-Lilienthal, L. K., & Fahey, G. C. (2005). Influence of supplemental high
545   molecular weight pullulan or gamma-cyclodextrin on ileal and total tract nutrient digestibility,
546   fecal characteristics, and microbial populations in the dog. *Archives of Animal Nutrition, 59*(4),
547   257-270.

548   Strojny, L., Bomba, A., Hijova, E., Chmelarova, A., Mojzisova, G., Bertkova, I., Koprovicova, J.,
549   Pomfy, M., Strompfova, V., & Molokacova, M. (2011). Effects of a probiotic in combination with
550   prebiotics on intestinal lactobacilli and coliforms and activities of bacterial enzymes in 1,2-
551   dimethylhydrazine exposed rats. *Czech Journal of Animal Science, 56*(3), 99-106.

552   Szejtli, J. (1998). Introduction and general overview of cyclodextrin chemistry. *Chemical Reviews,*
553   *98*(5), 1743-1753.

554   Szkaradkiewicz, A. K., & Karpiński, T. M. (2013). Probiotics and prebiotics. *J. Biol. Earth Sci, 3*,
555   M42-M47.

556   Truter, T. (2012). Probiotics and prebiotics. *Prof. Nurs. Today, 16*, 24-31.

557   Ziemer, C. J., & Gibson, G. R. (1998). An overview of probiotics, prebiotics and synbiotics in the
558   functional food concept: Perspectives and future strategies. *International Dairy Journal, 8*(5-6),
559   473-479.

Paper IV

1   # Celullose-Based Edible Films for Probiotic

2   # Entrapment and Delivery

3   *Poonam Singh[a], Solange Magalhães[a], Luis Alves[a], Filipe Antunes[a], Maria Miguel[a], Björn Lindman[b], Bruno Medronho[c,*]*

4

5

6   [a]Coimbra Chemistry Centre, Department of Chemistry, University of Coimbra, 3004-535 Coimbra, Portugal

7   [b]FSCN, Mid Sweden University, SE-851 70 Sundsvall, Sweden

8   [c]Faculty of Sciences and Technology (MeditBio), Ed. 8, University of Algarve, Campus de Gambelas, 8005-139 Faro, Portugal

9

10

11

12   *Corresponding author:

13   Electronic mail: bfmedronho@ualg.pt (B. Medronho)

14

15   Abstract

16   The encapsulation with edible coatings is a promising approach that may solve the

17   disadvantages associated with the use of bioactive compounds as food additives. This is

18   particularly relevant in the case of probiotics, since their stability and survival in food matrices

19   and in the gastrointestinal tract may be rather poor. Therefore, in this work, new cellulose-

20   based edible films have been developed and characterized. Sodium carboxymethyl cellulose

21   (CMC) and hydroxyethyl cellulose (HEC) were used for film preparation and cross-linked with

22   citric acid (CA) under reasonably mild conditions. Model probiotic bacteria (Lactobacillus

23   rhamnosus GG) were incorporated in the films either during the film formation and casting or

24   after the film synthesis, via bacteria diffusion and adsorption. The film formation and structure

were characterized as well as the viability of the bacteria under different conditions (notably

film composition and pH). Films with tunable mechanical properties and swelling ability could

be obtained by varying the HEC/CMC ratio and the amount of CA. Overall, these new films

could efficiently entrap and preserve viable bacteria thus being promising matrices for food

applications.

1. Introduction

The use of edible coatings to improve the quality of food products is an interesting

approach, which is employed routinely nowadays. Typically, these systems work as physical

barriers for gases (e.g. oxygen, carbon dioxide), moisture (thus providing humidity control) and

other molecules such as aromas and lipids (Biquet & Labuza, 1988; Cuq, Gontard & Guilbert,

1995; Kester & Fennema, 1986; Quiros-Sauceda, Ayala-Zavala, Olivas & Gonzalez-Aguilar,

2014). Apart from the barrier functionality, some innovative applications have considered the

use of these edible matrices to entrap bioactive compounds of interest combined with later

controlled release and availability of the cargo at a specific place, time and defined rate. These

functionalized systems are interesting not only to extend shelflife and reduce the risk of

pathogen growth on food products, but also to provide a functional product with health

benefits to the consumer (Dhall, 2013; Pothakamury & BarbosaCanovas, 1995). Moreover, the

entrapment of the bioactive species in edible coatings may also contribute to mask their

potential inherent undesired off-flavors and improve their premature loss of functionality (e.g.

degradation due to the food matrix characteristics, such as low pH) (Ayala-Zavala, Soto-Valdez,

Gonzalaz-Leon, Alvarez-Parrilla, Martin-Belloso & Gonzalez-Aguilar, 2008; Ayala-Zavala et al.,

2011; Silva-Weiss, Ihl, Sobral, Gomez-Guillen & Bifani, 2013). Antioxidants, nutraceutical

2

51   compounds, antimicrobials, flavors and probiotics are among the most used bioactive agents

52   (Espitia, Batista, Azeredo & Otoni, 2016; Muranyi, 2013). Among the latter, probiotic bacteria,

53   are particularly relevant since these living microorganisms are believed to provide

54   beneficial health effects to the host by replenishing the natural gastrointestinal

55   microbiota (Espitia, Batista, Azeredo & Otoni, 2016; Holzapfel, Haberer, Snel, Schillinger

56   & Huis in't Veld, 1998; Pamer, 2016; Salminen, Ouwehand, Benno & Lee, 1999). The

57   most commonly used microorganisms are bifido bacteria, lactic acid bacteria and certain types

58   of yeast. Among the beneficial effects, probiotics have been reported to shorten or even

59   prevent diarrhea and respiratory tract infections, reduce the risk of necrotizing enterocolitis in

60   premature infants, mitigation of lactose intolerance symptoms, treatment of food allergy, and

61   binding of toxins and pathogens from ingested foods or from the gastrointestinal tract

62   (Salminen, Ouwehand, Benno & Lee, 1999; Sanchez, Delgado, Blanco-Miguez, Lourenco,

63   Gueimonde & Margolles, 2017). Probiotics can also be used as antimicrobial compounds

64   against food pathogens (Sharafi et al., 2013). Encapsulation of probiotics into a polymeric

65   matrix can protect them from premature degradation and enhance a controlled release

66   (Corona-Hernandez, Alvarez-Parrilla, Lizardi-Mendoza, Islas-Rubio, de la Rosa & Wall-Medrano,

67   2013; Haffner, Diab & Pasc, 2016; Singh, Medronho, Alves, da Silva, Miguel & Lindman, 2017).

68   In food science, encapsulation can be achieved by polymeric coatings (Espitia, Batista, Azeredo

69   & Otoni, 2016; Quiros-Sauceda, Ayala-Zavala, Olivas & Gonzalez-Aguilar, 2014). The

70   practicability of coatings based on edible polysaccharides (e.g. alginate or gellan films) to carry

71   and support viable bifido bacteria in food products was first demonstrated by Tapia et al. in

72   fresh-cut fruit (Tapia, Rojas-Grau, Rodriguez, Ramirez, Carmona & Martin-Belloso, 2007). Later,

73   in a related study, *L. acidophilus* probiotics have been immobilized in an alginate-coated

74   surface for strawberries (Moayednia, Ehsani, Emamdjomeh, Asadi, Mizani & Mazaheri, 2010).

75   The microbiological analysis has revealed a high load of probiotic bacteria in fruits for high

76   concentrations of sodium alginate in the coating formulation. Furthermore, such

77   immobilization of *L. acidophilus* in the alginate-based film effectively protected the bacteria

78   cells against the low temperature storage, with no significant change in the viability count

79   (Moayednia, Ehsani, Emamdjomeh, Asadi, Mizani & Mazaheri, 2010). López de Lacey et al.

80   have successfully incorporated *L. acidophilus* and *Bifidobacterium bifidum* into edible gelatin

81   coatings and evaluated their effect on fish during chilled storage. It was observed that the

82   application of an edible gelatin packaging incorporated with bacteria can be a promising

83   approach for fish preservation (de Lacey, Lopez-Caballero, Gomez-Estaca, Gomez-Guillen &

84   Montero, 2012).

85   Among the systems developed so far, a high focus has been given to biopolymers such as

86   chitosan, gums, cellulose, pectins and seaweed extracts (Baldwin, Hagenmaier & Bai, 2012;

87   Bourtoom, 2008; Espitia, Du, Avena-Bustillos, Soares & McHugh, 2014). Among them,

88   cellulose, as the most available, renewable and biocompatible biopolymer, emerges as a future

89   key material for a sustainable planet (Klemm, Heublein, Fink & Bohn, 2005; Singh et al., 2015).

90   Cellulose-based films have been developed and a striking example is cellophane. Cellulose

91   derivates are also widely used for film production but their synthesis often requires the use of

92   harsh chemicals and cross-linking agents (such as formaldehyde-based compounds) that limit

93   their potential use in food applications. An interesting alternative considers the use of citric

94   acid (CA) as a natural cross-linker and, therefore, the resulting materials are of great interest in

95   food and medical fields, due to their excellent biocompatibility and hydrophilicity (Demitri et

96   al., 2008; Raucci et al., 2015). Even if not well documented in literature available, cellulose

97   systems chemically cross-linked by CA are expected to form three-dimensional networks

98   poorly soluble in water (or in biological fluids) (Coma, Sebti, Pardon, Pichavant & Deschamps,

99   2003; Glusker, 1980; Wang & Chen, 2005; Xie, Liu & Cui, 2006; Yang & Wang, 1998). These

100   hydrogels have also been suggested as new superabsorbent systems potentially interesting in

101   personal care (i.e. diapers and napkins) or in agriculture and horticulture (i.e. strategical

102   management of water in areas where it is scarce) applications (Demitri, Scalera, Madaghiele,

103   Sannino & Maffezzoli, 2013; Sannino, Demitri & Madaghiele, 2009). To the best of our

104   knowledge, the potential use of such systems to entrap probiotic bacteria has never been

105   explored before and may constitute an interesting approach particularly relevant for food

106   applications. Therefore, in the present work, two cellulose derivatives, sodium

107   carboxymethylcellulose and hydroxyethylcellulose were used for film preparation (cross-linked

108   with CA) and posterior loaded with probiotic bacteria. The film formation and structure were

109   characterized, as well as the viability of the bacteria under different conditions (i.e. film

110   composition and pH).

111

112   **2.   Experimental**

113   *2.1. Materials and Methods*

114   The cellulose derivatives , CMC (Mw of ca. 250 kDa) and HEC (Mw of ca. 720 kDa), were

115   purchased from VWR and Sigma Aldrich, respectively, and used as received. The citric acid

116   was obtained from Sigma Aldrich. Lactobacillus rhamnosus GG LMG 18243 (LGG) was

117   bought from the Belgian Coordinated Collection of Microorganisms (BCCM). The MRS broth

118   pH 6.4 and MRS agar pH 5.7 were obtained from VWR International. The PBS buffer was

119   prepared in the laboratory using disodium hydrogen phosphate, sodium chloride, potassium

120   chloride and potassium dihydrogen phosphate (all analytical grade) obtained from Sigma-

121   Aldrich.

122

123   *2.2. Film formation*

124   The films were obtained by mixing different amounts of CMC (sodium form), HEC and

125   CA in water until full dissolution was achieved. The total polymer concentration was set to 2 wt

126   % while the ratio between the cellulose derivatives was systematically varied. The CA (cross-

127   linking agent) amount ranged from 5 to 10 wt%. Lower amounts of CA were also tested but the

128   films produced were not satisfactory (i.e. non-handable fragile films). After obtaining a clear

solution, 10 g of it were poured into Petri dishes and allowed to cure in an oven at 50 ºC for 15

129   h to allow the cross-linking reaction between the cellulose derivatives and CA to occur.

130   Depending on the amount of CA used, the film thickness varied from 0.05 to 0.2 mm. It should

131   be noted that this is a fairly mild procedure in comparison with the standard cross-linking

132   approach reported elsewhere (i.e. 80 ºC for 24h) (Demitri et al., 2008).

133

134   *2.3. Lactobacillus rhamnosus GG culture and entrapment in the films*

135   All culture media and buffers were autoclaved for sterilization at 121 ºC for 15

136   minutes. Freeze-dried cells of *Lactobacillus rhamnosus* GG were rehydrated in 5 mL MRS

137   broth and incubated at 37 °C for 40 hours in a CO_2 incubator, the growth being followed for

138   two days. When the broth became turbid, the bacterial growth was visually confirmed by the

139   optical density and was compared with the non-inoculated broth. To evaluate the purity of the

140   bacteria, one inoculation loop with bacteria was streaked on a MRS agar plate while a plate

141   with pure sterilized culture was treated as control. The optical density was measured with a

142   UV/vis spectrophotometer. The incorporation of bacteria into the films was performed in two

143   ways: 1) soaking the cross-linked films in a bacteria medium for 30 min at room temperature,

144   and removing the excess of medium afterwards. 2) mixing an appropriate amount of bacteria

145   inoculum in the CMC/HEC/CA mixture before casting and curing the mixture.

146   While in the former approach the bacteria are expected to diffuse and adsorb into the film

147   during its swelling and solvent uptake, in the latter the bacteria are expected to be entrapped in

148   the cellulosic polymer matrix already from the beginning. The virtues and drawbacks with both

149   methodologies will be discussed later.

150

151   *2.4. Evaluation of the Viability of Lactobacillus rhamnosus GG.*

152   To estimate the viable counts and matrix effect, the encapsulated bacteria were released

153   from the films (ca. 0.01 gm) by re-suspending them in a PBS buffer solution (pH 7.4) at 37 ºC

154   for 30 minutes, under stirring. Sequential dilutions were performed following the

155   Miles and Misra approach to count the number of v iable bacteria (Miles, Misra & Irwin, 1938).

156   All different dilutions were plated in triplicates and kept in CO_2 incubator for 48 hours before

157   the bacterial colony was counted using a colony reader. The experiments were performed in

158   Faster BH-EN and BHG Class II Microbiological Safety Cabinets.

159

160   *2.5. Rheology*

161   The rheological measurements on the gel-like films were carried out on a HAAKE

162   MARS III rheometer (Thermo Fisher Scientific, Germany) set with a plate-plate geometry (35

163   mm, 0.2 mm gap). A Peltier unit was used to ensure strict temperature control, which was

164   fixed at 20.0 ± 0.1 ºC. The storage modulus (G') was accessed by performing dynamic

165   oscillatory experiments from 10 to 0.01 Hz, at a constant stress of 5 Pa.

166

167   *2.6. Fourier transform infrared spectroscopy (FTIR)*

168   The cross-linking between the cellulose derivatives and CA in the film was investigated by

169   FTIR at 25 ºC with an ATR-FTIR spectrophotometer Thermo Nicolet, IR300 (USA), using an

170   universal ATR sampling accessory. The FTIR spectral analysis was performed within the

171   wavenumber range of 400–4000 cm^{-1}. A total of 256 scans were performed for each spectrum,

172   at a resolution of 1 cm^{-1}, in the transmission mode.

173

174   *2.7. Thermal gravimetric analysis (TGA)*

175   The thermal gravimetric analysis (TGA) was performed on a TG 209 F3Tarsus

176   thermogravimetric analyzer (Netzsch Instruments). The films (ca. 8-10 mg) were weighed

177   in alumina pans and were heated from 30 to 650 ºC at a heating rate of 10ºC min^{-1} under N_2

178   atmosphere (flow rate of 20 mL min^{-1}).

179

180   *2.8. Water uptake*

181   The equilibrium swelling measurements for all films were carried out in distilled water or

182   in aqueous media of different pHs. The percentage of swelling (S) was estimated by weighing a

183   ca. 1g square-shaped specimen before and after its immersion in distilled water for about 24 h

184   (the films reach their swelling equilibrium within this period). S is defined as follows:

185

$$S = \frac{(Ws - Wd)}{Wd} \times 100$$

186

187   where W_s is the weight of the swollen film and W_d is the weight of the dried sample.

188

189   *2.9. Scanning Electron Microscopy (SEM)*

190   A VEGA3 SBH from TESCAN scanning electron microscope, equipped with a selected

191   energy dispersive X-ray microanalyser (EDX) was used to observe the morphology of the

192   cross-linked dried films. Briefly, the freeze-dried samples were deposited directly over the

193   carbon tape on the support and sputtered with an approximately 6 nm thin Au/Pd film by

194   cathodic pulverization using a SPI Module Sputter Coater before SEM analysis, during 90 s,

195   and with a current of de 15 mA. The accelerating voltage ranged from 5 to 15 kV.

196

197   *2.10. Statistical analysis*

198   The experiments were performed in triplicate and data was subjected to one-way analysis

199   of variance (ANOVA). Multiple comparisons were performed by LSD test. Statistical

200   significance was set at $P<0.05$ using SPSS (SPSS Inc, USA).

201

202   **3.   Results and discussion**

203   *3.1. Characterization of the cellulose-based films*

204   Photographs of the films formed following the procedure described in the

205   experimental section are presented in Figure 1. The films made from HEC (#1) and CMC (#2)

206   alone are reasonably flexible and transparent. The same is observed for the physical mixture of

207   HEC and CMC (#3). On the other hand, the addition of CA followed by cross-linking resulted

208   in less flexible, and brittle, films and the transparency is observed to decrease with the amount

209   of CA. While the HEC (#1), CMC (#2) and their physical mixture (#3) dissolve in water, the

210   cross-linked films (#4 and #5) do not.

211
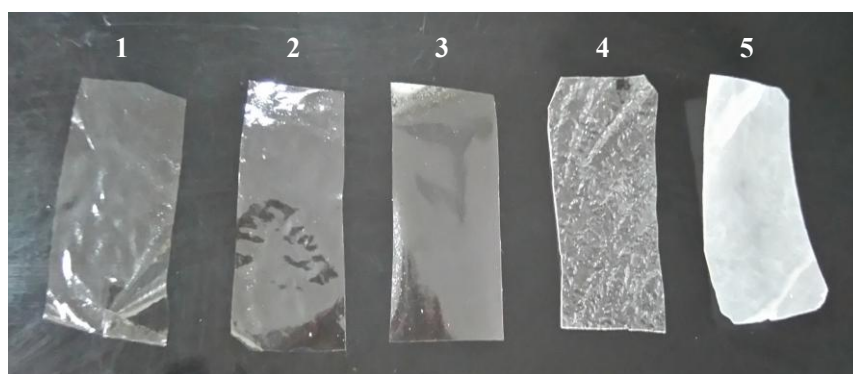
217   Figure 1. Photograph of cellulose-based film strips after being casted and dried in Petri dishes.

218   1) 1 wt% HEC; 2) 1 wt% CMC; 3) 1 wt% HEC + 1 wt% CMC; 4) 1 wt% HEC + 1 wt% CMC

219   + 5 wt%CA; 5) 1 wt% HEC+ 1 wt% CMC + 10 wt% CA.

220

221   The synthesized films were further characterized by FTIR spectroscopy (Figure 2) and

222   the spectra compared to those of the individual compounds. As can be seen in the spectrum of

223   CMC (b), the absorption band at 1590 cm^{-1} can be assigned to the asymmetrical stretching of

224   the COO^- of CMC (Hatanaka, Yamamoto & Kadokawa, 2014). The bands at 1414 and 1320 cm

225    $^{-1}$ are attributed to the symmetrical stretching vibrations of the carboxylate groups and to the

226   C–H bending mode, respectively (Fan et al., 2014). The broad band in the 1080-980 cm^{-1} range

227   is assigned to the stretching of the C–O–C bonds (Qi et al., 2016). The HEC spectrum (c)

228   broad band at 3480 cm^{-1} possibly assigned to the alcohol group and another broad band at

229   2920-2820 cm^{-1} region corresponding to the C-H stretching modes of the CH_2 groups. The bands in the

230   1450-1380 cm^{-1} are due to the symmetrical deformations of the CH_2 and C-OH groups.

231   The bands due to the alcoholic CH_2OH stretching and CH_2 twisting modes appear at around

232 1070 and 1010 cm^{-1}, respectively (Deyab, 2015). On the other hand, the FTIR spectrum of CA

233 (a) presents a band at 3490 cm^{-1}, which can be assigned to the stretching mode of the OH

234 group. The strong band at 1740-1700 cm^{-1} is attributed to the C=O stretch vibration of the

235 carboxylic acid group.

236 For the cross-linked films, a new band is observed at 1715 cm^{-1} which is assigned to the

237 stretching mode of the C=O ester bond, expected to appear at higher frequencies than for

238 carboxylic acids. All the remaining bands of CMC and HEC are essentially kept after reaction.

239 Overall, the FTIR data supports the success of the esterification reaction between the cellulose

derivatives and CA.
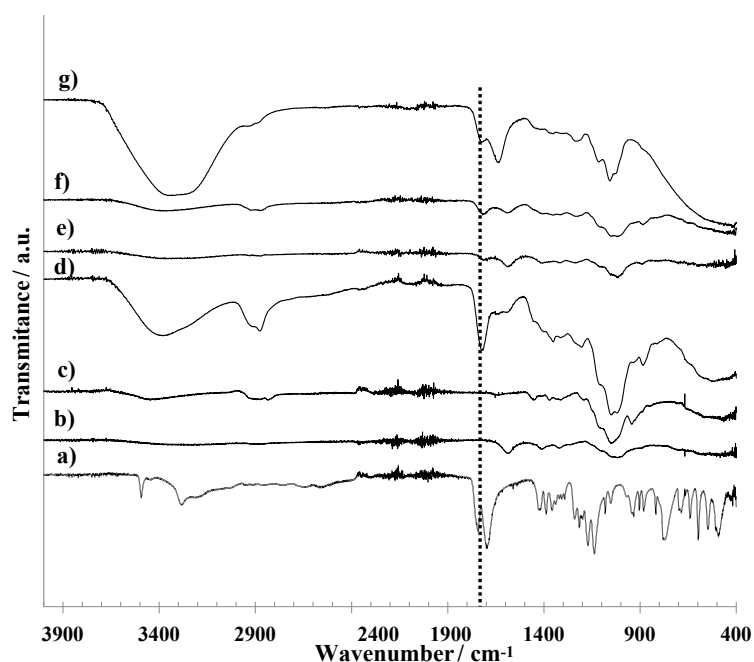
251 Figure 2. FTIR spectra of CA, CMC, HEC and the different films formed after cross-linking. a)

252 citric acid (CA); b) CMC; c) HEC; d) HEC + 5% CA; e) CMC + 5% CA; f) HEC + CMC + 5%

253 CA; g) HEC + CMC + 10% CA.

254

255 The amount of water adsorbed by the different films was measured after 24h of equilibration in

256 distilled water. All the physical films, i.e. without chemical cross-linking,

257 dissolved in water after a couple of minutes and thus only the equilibrium average swelling for

258 the films, which were cross-linked by CA, is presented in table 1.

259

260 Table 1. Average swelling percentage of the cross-linked films in water, at 25 ºC and neutral

261 pH.

Sample	Average swelling / %
CMC + 5%CA	236
HEC + 5%CA	2630
CMC + HEC + 5%	280
CA CMC + HEC + 10%CA	86

262

263 The results show that the cross-linked HEC film presents the highest swellability. The

264 drawback of such a huge water uptake is that the highly swollen film behaves as a weak gel

265 (rheology data in Figure 3) and thus its handability is rather modest in contrast with the other

266 formulations. Comparing the films containing only CMC and CMC/HEC, both cross-linked

267 with 5% CA, it is interesting to note an increase in swelling when HEC is present. The data

268 suggests that CMC is more reactive under the present conditions, leading to a better cross-

269 linking when compared with the HEC film. Previous work reported a different trend, the higher

270 HEC reactivity being attributed to the lower sterical hindrance presented by HEC when

271 compared with CMC (Demitri et al., 2008). Since at these pHs, CMC is charged, swelling may

272 induce some structural changes/rearrangements that are energetically not favored, thus

273 restricting an extreme expansion. Another interesting observation is related to the lower

274 swelling of the films when the CA concentration increases. Most likely, the increment in CA

275 concentration leads to an increase in the cross-linking density thus reducing the swelling ability

276 due to an increase in rigidity of the highly cross-linked polymer network.

277   The effect of pH on the film stability and swellability was further evaluated. It was

278 observed that all the tested films present a rather similar trend with a low swelling capacity at

279 low pH (ca. pH 2) and an up to four-fold swelling increment at high pH, ca. pH 10. In addition,

280 the film integrity was essentially preserved regardless of the pH used. If not protected, the

281 growth and survival of probiotics during their transit in the gastrointestinal tract may be

282 seriously compromised. Moreover, the inherent physical and chemical properties of food

283 carriers such as the low pH (e.g. fruit juices, salads and condiments) may represent an

284 additional problem for probiotic survival (Rodgers, 2007). The data suggests that these

285 cellulose-based films, cross-linked with CA (or related systems, such as microparticles), may be

286 a viable alternative for entrapping viable probiotics and protect them from any unfavorable

287 food matrix properties or even from the harsh gastrointestinal conditions (e.g. low pH in the

288 stomach).

289 As previously mentioned, after soaking and swelling the films for 24h in water they

290 behave as jelly-like materials. The rheological mechanical spectra are represented in Figure 3.

291
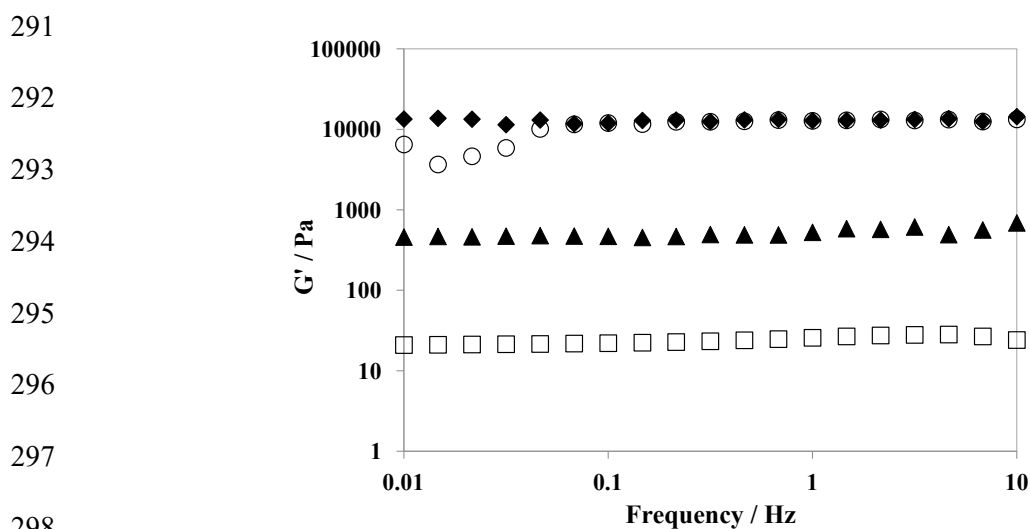
299 Figure 3. Mechanical spectra (frequency sweep) of the films after 24h swelling in water

300 (neutral pH) at 25 ºC. 1 wt% CMC + 5 wt% CA (♦); 1 wt% HEC + 5 wt% CA (□); 1 wt%

301 HEC + 1 wt% CMC + 5 wt% CA (▲);1 wt% HEC + 1 wt% CMC + 10 wt% CA (○).

302

303   The cross-linked CMC films present a high storage modulus, G', almost three orders of

304   magnitude higher than the cross-linked HEC films, which behave as a weak gel-like material.

305   Nevertheless, as observed in table 1, such high elasticity compromises the extension of

306   swelling (i.e. HEC films have a lower cross-linking density and thus show up to one order

307   magnitude higher swelling than the CMC films). The combination of the two polymers results

308   in films with interesting rheological properties (i.e. G' in between the values of the films of the

309   individual polymers) and a swelling degree higher than the film of CMC alone. The role of CA

310   cannot be neglected; an increase in CA concentration from 5 to 10 wt% leads to a significant

311   increase in rigidity of the polymer network (highest G' value observed) and consequently to a

312   very poor swelling ability. Therefore, the mechanical and swelling properties can be optimized

313   by tuning the CMC/HEC/CA ratios.

314   TGA was used in order to evaluate the thermal stability of the different film

315   formulations. Figure 4 shows the thermal decomposition of the different films as well as the

316   corresponding derivative thermogravimetric curves (DTG).

317
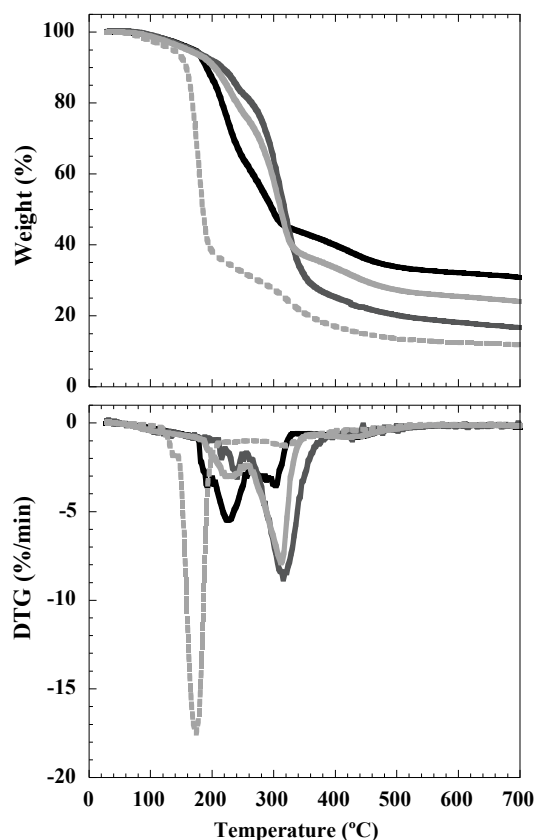
329

330   Figure 4. TGA (top) and corresponding DTG (bottom) of cellulose-based cross-linked films. 1

331   wt% CMC + 5 wt% CA (full black line); 1 wt% HEC + 5 wt% CA (full grey line); 1 wt% HEC

332   + 1 wt% CMC + 5 wt% CA (full light grey line); 1 wt% HEC + 1 wt% CMC + 10 wt% CA

333   (dashed light grey line).

334

335   The CMC-based films generally present a lower thermal stability when compared with the

336   formulations using HEC. The thermal degradation, T_{dm}, of the native polymers HEC and CMC

337   occurs at ca. 310 ºC and 280 ºC, respectively (data not shown) but after the cross-linking

338   reaction with 5 wt% CA, T_{dm} is shifted to ca. 315 and 230 ºC, respectively. That is, while the

339   HEC films slightly improve their stability, the CMC based films display a substantial reduction.

340   Moreover, it is interesting to note that the film containing both HEC, CMC and 5% CA presents

341   a T_{dm} similar to HEC cross-linked with CA but with a final mass loss intermediate of the

342   individual cross-linked polymers. The formulation containing 10 wt% CA results in films with

343   decreased thermal stability (i.e. T_{dm} is ca. 175 ºC). This reduction in T_{dm} can be related to a

344   higher disorder in the structure due to the high concentration of CA in the reaction. There are

345   other systems where a too high cross-linking density leads to a less organized material and

346   consequently to a lower thermal stability. Nevertheless, overall the TGA curves indicate that the

347   obtained chemically cross-linked cellulose-based films are thermally stable in the temperature

348   range suitable for entrapment and delivery of probiotic bacteria.

349   The morphology of the cross-linked films was characterized using scanning electron

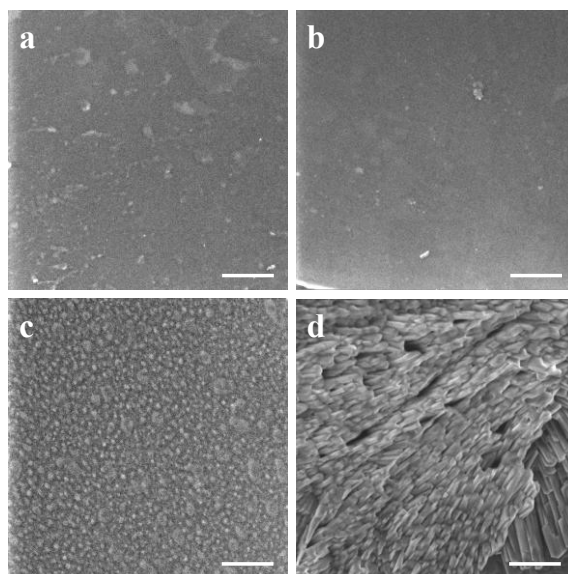350   microscopy (Figure 5).

351

352

353

354

355

356

357

358

359

360

361

362

363

364

365   Figure 5. SEM images of different cross-linked films: a) 1 wt% CMC + 5 wt% CA; b) 1 wt%

366   HEC + 5 wt% CA; c) 1 wt% HEC + 1 wt% CMC + 5 wt% CA; 1 wt% HEC + 1 wt% CMC +

367   10 wt% CA. The scale bar represents 5 µm.

368

369   The cross-linked films of HEC or CMC alone (Figures 5a and 5b) present a rather similar and

370   homogeneous morphology with an apparent low porosity, which contrasts to the much less

371   dense structure and higher porosity of the non-cross-linked homologues (data not shown).

372   When CMC and HEC are mixed and cross-linked together, the porosity and heterogeneity

373   increase (Figure 5C) and a "fibrillar"-like morphology is obtained for the highest CA

374   concentration used (Figure 5D). Such an aggregated fibrillar structure is expected to account

375   for the high elasticity and good mechanical resistance of the wet films (see Figure 3).

376   Nevertheless, the increased heterogeneity in the film with visible fracture points may be

377   responsible for the brittleness and observed decrease in thermal stability (see Figure 4).

378

379   *3.2.   Probiotic encapsulation and viability*

380   In order to evaluate the ability of the different cellulose-based films to work as matrices

381   for probiotic entrapment and delivery, LGG was selected as model bacteria. The bacteria

382   entrapment in the films was performed following two distinct approaches as described in the

383   experimental section. Briefly, in a first approach, LGG was mixed directly with all compounds

384   and casted in the Petri dishes. A typical SEM example of LGG embedded in the film matrix is

385   shown in Figure 6a (with zoom-in presented in Figure 6b). However, even if the curing

386   conditions for the cross-linking reaction are far milder than the standard procedure reported in

387   literature, the entrapped bacteria are found to have a quite low viability as qualitatively

388   evaluated by fluorescence microscopy using a Dead/Alive kit (Figure 6d). In this test, the viable

389   bacteria appear as green rods while the dead bacteria are red and, as is clearly visible, the curing

390   conditions (i.e. 50 ºC, 24h) are still too harsh with the majority of the bacteria being found dead;

391   3 Log CFU/mL (CFU: colony-forming units) is estimated from the plate counting method. It

392   has been speculated that some of the mechanisms behind the probiotic health effects may not

393   entirely dependent on the viability of the cells but may also depend on other factors such as

394   probiotic adhesion. It has been argued that probiotic adhesion to host tissues facilitates the host-

395   microbial interactions such as the effects of microbes on the immune system of the host. In fact,

396   some reports suggest that viable and non-viable probiotics are equally adherent to intestinal

397   mucus (Lahtinen, 2012). Apart from the hypothetic effect of non-viable probiotics, further

398   studies are planned to improve the synthesis conditions in order to guarantee a higher probiotic

399   viability in the films.
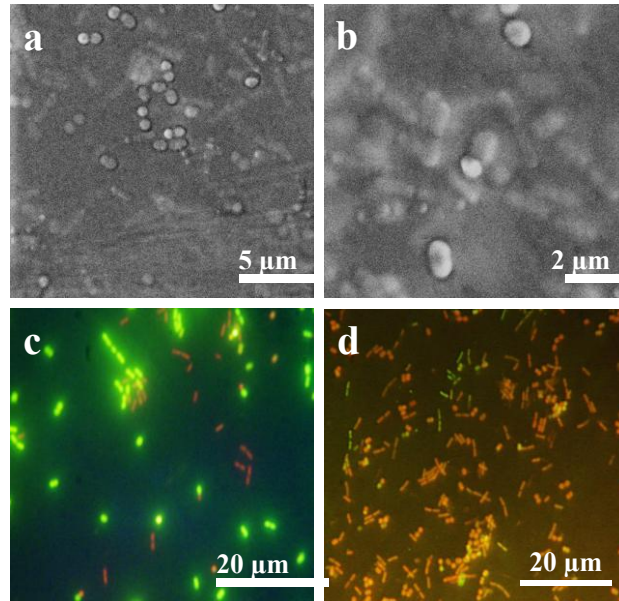
400

401

402

403

404

405

Figure 6. SEM of probiotic bacteria entrapped in CMC-based films (A and B) and the

corresponding fluorescent microscopy image using the Dead/Alive kit (D). The control of LGG

in the polymer matrix before curing is presented in panel C.

An alternative approach was tested to endow the films with viable cells. The method is based

on probiotic adsorption onto the films via soaking them in a LGG solution for 30 min at room

temperature. The ability of the films to release bacteria into aqueous media of different pH was

also evaluated. As can be seen in Figure 7 (a and b), the majority of the bacteria appear as

green, which is a strong qualitative indication of high viability even after exposure to the

different pH conditions. Note that the images in Figure 7 are not as clear as those in Figure 6

since the cross-linked mixture of CMC and HEC results in films with poorer transparency,

which contributes to blur the fluorescence images. Additionally, during the cell diffusion into

the film matrix, it is expected that bacteria accumulate in the larger pores and defects in the

films thus resulting in a less homogeneous distribution of the bacteria. This can be inferred

from Figure 7b where a rather large green area is observed. The viability of LGG after

entrapment in the films was also quantitatively checked by plate counting (Figure 7).

432

433

434

435

436

437

438

439

440

441

442

443
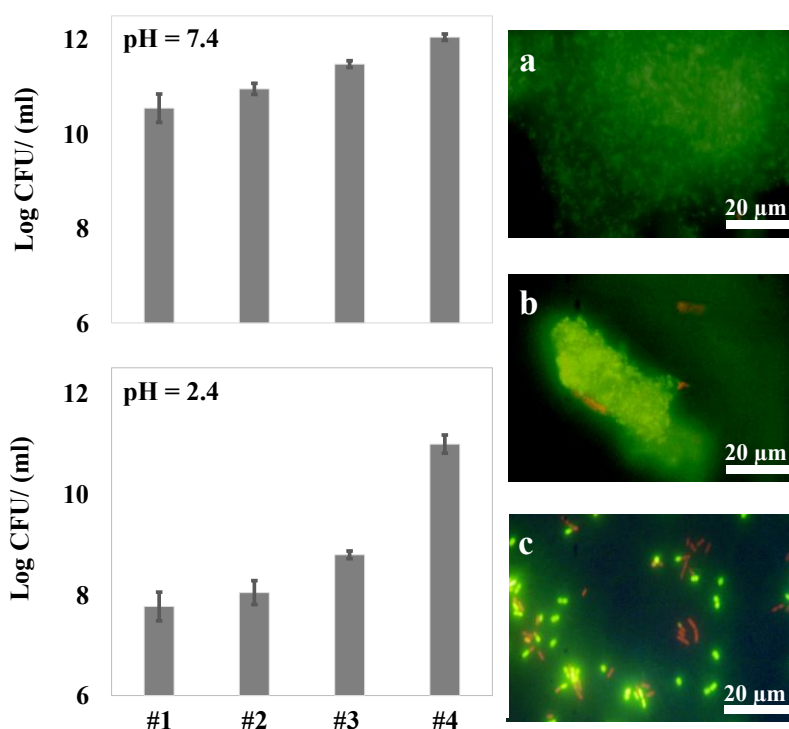
444 Figure 7. Left: Viability counts in Log CFU/mL of the different systems developed after the

445 bacteria have been released in PBS, pH 7.4 (top) and in an aqueous solution of HCl, pH 2.4

446 (bottom). #1: 1 wt% CMC + 5 wt% CA; #2: 1 wt% HEC + 1 wt% CMC + 5 wt% CA; #3: 1 wt

447 % HEC + 1 wt% CMC + 10 wt% CA; #4: control. Fluorescence microscopy images of the 1 wt

448 % HEC + 1 wt% CMC + 5 wt% CA film after bacteria soaking and later exposure to entrapped

449 bacteria of the CMC + HEC + 10% CA films after their exposure to a) pH 2.4 and b) pH 7.4.

450 Image "c" refers to naked bacteria. The films were stained with the Live and Dead viability kit.

451 The error bars represent the standard deviation.

452

453 The cross-linked CMC film presented the lower cell counting at both pHs but the viability

454 increases if HEC is added to the formulation. Moreover, the higher the content of CA, the higher

455 the cell counting (statistically relevant). This observation is most likely related to the fact that

456 the degree of porosity and film defects increases with CA (see Figure 5). Note that the HEC

457 film was not selected for these tests since the mechanical properties of the wet film are

458   rather poor. While at higher pH (7.4) the viability for all films tested is very high (above ca. 10

459   log CFU/mL) it is striking that at low pH (2.4.) the viability count drops significantly (ca. 7-8

460   log CFU/mL). This viability counting is expected to be underestimated due to remaining

461   entrapped bacteria in the film matrix, bacteria which are not released (poor swelling) as the

462   florescence data suggests. On the other hand, at high pH, film swelling is favored and the

463   bacteria are more efficiently released thus resulting in a higher viability counting.

464   In general, viable LGG bacteria can be effectively entrapped in the cross-linked cellulose based

465   films and their release is strongly dependent on the film composition and pH of the media.

466

467   *4.   Conclusions*

468   Both CMC and HEC can be successfully cross-linked using CA, via an esterification reaction

469   among the COOH groups of CA and the OH groups of the cellulose derivatives. This reaction

470   can be successfully followed by FTIR by monitoring the appearance of the vibrations modes

471   corresponding to ester groups. Different concentrations of cross-linking agent (CA) result in

472   films with different properties. An increase in CA concentration leads to a decrease in swelling

473   ratio of the films, which can be attributed to an increase in cross-linking density of the polymer

474   chains. As a direct consequence, the swelling obtained is reduced due to an increased rigidity of

475   the highly cross-linked polymer network. The presence of HEC favours the swelling of the

476   films, but the increase in CA reduces significantly the swelling ratio. The film containig only

477   HEC and CA present a very large swelling ratio but its integrity is compromised after

478   hydration, as is supported by the rheological data (i.e. poor elasticity). In contrast, the film

479   containing CMC and CA is highly stable and after hydration a strong wet film is obtained. The

480   mixture of the two polymers gives rise to films of intermediate sweling and mechanical

481   properties. The higher the CA content, the higher the porosity of the films until fibrillar-like

482   aggregates are observed by SEM. This curious morphology explains not only the improved

483   elasticity and good mechanical resistance of the obtained films before and after hydration, but

      also the higher

484 release of bacteria at different pHs. Viable LGG could be effectively entrapped in the films after

485 soaking them in bacteria medium. Their release could be effectively controlled depending on

486 the pH of the release media and film composition. On the other hand, the direct mixing of

487 bacteria with the film components followed by casting and curing was found to be very harsh

488 for LGG even if the curing conditions developed in this work are far milder than the standard

489 one previously reported in literature. Overall, the films developed proved to be promising

490 matrices for bacteria entrapment and release, for instance, in food applications where the

491 mechanical, swelling and release properties can be tuned by HEC/CMC ratio and amount of

492 cross-linker. Clearly, these results represent promising advances in the search for new

493 applications of edible cellulose based films and coatings as carriers of diverse probiotics, and

494 open new possibilities for the development of novel food probiotic products. For instance, these

495 films may inspire the formation of related systems such as micro-beads as carriers for probiotic

496 bacteria and delivery at the gut. Indeed, the data suggests that particles based on the developed

497 formulations can be used to entrap bacteria, protect them during the harsh conditions of the

498 stomach (reduced swelling at low pH) and effectively release them at the intestine (improved

499 swelling at high pH). Future work is planned to consider other different morphologies such as

500 particles based on the innovative approach discussed in this work.

501

509

References

Ayala-Zavala, J. F., Soto-Valdez, H., Gonzalaz-Leon, A., Alvarez-Parrilla, E., Martin-Belloso, O., & Gonzalez-Aguilar, G. A. (2008). Microencapsulation of cinnamon leaf (Cinnamomum zeylanicum) and garlic (Allium sativum) oils in beta-cyclodextrin. *Journal of Inclusion Phenomena and Macrocyclic Chemistry, 60*(3-4), 359-368.

Ayala-Zavala, J. F., Vega-Vega, V., Rosas-Dominguez, C., Palafox-Carlos, H., Villa-Rodriguez, J. A., Siddiqui, M. W., Davila-Avina, J. E., & Gonzalez-Aguilar, G. A. (2011). Agro-industrial potential of exotic fruit byproducts as a source of food additives. *Food Research International, 44*(7), 1866-1874.

Baldwin, E. A., Hagenmaier, R. D., & Bai, J. (2012). Edible coatings and films to improve food quality. CRC Press Llc, Boca Raton.

Biquet, B., & Labuza, T. P. (1988). Evaluation of the Moisture Permeability Characteristics of Chocolate Films as an Edible Moisture Barrier. *Journal of Food Science, 53*(4), 989-998.

Bourtoom, T. (2008). Edible films and coatings: characteristics and properties. *Int Food Res J, 15*, 237-248.

Coma, V., Sebti, I., Pardon, P., Pichavant, F. H., & Deschamps, A. (2003). Film properties from crosslinking of cellulosic derivatives with a polyfunctional carboxylic acid. *Carbohydrate Polymers, 51*(3), 265-271.

Corona-Hernandez, R. I., Alvarez-Parrilla, E., Lizardi-Mendoza, J., Islas-Rubio, A. R., de la Rosa, L. A., & Wall-Medrano, A. (2013). Structural Stability and Viability of Microencapsulated Probiotic Bacteria: A Review. *Comprehensive Reviews in Food Science and Food Safety, 12*(6), 614-628.

Cuq, B., Gontard, N., & Guilbert, S. (1995). Edible films and coatings as active layers. In: Active food packaging. Springer, pp 111-142.

de Lacey, A. M. L., Lopez-Caballero, M. E., Gomez-Estaca, J., Gomez-Guillen, M. C., & Montero, P. (2012). Functionality of Lactobacillus acidophilus and Bifidobacterium bifidum incorporated to edible coatings and films. *Innovative Food Science & Emerging Technologies, 16*, 277-282. Demitri, C., Del Sole, R., Scalera, F., Sannino, A., Vasapollo, G., Maffezzoli, A., Ambrosio, L., & Nicolais, L. (2008). Novel superabsorbent cellulose-based hydrogels crosslinked with citric acid. *Journal of Applied Polymer Science, 110*(4), 2453-2460.

Demitri, C., Scalera, F., Madaghiele, M., Sannino, A., & Maffezzoli, A. (2013). Potential of Cellulose-Based Superabsorbent Hydrogels as Water Reservoir in Agriculture. *International Journal of Polymer Science*.

543   Deyab, M. A. (2015). Hydroxyethyl cellulose as efficient organic inhibitor of zinc–carbon

544   battery corrosion in ammonium chloride solution: Electrochemical and surface morphology

545   studies. *Journal of Power Sources, 280*, 190-194.

546   Dhall, R. K. (2013). Advances in Edible Coatings for Fresh Fruits and Vegetables: A Review.

547   *Crit Rev Food Sci Nutr, 53*(5), 435-450.

548   Espitia, P. J. P., Batista, R. A., Azeredo, H. M. C., & Otoni, C. G. (2016). Probiotics and their

549   potential applications in active edible films and coatings. *Food Research International, 90*,

550   42-52.

551   Espitia, P. J. P., Du, W. X., Avena-Bustillos, R. D., Soares, N. D. F., & McHugh, T. H. (2014).

552   Edible films from pectin: Physical-mechanical and antimicrobial properties - A review. *Food*

553   *Hydrocolloids, 35*, 287-296.

554   Fan, L., Peng, M., Zhou, X., Wu, H., Hu, J., Xie, W., & Liu, S. (2014). Modification of

555   carboxymethyl cellulose grafted with collagen peptide and its antioxidant activity.

556   *Carbohydrate Polymers, 112*, 32-38.

557   Glusker, J. P. (1980). Citrate Conformation and Chelation - Enzymatic Implications. *Accounts*

558   *of Chemical Research, 13*(10), 345-352.

559   Haffner, F. B., Diab, R., & Pasc, A. (2016). Encapsulation of probiotics: insights into academic

560   and industrial approaches. *Aims Materials Science, 3*(1), 114-136.

561   Hatanaka, D., Yamamoto, K., & Kadokawa, J.-i. (2014). Preparation of chitin nanofiber-

562   reinforced carboxymethyl cellulose films. *International Journal of Biological Macromolecules,*

563   *69*, 35-38.

564   Holzapfel, W. H., Haberer, P., Snel, J., Schillinger, U., & Huis in't Veld, J. H. J. (1998).

565   Overview of gut flora and probiotics. *International Journal of Food Microbiology, 41*(2),

566   85-101.

567   Kester, J. J., & Fennema, O. R. (1986). Edible Films and Coatings - a Review. *Food*

568   *Technology, 40*(12), 47-59.

569   Klemm, D., Heublein, B., Fink, H. P., & Bohn, A. (2005). Cellulose: Fascinating biopolymer

570   and sustainable raw material. *Angewandte Chemie-International Edition, 44*(22), 3358-3393.

571   Lahtinen, S. J. (2012). Probiotic viability - does it matter? *Microb Ecol Health Dis, 23*.

572   Miles, A. A., Misra, S. S., & Irwin, J. O. (1938). The estimation of the bactericidal power of the

573   blood. *Journal of Hygiene, 38*(6), 732-749.

574   Moayednia, N., Ehsani, M. R., Emamdjomeh, Z., Asadi, M. M., Mizani, M., & Mazaheri, A. F.

575   (2010). Effect of refrigeration on viability of immobilized probiotic bacteria in alginate coat of

576   strawberry. *World Appl Sci J, 10*, 472-476.

577   Muranyi, P. (2013). Functional Edible Coatings for Fresh Food Products. *J Food Process*

       Technol, 4, e114.

578   Pamer, E. G. (2016). Resurrecting the intestinal microbiota to combat antibiotic-resistant

579   pathogens. *Science, 352*(6285), 535-538.

580   Pothakamury, U. R., & BarbosaCanovas, G. V. (1995). Fundamental aspects of controlled

581   release in foods. *Trends in Food Science & Technology, 6*(12), 397-406.

582   Qi, X.-M., Liu, S.-Y., Chu, F.-B., Pang, S., Liang, Y.-R., Guan, Y., Peng, F., & Sun, R.-C.

583   (2016). Preparation and Characterization of Blended Films from Quaternized Hemicelluloses

584   and Carboxymethyl Cellulose. *Materials, 9*(1), 4.

585   Quiros-Sauceda, A. E., Ayala-Zavala, J. F., Olivas, G. I., & Gonzalez-Aguilar, G. A. (2014).

586   Edible coatings as encapsulating matrices for bioactive compounds: a review. *Journal of Food

587   Science and Technology-Mysore, 51*(9), 1674-1685.

588   Raucci, M. G., Alvarez-Perez, M. A., Demitri, C., Giugliano, D., De Benedictis, V., Sannino,

589   A., & Ambrosio, L. (2015). Effect of citric acid crosslinking cellulose-based hydrogels on

590   osteogenic differentiation. *Journal of Biomedical Materials Research Part A, 103*(6),

591   2045-2056.

592   Rodgers, S. (2007). Incorporation of probiotic cultures in foodservice products: an exploratory

593   study. *J Food Serv, 18*, 108-118.

594   Salminen, S., Ouwehand, A., Benno, Y., & Lee, Y. K. (1999). Probiotics: how should they be

595   defined? *Trends in Food Science & Technology, 10*(3), 107-110.

596   Sanchez, B., Delgado, S., Blanco-Miguez, A., Lourenco, A., Gueimonde, M., & Margolles, A.

597   (2017). Probiotics, gut microbiota, and their influence on host health and disease. *Molecular

598   Nutrition & Food Research, 61*(1).

599   Sannino, A., Demitri, C., & Madaghiele, M. (2009). Biodegradable Cellulose-based Hydrogels:

600   Design and Applications. *Materials, 2*(2), 353-373.

601   Sharafi, H., Alidost, L., Lababpour, A., Shahbani Zahiri, H., Abbasi, H., Vali, H., & Akbari

602   Noghabi, K. (2013). Antibacterial Activity of Probiotic Lactobacillus plantarum HK01: Effect

603   of Divalent Metal Cations and Food Additives on Production Efficiency of Antibacterial

604   Compounds. *Probiotics Antimicrob Proteins, 5*(2), 121-130.

605   Silva-Weiss, A., Ihl, M., Sobral, P. J. A., Gomez-Guillen, M. C., & Bifani, V. (2013). Natural

606   Additives in Bioactive Edible Films and Coatings: Functionality and Applications in Foods.

607   *Food Engineering Reviews, 5*(4), 200-216.

608   Singh, P., Duarte, H., Alves, L., Antunes, F., Le Moigne, N., Dormanns, J., Duchemin, B.,

609   Staiger, M. P., & Medronho, M. (2015). *"From Cellulose Dissolution and Regeneration to

610   Added Value Applications - Synergism Between Molecular Understanding and Material

611   Development, Cellulose - Fundamental Aspects and Current Trends", Dr. Matheus Poletto

       (Ed.), InTech, DOI: 10.5772/61402.*

612   Singh, P., Medronho, B., Alves, L., da Silva, G. J., Miguel, M. G., & Lindman, B. (2017).

613   Development of carboxymethyl cellulose-chitosan hybrid micro- and macroparticles for

614   encapsulation of probiotic bacteria. *Carbohydrate Polymers, 175*, 87-95.

615   Tapia, M. S., Rojas-Grau, M. A., Rodriguez, F. J., Ramirez, J., Carmona, A., & Martin-

616   Belloso, O. (2007). Alginate- and gellan-based edible films for probiotic coatings on fresh-cut

617   fruits. *Journal of Food Science, 72*(4), E190-196.

618   Wang, C. C., & Chen, C. C. (2005). *Appl Catal A, 293*, 171.

619   Xie, X. S., Liu, Q., & Cui, S. W. (2006). *Food Research International, 39*, 332.

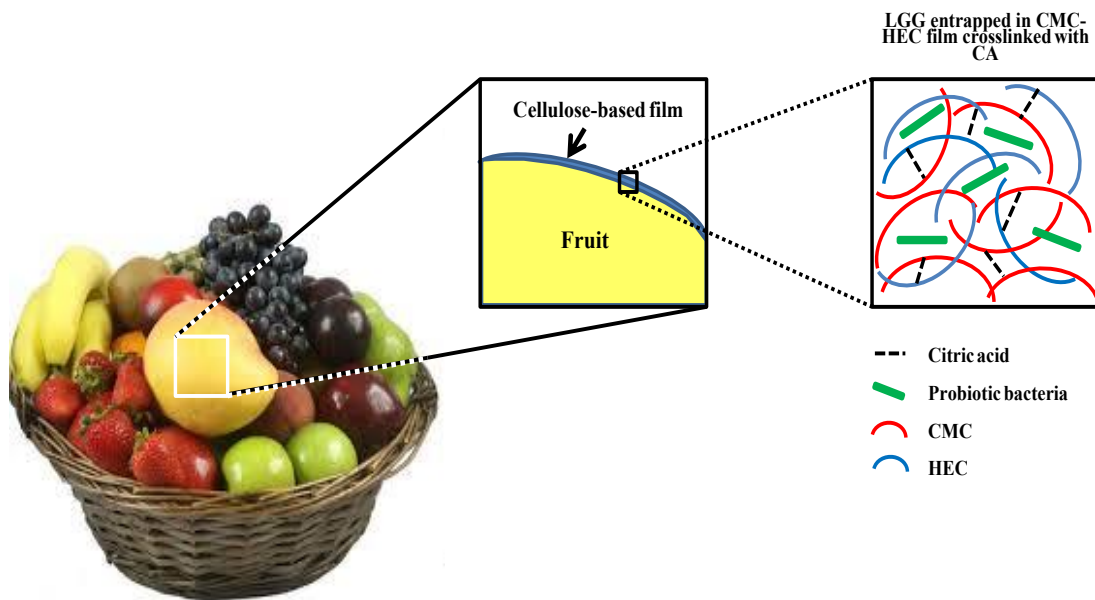620   Yang, C. Q., & Wang, X. J. (1998). *Journal of Applied Polymer Science, 70*, 2711.

Graphical abstract

"Celullose-Based Edible Films for Probiotic Entrapment and Delivery"

Poonam Singh, Solange Magalhães, Luis Alves, Filipe Antunes, Maria G. Miguel,

Björn Lindman and Bruno Medronho*

*corresponding author: bfmedronho@ualg.pt

Paper V

On the viability, toxicity and stability of probiotic bacteria entrapped in cellulose-based particles

Poonam Singh[§], Bruno Medronho[‡,], Tiago Santos, Isabel Nunes[§], Maria G. Miguel[§] and Björn Lindman[‖]*

[§]CQC, University of Coimbra, Department of Chemistry, 3004-535 Coimbra, Portugal

[‡]Faculty of Sciences and Technology (MeditBio), Ed. 8, University of Algarve, Campus de Gambelas, 8005-139 Faro, Portugal

[†]*CQC*, University of Coimbra, Department of Chemistry, 3004-535 Coimbra, Portugal

[‖]FSCN, Mid Sweden University, SE-851 70 Sundsvall, Sweden

*Corresponding author: bfmedronho@ualg.pt

Abstract

Probiotics are increasingly gaining popularity in vast food applications due to their recognized health benefits to the hosts. However, their passage through the gastrointestinal (GI) tract is not smooth and a significant number of physiological obstacles (e.g. low pH, bile salts, enzymes, peristaltic movements, etc.) may considerably affect their viability. The entrapment of probiotics in protective matrices, such as hydrogels particles, is a viable approach to minimize cell death. Therefore, in this work, novel cellulose/chitosan-based particles have been developed to entrap model probiotic *Lactobacillus rhamnosus* GG. The particle aging, storing and stability was studied at different temperatures and in simulated GI fluids with and without cross-linking agents or protein and lipid additives. Moreover, the effect of the particles on an intestinal cell line was evaluated. The formulations containing casein displayed the best bacterial survival even when exposed to the GI fluids. Overall, the storage and viability of the probiotics were observed to be improved in the different biopolymer-based systems presenting a low toxicity profile to the cell line. Thus, the CMC-Cht based particles may be regarded as interesting matrices for probiotic encapsulation and delivery in food products.

Keywords: Probiotic; carboxymethyl cellulose; chitosan, genipin, casein, lechitin, particles,

Introduction:

The Human intestine hosts more than 1000 species of bacteria including probiotic strains, such as the gram-positive genus Lactobacillus, which constitutes the microbiota. The Lactobacillus bacteria are known for their beneficial health effects and are mostly delivered through foods and nutraceuticals (Bosnea et al., 2014). In fact, the delivery of the probiotics into the gut has been suggested to combat many diseases and harmful pathogens (Iannitti & Palmieri, 2010). Although regarded as valuable food additives, probiotics are reasonably fragile when nakedly exposed to the harsh conditions of the GI tract (i.e. low pHs, oxidative stress, bile juices, etc.) or even during the storage in a given food matrix whose characteristics may irreversibly affect the probiotic viability. Thus, the protection of the bacteria in suitable carriers is an often-used procedure not only to minimize bacteria death but also to offer the systems "smart" features such as targeted release (i.e. delivery of the cargo at specific sites) or triggered release (i.e. delivery of the load activated by enzymes, changes in pH, ionic strength, temperature, etc.) (James et al., 2014). In this respect, the microencapsulation in biopolymer-based particles has been increasingly explored. So far, among the many systems reported, the high focus has been given to sugar-based biopolymers for biocompatibility and availability reasons (Chang & Zhang, 2011). It is thus not surprising that a lot of work has been carried out with chitin and cellulose-based systems (Dutta et al., 2004; Klemm, Heublein et al., 2005; Kumar, 2000). Systems containing alginate and hyaluronic acid are also among the most studied ones (Sharpe et al., 2014). Recently, some of us have reported the formation of novel micro- and macro particles based on chitosan and carboxymethyl cellulose by different methods. An extensive characterization was performed to understand their physicochemical properties, swelling behavior, and morphological features. The systems were found to successfully entrapped model probiotic (LGG) with acceptable viability count for practical uses (Singh et al., 2017). Moreover, the cross-linking of the particles with genipin, a low acute toxicity natural extract from the gardenia plant, was found to strengthen the polyion complex and improve the mechanical properties of the hydrogel particles. This is a very attractive approach not only due to the safety and biocompatibility profiles of the molecules involved but also due to their high availability which may turn feasible a hypothetical scale-up of the process. In this work, the novel Cht-CMC particles were improved regarding their colloidal stability using lecithin and sodium caseinate (Donthidi et al., 2009). The particle was also submitted to an *in vitro* study in simulated GI fluids and, in order to mimic the in vivo intestinal conditions, a Caco-2 cell line was used to evaluate the cytotoxicity of the novel cellulose-based particles with and without probiotics. Finally, the storage stability of the particles was also studied since in food industry, a manufactured

2

product may take different paths and time to reach to the customer and therefore their self-life must be considered (Li et al., 2009).

Materials and Methods

2.1. Materials

Chitosan (deacetylation $\geq$ 85 % and Mw of ca. 370 kDa), sodium caseinate (SC) from bovine milk (Mw 24kDa), L- α -Phosphatidylcholine (average Mw 776 Da) were purchased from Sigma-Aldrich. Sodium carboxymethyl cellulose, CMC, (Mw of ca. 250 kDa) was obtained from VWR chemicals. Lactobacillus rhamnosus GG LMG 18243 (LGG) was bought from the Belgian Coordinated Collection of Microorganisms (BCCM). The MRS broth pH 6.4 and MRS agar pH 5.7 were obtained from VWR International. The PBS buffer was prepared with sodium hydrogen phosphate, sodium chloride, potassium chloride and potassium dihydrogen phosphate, all obtained from Sigma-Aldrich. Sodium hydrogen carbonate, magnesium chloride hexahydrate, ammonium carbonate and calcium chloride (all analytical grade) were also obtained from Sigma-Aldrich. The Live/Dead® BacLight™ Bacterial Viability Kit L7012 and α-Minimum Essential Medium Eagle was purchased from Thermofisher Scientific, USA. The porcine pepsin (EC 3.4.23.1), porcine trypsin (EC 3.4.21.4), bovine chymotrypsin (EC 3.4.21.1), porcine pancreatic α-amylase (EC 3.2.1.1), porcine pancreatic lipase (EC 3.1.1.3), porcine pancreatic colipase and bile extract B8631 (porcine) were all purchased from Sigma Aldrich. Caco-2 cell line was obtained from ATCC. Fetal bovine serum was acquired from Biowest and 1% penicillin/streptomycin were purchased from Invitrogen Corp. Milli-Q water (18.2 MΩ.cm-1 at 25 °C, MQ) was used for the preparation of all samples.

2.2. Preparation of CMC-Cht particles

Physical and chemical CMC-Cht macroparticles (MP) were selected to evaluate the effect of sodium caseinate or soy lecithin in the particle formation and stability following the procedure reported before (Singh, et al., 2017). Briefly, a 1 wt% CMC solution (50 ml) was carefully dropped-wise into a 1 wt% Chit solution (300 mL) using a manually operated syringe with a 0.7 mm cannula under continuous stirring. When sodium caseinate or soy lecithin were used in the formulation, their content was kept constant at 1 wt % in all the formulations. The hydrogel particles formed were removed from the Cht solution by gentle filtration after 30 minutes aging. The microspheres (mP) were prepared in a similar way using a nozzle spray apparatus (Singh et al., 2017). Moreover, 0.5 wt % genipin solution (pH 7) was used for the preparation of chemical cross-linked particles as previously described.

2.3. Thermal and morphological characterization

The effect of casein and soy lecithin on the original CMC-Cht particles has been evaluated by thermal gravimetric analysis using a TG 209 F3 Tarsus thermogravimetric analyzer (Netzsch Instruments). Samples (ca. 10 mg) were weighed in alumina pans and were heated from 30 to 500 °C at a constant heating rate of 10 °C min−1 under N2 atmosphere (flow rate of 20 mL min−1).

Scanning Electron Microscopy (SEM) was performed on MERLIN with the GEMINI II column combines ultra-fast analytics, high- resolution imaging using advanced detection modes. Generally, freeze-dried particles were deposited directly onto the carbon tape on the support and sputtered with approximately 6 nm thin Au/Pd film by cathodic pulverization using an SPI Module Sputter Coater, during 90 s and with a current of 91pA.

2.5. Growth and entrapment of *Lactobacillus rhamnosus* GG

All the polymers and compounds were initially sterilized using UV radiation for 30 minutes while the culture media and buffers were autoclaved for sterilization at 121 °C for 15 minutes. Freeze-dried cells of Lactobacillus rhamnosus GG were rehydrated in 5 ml MRS broth and incubated at 37 °C for 40 hours in a CO2 incubator and their growth was analyzed during two days. When the broth became turbid, the bacterial growth was evaluated by the optical density using a UV/vis spectrophotometer and compared with the non-inoculated broth. To evaluate the purity of the bacteria, one inoculation loop of bacteria were streaked on an MRS agar plate while a plate with pure culture was treated as control. Colonies from the plate were grown by two successive transfers and then inoculated in 250-mL Erlenmeyer flasks containing 100 mL of MRS broth. In a later step, 10 mL of the cultured broth was divided into 10 eppendorfs and centrifuged for 30 minutes at 3000 rcf. The supernatant was discarded and 1 ml PBS was added to each of the pellets followed by centrifugation at 3000 rcf for 20 minutes. This washing procedure was repeated twice. Finally, the PBS rich supernatant was discarded and 5 bacterial pellets were mixed with 20 ml of 1 wt % of CMC aqueous solution and were mixed (drop-wise or via nozzle spray) with the Cht aqueous solution with or without the protein (casein) and lipid (lecithin) additives or cross-linker (genipin).

2.6. Preparation of the salivary, gastric and intestinal fluids

The Simulated Salivary Fluid (SSF), Simulated Gastric Fluid (SGF) and Simulated Intestinal Fluid (SIF) were prepared from the corresponding electrolyte stock solutions, enzymes and water as described in Minekus et al. 2014. The SSF was prepared using stock solutions of the following electrolytes: K^+ (18.8 mmol/L), Na^+ (13.6 mmol/L), Cl^- (19.5 mmol/L), $H_2PO_4^-$(3.7 mmol/L), HCO_3^- (13.7 mmol/L), Mg^{2+}(0.15 mmol/L), NH_4^+ (0.12 mmol/L), Ca^{2+}(1.5 mmol/L). In a typical

4

example, five CMC-Cht particles were mixed with 5 ml of SSF electrolyte stock solution. Human salivary α-amylase (EC 3.2.1.1) was further added to achieve 75 U/mL in the final mixture, followed by $CaCl_2$ (0.75mM) and the required amount of water to dilute the stock solution of SSF. Note that the recommended contact time with the enzyme is 2 min at 37 ℃ (pH 7) and therefore all reagents were pre-heated before mixing (Minekus et al., 2014).

For the SGF fluid, the electrolyte stock solution was prepared to achieve the following ion concentrations; K^+ (7.8 mmol/L), Na^+ (72.2 mmol/L), Cl^- (70.2 mmol/L), $H_2PO_4^-$ (0.9 mmol/L), HCO_3^- (25.5 mmol/L), Mg^{2+}(0.1 mmol/L), NH_4^+ (1 mmol/L), Ca^{2+}(0.15 mmol/L). Later, porcine pepsin (EC 3.4.23.1) was added to achieve 2000 U/mL in the SGF electrolyte mixture. 1 M HCl was added to adjust the pH to 3. Typically, the obtained gastric chyme was kept in contact with the particles for 2 hours at 37 °C (recommended conditions for digestion (Minekus, et al., 2014)). Finally, for the SIF fluid preparation, five parts of simulated gastric chyme were mixed with four parts of a SIF electrolyte stock solution composed of K^+ (7.6 mmol/L), Na^+ (123.4 mmol/L), Cl^- (55.5 mmol/L), $H_2PO_4^-$ (0.8 mmol/L), HCO_3^- (85 mmol/L), Mg^{2+} (0.33 mmol/L) and Ca^{2+} (0.6 mmol/L) to obtain a final ratio of gastric chyme to SFI of 50:50 (v/v) after addition of other recipients and water. The mixture was neutralized to pH 7.0 with 1 M NaOH. Individual enzymes: porcine trypsin (EC 3.4.21.4) 100 U/mL, bovine chymotrypsin (EC 3.4.21.1) 25 U/mL, porcine pancreatic α-amylase (EC 3.2.1.1) 200 U/mL, porcine pancreatic lipase (EC 3.1.1.3) 2000 U/mL, porcine pancreatic colipase 100 U/mL and bile extract B8631 (porcine) 10 mM were added to the digestion mixture to achieve the desired activities in the final mixture. Typically, the SIF fluid was kept in contact with the particles for 2 hours at 37 °C (recommended conditions for intestinal digestion) and pH 7.0 (Minekus et al., 2014).

2.6.1. Evaluation of LGG culturability and viability: plate counting and fluorescence microscopy

The synthesized particles were transferred to a PBS buffer solution at 37 ⁰C for 30 minutes. The viability count corresponds to 1 suspended particle in 1 ml of PBS buffer. Sequential dilutions were performed by dissolving the particles from each composition in the PBS buffer following the Miles and Misra approach to count the number of viable bacteria (Miles, et al., 1938). All different dilutions were plated in triplicates and kept in a CO_2 incubator for 48 hours before the bacterial colony was counted using a colony reader. For the particles treated with the different gastrointestinal fluids (in vitro tests), the procedure was rather similar. Briefly, after exposing the particles to the different fluids, the samples were centrifuged at 3000 rcf for 10 min at 4 °C. The particles (or what remains from them) were re-suspended in 900 µL of a phosphate buffer (0.1 M,

pH 7.0) followed by gentle shaking at room temperature for 15 min. Sequential dilutions and plating in MRS agar were performed as previously described to estimate the number of viable cells. For the storage stability trials, the particles were stored at different temperatures (i.e. 25, 4 and -20 ⁰C) and the viability assessed periodically through plate counting for one month.

All these experiments were performed in a Faster BH-EN and BHG Class II Microbiological Safety Cabinets.

In addition to the plate counting, the bacteria viability was also inferred using a Dead/Alive kit (commercial LIVE/DEAD® BacLight™). Generally, the bacteria in the particles were stained with 2 µl of SYTO 9 dye and 2 µl of propidium iodide from the kit and observed in a fluorescence Olympus microscope (100x immersion objective).

2 .6.2. Flow Cytometry

This analysis was performed using a FACS Calibur flow cytometer (BD Biosciences) equipped with a 488-nm argon ion laser. The green fluorescence was measured at 530/30 nm (FL1) while the red fluorescence was measured at 670 nm (FL3). The data analysis was done using the BD Cell Quest Pro software. The fluorescent probes Syto 9 (3.34 mM in DMSO) and propidium iodine (PI) (20 mM in DMSO) were used to stain all bacteria and the ones with a compromised membrane, respectively. Typically, 5 µL of live/dead working solution was added to 5 µL of a diluted particle sample and 490 µL of filtered PBS. The mixture was further incubated at 37 °C for 15 minutes in an incubator.

The collected data during the in vitro study was analyzed by defining a region around the Syto 9 positive cells (R1) and discriminating the PI-positive cells (R2 – dead cells) from the ones only labeled with Syto 9 (R1 and not R2 – live cells). At least 40000 events gated on R1 were collected for analysis.

In the storage stability trials, the data was periodically analyzed, as done for plate counting, by drawing a region around the Syto 9 positive cells and discriminating the PI-positive cells (R3 – dead cells) from the ones only labeled with Syto 9 (R4) and a region which is positive for both Syto 9 and PI (R4 the intermediate undefined cells). Heat-killed bacteria (i.e. 90 ⁰C for 15 minutes) were used as positive control whereas free bacteria were used as a negative control. Events were gated with 400 µL of the prepared mixtures.

2.7. Cell Culture

The Caco-2 (the passage number ranged 9-15) intestine cell line was cultured at 37 °C in 5 % CO2 in α-Minimum Essential Medium Eagle, supplemented with 10 wt% fetal bovine serum and 1 wt% penicillin/streptomycin. A hemocytometer was used to determine the cell culture concentration of

6

Caco-2 cell line in log phase, that were trypsinized from a 75 cm2 flask using 1 mL of 0.05 wt% trypsin and a 10 µL aliquot. For experimental purposes, 5×10^4 cells were seeded in a 12 well tissue culture plate (corning) and incubated for 24 h to allow proper adhesion (the cell number did not change significantly in the first 24h). After 24 hrs, the medium was replaced by either 1ml of medium containing the different CMC-Cht based particles with and without LGG and/or their respective conditioned medium. The samples to be tested were weighted (ca. 2-4mg) and added to their respective mediums to fulfill a final concentration of 2-4mg/ml before adding to the cells. In the case of the conditioned medium, the same procedure was performed although the materials were incubated at 37 °C in 5 % CO2 for 24h prior to the addition of the cells. After 24 h of incubation, the medium was removed, washed thrice with PBS 1x and 20 % (v/v) of resazurin (final volume of 1ml) was added in each well. The fluorescence signal was developed for 4 h prior to reading and data evaluation. Aliquots (100 µl) of the resulting solutions were transferred in 96-well plates and the fluorescence measurements were performed on a fluorimeter (SynergyMx, BioTek®) using a 560 nm excitation/590 emission filter set. Results are presented as the cell viability percentage when compared to the untreated cells (negative control).

2.8. Statistical analysis

The experiments were performed in triplicate and data was subjected to one-way analysis of variance (ANOVA). Multiple comparisons were performed by LSD test. Statistical significance was set at $P < 0.05$ using SPSS (SPSS Inc, USA). The toxicity data is presented as mean ± standard deviation and excel software was used to perform statistical analysis and $p < 0.05$ indicates the statistical significance.

Results and Discussion

Improving the stability and formation of CMC-Cht particles: Effect of casein and lecithin

In our previous study, physical and chemically cross-linked CMC-Cht hybrid micro- and macro particles were successfully developed for the first time and shown to be capable to entrap viable probiotic bacteria (Singh et al., 2017). Nevertheless, through their preparation, in particular during the centrifugation and filtration washing steps, undesired particle aggregation was often observed. Particles were even more susceptible to aggregation after being cross-linked with genipin. The reason for this was their average zeta potential which considerably decreased to ca. -8 mV (due to the reaction of genipin with the charged amino groups) and thus particles became less charged. Since the incorporation of LGG (negatively charged probiotics) was observed to make the particles more negatively charged thus giving a higher colloidal stability and a reduced tendency to

7

aggregation it was reasonable to assume that electrostatics play a crucial role in particle stability. Therefore, in this follow up study, this major aggregation problem has been tackled by using biocompatible protein and lipid additives.

After an initial screening using different concentrations of milk protein sodium caseinate (SC) and lipid soy lecithin (SL), 1% w/v of either of the biopolymers was found to be optimum and further used in the formation of the CMC-Cht particles. As can be seen in Figure 1, it is clear that the MP doped with SL or SC do not aggregate while the in original CMC-Cht formulation particles stick to each other. Thus, it is suggested that the incorporation of SC or SL increases the particle charge density and therefore the electrostatic inter-particle repulsion is enhanced preventing aggregation. The same qualitative observations were found for the micro particles and for the chemically cross-linked systems.
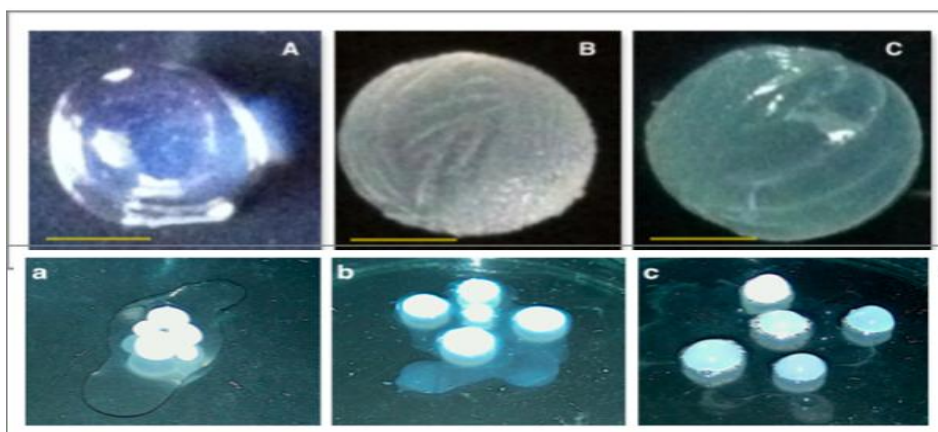
Figure 1. Optical images of (A, a) CMC-Cht, (B, b) CMC-Cht with soy lecithin (C, c) CMC-Cht with casein. Scale bar corresponds to 2 mm.

The outer surface of the CMC-Cht particles is also clearly affected when SL and SC are added to the formulation. Not only the aggregation is minimized but also the particles become less translucent. The morphology of the surface was investigated by SEM and representative pictures are shown in Figure 2. While the CMC-Cht particles are significantly porous, the systems containing SC and SL present a much denser and smooth surface with no perceptible porosity. This difference in porosity can explain the observed differences in the degree of transparency of the particles in Figure 1.
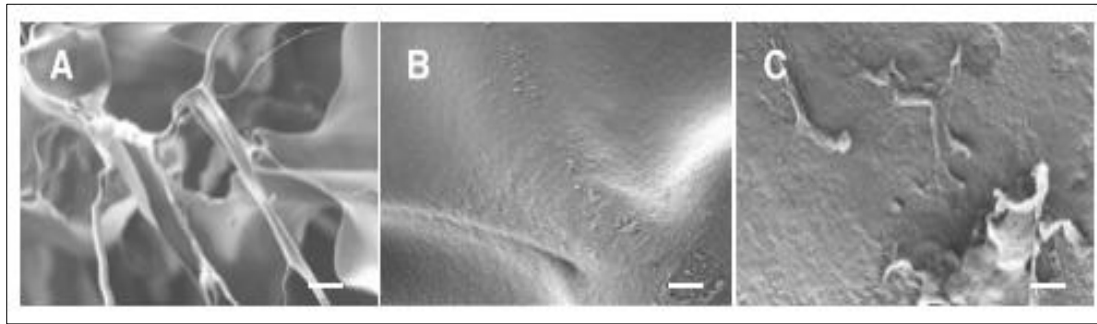
Figure 2. SEM images of CMC-Cht (A), CMC-Cht with soy lecithin (B) CMC-Cht with casein (C). Scale bar is **1**μm.

The thermogravimetric analysis (TGA) was used to evaluate the thermal stability of CMC-Cht particles containing SC or SL. For the original non-doped particles, two main degradation steps can be identified with a ca. 25% mass loss in the first step and a more significant mass lost (35-45%) in the second step. While the first step consists in the evaporation of bound water, the second transition may be attributed to the complex dehydration of the saccharide rings followed by depolymerization, and pyrolytic decomposition of the polysaccharide structure with vaporization and elimination of CO_2 and other volatile products (Wang et al., 2005). It should be noticed that the loss of water in these particle systems is substantially higher than in the native polymers (Singh et al., 2017). More importantly, the major difference detected in the first step where the systems doped with SL or SC show less than 10 % mass lost. Such finding is consistent with the morphological analysis (Figures 1 and 2). Since the systems with SL or SC have a more denser and low porosity surface that hinders water diffusion and thus dehydration is minimized. These features might be important in an in vivo scenario where particle dehydration due to thermal or osmotic effects can be substantially reduced and thus bacteria viability preserved in the GI tract for a longer time.
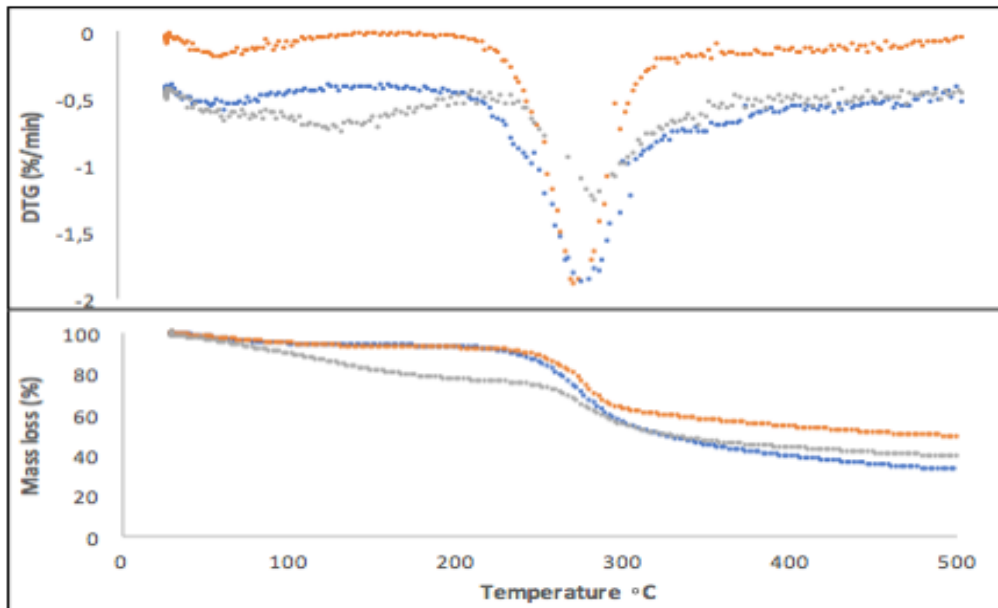
9

Figure 3. Thermograms and first derivative of the particles CMC-Cht (grey), CMC-Cht with casein (orange) and CMC-Cht with soy lecithin (blue).

As the particles are formed with charged biopolymers, the systems are highly sensitive to pH changes as concluded in our previous work (Singh et al., 2017). The presence of SL and SC did not affect the qualitative trend observed before (i.e. little swelling at pH 2-4 and considerably swelling at high pH) (Figure 1 SL). Nevertheless, the particles containing SL generally show an improved swelling at all pH range tested since the SL phosphate groups have a pKa of 1.5 (Israelachvili, 1992; Ogawa et al., 2004) and On the preparation of lecithin-stabilized oil-in-water emulsions by multi-stage premix membrane emulsification) and thus their ionization is expected to contribute to a more expanded state of the particles which is a process typically controlled by the osmotic pressure exerted by the mobile counterions neutralizing the network charges. The SC effect is similar to SL, particularly at pHs above its isoelectric point (ca. pH 4.6). Overall, the observed swelling behavior of the CMC-Cht particles with SL and SC is still very suitable for the delivery of probiotics in the intestinal tract since particles undergo little swelling at pH 2-4 (particles stable at pH values typical for the stomach) while they undergo considerable swelling at pH conditions typically found in the intestinal tract (pH ≈ 8).

The *in vitro* data revealed a strong correlation between the number of viable cells detected by FACS and plate count techniques. Total probiotic counts varied across 7 orders of magnitude during plate counting study and 5 orders in flow cytometry. Nevertheless, tested enumeration methods remained sufficiently close as the techniques give culturable and viable cells respectively. Figure 4 shows the data obtained by plate enumeration. The culturability of encapsulated bacteria on MRS agar, during simulated gastric digestion infers that the CMC-Cht particles with casein showed best survival/viable and culturable abilities significantly higher than the CMC-Cht cross linked ones during human simulated gastric digestion, exhibiting the lowest loss in correlation with the initial value.
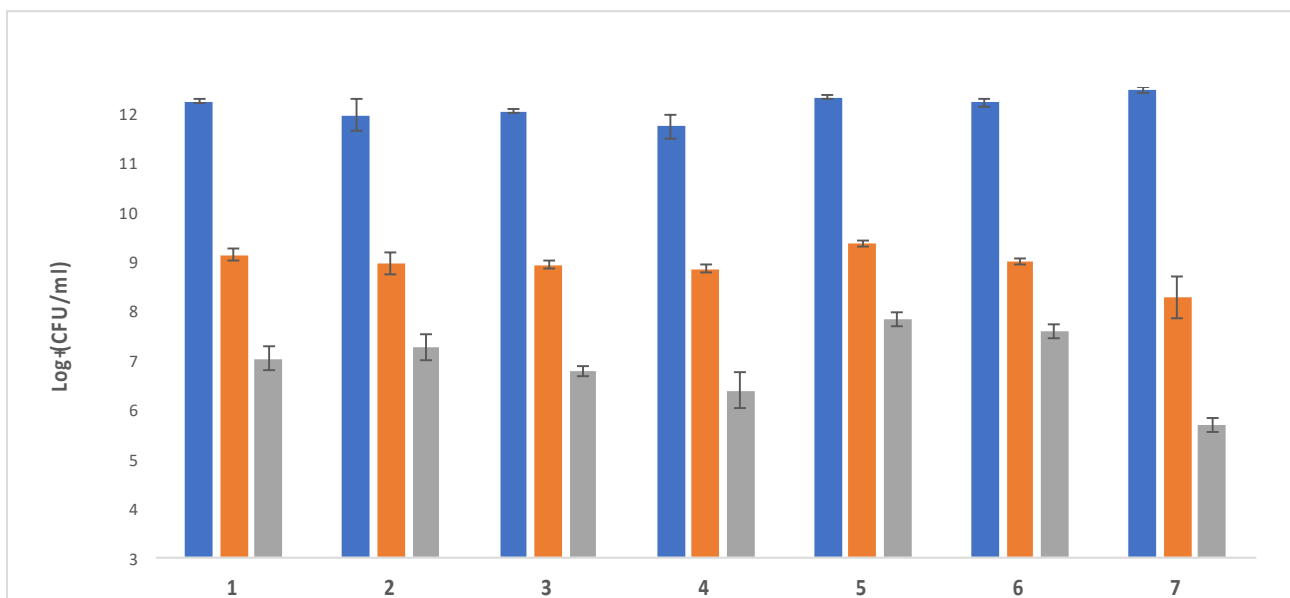
Figure 4. The bar diagram showing the viability of the particles during simulated *in vitro* digestion 1. CMC-Cht (Mp), 2. CMC-Cht gen (Mp), 3. CMC-Cht (mp), 4. CMC-Cht gen (mp), 5. CMC-Cht with casein, 6. CMC- Cht with soy lecithin and 7. control or the naked cells. The different colour of the bars correspond to the distinct stages in the digestion Blue SSF, Orange SGF and Grey SIF respectively.

To compare the plate counting data, rapid alternative enumeration technique with reinforced results has been obtained using Flow Cytometry in Figures 5, 6 and 7. The bar chart in Figure 5 shows the survival ability of the particles and naked bacteria during SSF, SGF & SIF simulated fluids, calculated by flow cytometry. In the encapsulated particles during simulated *in vitro* digestion viability of bacterial cells was more than the control. There was significant difference in the viability ($p<0.05$) between the CMC-Cht with casein in comparison to all other samples. Whey

11

protein was studied to entrap *Lactobacillus rhamnosus* GG during storage, heat and acid stress (Doherty et al., 2010), it also emerged as a platform for delivery of bioactive components. Thus, protein matrices are believed to be environmental friendly and a growth source for *L. rhamnosus* GG.
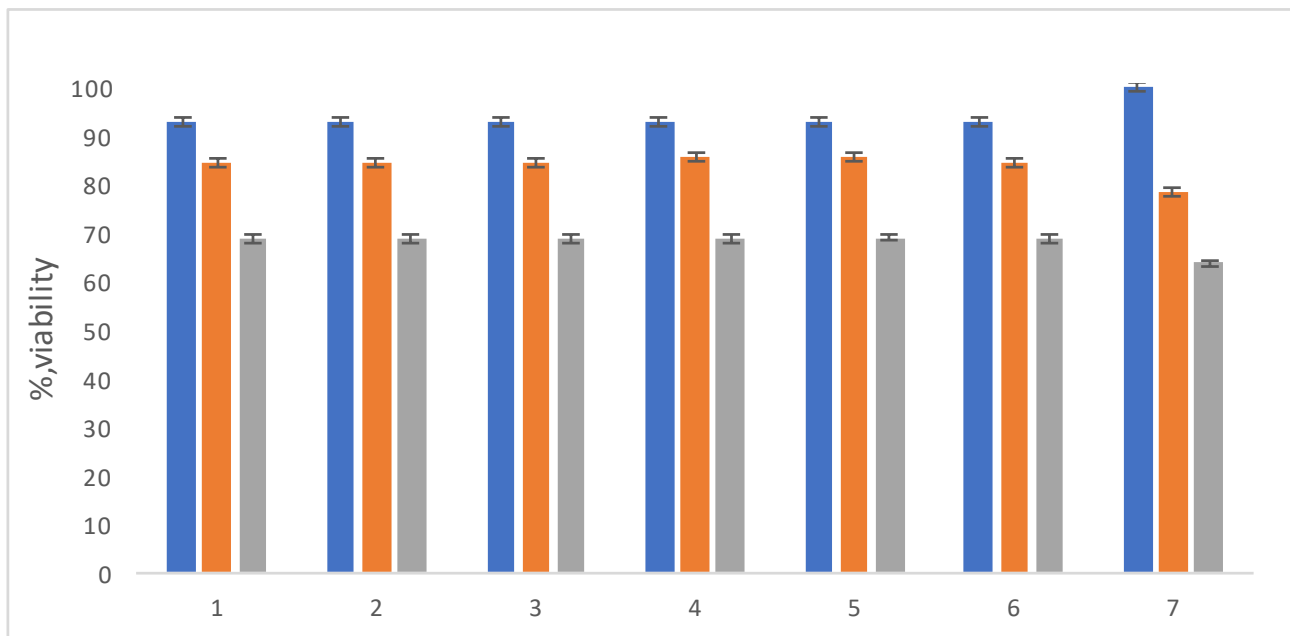

Figure 5. The bar diagram showing the % viability of the particles during simulated *in vitro* digestion obtained with flow cytometer 1. CMC-Cht (Mp), 2. CMC-Cht gen (Mp), 3. CMC-Cht (mp), 4. CMC-Cht gen (mp), 5. CMC-Cht with casein, 6. CMC- Cht with soy lecithin and 7. control or the naked cells. The different color of the bars corresponds to the distinct stages in the digestion Blue SSF, Orange SGF and Grey SIF respectively.

Exposure of bacteria (both encapsulated and naked) to acidic conditions using simulated gastric conditions at pH 2.0 and simulated intestinal conditions pH 7.4 clearly showed the difference in the population of bacterial cells observed and collected (Figure 6. I, II & III).

Live, dead and injured cells could be easily distinguished based on fluorescent properties of PI and Syto 9, respectively as *lactobacilli* are not spherical, FSC and SSC were adjusted to the amplifications to collect the entire rod-shaped population appearing on the scale with a substantial concentration for gating. Regions were carefully drawn to avoid any background noise also the buffer augmentation. Fig. 6, (I), (II) and (III) show that the digested *L. rhamnosus* GG successfully preserved membrane integrity and continued to emit the strong fluorescent signal. The purpose of enumerating viable bacteria in the particles was to ensure that it's an easy, fast and efficient method, as the task could take over 3 days to achieve by plate counting.
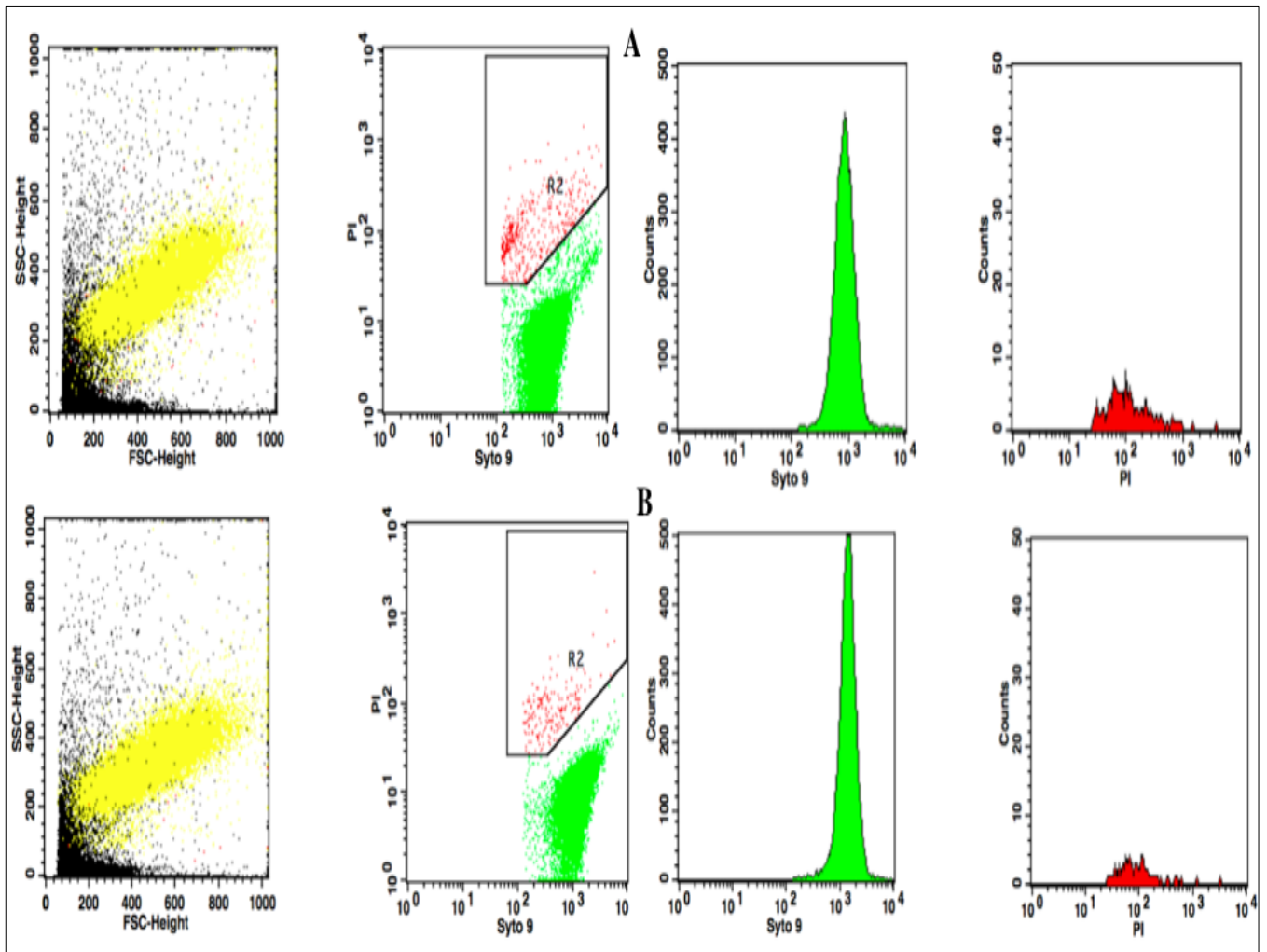
12

Figure 6 (I). Dot plots and histograms of the released bacteria from the samples during SSF *in vitro* digestion **A**. CMC-Cht particles with casein and **B**. control or the naked cells.

The advantage of using flow cytometry is that staining the released bacteria from the matrix with red fluorescent PI with a green fluorescent total cell stain (SYTO9) gives a distinctive and reproducible fluorescence pattern.
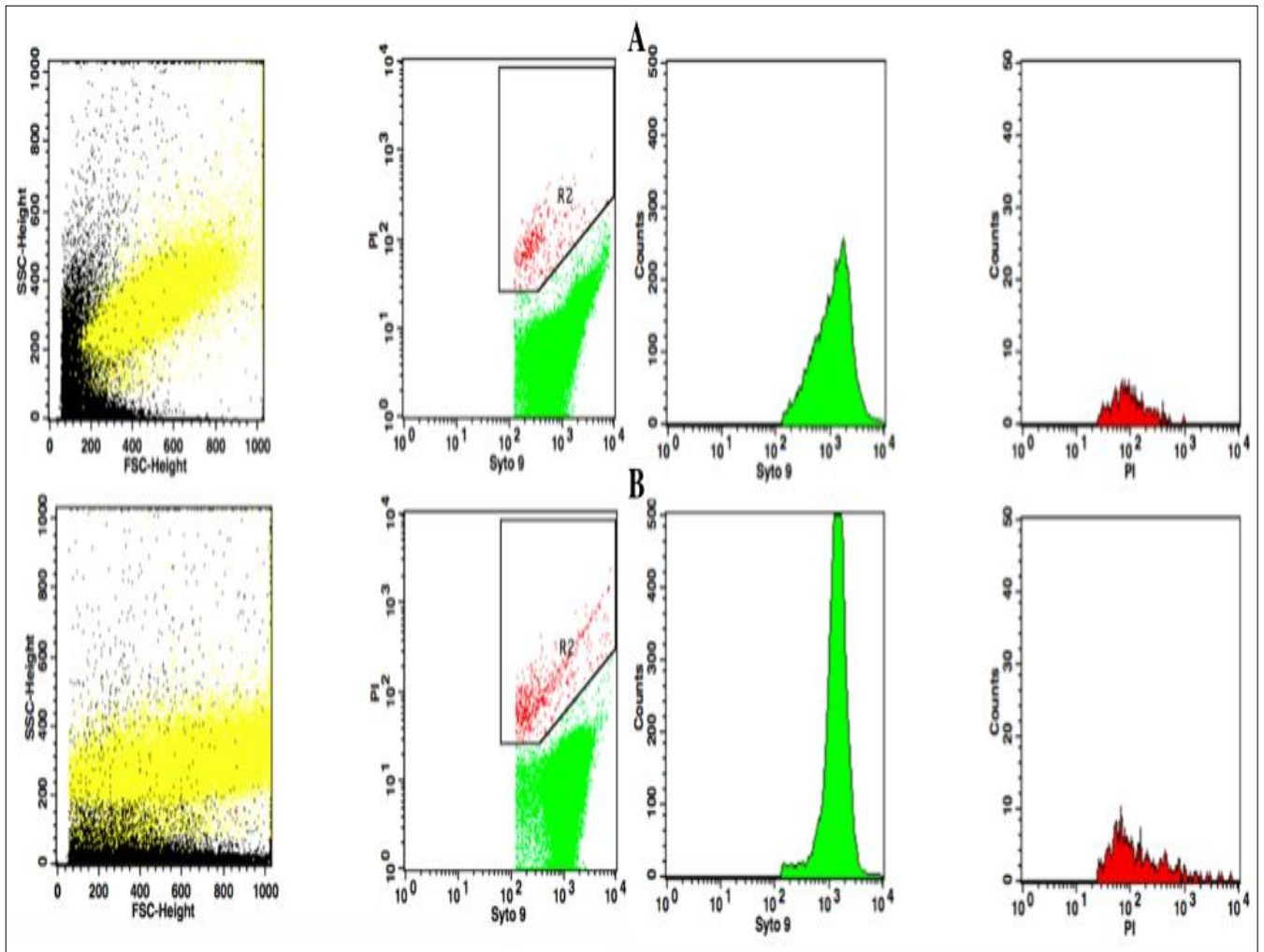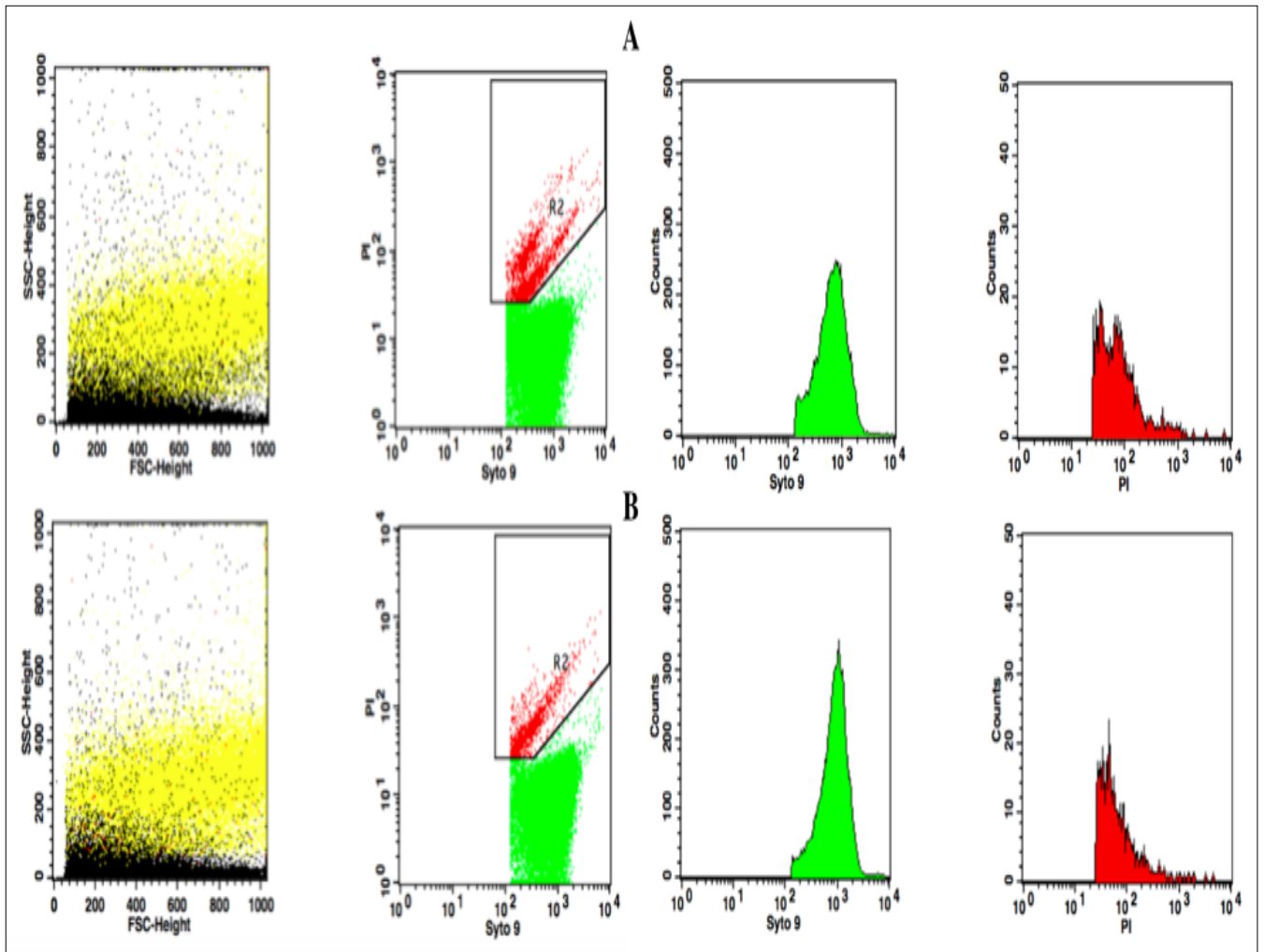
Figure 6 (II). Dot plots and histograms of the released bacteria from the samples during SSF *in vitro* digestion **A**. CMC-Cht particles with casein and **B**. control or the naked cells.

The viable bacterial population demonstrated as green histogram contrary to the dead ones with a red fluorescence (Fig. 6 and 8). During the gastric simulated digestion in Figure 6 I (B and C), some of the released cells have specifically a different population density if compared to what was seen during the salivary fluid simulation.

Figure 6 (III). Dot plots and histograms of the released bacteria from the samples during SIF *in vitro* digestion **A**. CMC-Cht particles with casein and **B**. control or the naked cells.

The encapsulation efficiency of different types of particles calculated was CMC-Cht (Mp) 98.2%, CMC-Cht gen 95.9% (Mp), CMC-Cht (mp) 96.6%, CMC-Cht gen (mp) 94%, CMC-Cht with casein 98.8%, and CMC-Cht with soy lecithin 98%. Also, the encapsulated samples in all different particles had a significantly higher viability than the control after going through the harsh conditions. The data demonstrate that microscopic viability counting yielded consistently higher counts (10- 20-fold) than the plate counting.

The results from storage studies using plate count methods showing the culturable bacteria for a duration of 1 month Figure 9. The statistical analysis showed that there was a significant higher survival rate in the encapsulated bacteria than the free, naked cells in all the three different temperatures studied for shelf life. Also, particles with caseinate have considerably highest viability among all. The storage studies show that the encapsulated bacteria have a higher culturablility and

15

viablilty at lower temperatures i.e. 4 ℃ and -20 ℃. However, the bacteria at room temperature (25 ℃) is found culturable until 5 log units.
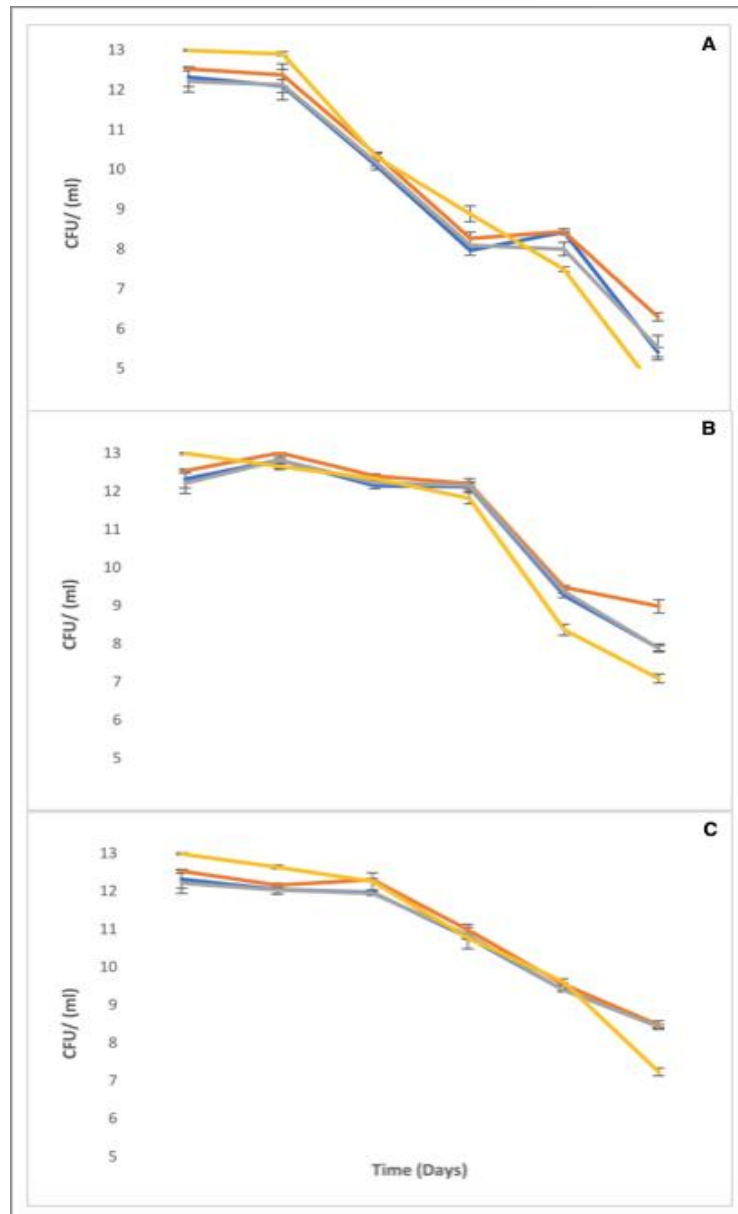

Figure 7. The graph represents the viability during the storage of samples at three different temperatures A) 25 ℃, B) 4 ℃ and C) -20 ℃ during 30 days of period. Orange line refers to CMC-Cht particles with casein, Blue CMC-Cht particles, Grey CMC- Cht particles with soy lecithin and yellow is the control or the naked cells.

If looked carefully in the dot plot of storage diagrams Figure 8(I) distinctive pattern of the cells which are positive for both Syto9 and PI can be observed, that belong to strong green and weak red

fluorescence intensity suggesting that an intermediate state of the cells is occurring. This pattern is recurrent in all the studied temperatures.

This may be inferred as there might be high degree of clumping formed, and due to stress response as seen during storage studies in the region R4 the bacteria are not culturable therefore, there is a difference in count of the survival of the bacteria from two different techniques.

Storage studies at temperatures 25, 4 & -20°C showed the fundamental variance in the cell population generated by FACS with a fact that higher cell counts were enumerated relative to plate count. It can be related with the fact that FACS detects injured and dead probiotic populations as well together with the normal population, because injured cells which may be non-culturable by plate method would remain effective and detectable by FACS.
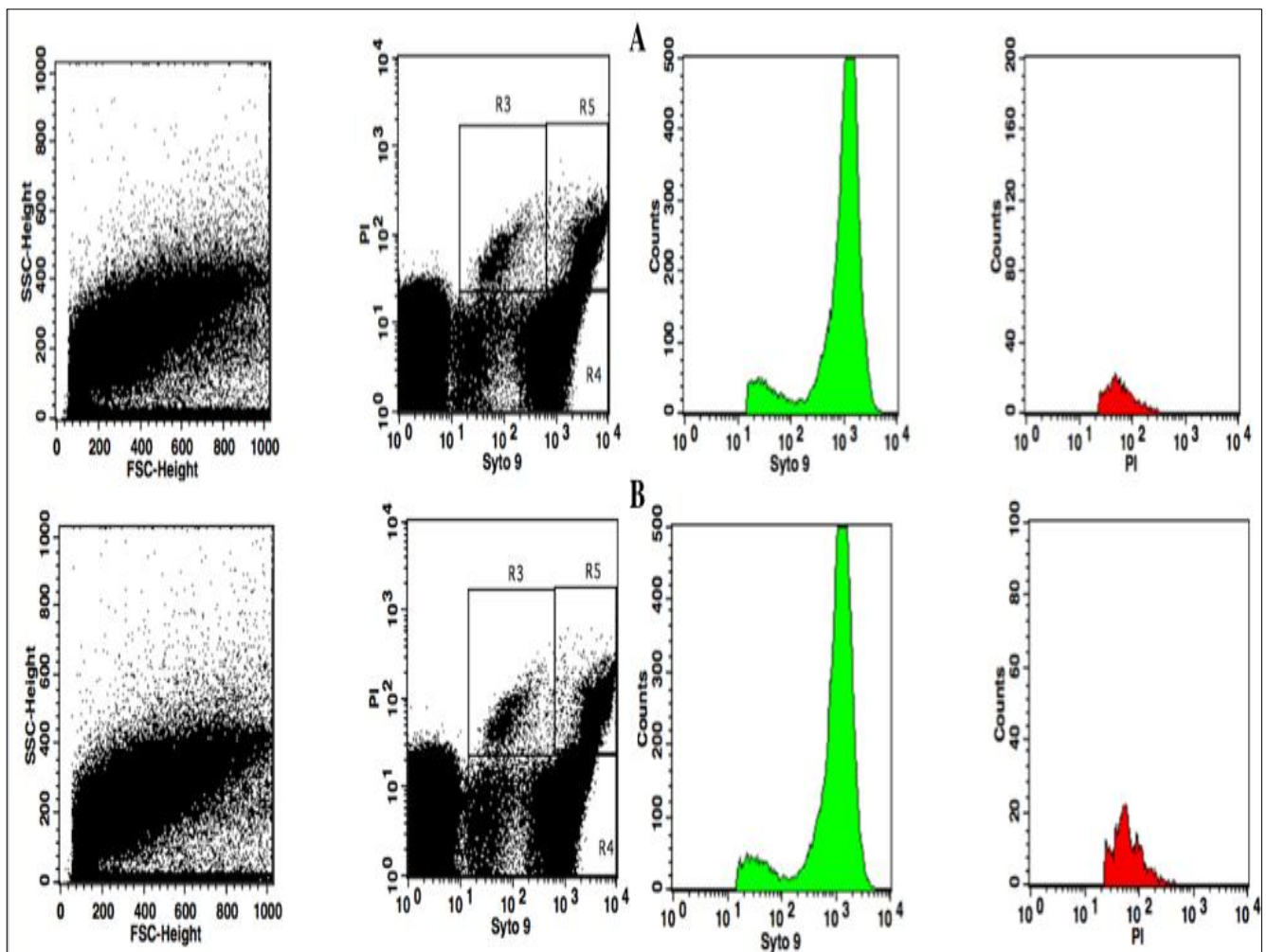

Figure 8 (I). Dot plots and histograms of the released bacteria from the samples during storage at 25 ºC on the 1st day **A**. CMC-Cht particles with casein and **B**. control or the naked cells.
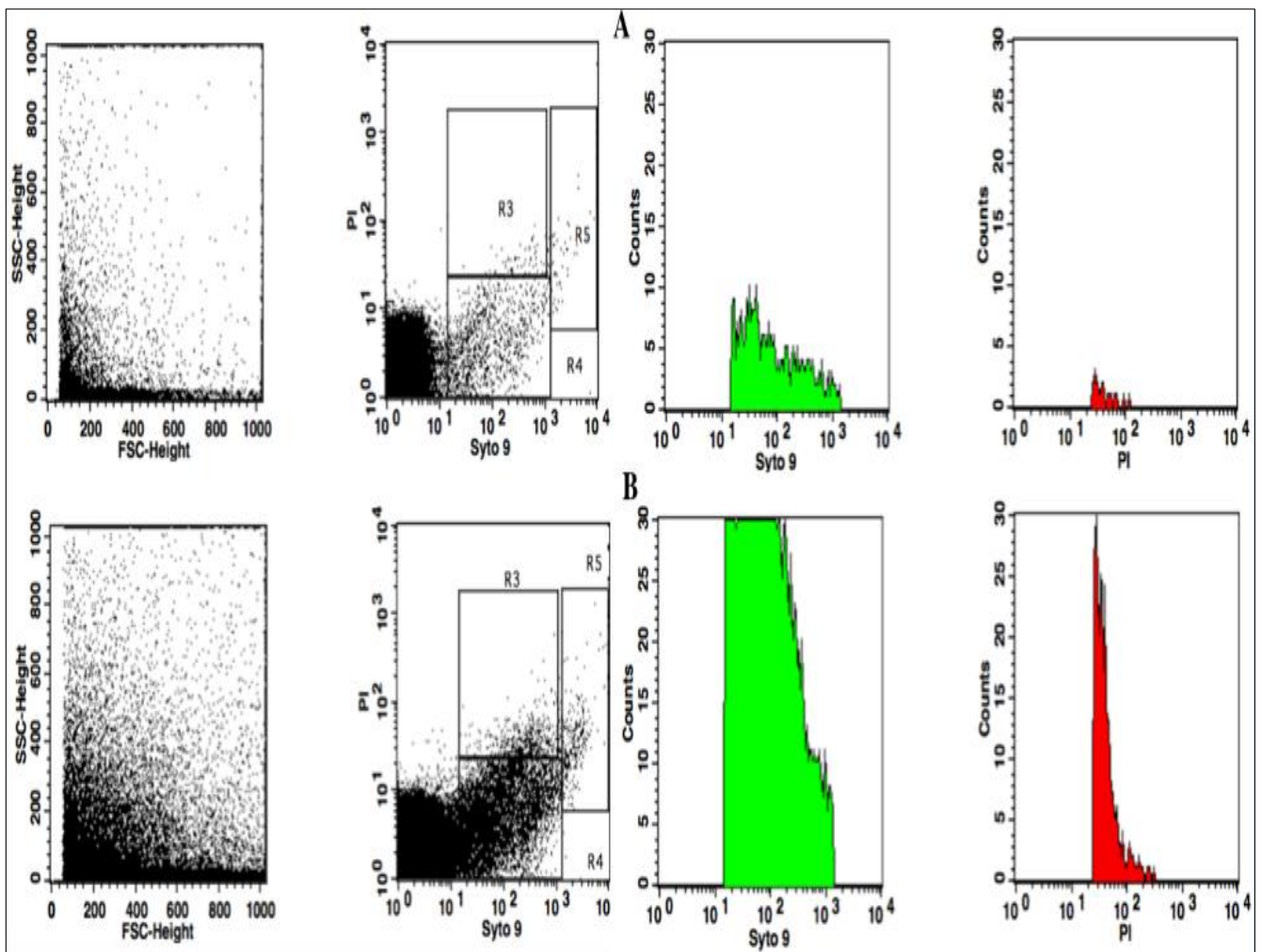
Figure 8 (II). Dot plots and histograms of the released bacteria from the samples during storage at 25 ºC on the 31st day **A**. CMC-Cht particles with casein and **B**. control or the naked cells.

In the dot plot a distinctive region can be observed in shelf life studies Figure 8 (I, II). A bacterial cluster has a selective behaviour suggesting an occurrence of intermediary state, which are characterized by different intracellular concentrations of SYTO9 and PI Figure 8 I. In all the three different temperatures calculated at specific days this pattern was visible, however with decrease in total population of the bacteria this population tend to diminish as well Figure 8 II.

The decline in the viability during the shelf life evaluation at 25°C in CMC-Cht particles (Mp) 56.2%, CMC-Cht particles with casein 49%, CMC- Cht particles with soy lecithin 54%. and control or the naked cells 60%. At 4 °C it was 44%, 36%, 43%, 47% and at -20°C was 31%, 32%, 31%, 44% respectively.
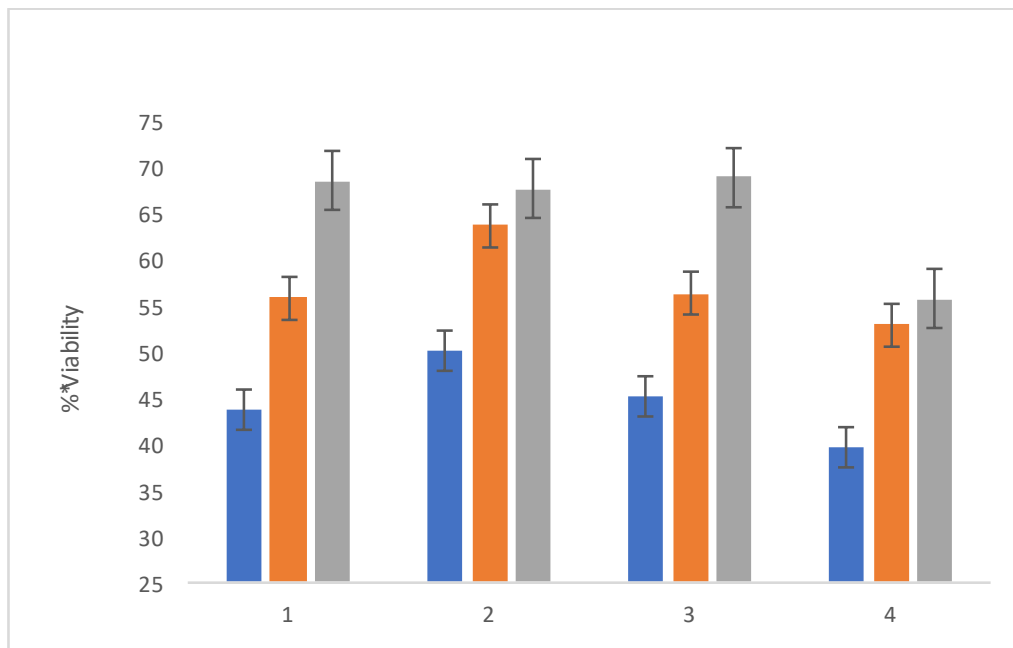
Figure 9. The graph represents the % viability during the storage of samples at three different temperatures 25 ℃ (blue bar), 4 ℃ (orange bar) and -20 ℃ (grey bar) after 30 days. 1. refers to CMC-Cht particles, 2. CMC-Cht particles with casein, 3. CMC- Cht particles with soy lecithin and 4. is the control or the naked cells.

The qualitative cell viability in the CMC-Cht particles prepared with SC or SL was also evaluated by fluorescence microscopy using a Dead/Alive kit. In this test the viable bacteria appear as green while the dead bacteria are red/orangish. As can be seen in Figure 10, the fluorescence microscopy images substantiate the results from microbiological studies. While the particle with SL and particle without any blend is more "orange-like" (Figure 10F) the SC samples (Figures 10E) are "greener" thus suggesting a higher number of viable cells.
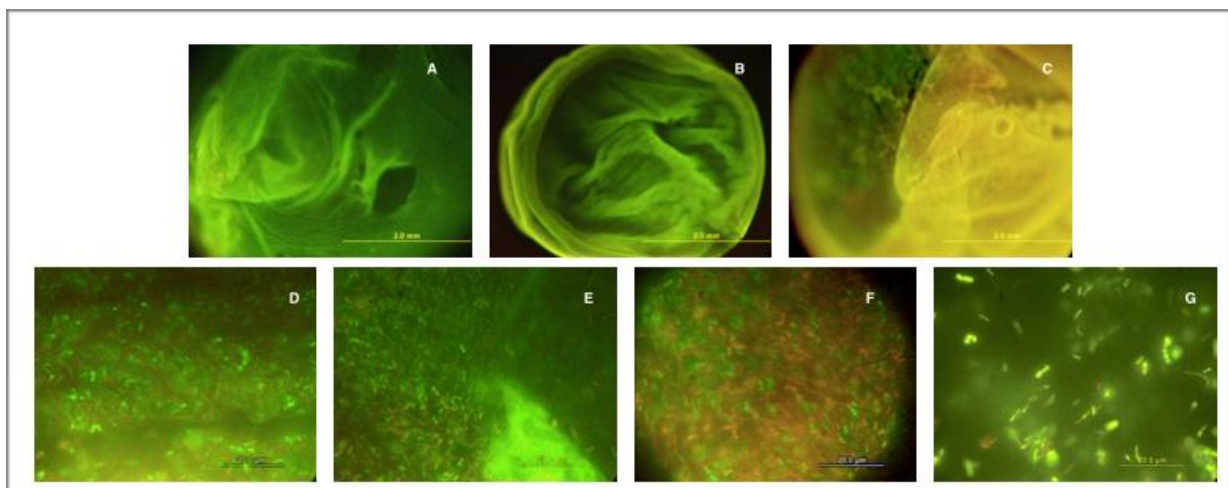
Figure 10. The images obtained through fluorescent microscope represents the particles with the entrapped bacteria. A. CMC-Cht particles, B. CMC-Cht particles with casein (CS), C. CMC- Cht particles with soy lecithin (SL). The scale bar corresponds to **2** mm in A, B and C.

The images obtained through fluorescent microscope represents the viability of the encapsulated bacteria D. CMC-Cht particles, E. CMC-Cht particles with casein, F. CMC- Cht particles with soy lecithin and G the naked cells. The scale bar corresponds to **20** μm

The consequential results showing encapsulated *L. rhamnosu*s could be also protected during non-refrigerated storage with exposure to oxygen and humidity for 30 days is particularly promising, this demonstrates the potential of encapsulation vehicle to widen the application of environmentally sensitive probiotics to long-shelf-life food and pharmaceutical products even at the room temperature.

The cytotoxicity results obtained after the exposure of the Caco-2 cells system to different particles determined their viability. The particles were investigated at two different mediums, among different particles in presence and absence of LGG with resazurin assay, mainly to evaluate epithelial barrier damages caused by exposure. Resazurin assay was used as an indicator for cell viability in mammalian cell cultures. The results obtained express a moderate to low toxicity to the cell line. When the particles have encapsulated bacteria, they show better viability of the cultured cell line (Figure 11).
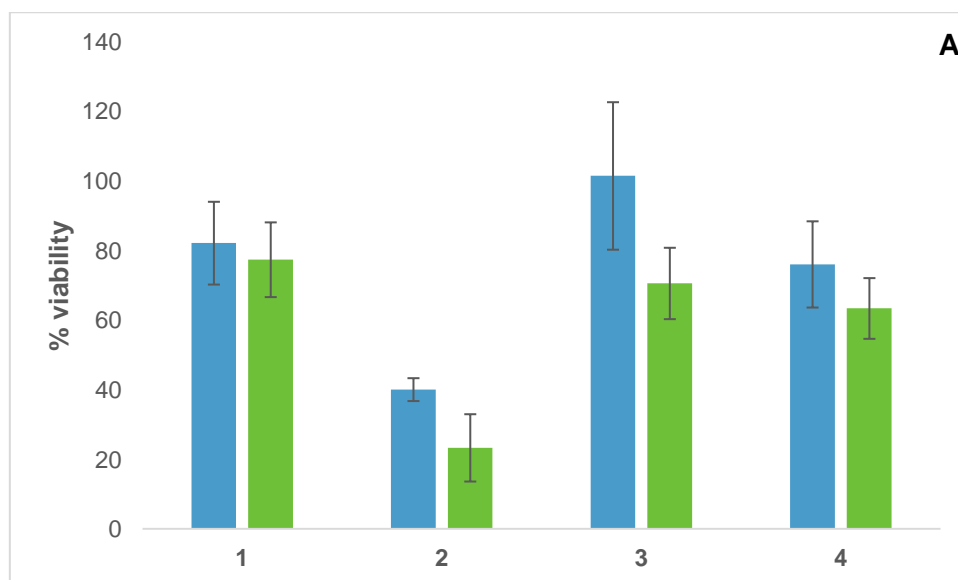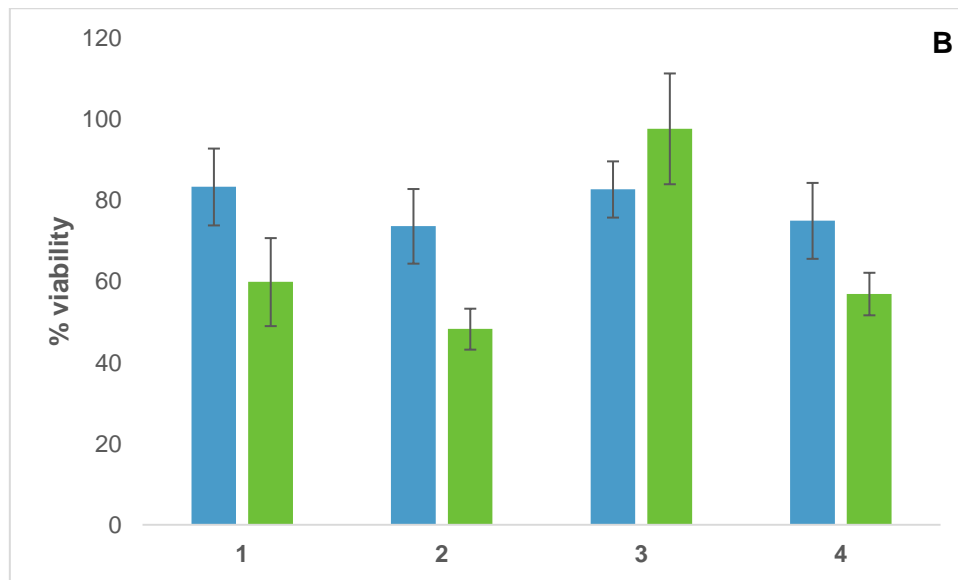
Figure 11. The bar graph represents the exposure of the particles to Caco-2 cell line (green bars with direct contact medium and blue bars with conditioned medium) A) without LGG B) encapsulating LGG. The numbers on horizontal axis represent the variation in composition of CMC- Cht particles 1. without modification 2. with soy lecithin (SL) 3. with casein (CS), 4. crosslinked with genipin

The cell concentration in direct media seemed to be more sensitive in all the compositions except sodium caseinate entrapped with LGG, besides the particles with the protein show the highest number of viability in both the mediums with and without LGG. As the earlier viability results show mitigated release of probiotic bacteria with chemically cross-linked particles (the assumption was both the antibacterial property and pore less matrix because of genipin), contrary to that the toxicity to the cell line was minimal, somewhat similar to physical particles. Thus, the particle composition of the used polymers, doesn't decrease cell viability considerably proving the integrity of the monolayer is not compromised except in the particles where soy lecithin is used and the toxicity is high almost 60% in direct contact medium.

Conclusion

The initially developed CMC-Cht particle matrix was further enhanced through the addition of a a lipid molecule, soy lecithin or a protein sodium caseinate at an optimum concentration for detection with *L. rhamnosu*s GG. The ability of the particles to protect LGG during gastrointestinal conditions assessed in a two-stage in vitro model simulating conditions in the human stomach and small intestine showed an enhancement of the viability of encapsulated bacteria to non-encapsulated. The decrease was more prominent in the culturable bacteria in relation to the viable one. The reduction in culturability and viability may be governed by the hydrophilic character of *L. rhamnosus* GG, which is because electrostatic repulsion, preventing the adherence of the bacteria on and inside the particle surface. The surface charge and hydrophobicity of the bacteria contributes to its interaction with proteins or any matrix (Li et al., 2008). The entrapment and relationship of probiotics is strain specific and the type of milk protein and pH affect these interactions being non-specific in case of casein (Burgain et al., 2013b). Results obtained in the present study provide information on principal factors affecting the viability of the bacteria, such as the, matrix, initial pH of the stomach and intestine in the simulated digestion model. The combination of flow cytometry model complies to get a dynamic view of the survival of organisms as they pass through the GI tract and storage profile in different polymers associated CMC-Cht particles. It is interesting to highlight that although the data showed a more significant effect of low pH on bacterial survival nonetheless, the particle matrices showed a great survival during both *in vitro* and storage studies.

References

- Bosnea, L. A., Moschakis, T., & Biliaderis, C. G. (2014). Complex Coacervation as a Novel Microencapsulation Technique to Improve Viability of Probiotics Under Different Stresses. *Food and Bioprocess Technology*, 7, 10, 2767-2781.
- Burgain, J., Gaiani, C., Cailliez-Grimal, C., Jeandel, C., & Scher, J. (2013). Encapsulation of Lactobacillus rhamnosus GG in microparticles: Influence of casein to whey protein ratio on bacterial survival during digestion. *Innovative Food Science and Emerging Technologies*, 19, 233-242.
- Chang, C. Y., & Zhang, L. N. (2011). Cellulose-based hydrogels: Present status and application prospects. *Carbohydrate Polymers*, 84(1), 40-53.
- Donthidi, A. R., Tester, R. F., & Aidoo, K. E. (2009). Effect of lecithin and starch on alginate-encapsulated probiotic bacteria. *Journal of Microencapsulation*, 27, 1, 67-77.

- Dutta, P. K., Dutta, J., & Tripathi, V. S. (2004). Chitin and chitosan: chemistry, properties and applications. *Journal of Scientific and Industrial Research*, 63, 20-31.

- Iannitti, T., & Palmieri, B. (2010). Therapeutical use of probiotic formulations in clinical practice. *Clinical Nutrition*, 29(6), 701-725.

- Israelachivili, J. N. (1992). Intermolecular and surface forces. London, England: Academic Press.

- James, P. H., John, R., Alex, A., & Anoop, K. R. (2014). Smart polymers for the controlled delivery of drugs - a concise overview. *Acta Pharm Sin* B, 4(2), 120-127.

- Klemm, D., Heublein, B., Fink, H.P., & Bohn, A. (2005). Cellulose: Fascinating Biopolymer and Sustainable Raw Material. *Angewandte Chemie*, 44, 22, 3358.

- Li, W., Sun, B., & Wu, P. (2009). Study on hydrogen bonds of carboxymethyl cellulose sodium film with two-dimensional correlation infrared spectroscopy. *Carbohydrate Polymers,* 78, 3, 454-461.

- Li, X. J., Yue, L. Y., Guan, X. F., & Qiao, S. Y. (2008). The adhesion of putative probiotic lactobacilli to cultured epithelial cells and porcine intestinal mucus. *Journal of Applied Microbiology*, 104, 4, 1082-91.

- Minekus, M., Alminger, M., Alvito, P., Ballance, S., Bohn, T., Bourlieu, C., Carriere, F., Boutrou, R., Corredig, M., Dupont, D., Dufour, C., Egger, L., Golding, M., Karakaya, S., Kirkhus, B., Le Feunteun, S., Lesmes, U., Macierzanka, A., Mackie, A., Marze, S., McClements, D. J., Menard, O., Recio, I., Santos, C. N., Singh, R. P., Vegarud, G. E., Wickham, M. S. J., Weitschies, W., & Brodkorb, A. (2014). A standardised static in vitro digestion method suitable for food - an international consensus. *Food & Function*, 5(6), 1113-1124.

- Ogawa, S., Decker, E. A., & McClements, D. J. (2003a). Production and character- ization of O/W emulsions containing droplets stabilized by lecithin-chitosan membranes. *Journal of Agriculture and Food Chemistry*, 51, 2806–2812.

- Sharpe, L. A., Daily, A. M., Horava, S. D., & Peppas, N. A. (2014). Therapeutic applications of hydrogels in oral drug delivery. *Expert Opinion on Drug Delivery*, 11, 6, 901-15.

- Singh, P., Medronho, B., Alves, L., da, S. G. J., Miguel, M. G., & Lindman, B. (2017). Development of carboxymethyl cellulose-chitosan hybrid micro- and macroparticles for encapsulation of probiotic bacteria. *Carbohydrate Polymers*, 175, 87-95.

- Wang, S. F., Shen, L., Tong, Y. J., Chen, L., Phang, I. Y., Lim, P. Q., & Liu, T. X. (2005). Biopolymer chitosan/montmorillonite nanocomposites: Preparation and characterization. *Polymer Degradation and Stability*, 90, 1, 123-131.